



Studier af rekrySTALLISATION med 3DXRD

Juul Jensen, Dorte

Publication date:
2013

Document Version
Publisher's PDF, also known as Version of record

[Link back to DTU Orbit](#)

Citation (APA):
Juul Jensen, D. (Author). (2013). Studier af rekrySTALLISATION med 3DXRD. Sound/Visual production (digital), Dansk Metallurgisk Selskab.

General rights

Copyright and moral rights for the publications made accessible in the public portal are retained by the authors and/or other copyright owners and it is a condition of accessing publications that users recognise and abide by the legal requirements associated with these rights.

- Users may download and print one copy of any publication from the public portal for the purpose of private study or research.
- You may not further distribute the material or use it for any profit-making activity or commercial gain
- You may freely distribute the URL identifying the publication in the public portal

If you believe that this document breaches copyright please contact us providing details, and we will remove access to the work immediately and investigate your claim.

Karakterisering på alle længdeskalaer

DMS

DANSK METALLURGISK SELSKAB
Vintermødet
2013
Koldingfjord

Foredrag
præsenteret ved
Vintermødet 16. til 18. januar 2013
Hotel Koldingfjord
Kolding

Redaktion:
Trine Nybo Lomholt

Eftertryk kun tilladt med forfatternes tilladelse

FORORD

Dansk industri skal bl.a. overleve på kvalitet, og det er vigtigt, at virksomhederne kan dokumentere denne kvalitet overfor deres kunder. Vintermødet 2013 har derfor fokus på karakterisering af materialer, processer og komponenter, som spænder fra nanometer til meterskala og fra forskning & udvikling til monitorering af komponenter i drift.

Vintermødet sigter mod en bred dækning af emnet med foredrag, der bl.a. dækker mikroskopi, kemisk analyse, mekanisk prøvning, skadesanalyse, kvalitetskontrol mm.

Dette års virksomhedsbesøg foregik på Alfa Laval i Kolding. Alfa Laval Kolding er specialist i løsninger til håndtering af væsker af enhver viskositet, hurtig rengøring af lukket procesudstyr og intelligent, automatiseret kontrol. På fabrikken i Kolding produceres pumper og ventiler til fødevareindustrien, bryggerier, mejerier, farmaceutiske- og kosmetiske industrier. Alfa Laval Kolding beskæftiger i dag ca. 550 medarbejdere.

Trine Nybo Lomholt

INDHOLDSFORTEGNELSE

Fracture mechanics - Some basic concepts and recent trends Erling Østby, SINTEF	1
Off-line testing af friktion og smøring i pladeformgivning Niels Bay, DTU Mekanik	24
Industriens udnyttelse af de store internationale røntgen og neutronfaciliteter Henning Friis Poulsen, DTU Fysik	48
Studier af rekrytation med 3DXRD Dorte Juul Jensen, DTU Vindenergi	60
Den nyeste generation af røntgen diffraktometre med tilhørende temperaturcelle Flemming Grumsen, DTU Mekanik	78
NDT – relevante teknikkers muligheder og begrænsninger Peter Villumsen, Force	89
Metrology and Quality Assurance Maria Holmberg, Teknologisk Institut	101
Determining geometrically necessary dislocation densities by EBSD Philip Littlewood, DTU Mekanik	111
Transformation af udskillelser på atomar skala Hilmar Danielsen, DTU Mekanik	121
Structural and chemical characterization by electron microscopy – spanning the micro and nano regime Jakob Birkedal Wagner, DTU CEN	133
Nanostruktur og styrke af stål deformeret ved valsning og med shot peening Niels Hansen, DTU Vindenergi	144
Homogen og lokaliseret tøjningsudvikling af nanostruktureret aluminium Jacob Kidmose, DTU Vindenergi	164
Baggrund for Innovationskonsortiet REEgain om magnetiske materialer Jens Christiansen, Teknologisk Institut	175

Superleder tapes karakteriseret fra nanometer pinning til meter store spoler Asger Bech Abrahamsen, DTU Vindenergi	189
Mikrostruktur karakterisering af SG-støbejern Karl Martin Pedersen, Siemens Wind Power A/S	198
Kvalitetssikring af støbegods i MAN B&W motorer Knud Strande, MAN	212
Ny metode til kvantificering af grafitstørrelse og –morfologi i støbejern Steen Krogh Jensen, MAN	231
Materialevalg/Stålfremstilling Stig Rubæk, Metal-Consult	252
Varmebehandling og karakterisering af nye udskilningshærdbare superlegeringer Uffe Bihlet, MAN og DTU Mekanik	268
GD-OES applications Io Mizushima, IPU	286
Egenskaber for korrosion og rensbarhed af rustfrit ståloverflader Rasmus Lage	295

Fracture mechanics - Some basic concepts and recent trends

Erling Østby, SINTEF

Fracture Mechanics - Some basic concepts and recent trends

Erling Østby
(Erling.Ostby@sintef.no)

SINTEF Materials and Chemistry



Materials and Chemistry

1

SINTEF Materials and Chemistry

- SINTEF Materials and Chemistry is a contract research division offering high competence within
 - materials technology,
 - applied chemistry,
 - and applied biology
- 400 employees
 - 100 Oslo, 300 Trondheim, approx. 25% non-Norwegian from 44 countries
- 8 departments + staff
- Core areas of R&D
 - Oil & Gas industry, approx. 150 man-years
 - along the whole value chain from increased oil production, drilling, flow assurance, pipelines, to refineries and petrochemical
 - the largest independent research institution in the world on oil spill
 - Land-based industries, approx. 120 man-years
 - aluminum, ferro alloys, mineral industry, manufacturing industry, pharmaceutical industry (biotech), and food industry.
 - Environmentally friendly energy, approx. 120 man-years
 - Silicon-based solar, CCS, bio-refinery, offshore wind, hydrogen technology.



Executive Vice President Torstein Haarberg together with former and present employees at SINTEF Materials and Chemistry



Materials and Chemistry

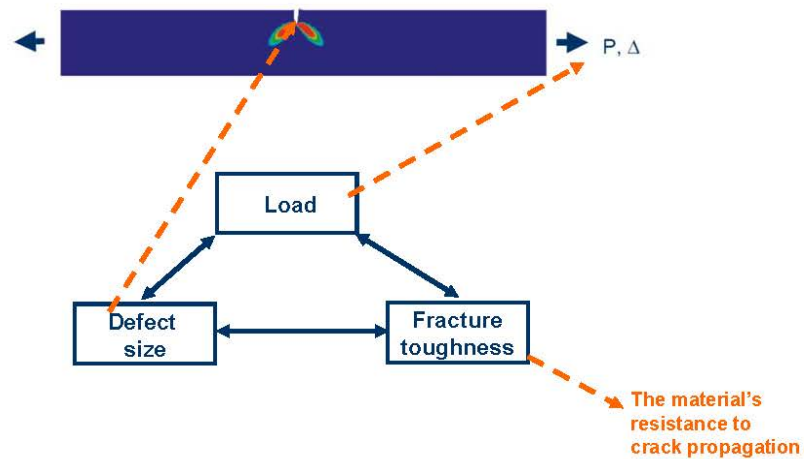
2

Outline

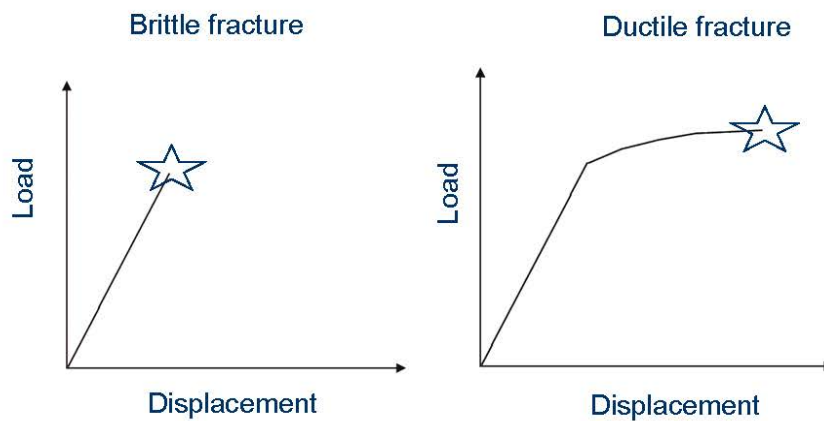
- Some basic fracture mechanics concepts
- Examples of emerging/new topics
 - Constraint effect – *"new knowledge"*
 - Fracture under large global deformations - *"application under harsher conditions"*
 - Use of numerical simulation tools – *"taking the analysis further"*
 - Testing techniques – *"new information"*
 - Probabilistic fracture assessments – *"quantified safety level"*
 - .. and a few words on multi-scale approaches – *"tomorrow"*
- Wrap-up

Some basic fracture mechanics

Basic fracture mechanics

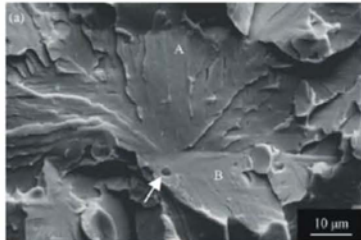


Types of fracture – global perspective



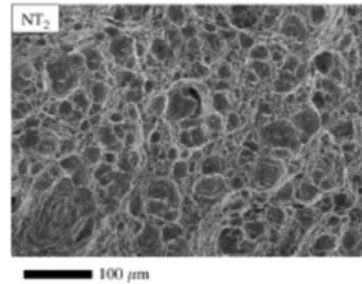
Types of fracture – materials perspective

Brittle fracture (cleavage fracture)



- Fracture propagates along given planes in the crystal
- Requires little energy for crack propagation

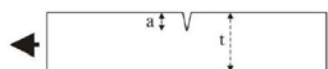
Ductile fracture



- Fracture propagates through formation and coalescence of voids in the material
- Requires more energy (and local deformation)

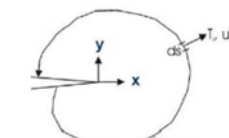
How to quantify the loading of the crack

■ Elastic conditions – Stress intensity factor, K



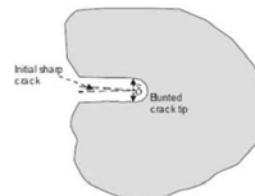
$$K = \sigma \sqrt{\pi a} f(a/t) \quad [\text{MPa}\sqrt{\text{m}}]$$

■ With significant plasticity – J-integral or CTOD (δ)



$$J = \int_{\Gamma} (w dy - T_i \frac{\partial u_i}{\partial x} ds)$$

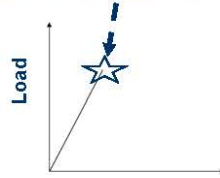
$$J = m \sigma_y \delta$$



When will the material fracture?

■ Brittle fracture:

- Fracture occurs when a critical K , J or CTOD value is reached

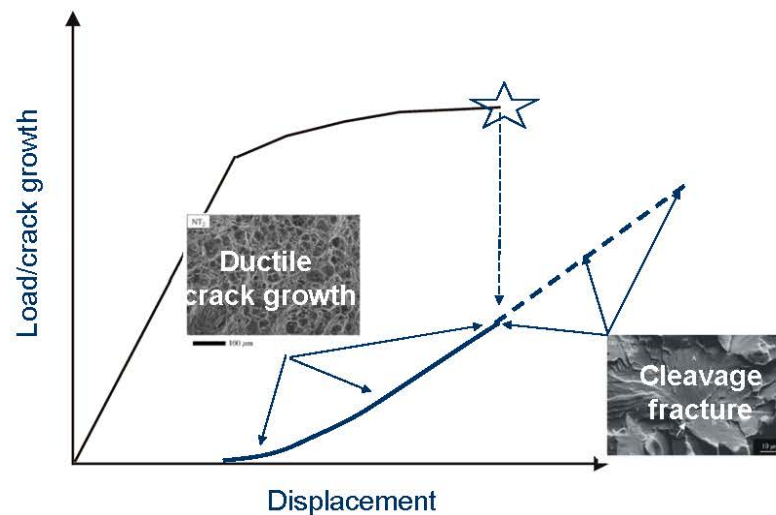


■ Ductile fracture:

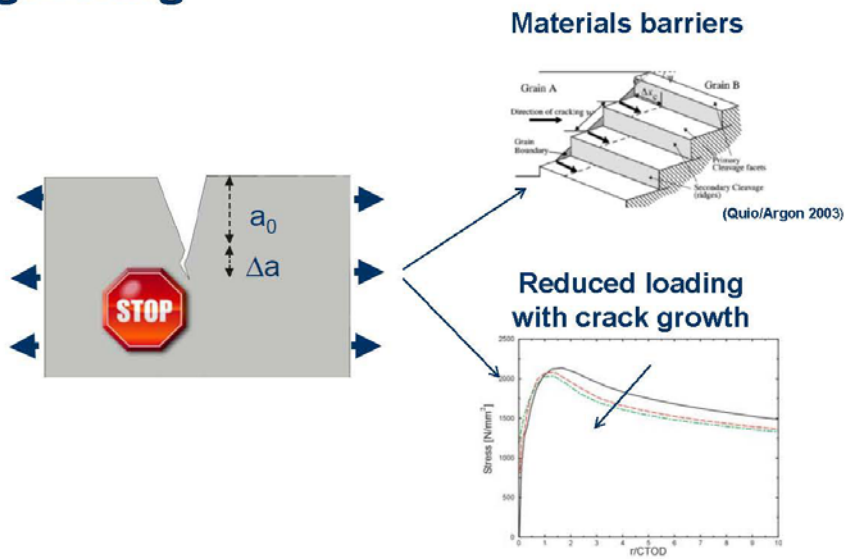
- The fracture resistance is not represented with a single value, but with a curve (either using J or CTOD)



A transition in fracture mechanism may sometimes occur



Crack arrest – *when cracks stop growing*



Emerging/new topics

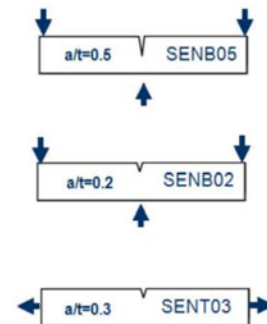
Constraint effects in fracture

Key points:

- *Fracture toughness no longer a material parameter!!!*
- There is an influence from the geometry and mode of loading applied

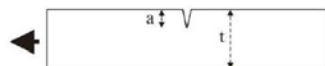
Case:

- The effect of specimen geometry in brittle fracture toughness of a HAZ microstructure



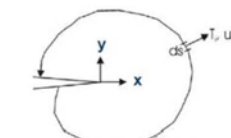
Classical fracture mechanics parameters – *Believed to fully describe the crack tip conditions....*

Elastic conditions – Stress intensity factor, K



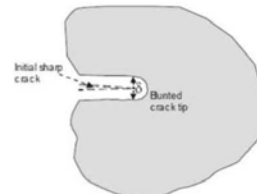
$$K = \sigma \sqrt{\pi a} f(a/t) \quad [\text{MPa}\sqrt{\text{m}}^{1/2}]$$

With significant plasticity – J-integral or CTOD (δ)

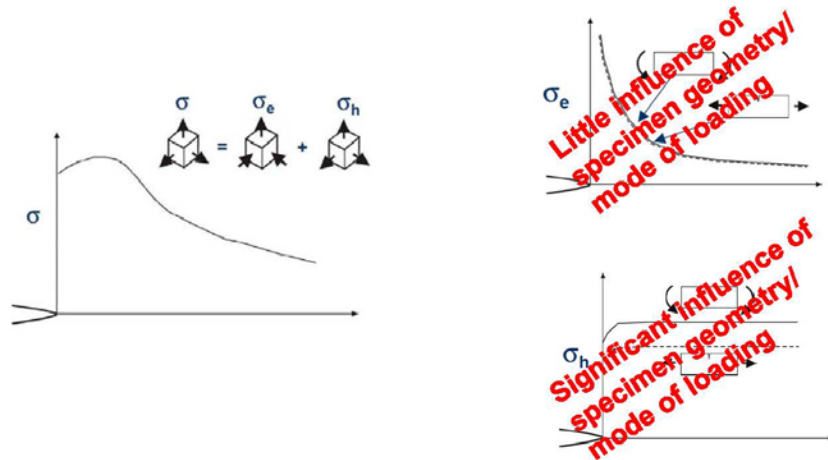


$$J = \int_{\Gamma} (w dy - T_i \frac{\partial u_i}{\partial x} ds)$$

$$J = m \sigma_y \delta$$

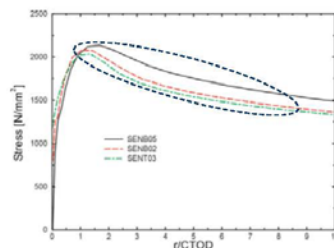
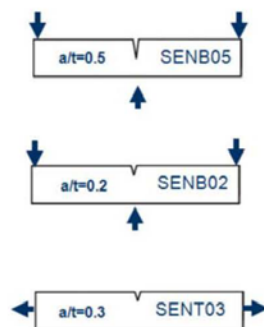


"... but there was more"

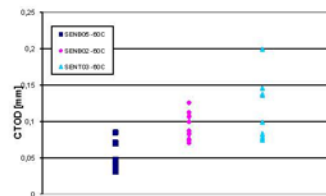


..and the so-called constraint effect was "born"

Example – effect of constraint on local crack-tip stress field/fracture toughness



Specimen geometry affects the local stress level in front of the crack, i.e. the constraint level...



..which in turns affects the fracture toughness

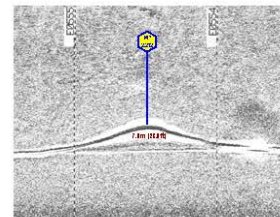
Fracture under large imposed deformations

Key points:

- Most fracture mechanics approaches developed for situations with macroscopic elastic behaviour
- Technological pull to allow for larger utilization of materials
- Need fracture assessment schemes that applies under large global deformations

Case:

- Fracture under large deformations in pipelines/strain-based design

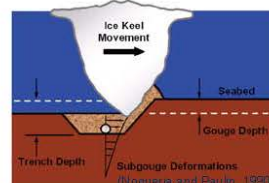


Large deformation scenarios for pipelines

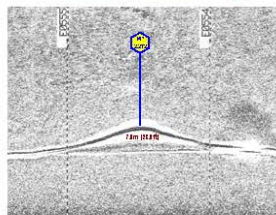
Pipeline installation



Ice loading



On-bottom snaking

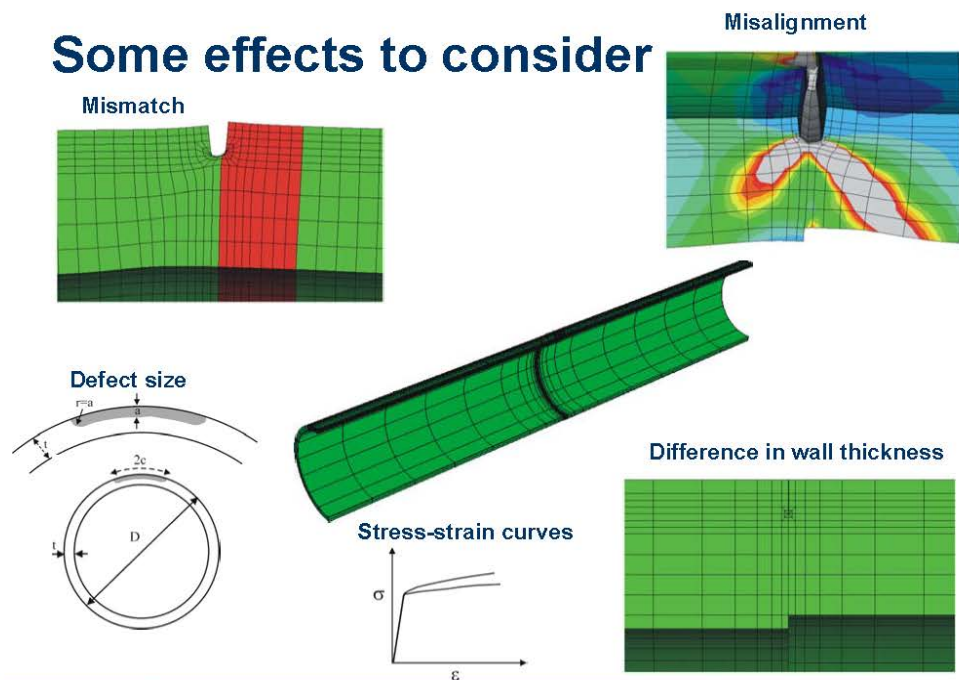


Earthquakes



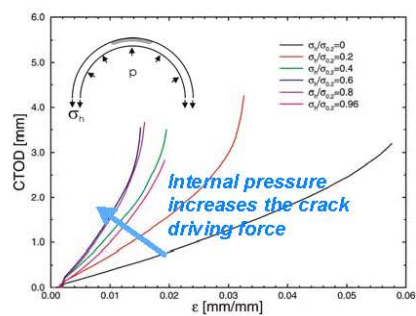
➔ Pipelines must in many cases be designed to withstand a given deformation or strain level – i.e. strain-based design principles should be used

Some effects to consider



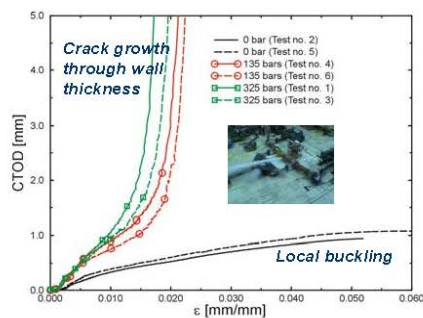
The effect of biaxial loading

Initial FE studies



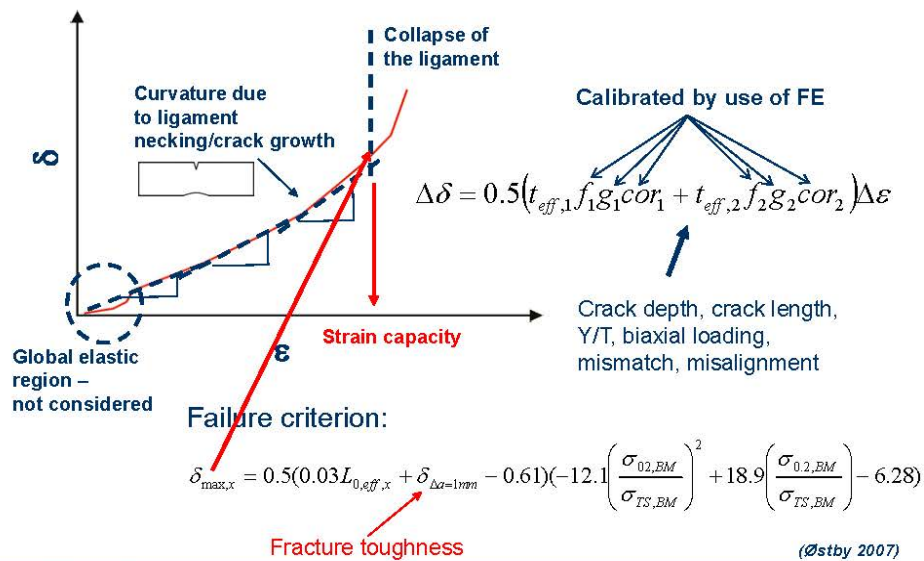
(Jayadevan et al. 2004, Østby et al. 2005)

Large-scale experimental validation



(Østby and Hellesvik 2007, 2008)

Simplified strain-based fracture assessment model



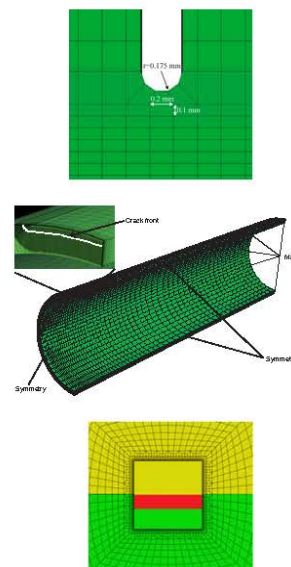
Numerical simulations

Key points:

- Analytical solutions often not accurate enough
- Numerical (FE) fracture mechanics simulations becoming more usual also in the industry
- Quicker implementation of new knowledge
- Coupling with more advanced material models and micromechanical-based fracture criteria becomes easier

Cases:

- Small and large-scale modelling of ductile fracture in pipelines
- The effect of local materials properties in ductile fracture
- Geometry and materials constraint effects in brittle fracture
- Including "microstructure"



The Gurson-Tvergaard-Needleman model and criterion for void coalescence

Yield function:

$$\phi(q, \bar{\sigma}, f, \sigma_m) = \frac{q^2}{\bar{\sigma}^2} + 2q_1 f \cosh\left(\frac{3q_2 \sigma_m}{2\bar{\sigma}}\right) - 1 - (q_1 f)^2 = 0$$

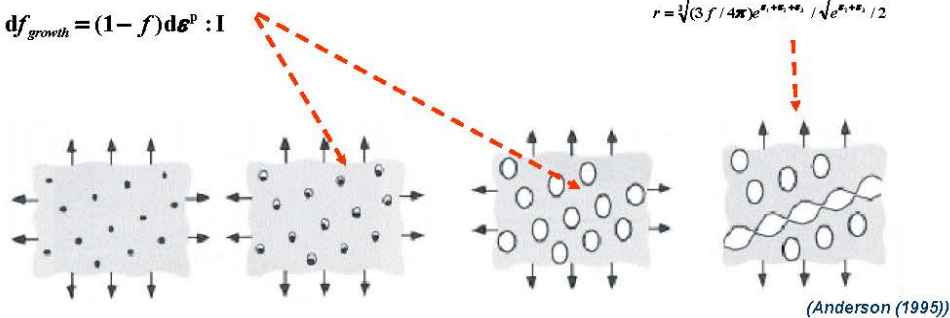
Void growth

$$df_{growth} = (1-f)d\epsilon^p : I$$

Thomason's limit load criterion

$$\frac{\sigma_1}{\bar{\sigma}} < \left(\alpha \left(\frac{1}{r} - 1 \right)^2 + \frac{\beta}{\sqrt{r}} \right) (1 - \pi r^2)$$

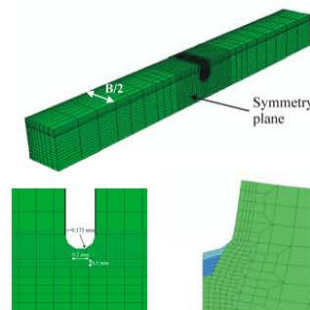
$$r = \sqrt[3]{(3f/4\pi)e^{q_1 + q_2 + q_3}} / \sqrt{e^{q_1 + q_2 + q_3} / 2}$$



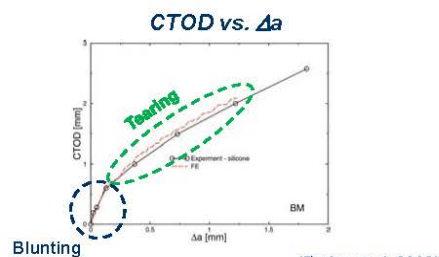
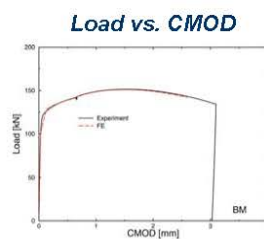
- An interesting approach for modelling of ductile crack growth

Crack growth modelling – SENT small-scale testing

Seamless X65 pipe



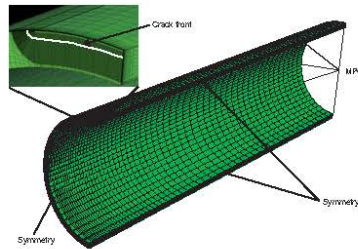
Comparisons between experiment and simulation



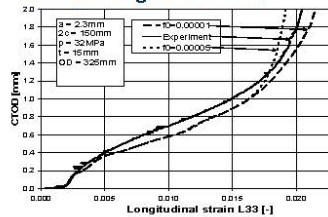
(Østby et al. 2008)

Crack growth modelling - Large-scale testing

325 bar internal pressure

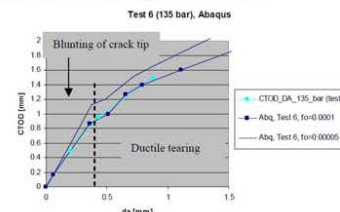


CTOD vs. global strain



(Sandvik et al. 2008)

Ductile tearing resistance



(Dybwad et al. 2009)



Materials and Chemistry

25

Invers modelling... to help understanding the influence of local features – Ex. HAZ X80 weld

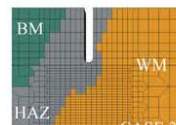
FE configuration

Comparison with experiment

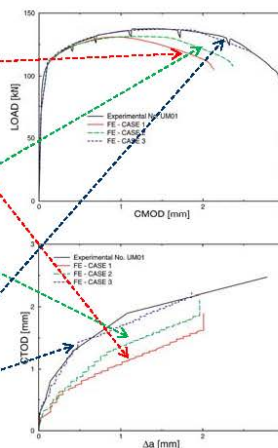
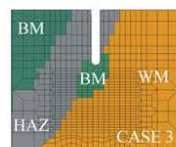
Defect at fusion line



Defect shifted somewhat into HAZ
-The effect of defect position



Defect shifted somewhat into HAZ with local increase in strength
-The effect of defect position
-The effect of crack-tip shielding



(Østby et al. 2009)



Materials and Chemistry

26

Micromechanical models for brittle fracture – The Weibull stress approach

Failure probability, P_f :

$$P_f = 1 - \exp\left(-\left(\frac{\sigma_w}{\sigma_u}\right)^m\right)$$

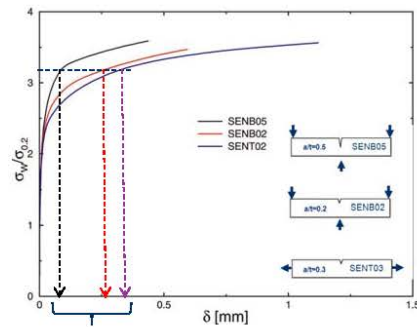
The Weibull stress:

$$\sigma_w = \sqrt[m]{\frac{1}{V_0} \int (\sigma_1)^m dV}$$

Scaling volume

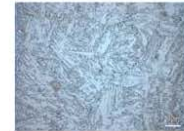
Principal stress

Toughness scaling principle

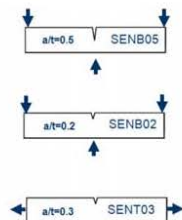


Equivalent CTOD values in different specimen geometries

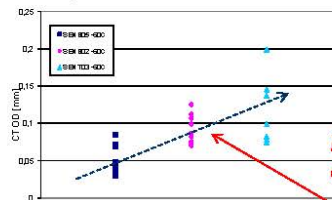
Constraint effect – Ex. HAZ microstructure



ICCGHAZ 420 Mpa steel

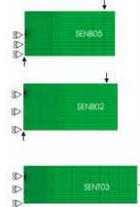


Experimental CTOD values

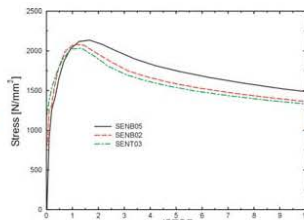


Description of constraint effect

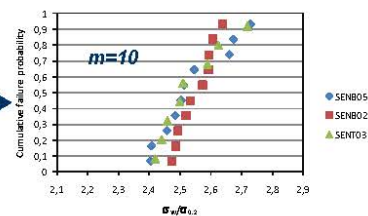
FE modeling



Local crack tip fields



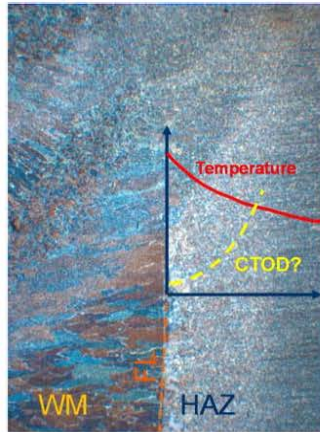
Calibration using Weibull stress



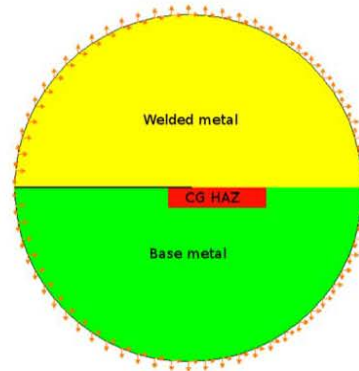
(Østby et al. 2011b)

FE modeling of inhomogeneous material systems - HAZ

Real HAZ

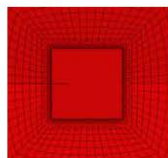


Idealized FE representation

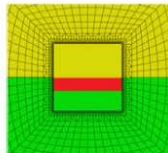


Transferability from weld thermal simulation to real HAZ toughness using the Weibull stress model

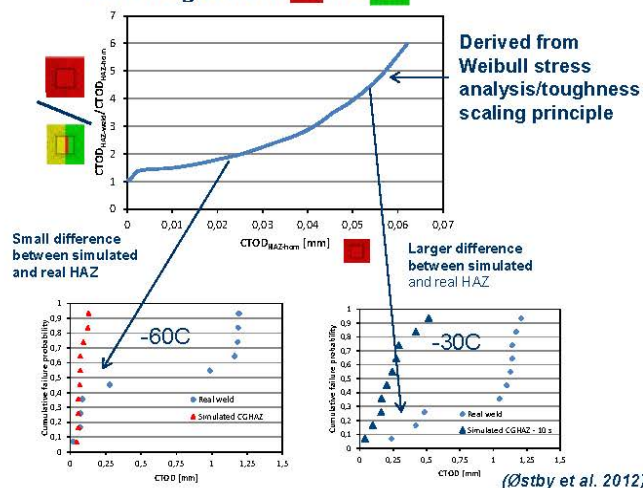
"Homogeneous" HAZ



"HAZ" in weld



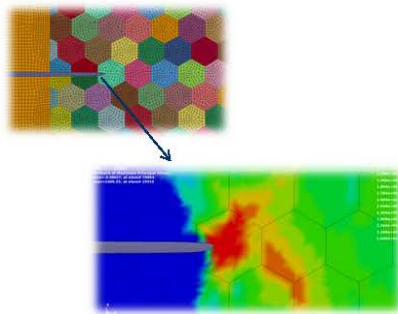
"How to get from  to 



(Østby et al. 2012)

Including "microstructure"...

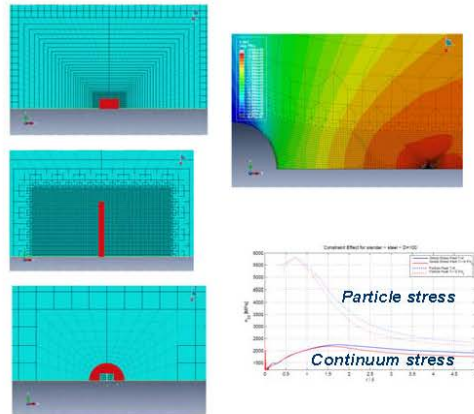
Grains



Crystal plasticity – accounting for grain orientation

(Kane et al. 2011)

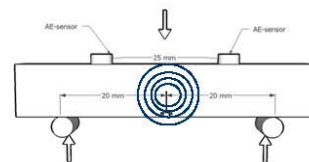
Particles/inclusions



Testing techniques

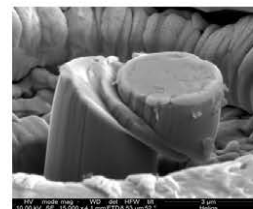
Key points:

- More knowledge about properties at lower levels ("Karakterisering på alle længdeskalaer")
- Helpful for improved understanding of fracture
- Modelling requires more input regarding material properties



Cases:

- Acoustic emission and local crack arrest
- FIB/Nano indentation
- FIB/TEM

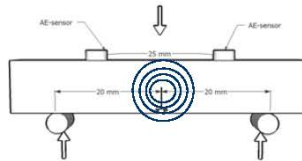
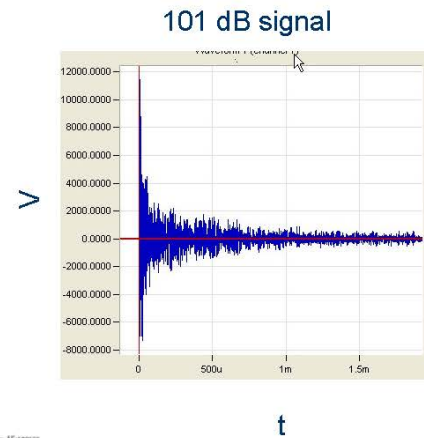


Interpretation of acoustic emission signals

AE signal:

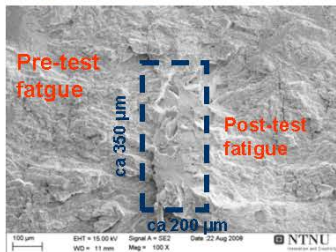
$$A = 20 \log \left(\frac{V}{V_{ref}} \right) - A_{pre_amp} \text{ [dB]}$$

- A – amplitude in dB
- V – voltage signal transducer
- V_{ref} – reference voltage (1 μ V)
- A_{pre_amp} – pre-amplification used (in this case -20dB)

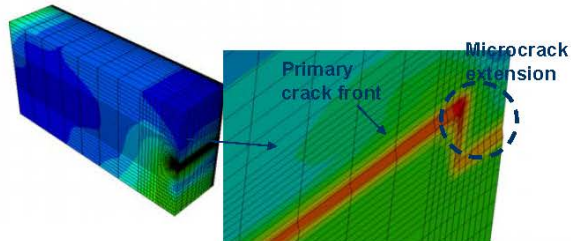


Correlation between AE signals and arrested microcracks

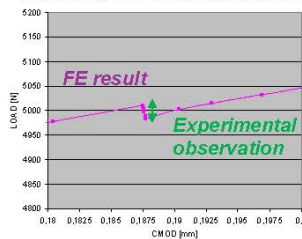
Experimentally observed microcrack



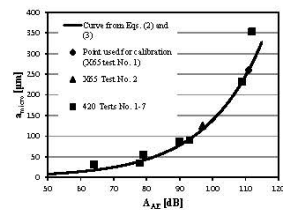
FE modelling of microcrack extension



Load drop due to introduction of microcrack



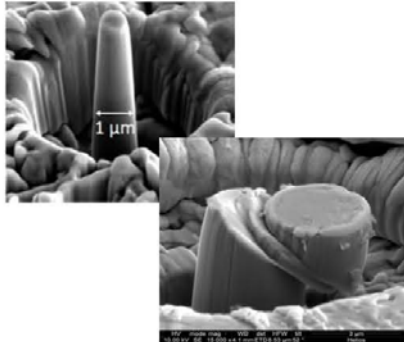
Assistance in validation of correlation between AE signal amplitude and microcrack size



(Østby et al. 2012)

FIB/nano indentation/TEM

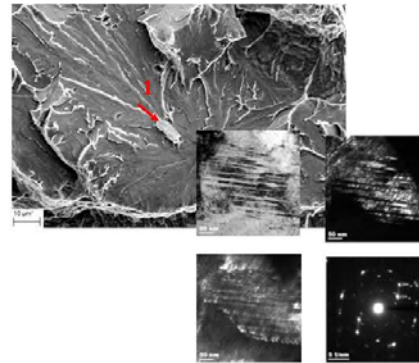
FIB/nanoindentation



Plastic properties at small-scales

(Haugen et al. 2012)

FIB/TEM



Investigation of nature of fracture initiating particles

(Mohseni et al. 2012)



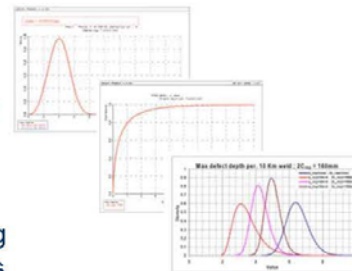
Materials and Chemistry

35

Probabilistic fracture mechanics

Key points:

- Natural scatter and variability in parameters entering the problem
- Deterministic analysis in some cases of limited value
- Uncertainty around accuracy of models
- Probabilistic approaches open for linking to given failure probabilities/safety levels



Case:

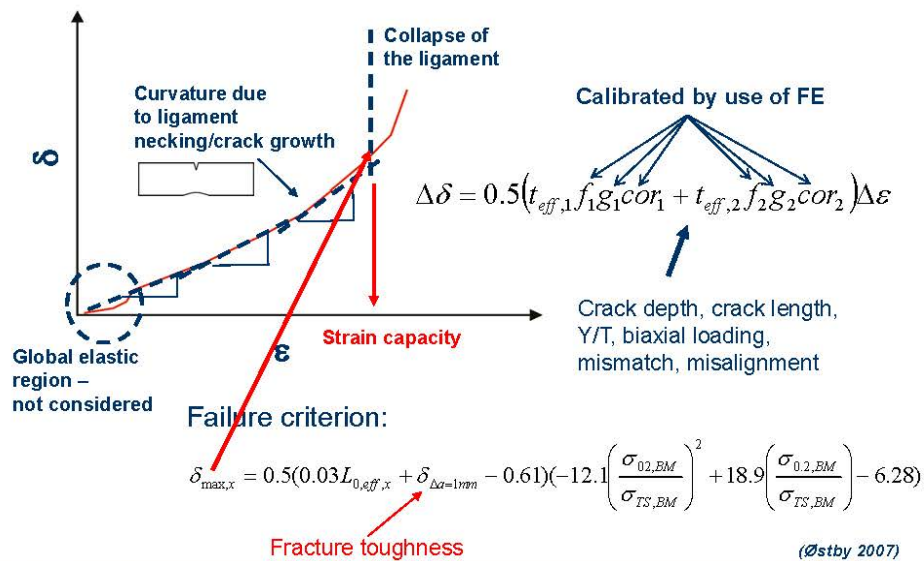
- Calibration of safety factors in fracture assessment of pipelines



Materials and Chemistry

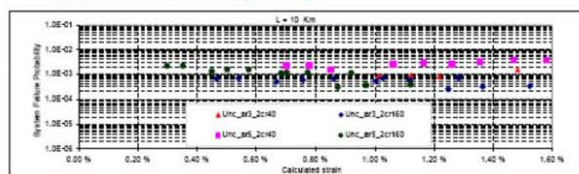
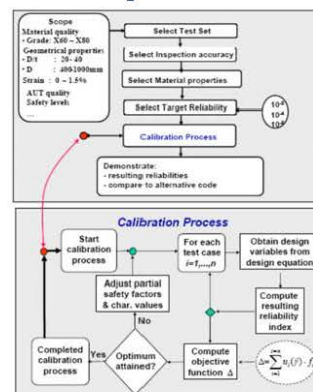
36

Simplified fracture assessment model



Calibration of partial safety factors

- Scatter in input parameters
- Model uncertainty
- Variability in applied strains (basis from Hotpipe project)
- Statistical distributions of defects (valuable input from Hydro)



(G. Sigurdsson, DNV)

Proposed design format

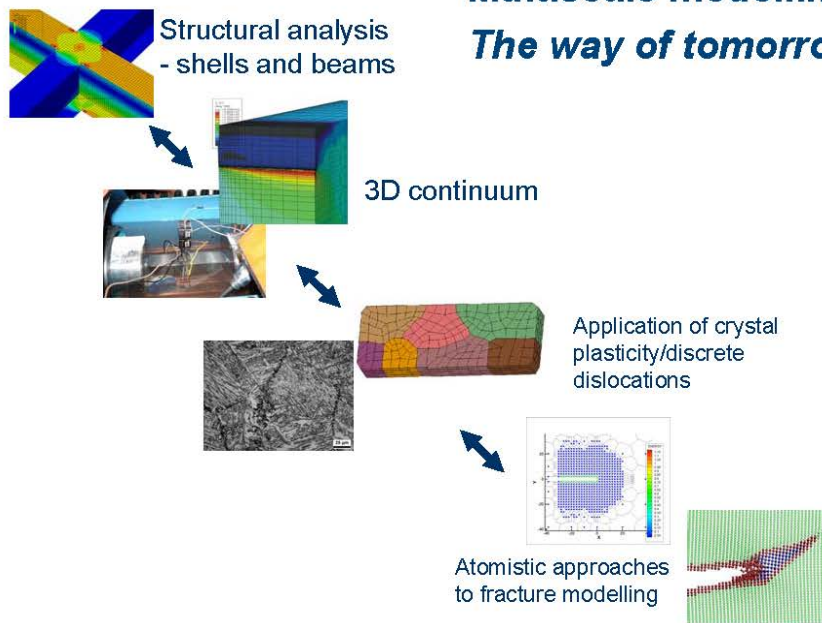
$$\varepsilon_{\max} \leq \min \left\{ \frac{\varepsilon_{\text{cap}}^c(t_c; \sigma_h; a_c \cdot \gamma_a; 2c_c; \alpha_c / \gamma_j; (a_{\text{rep}} \text{ or } Std(a_m)))}{\gamma_L} \right\}$$

- ε_{\max} – best estimate applied strain
- ε_{cap} – deformation capacity
(calculated based on simplified model)
- γ_L – safety factor applied strain
- γ_a – safety factor defect depth
- γ_j – safety factor fracture toughness

- Safety factors depend on the safety class
- Different safety factors for installation (system effect) and operation
- Safety factor for applied strain under operation depends upon "CoV" of best estimate

Tomorrow....?

Multiscale modelling – *The way of tomorrow?*



Wrap-up...

- Fracture mechanics has been developed into a useful tool:
 - Materials developments
 - Design/structural integrity assessments
- New issues are being introduced and new application areas emerge
- The use of numerical simulation tools is becoming increasingly more important
- Important future development trends:
 - Further development of link to materials science
 - Development of multiscale schemes
- **Vision...**
 - ***...predictions rather than calibration/"description"***

Acknowledgments

- The financial support from the Norwegian Research Council and the industry to the Fracture Control Offshore Pipelines and Arctic Materials projects is greatly acknowledged
- The contributions from colleagues at SINTEF, NTNU, and DNV is also highly acknowledged

Off-line testing af friktion og smøring i pladeformgivning

Niels Bay, DTU Mekanik

Off-line testning af friktion og smøring i pladeformgivning

Niels Bay, Ermanno Ceron

DTU-Mekanik

Projektpartnere:

Grundfos, SSAB, Outokumpu Stainless, Uddeholm

Dansk Metallurgisk Selskabs Vintermøde

Kolding

Januar 2013

1

Niels Bay, Ermanno Ceron – Off-line testning af friktion og smøring i pladeformgivning
Dansk Metallurgisk Selskabs Vintermøde, Kolding, Januar 2013

Indhold

- Introduktion
- Faldgruber ved off-line testning
- Off-line plade-tribo-testning
- Eksempel på analyse af konkret produktion
- Off-line test resultater
- Produktionstest resultater, sammenligning med off-line test
- Konklusion

2

E. Ceron, N. Bay

Niels Bay, Ermanno Ceron – Off-line testning af friktion og smøring i pladeformgivning
Dansk Metallurgisk Selskabs Vintermøde, Kolding, Januar 2013

Introduction

Legislation

Since 2000 legislation in Europe and Japan has been increasingly restrictive as regards industrial application of hazardous lubricants

2006-2007 EU introduced new legislations, REACH, aiming at high level of protection of human health and the environment from risk posed by chemicals.

REACH makes industry responsible for assessing and managing the risks and providing appropriate safety information to their users.

The new legislations have forced metal forming industry to look for new environmentally benign tribo-systems.

This causes however great challenges.

3 N. Bay

Niels Bay, Ermanno Ceron – Off-line testning af friktion og smøring i pladeformgivning
Dansk Metallurgisk Selskabs Vintermøde, Kolding, Januar 2013

Lubrication in tribologically difficult sheet metal forming

Tribologically difficult materials:

High strength steel, stainless steel, aluminium, titanium

Tribologically difficult processes:

Deep drawing with low radius of curvature

Ironing

Fine blanking

Chlorinated additives

Chloroparaffins suspected to have harmful effects on human health

- Risk of dioxin formation
- High recycle costs

4 N. Bay

Niels Bay, Ermanno Ceron – Off-line testning af friktion og smøring i pladeformgivning
Dansk Metallurgisk Selskabs Vintermøde, Kolding, Januar 2013

Tribological problems in sheet metal forming

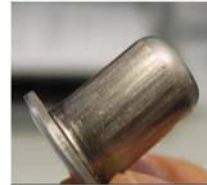
- High normal pressures
- Elevated tool/work piece interface temperatures

i.e. severe stressing of the lubricant with possible breakdown as a consequence.

Breakdown may cause:

- Local pick-up on tool surface
- Scoring of subsequently formed work piece surface

The sequence of events normally referred to as galling



5

N. Bay

Niels Bay, Ermanno Ceron – Off-line testning af friktion og smøring i pladeformgivning
Dansk Metallurgisk Selskabs Vintermøde, Kolding, Januar 2013

Challenges

- Introduction of new lubricants in manufacturing production is costly (production breaks, cleaning of tools)
- Industry is reluctant to carry out production tests due to bad experience (premature galling leading to unexpected production stops)
- Off-line testing of new tribo-systems
- It is vital to ensure testing conditions emulate production conditions
- Otherwise a tribo-system, which is approved in the simulative test, may turn out to be malfunctioning in the production tool, thus leading to the problems described above.

6

N. Bay

Niels Bay, Ermanno Ceron – Off-line testning af friktion og smøring i pladeformgivning
Dansk Metallurgisk Selskabs Vintermøde, Kolding, Januar 2013

Environmentally friendly sheet forming lubricants (except dry film)

Only a few lubricant manufacturers have focused on development of new, environmentally friendly lubricants

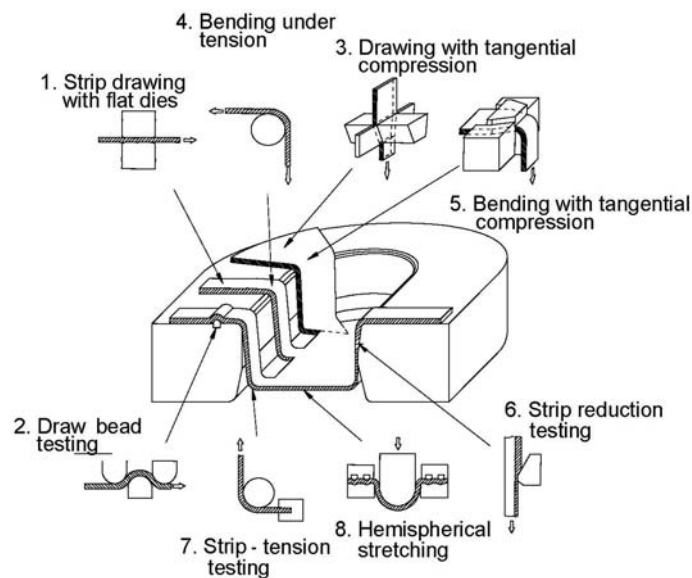
- **Masa Oil, Finland:** Biodegradable oils derived from tall oil extracted from fir tree. Fatty acid ester based.
- **Rhenus Lub, Germany:** Refined mineral oils with special additives of natural fatty components, synthetic esters, sulphur additives.
- **IRMCO Fluids, USA:** Oil free, low viscosity, water soluble lubricants made from vegetables and fruit.

7

E. Madsen, E. Ceron, N. Bay

Niels Bay, Ermanno Ceron – Off-line testning af friktion og smøring i pladeformgivning
Dansk Metallurgisk Selskabs Vintermøde, Kolding, Januar 2013

Simulative sheet tribo-tests



8

N. Bay, K. Krebs Nielsen

Niels Bay, Ermanno Ceron – Off-line testning af friktion og smøring i pladeformgivning
Dansk Metallurgisk Selskabs Vintermøde, Kolding, Januar 2013

Indhold

- Introduktion
- **Faldgruber ved off-line testning**
- Off-line plade-tribo-testning
- Eksempel på analyse af konkret produktion
- Off-line test resultater
- Produktionstest resultater, sammenligning med off-line test
- Konklusion

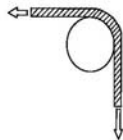
9

E. Ceron, N. Bay

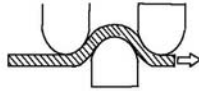
Niels Bay, Ermanno Ceron – Off-line testning af friktion og smøring i pladeformgivning
Dansk Metallurgisk Selskabs Vintermøde, Kolding, Januar 2013

Selected off-line tests Sheet forming tribology

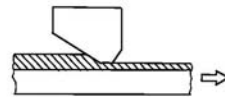
Bending-Under-Tension



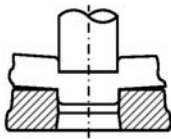
Draw Bead Test



Strip Reduction Test



PUnching Test



Test	Normal pressure	Surface expans.	Temp.	Tribological severity
BUT	low	0	low	low
DBT	medium	0	medium	medium
SRT	high	medium	high	high
PUT	medium-high	infinite	very high	very high

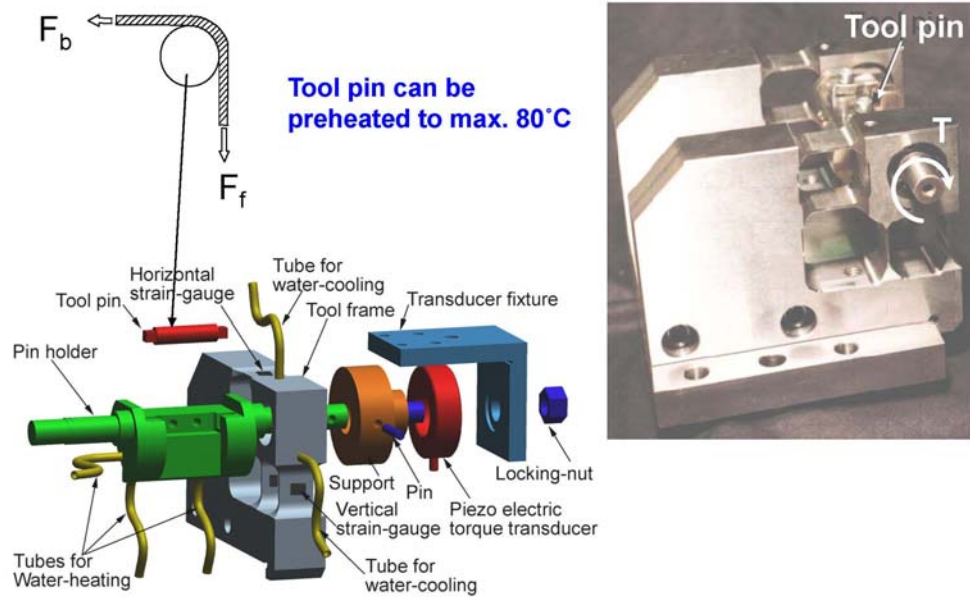
10

N. Bay

Niels Bay, Ermanno Ceron – Off-line testning af friktion og smøring i pladeformgivning
Dansk Metallurgisk Selskabs Vintermøde, Kolding, Januar 2013

Bending under tension - BUT

11

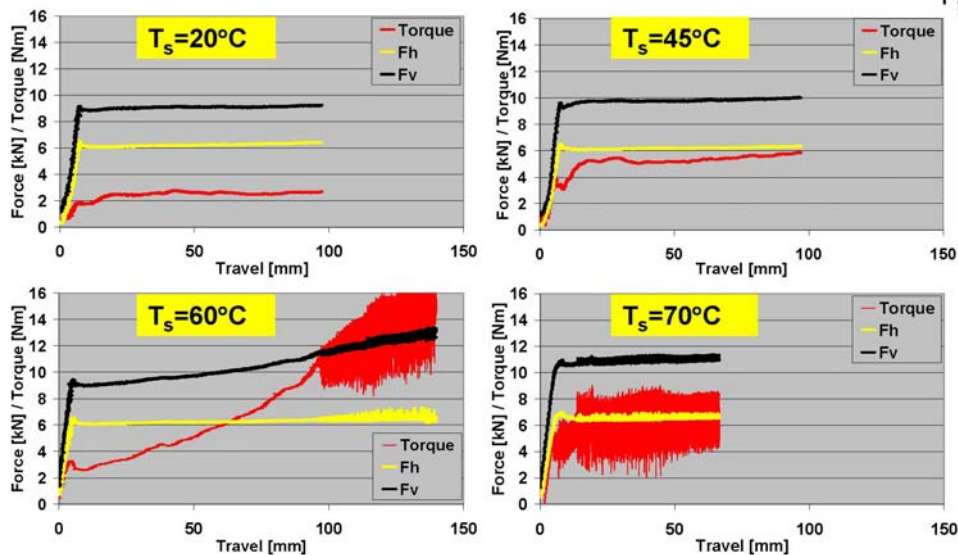
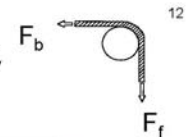


D.D. Olsson, K. Chodnikiewicz,
J.L. Andreasen, N. Bay

Niels Bay, Ermanno Ceron – Off-line testning af friktion og smøring i pladeformgivning
Dansk Metallurgisk Selskabs Vintermøde, Kolding, Januar 2013

Bending Under Tension - BUT

Stainless steel Wn.1.4401, Plain mineral oil without additives,
 $v=80\text{mm/s}$



J.L. Andreasen, D.D. Olsson, K.
Chodnikiewicz, N. Bay

Niels Bay, Ermanno Ceron – Off-line testning af friktion og smøring i pladeformgivning
Dansk Metallurgisk Selskabs Vintermøde, Kolding, Januar 2013

Faldgruber ved off-line testning -1

- For lav værktøjstemperatur
- For lav emnetemperatur (flertrinsoperationer)
- Ændrede procesparametre
 - Normaltryk
 - Glidelængde
 - Glidehastighed
 - Overfladeekspansion
 - Tid mellem tests
 - Kontakt/ikke kontakt mellem slag
- Ændrede smørebetingelser
 - Påføringsteknik
 - Emne- og værktøjsgeometri
- For få gentagelser

13

E. Ceron, N. Bay

Niels Bay, Ermanno Ceron – Off-line testning af friktion og smøring i pladeformgivning
Dansk Metallurgisk Selskabs Vintermøde, Kolding, Januar 2013

Faldgruber ved off-line testning - 2

- Ændrede egenskaber af emnemateriale
 - Flertrins operationer, f.eks. dybtrækning + krængetrækning/re-trækning
 - Dybtrækning + strækningsreduktion
- Ændret overfladetopografi
 - Emne (f.eks. ved flertrinsoperationer)
 - Værktøj (retning af hypper ved drejning, slibning, polering)

Production tool



Simulative tool (BUT)



14

E. Ceron, N. Bay

Niels Bay, Ermanno Ceron – Off-line testning af friktion og smøring i pladeformgivning
Dansk Metallurgisk Selskabs Vintermøde, Kolding, Januar 2013

Indhold

- Introduktion
- Faldgruber ved off-line testning
- **Off-line plade-tribo-testning**
- Eksempel på analyse af konkret produktion
- Off-line test resultater
- Produktionstest resultater, sammenligning med off-line test
- Konklusion

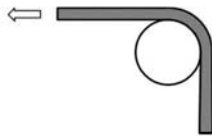
15

E. Ceron, N. Bay

Niels Bay, Ermanno Ceron – Off-line testning af friktion og smøring i pladeformgivning
Dansk Metallurgisk Selskabs Vintermøde, Kolding, Januar 2013

New, universal sheet tribotester

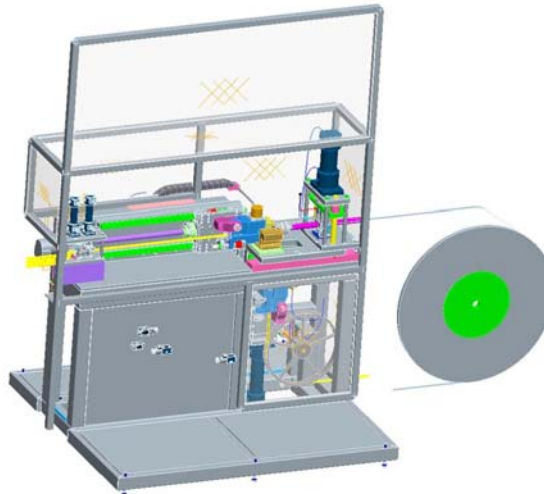
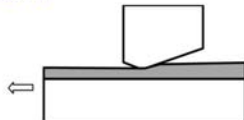
BUT



DBT



SRT



16

E. Ceron, N. Paldan,
J. Gregersen, N. Bay

Niels Bay, Ermanno Ceron – Off-line testning af friktion og smøring i pladeformgivning
Dansk Metallurgisk Selskabs Vintermøde, Kolding, Januar 2013

Universal sheet tribo-tester

- Automatic PLC controlled running of repeated tests
- Material feed from coil of more than 1000m
- Adjustable sliding lengths, speed, cycle time and total number of strokes
- Ensuring appropriate emulation of production conditions with heating and cooling cycle
- Easy programming by Labview


BUT_test_running_detail.avi

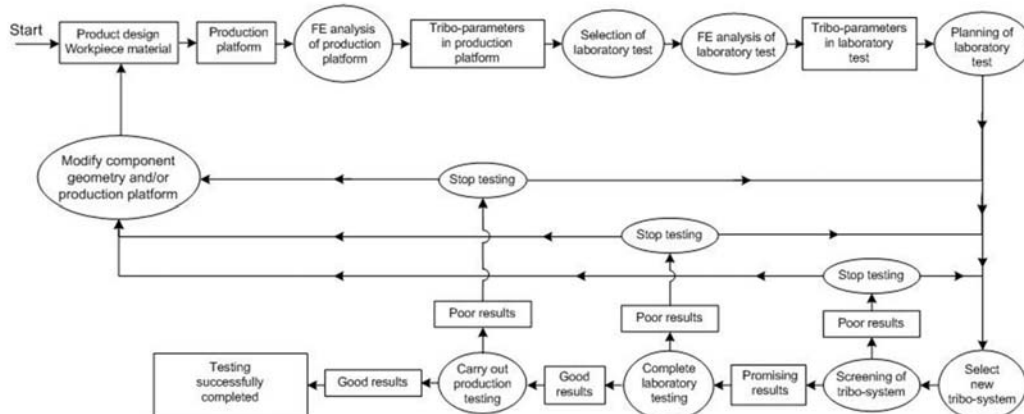

BUT_test_running.avi



E. Ceron, N. Paldan,
J. Gregersen, N. Bay

17

Methodology for predicting lubrication performance in production



E. Ceron, N. Bay

Niels Bay, Ermanno Ceron – Off-line testning af friktion og smøring i pladeformgivning
Dansk Metallurgisk Selskabs Vintermøde, Kolding, Januar 2013

18

Indhold

- Introduktion
- Faldgruber ved off-line testning
- Off-line plade-tribo-tester
- **Eksempel på analyse af konkret produktion**
- Off-line test resultater
- Produktionstest resultater, sammenligning med off-line test
- Konklusion

19

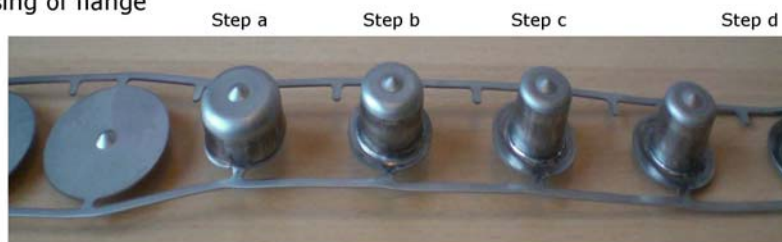
E. Ceron, N. Bay

Niels Bay, Ermanno Ceron – Off-line testning af friktion og smøring i pladeformgivning
Dansk Metallurgisk Selskabs Vintermøde, Kolding, Januar 2013

Production test example

Deep drawing in progressive tool - Grundfos

- Deep drawing
- 1st redrawing
- 2nd redrawing **Tribologically the most severe operation**
- Sharp pressing of flange



Workpiece material: EN 1.4301

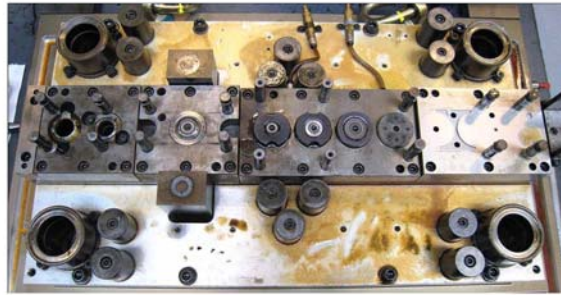
Production rate: 40 spm

Step c

E. Ceron, E. Madsen, N. Bay

Niels Bay, Ermanno Ceron – Off-line testning af friktion og smøring i pladeformgivning
Dansk Metallurgisk Selskabs Vintermøde, Kolding, Januar 2013

Deep drawing in progressive tool Grundfos

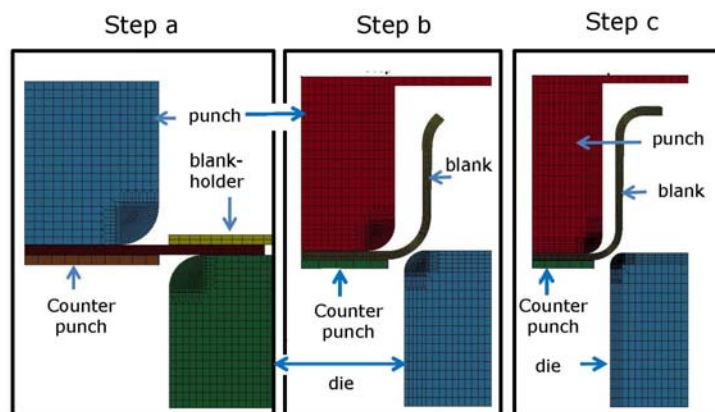


E. Ceron, E. Madsen, N. Bay

Ermanno Ceron – Off-line testning af friktion og smøring i pladeformgivning
Dansk Metallurgisk Selskabs Vintermøde, Kolding, Januar 2013

Simulation of deep drawing and 2 redrawings

- LS-DYNA 2D implicit model
- The blank is transferred from one process to the following updating flow stress and equivalent strain

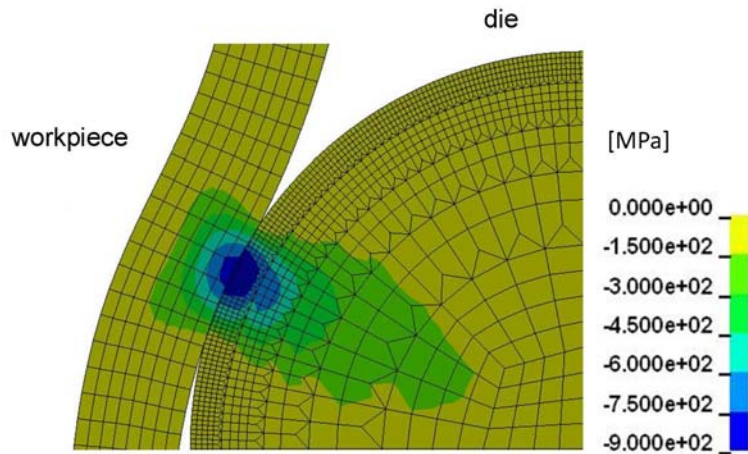


E. Ceron, N. Bay

Niels Bay, Ermanno Ceron – Off-line testning af friktion og smøring i pladeformgivning
Dansk Metallurgisk Selskabs Vintermøde, Kolding, Januar 2013

Distribution of radial stress in step c

Maximum contact pressure $p_{\max} = 900 \text{ MPa}$



23

E. Ceron, N. Bay

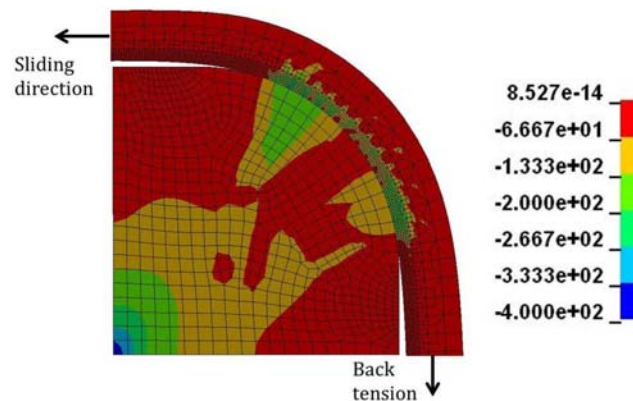
Niels Bay, Ermanno Ceron – Off-line testning af friktion og smøring i pladeformgivning
Dansk Metallurgisk Selskabs Vintermøde, Kolding, Januar 2013

Simulation of BUT test

Round pin with radius $R = 3,5$

Maximum contact pressure 360 Mpa
with maximum back tension 300 MPa

(i.e. only 40% of maximum pressure in production tool)



24

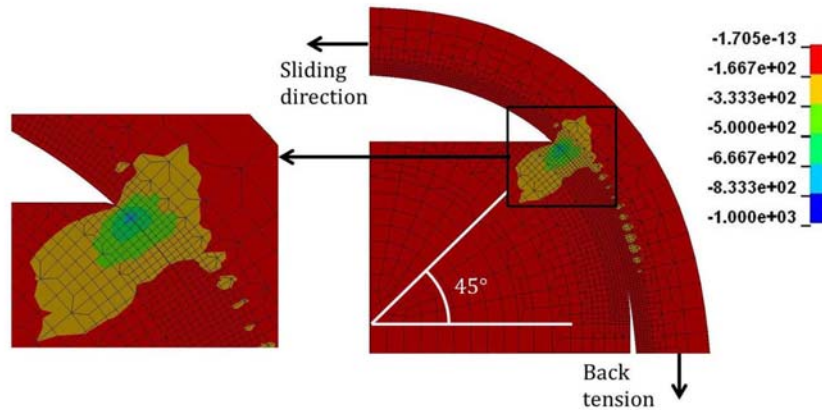
E. Ceron, N. Bay

Niels Bay, Ermanno Ceron – Off-line testning af friktion og smøring i pladeformgivning
Dansk Metallurgisk Selskabs Vintermøde, Kolding, Januar 2013

Distribution of radial stresses in BUT test

By modifying the BUT test tool to a 45° contact instead, sufficient contact pressure can be reached

Maximum contact pressure $p_{\max} = 1000 \text{ MPa}$ with back tension 300 MPa

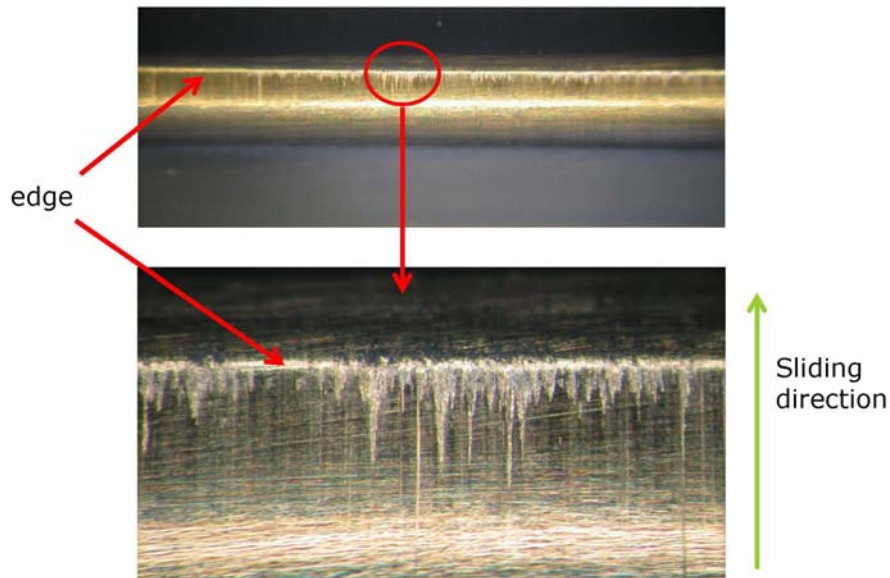


25

E. Ceron, N. Bay

Niels Bay, Ermanno Ceron – Off-line testning af friktion og smøring i pladeformgivning
Dansk Metallurgisk Selskabs Vintermøde, Kolding, Januar 2013

Lubricant film breakdown in BUT test Severe pick and galling



26

E. Ceron, N. Bay

Niels Bay, Ermanno Ceron – Off-line testning af friktion og smøring i pladeformgivning
Dansk Metallurgisk Selskabs Vintermøde, Kolding, Januar 2013

Tribo-systems investigated

Tribo-system	Workpiece material	Tool material	Lubricant
1	EN 1.4301	Vancron 40	rhenus SU 166 A
2	DP 800	Vancron 40	ANTICORIT PLS 100T
3	EN 1.4162 LDX 2101®	Vancron 40	rhenus SU 166 A

rhenus SU 166 A: mineral oil with EP additives, 160 mm²/s at 40°C

ANTICORIT PLKS 100T: mineral oil, 100 mm²/s at 40°C

27

E. Ceron, N. Bay

Niels Bay, Ermanno Ceron – Off-line testning af friktion og smøring i pladeformgivning
Dansk Metallurgisk Selskabs Vintermøde, Kolding, Januar 2013

Indhold

- Introduktion
- Faldgruber ved off-line testning
- Off-line plade-tribo-tester
- Eksempel på analyse af konkret produktion
- **Off-line test resultater**
- Produktionstest resultater, sammenligning med off-line test
- Konklusion

28

E. Ceron, N. Bay

Niels Bay, Ermanno Ceron – Off-line testning af friktion og smøring i pladeformgivning
Dansk Metallurgisk Selskabs Vintermøde, Kolding, Januar 2013

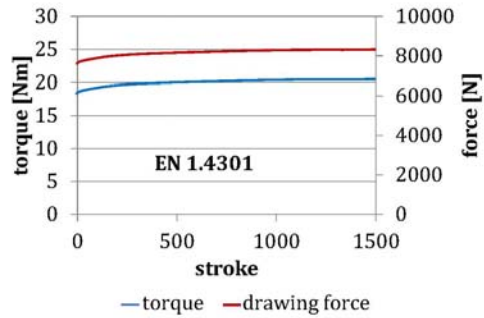
BUT test

Tribo-system 1:

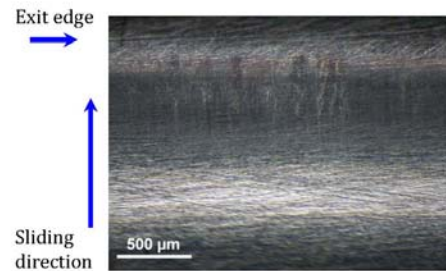
Material: EN 1.4301

Lubricant: rehenus SU 166 A

Test rate: 40 and 95 spm



Tool after 1500 tests



29

E. Ceron, N. Bay

Niels Bay, Ermanno Ceron – Off-line testning af friktion og smøring i pladeformgivning
Dansk Metallurgisk Selskabs Vintermøde, Kolding, Januar 2013

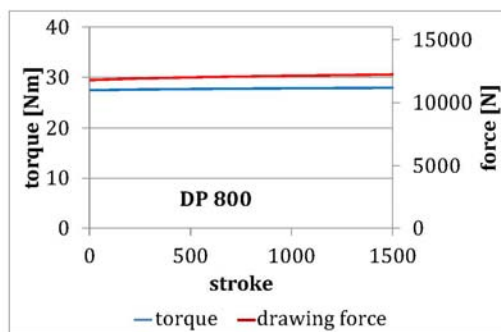
BUT test

Tribo-system 2:

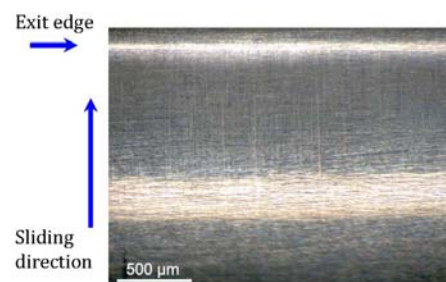
Material: DP 800

Lubricant: ANTICORIT PLS 100T

Test rate: 40 and 95 spm



Tool after 1500 tests



30

E. Ceron, N. Bay

Niels Bay, Ermanno Ceron – Off-line testning af friktion og smøring i pladeformgivning
Dansk Metallurgisk Selskabs Vintermøde, Kolding, Januar 2013

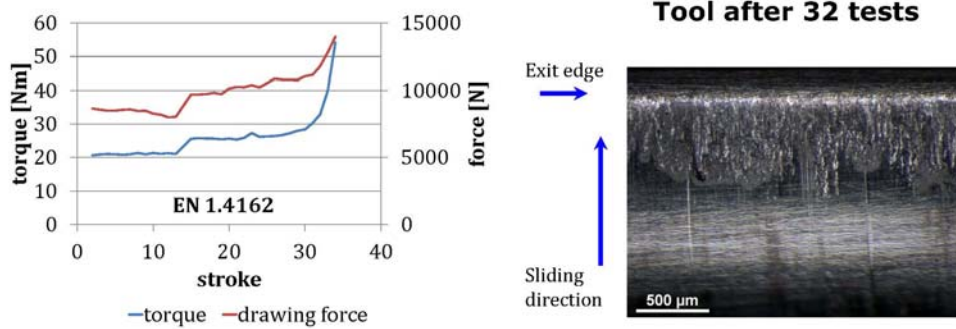
BUT test

Tribo-system 3

Material: EN 1.4162, LDX 2101®

Lubricant: rehus SU 166 A

Test rate: 40 spm



31

E. Ceron, N. Bay

Niels Bay, Ermanno Ceron – Off-line testning af friktion og smøring i pladeformgivning
Dansk Metallurgisk Selskabs Vintermøde, Kolding, Januar 2013

Indhold

- Introduktion
- Faldgruber ved off-line testning
- Off-line plade-tribo-tester
- Eksempel på analyse af konkret produktion
- Off-line test resultater
- **Produktionstest resultater, sammenligning med off-line test**
- Konklusion

32

E. Ceron, N. Bay

Niels Bay, Ermanno Ceron – Off-line testning af friktion og smøring i pladeformgivning
Dansk Metallurgisk Selskabs Vintermøde, Kolding, Januar 2013

Production tests

Tribo-system 1

Cup No. 1500



Tribo-system 2

Cup No. 1500



Tribo-system 3

Cup No. 40



Tribo system 1 and 2: no galling even at 95 spm

Tribo system 3: heavy galling after drawing 10 cups

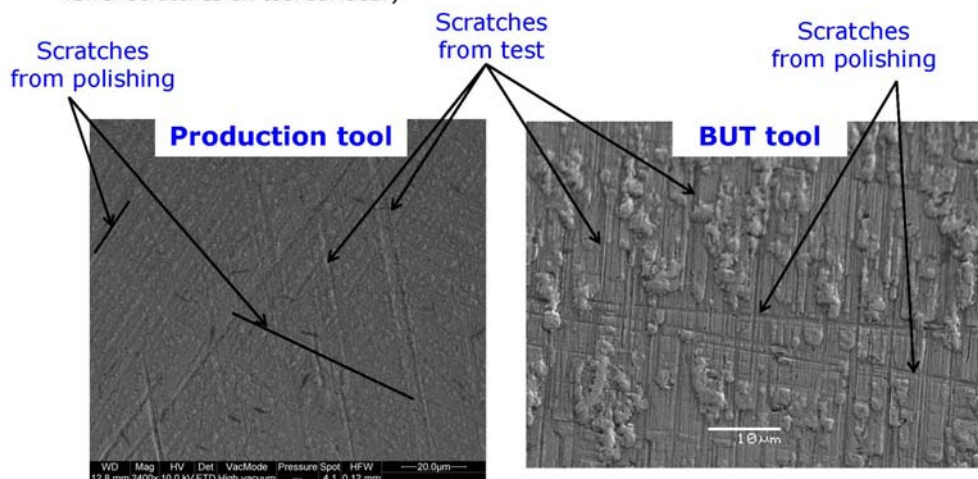
33

E. Ceron, N. Bay

Niels Bay, Ermanno Ceron – Off-line testning af friktion og smøring i pladeformgivning
Dansk Metallurgisk Selskabs Vintermøde, Kolding, Januar 2013

SEM pictures of tools - EN 1.4301

- Few scratches on the surface
- Slight amount of pick up can be seen like on BUT tool
- (part in EL RØR has less chromium oxide due to previous redrawing, may cause fewer scratches on tool surface?)

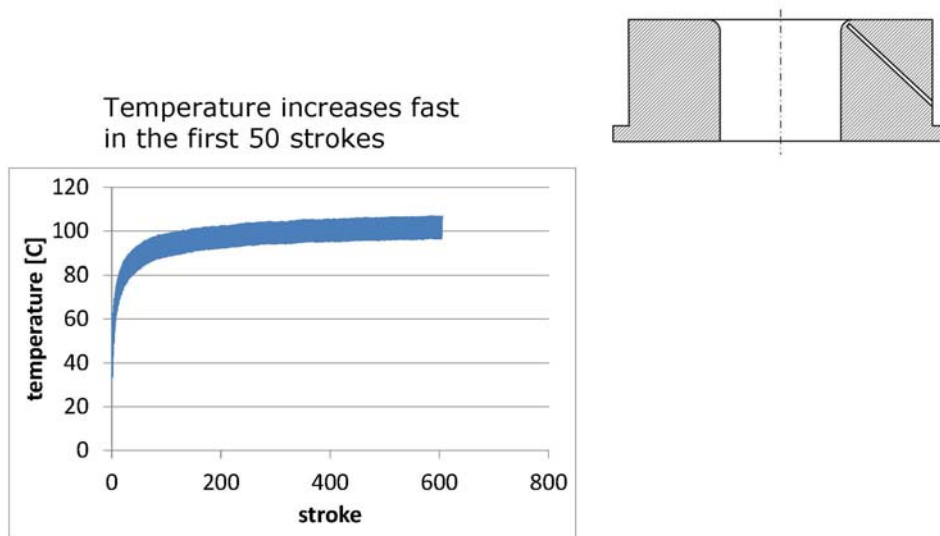


34

E. Ceron, N. Bay

Niels Bay, Ermanno Ceron – Off-line testning af friktion og smøring i pladeformgivning
Dansk Metallurgisk Selskabs Vintermøde, Kolding, Januar 2013

Tool temperature development – EN 1.4301



35

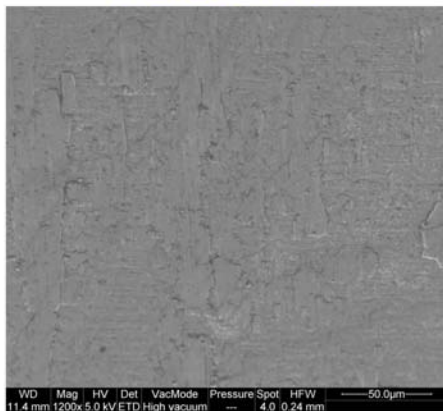
E. Ceron, N. Bay

Niels Bay, Ermanno Ceron – Off-line testning af friktion og smøring i pladeformgivning
Dansk Metallurgisk Selskabs Vintermøde, Kolding, Januar 2013

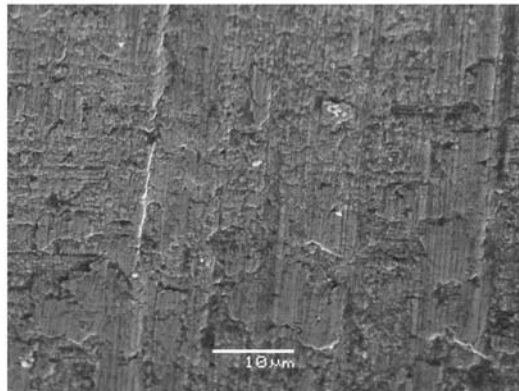
SEM pictures of tools – DP 800

- SEM picture of the tool surface
- Similar micro pick-up in production tool as in the BUT tool

Production tool



BUT tool



36

E. Ceron, N. Bay

Niels Bay, Ermanno Ceron – Off-line testning af friktion og smøring i pladeformgivning
Dansk Metallurgisk Selskabs Vintermøde, Kolding, Januar 2013

Production tool 2 – LDX 2101

- Parts are not acceptable. Severe galling along rolling direction
- Pick-up occurs already in operation 2.



37

E. Ceron, N. Bay

Niels Bay, Ermanno Ceron – Off-line testning af friktion og smøring i pladeformgivning
Dansk Metallurgisk Selskabs Vintermøde, Kolding, Januar 2013

Production tool 3 – LDX 2101

- Pick-up occurs also in operation 3



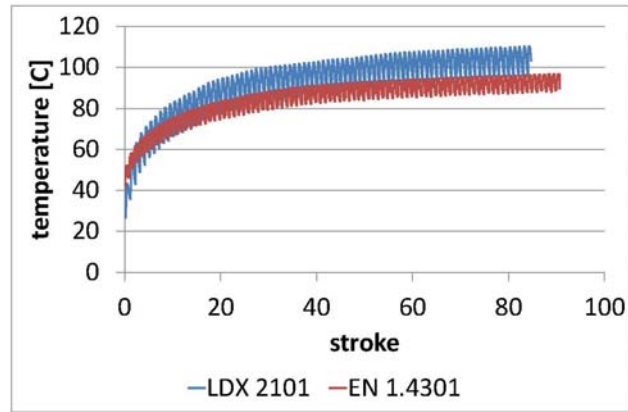
38

E. Ceron, N. Bay

Niels Bay, Ermanno Ceron – Off-line testning af friktion og smøring i pladeformgivning
Dansk Metallurgisk Selskabs Vintermøde, Kolding, Januar 2013

Tool temperature development

Comparison between LDX and EN 1.4301

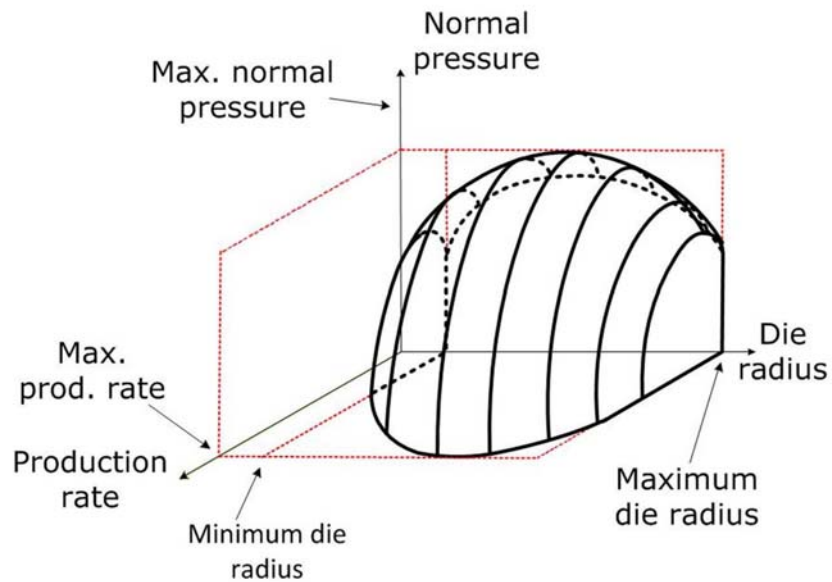


39

E. Ceron, N. Bay

Niels Bay, Ermanno Ceron – Off-line testning af friktion og smøring i pladeformgivning
Dansk Metallurgisk Selskabs Vintermøde, Kolding, Januar 2013

Evaluation of a tribo-system for deep drawing production



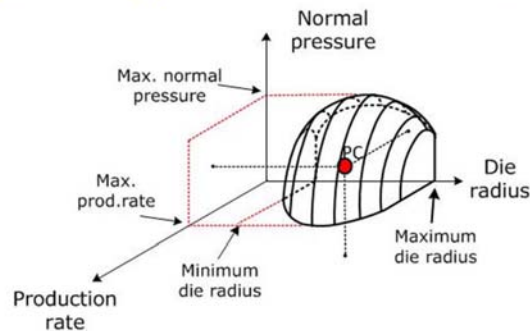
40

E. Ceron, N. Bay

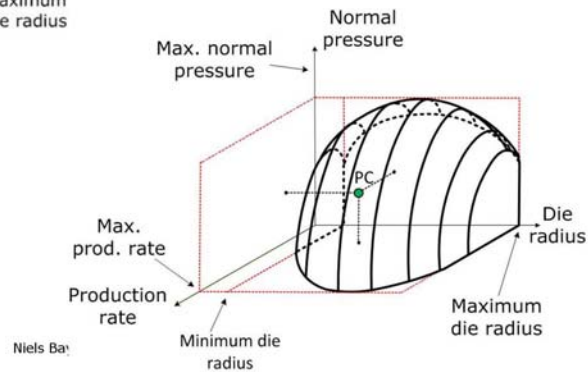
Niels Bay, Ermanno Ceron – Off-line testning af friktion og smøring i pladeformgivning
Dansk Metallurgisk Selskabs Vintermøde, Kolding, Januar 2013

Evaluation of a tribo-system for deep drawing production

Poor tribo-system production point above threshold surface



Promising tribo-system Production point below threshold surface



E. Ceron, N. Bay

41

Conclusion – differences between production and laboratory

	Production	Laboratory
Work hardening	High (max strain = 2)	Low (max strain = 0,2)
Surface topography	Completely different from original	Original
Normal pressure	≈1000 MPa	≈1000 MPa but smaller contact area
Initial specimen temperature	≈110C	25C
Temperature developed in the specimen	≈200C	≈90-100C
Temperature developed in the tool	≈110C (EN1.4301)	≈45C (EN1.4301)
Sliding speed	100-150mm/s	50mm/s
Thermal exchange	No workpiece/tool contact during idle time	workpiece/tool contact during idle time

E. Ceron, N. Bay

42

Niels Bay, Ermanno Ceron – Off-line testning af friktion og smøring i pladeformgivning
Dansk Metallurgisk Selskabs Vintermøde, Kolding, Januar 2013

Indhold

- Introduktion
- Faldgruber ved off-line testning
- Off-line plade-tribo-tester
- Eksempel på analyse af konkret produktion
- Off-line test resultater
- Produktionstest resultater, sammenligning med off-line test
- **Konklusion**

43

E. Ceron, N. Bay

Niels Bay, Ermanno Ceron – Off-line testning af friktion og smøring i pladeformgivning
Dansk Metallurgisk Selskabs Vintermøde, Kolding, Januar 2013

Konklusion

Metodik til forudsigelse af smøremiddel performance i produktion

- Numerisk modellering af produktionsbetingelser
- Valg af simulativ test
- Numerisk modellering af simulativ test
- Off-line testning
- Produktions testning

Miljøvenlige alternativer til kloreret paraffinolie

- rhenus SU 166 A

44

E. Ceron, N. Bay

Niels Bay, Ermanno Ceron – Off-line testning af friktion og smøring i pladeformgivning
Dansk Metallurgisk Selskabs Vintermøde, Kolding, Januar 2013

END

Industriens udnyttelse af de store internationale røntgen neutronfaciliteter

Henning Friis Poulsen, DTU Fysik

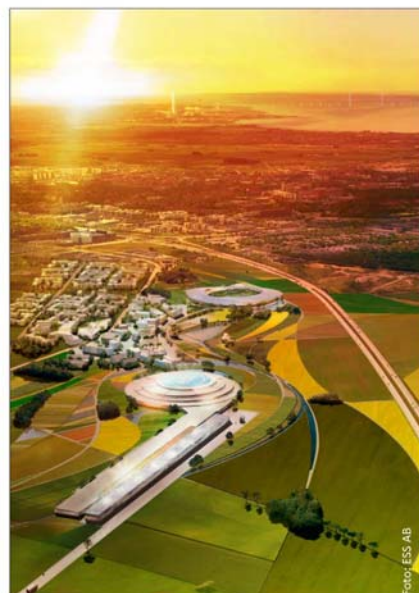
Industriens udnyttelse af de store internationale Røntgen og neutron faciliteter

Hening Friis Poulsen, DTU Fysik
hfpo@fysik.dtu.dk

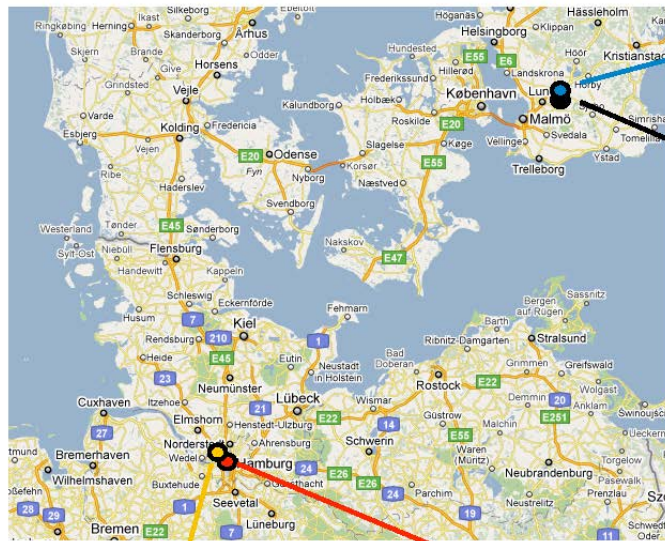


ESS & MAX-IV

- ESS og MAX IV i Lund
 - ESS (2019), verdens bedste neutronkilde, finansieret af 17 europæiske lande (ca. 1,5 mia. euro)
 - MAX IV (2015), synkrotron, svensk finansieret (500 mio. euro)
- Det danske bidrag
 - ESS: 1.4 Mia kroner + 12.5% drift
 - Data Management Center i Kbh (62 ansatte)
 - MAX-IV: Dansk beamlinie (74 Mkr) ?
- Science parks omkring Lund og Københavnsområdet



Verdens største mikroskop



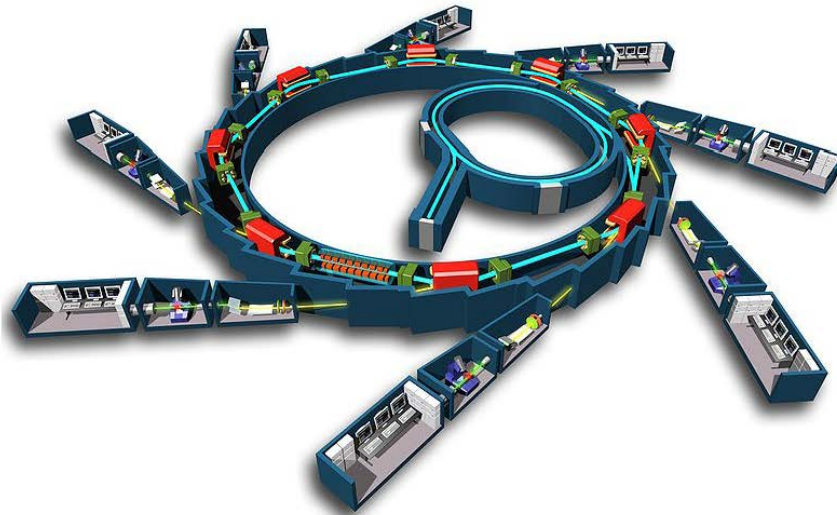
ESS, 2019
Neutroner
Dk medvært: 1.4 Gkr

Max-IV 2016
Medium energi Røntgen
Dk beamlinie: 74 Mkr ?

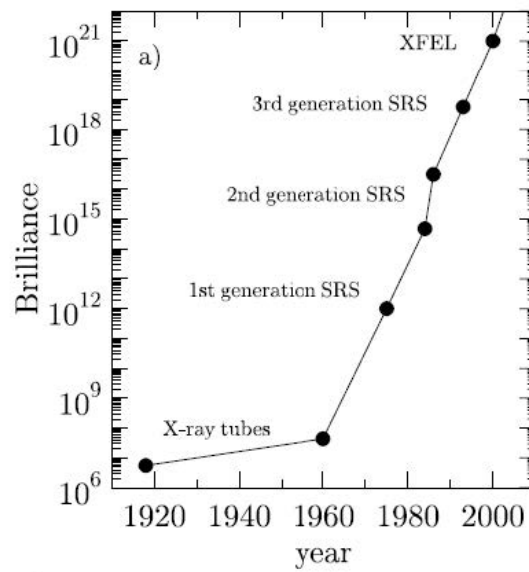
E-XFEL, 2016
Kohærent Røntgen
DK medlemskab: 11 Mkr/år

PETRA-III, 2011
Høj energi Røntgen
Dk bruger

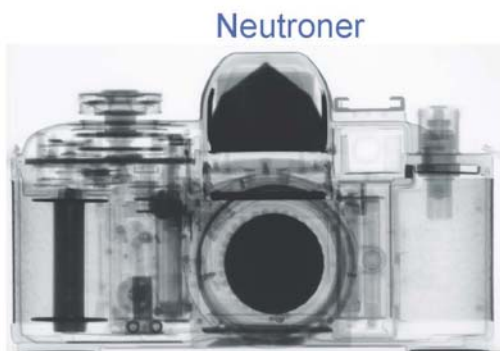
Hvad er en synkrotron?



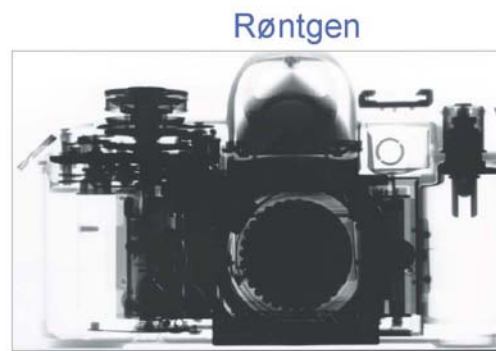
Hvorfor bruge en synkrotron?



Forskel i tværsnit



Ser: H, C, O,



Ser: høje Z-numre

Virksomheder som brugere af store faciliteter

Udfordringer:

- Manglende kendskab og ekspertise
- Ventetid og usikkerhed omkring måletid
- "Data analysen koster en halv PhD"

Haldor Topsøe, Astra Zeneca, Novo Nordisk, Carlsberg .. er stærkt involveret

Mulige danske løsninger:

- Strategiske partnerskaber
- Portaler/science hubs

Individuelle løsninger:

- Opsøg akademiske partnere
- Ansæt erhvervs-PhD studerende
- Science Link

SCIENCE LINK

Part-financed by the European Union (European Regional Development Fund)



SCIENCE LINK opens up research facilities for commercial R&D purposes

Partners:

MAX-lab, Lund
Desy, Hamburg
HZG & HZB, Berlin

DTU is Danish representative

Offers:

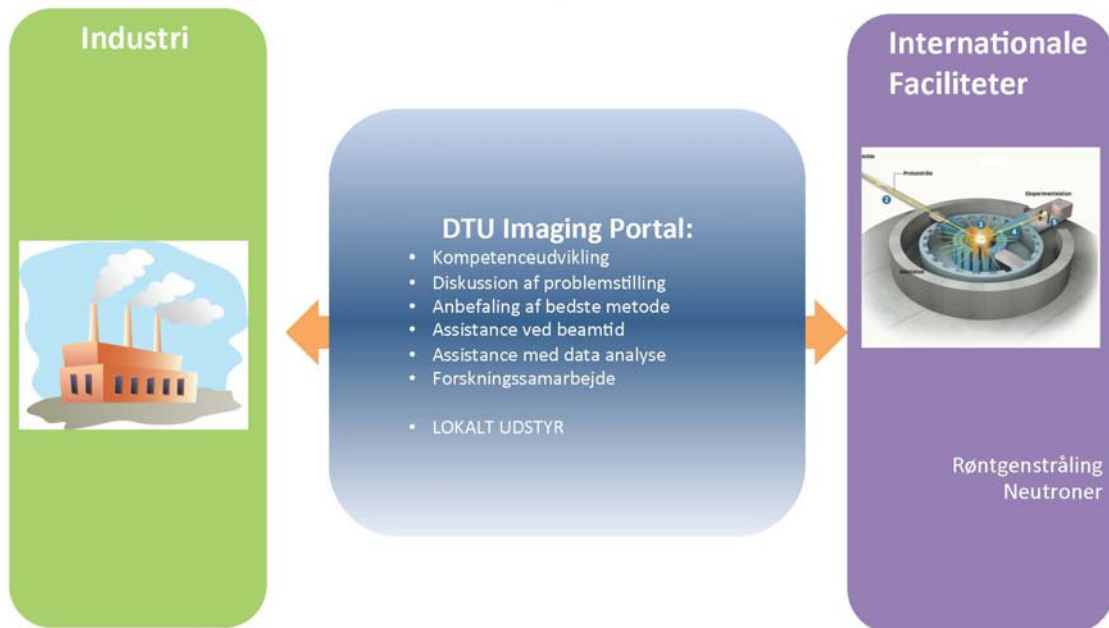
- Access to beamtime for industry
- Consultant for preparing, and executing beamtime
- Help with analyzing data

Contact: Martin Meedom Nielsen

DTU Physics
Phone: 51801561
mmee@fysik.dtu.dk



DTU som science hub/ portal for 3D imaging af materialer

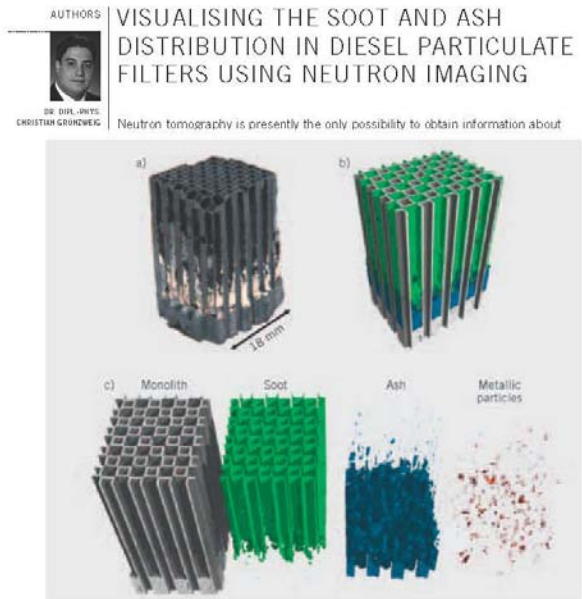
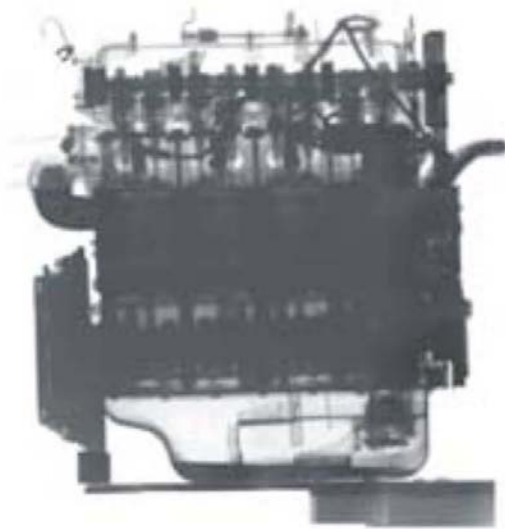


3D Imaging center



Best practice: University of Manchester
Strukturfondsprojekt (2013-2014): ESS og MAX-IV som vækstmotorer i regionen

Neutron Imaging

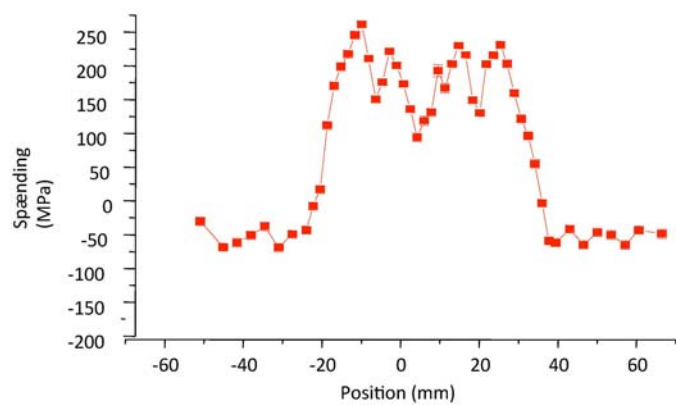


Courtesy: PSI, HMI/HZB, FRM2

Residual Spændinger

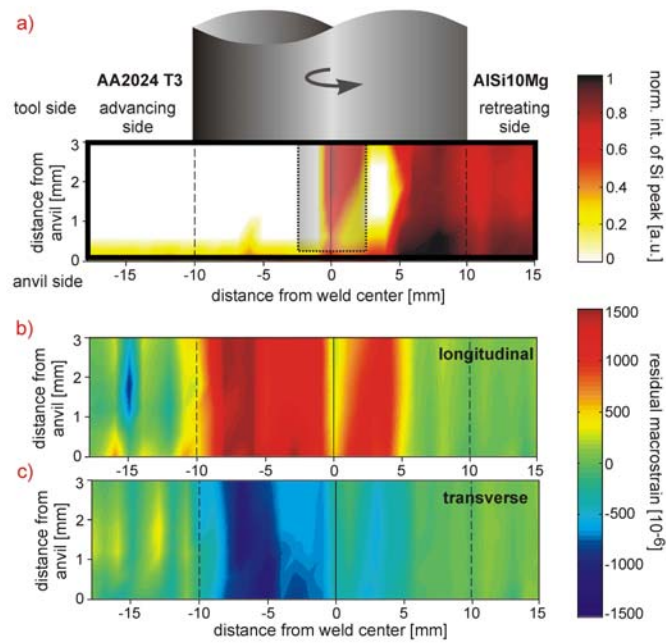


Svejsesøm: British Energy

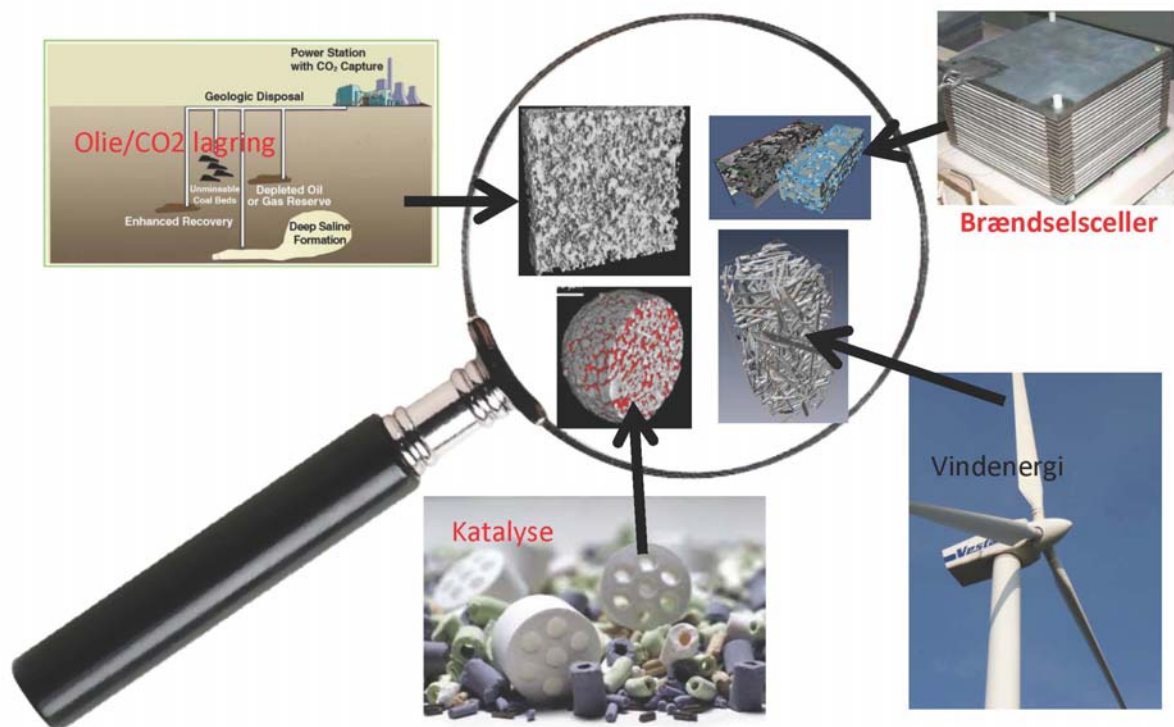


Courtesy: Open University, UK

3D strain map of friction stir weld

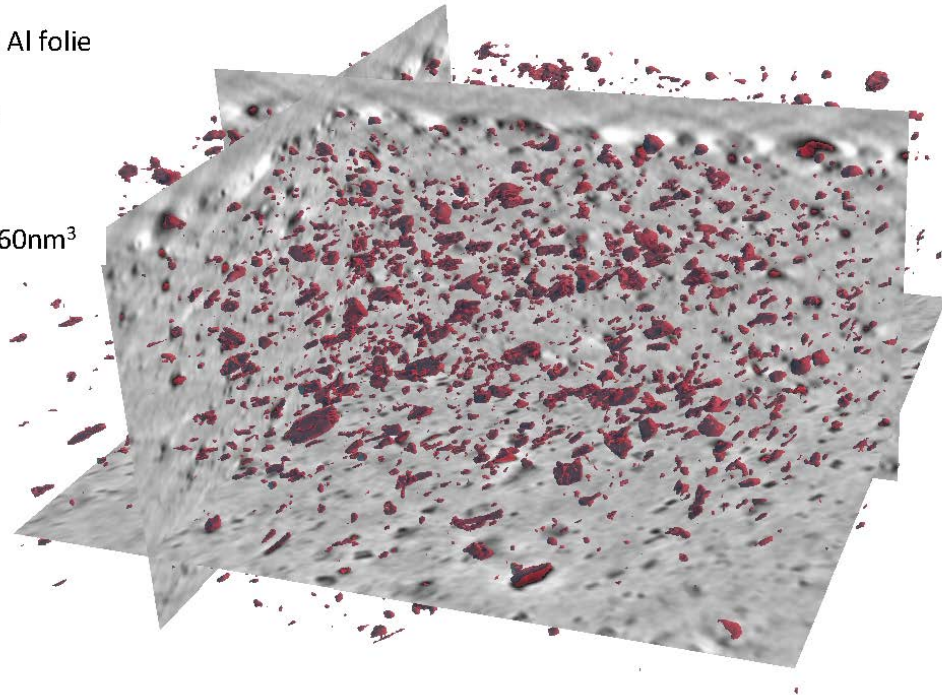


3D imaging of energimaterialer



Fase kontrast tomografi af Al folie

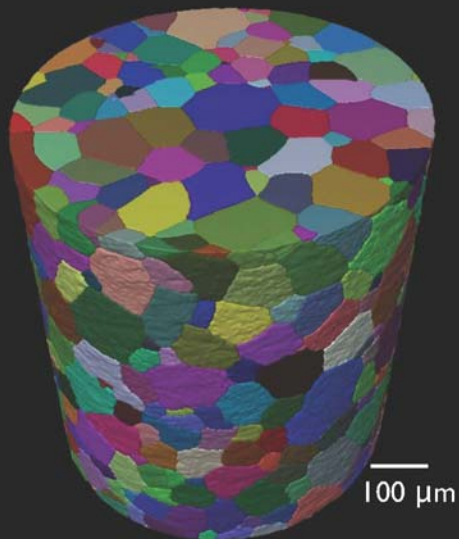
Materiale: Alcan Al folie
Type: Al8079
Energi: 17.5 keV
Volumen:
90x90x48 μm^3
Voxel størrelse: 60nm³



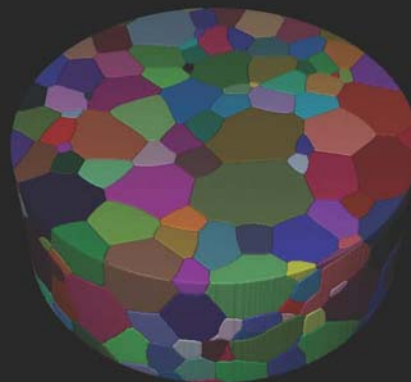
Slide fra P. Cloetens, ESRF

Kornvækst i Titanium

Eksperimentelt



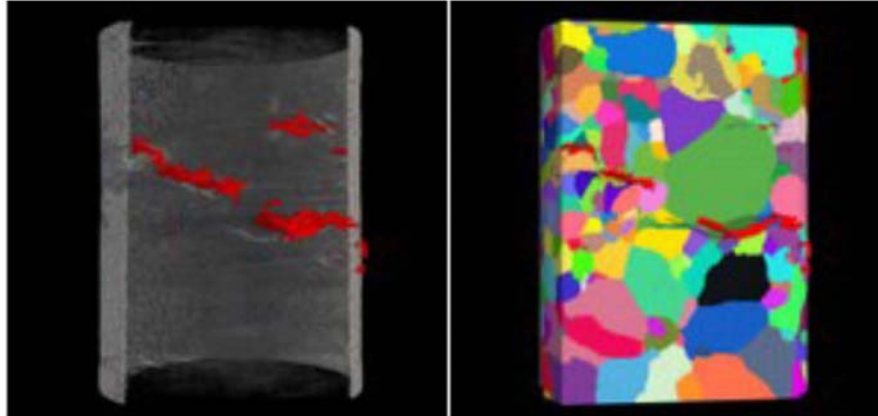
Phase field simuleringer



Risø: E.M. Lauridsen, S. Poulsen, A. Lyckegaard.
Northwestern: P. Voorhees, I. McKenna

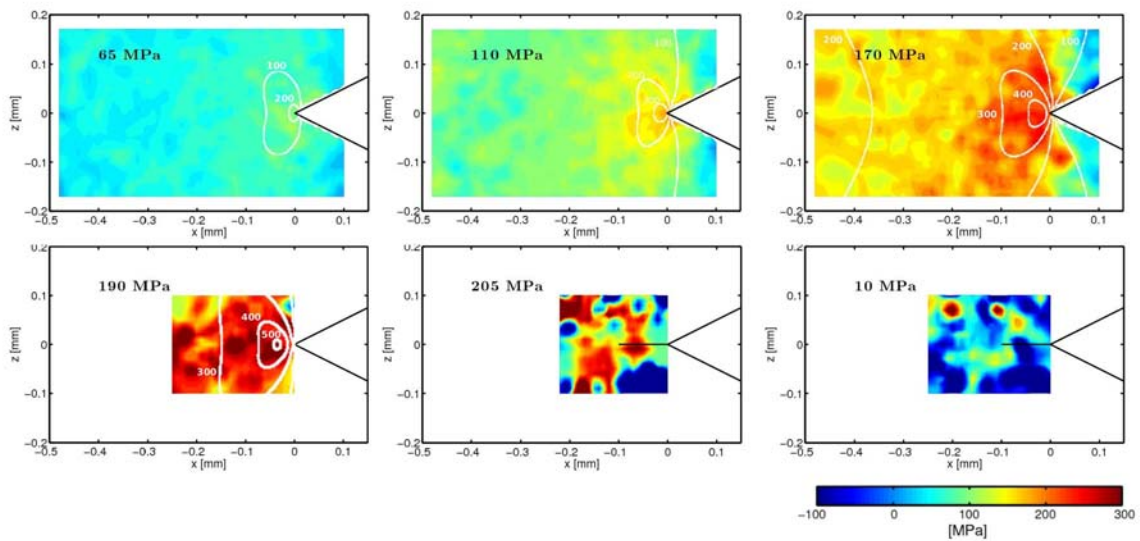
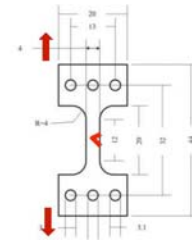
Navy Resarch Lab: R. Fonda
ESRF: W. Ludwig, A. King, S. Rolland

Stress corrosion revnedannelse i stål



A. King, G. Johnson, D. Engelberg, W. Ludwig, and J. Marrow, *Science* (2008) **321**, 382 - 385

Spændinger omkring revnespids i Mg



J. Oddershede, B. Camin, S. Schmidt, L.P. Mikkelsen, H.O. Sørensen, U. Lienert, H.F. Poulsen, W. Reimers.
Acta Mater. **60**, 3570-3580 (2012).

diffractions baseret

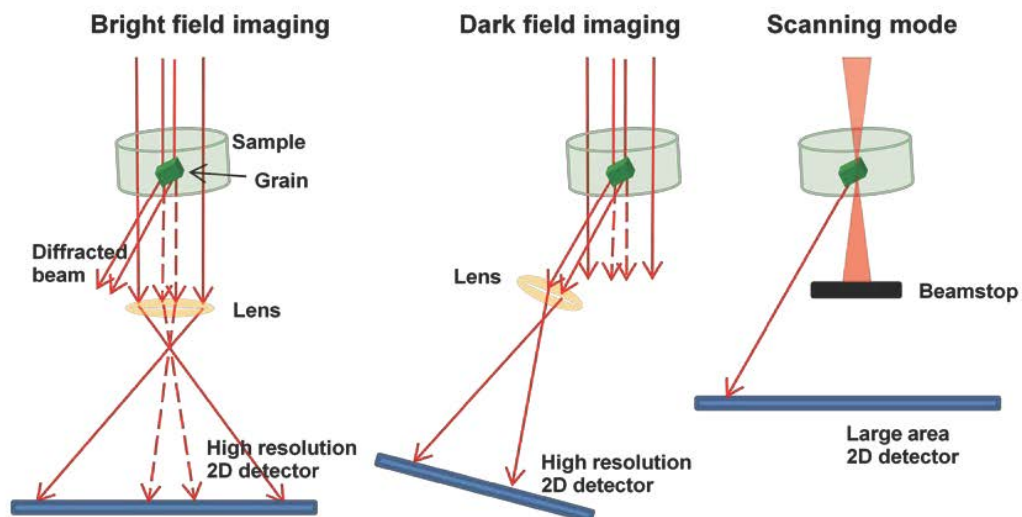
TEM

TXM



Opløsning:	1 Å	20-30 nm
Tykkelse:	1 korn in 2D	1000 korn in 4D
Orienteringer:	0.01-0.1 grad	0.001 – 0.1 grad
Spændinger:	(indirekte)	direkte

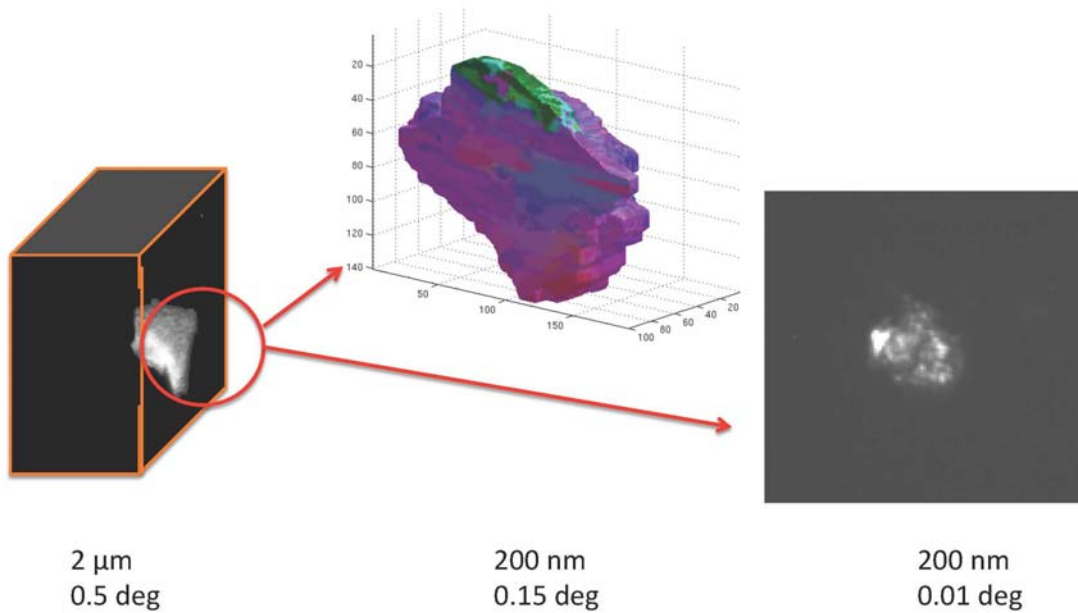
Diffractions baseret Transmission Røntgen Mikroskopi



Arbejdsgruppe:

DTU: H.F. Poulsen, E.M. Lauridsen, S. Schmidt, W. Pantleon, J. Oddershede, Y. Zhang, H. Simons, J. Hübner, F. Jense
 ESRF: A. Snigirev, I. Snigireva, W. Ludwig, A. King, C. Detlefs.

Mikroskopi



Arbejdsgruppe:

DTU: H.F. Poulsen, E.M. Lauridsen, S. Schmidt, W. Pantleon, J. Oddershede, Y. Zhang, H. Simons, J. Hübner, F. Jense
ESRF: A. Snigirev, I. Snigireva, W. Ludwig, A. King, C. Detlefs.

Studier af rekrySTALLISATION med 3DXRD

Dorte Juul Jensen

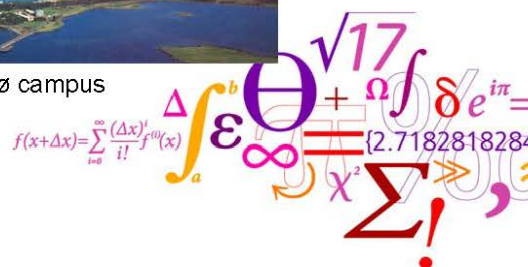
Studier af rekrytation med 3DXRD

D. Juul Jensen



Risø campus

DTU Wind Energy
Department of Wind Energy



Staff

MAC

KOM

**Senior scientists
(incl emerit.)**

7

8

Scientists

3

0

Engineers

0

6

Postdocs

3

3

PhD students

3

5

Technicians

3

7

Secretary

1

1

Guest scientists

3

1

DTU Wind Energy, Technical University of Denmark

Aim for Materials Science and Advanced Characterization (MAC) section



To perform materials science and development on a high international level with focus in particular on materials and components for wind energy applications

To advance existing techniques and to implement new characterization techniques and data analysis tools to match the needs of the scientific and engineering projects

Covering the whole range from basic science to applications

Work on length scales from nanometer to meter

DTU Wind Energy, Technical University of Denmark

DTU Wind Energy



Sections

Composites and Materials
Mechanics

Materials Science and
Advanced Characterization

Fluid Mechanics

Test and Measurement

Wind Turbines

Aeroelastic Design

Meteorologic Section

Wind Energy Systems

DTU Wind Energy, Technical University of Denmark

WIND ENERGY SYSTEMS

Wind resources and siting
Wind power integration and control
Offshore wind energy
Wind energy and society

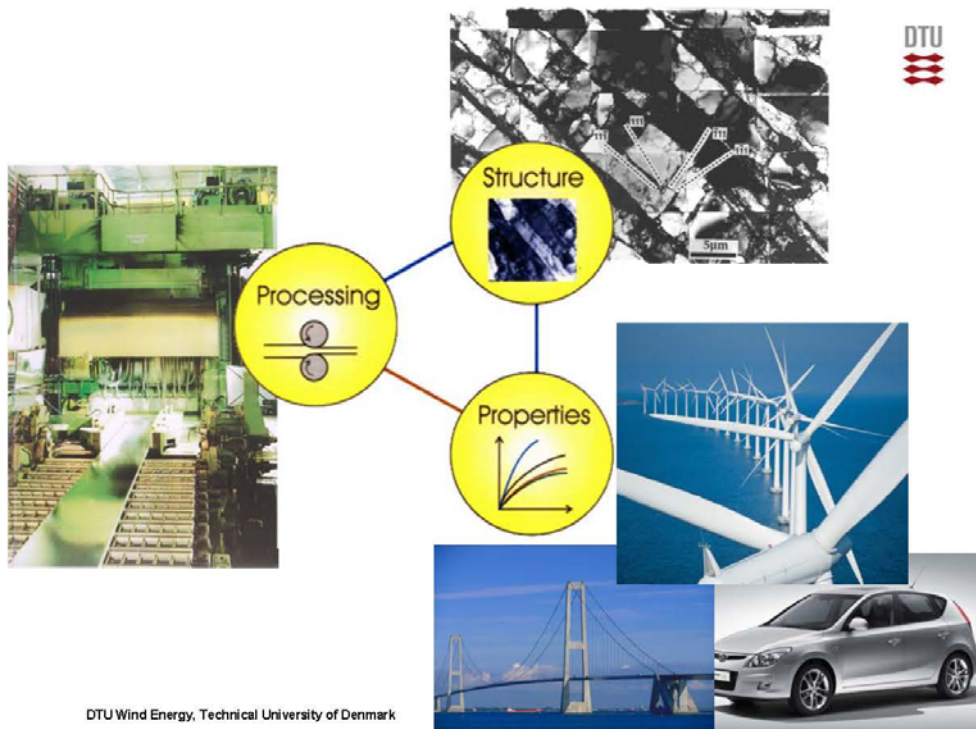
WIND TURBINE TECHNOLOGY

Aeroelastic design
Structural design and safety
Mechanical components
Electro-technical components

BASICS FOR WIND ENERGY

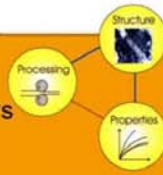
Aero and hydrodynamics
Boundary-layer meteorology and turbulence
Light, strong materials
Remote sensing and measurement technology

DTU Wind Energy, Technical University of Denmark



DTU Wind Energy, Technical University of Denmark

Materials:
Light and strong metals and alloys
Steels
Nanostructured materials

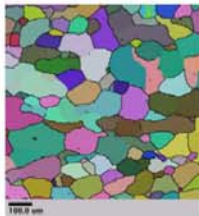


- Processing
Rolling, extrusion, etc.
Very high strain: ARB, DPD HPT
Annealing
- Structure
Advanced electron microscopy
Advanced x-ray characterization
Serial sectioning
- Properties
Mechanical testing (KOM)
Calometry
Hardness
Physical properties



DTU Wind Energy, Technical University of Denmark

Electron microscopes @ DTU Wind Energy



3 SEM & 3 TEM



ZEISS SUPRA 35



JEOL JMS-840



ZEISS EVO 60



JEOL JEM-3000F



JEOL JEM-2000FX

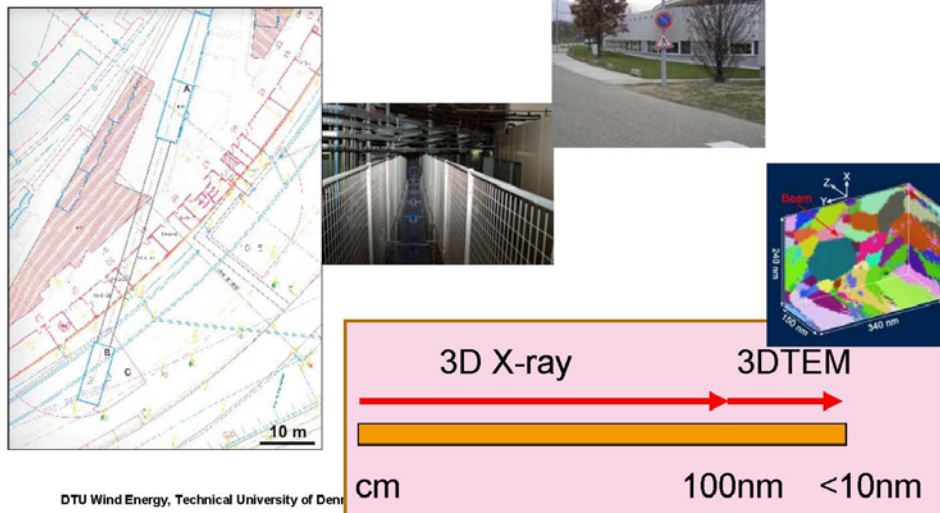
Funding achieved
Microscope
installed

200 kV



DTU Wind Energy, Technical University of Denmark

3D X-ray microscopes at ESRF in France, APS in USA and Hasylab in Germany



Hard and wear resistant steel components



- Characterize structure to determine stress and strain gradients as input for numerical modelling of e.g. friction and wear
- Develop reliable testing techniques (e.g. microsamples) to analyse structure and properties of components damaged by impact, wear or fatigue

Light and strong metals and alloys

- Optimize strength and formability by thermomechanical processing – bulk samples and multilayers
- Advance analytical and numerical modelling of recovery and recrystallization through 2D and 3D characterization

Technique development

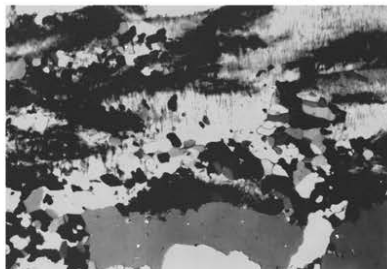
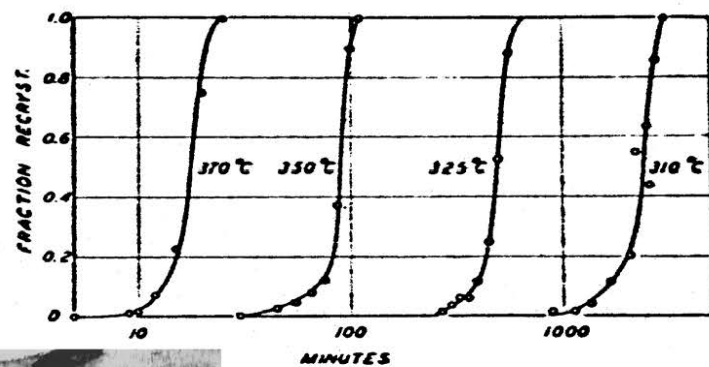
- Implement and develop techniques for characterization of damaged samples (incl lab residual stress measurements)
- Develop techniques for optimizing metals including surface hardening
- Superusers of all relevant 3D/4D techniques with focus on research results

DTU Wind Energy, Technical University of Denmark

Recrystallization Kinetics

DTU Wind Energy, Technical University of Denmark

Recrystallization kinetics - standard measurements



W.A. Anderson and R.F. Mehl: Trans. AIME, 1945, **161**, 140-172.

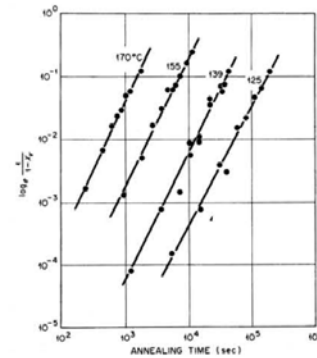
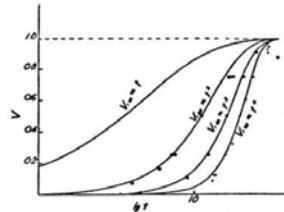
Recrystallization Kinetics – Standard model

Assuming:

- Random distribution of nucleation sites
- All grains grow with the same time-independent growth rate
- All nuclei develop at $t = 0$ or as a linear function of t

$$V_v = 1 - \exp(-Bt^k)$$

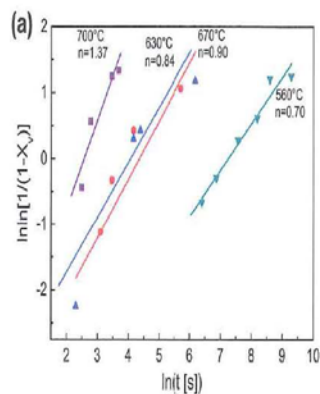
t Time
 B, k Constants related to nucleation rate, growth rate and dimensionality of growth



DTU Wind Energy, Technical University of Denmark

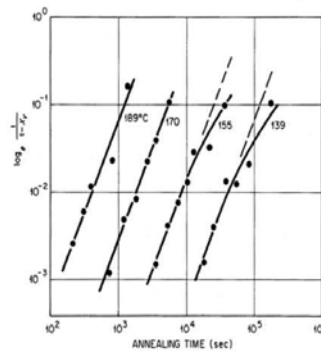
Experimental results - examples

Problems



Yaping Lü, Dmitri A. Molodov, Günter Gottstein, Acta Mat. 59 (2011) 3229-3243

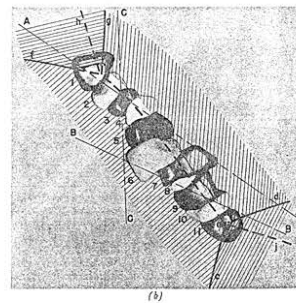
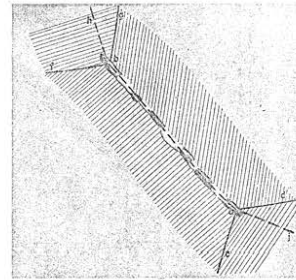
DTU Wind Energy, Technical University of Denmark



R.A. Vandermeer and P. Gorden: in 'Recovery and recrystallization of metals', (ed. L. Himmel), Interscience New York, 1963, 211-240

Clustered nucleation

Optical microscopy combined with serial sectioning



R. A. Vandermeer and P. Gordon: Trans. TMS-AIME, 1959, **215**, 577-588.

DTU Wind Energy, Technical University of Denmark

JMAK model

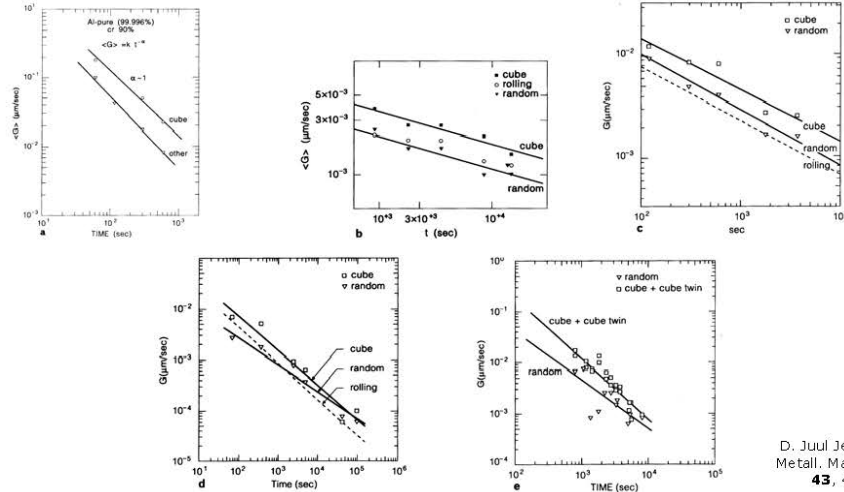
Assuming:

- Random distribution of nucleation sites
- All grains grow with the same time-independent growth rate
- All nuclei develop at $t = 0$ or as a linear function of t

DTU Wind Energy, Technical University of Denmark

Experimental methods and results

Average growth rates – time and orientation dependencies



Growth rates

- All grains grow with the same time-independent growth rate
- On average grains grow as $\langle G \rangle = k \cdot t^{-\alpha}$ or they have a fast decreasing growth rate followed by a period of constant growth and on average, cube grains often grow faster than other grains
- **What do individual grains do?**

3D X-ray Diffraction (3DXRD) 3D Microscope for in-situ characterization of recrystallization kinetics

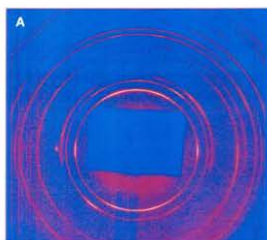
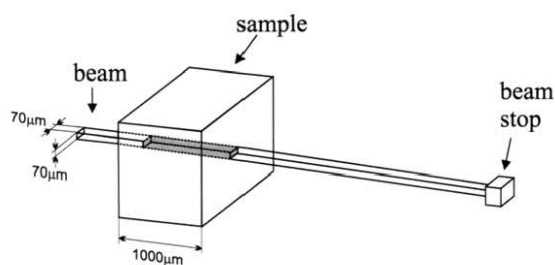


- Sub- μm spatial resolution
- Bulk penetration (0.1 mm – 1 cm)
- Non-destructive
- Fast measurements (seconds – minutes)



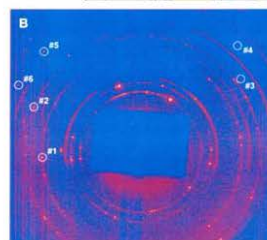
DTU Wind Energy, Technical University of Denmark

Recrystallization kinetic measurements



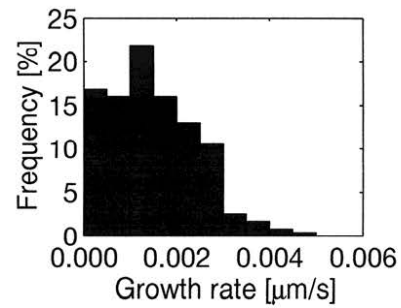
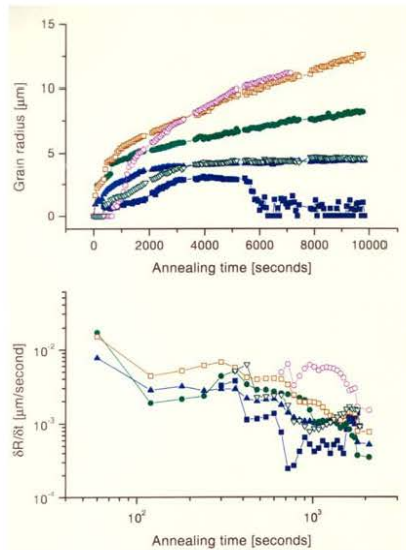
T = 0 min

DTU Wind Energy, Technical University of Denmark



T = 162 min

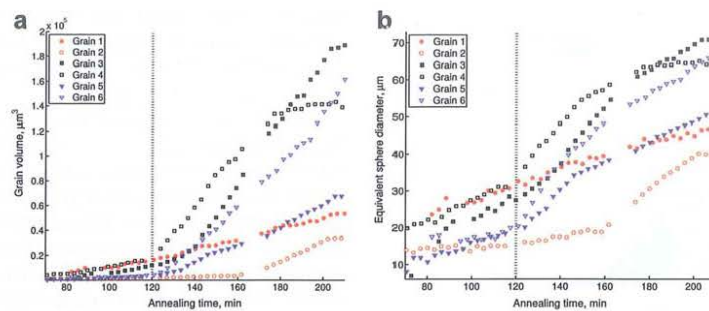
Al (AA 1050) cr 90%



E.M. Lauridsen, H.F. Poulsen, S.F. Nielsen and D. Juul Jensen: Acta Mater., 2003, **51**, 4423-4435
E.M. Lauridsen, D. Juul Jensen, H.F. Poulsen and U. Lienert: Scripta Mater., 2000, **43**, 561-566

DTU Wind Energy, Technical University of Denmark

Al (AA 1050) cr 50%



S.O. Poulsen et al. (2011)
Scripta Mater. **64**, 1003-1006.

DTU Wind Energy, Technical University of Denmark

Grain averaged activation energy for individual grains determined by 3DXRD



$$v = M \cdot F$$

$$v = M_0 \exp\left(-\frac{Q}{RT}\right) F$$

$$Q = R \left(\frac{1}{T_1} - \frac{1}{T_2} \right) \ln \frac{v_2}{v_1}$$

v	Growth rate
M	Mobility
F	Driving force
R	Gas constant
T	Absolute temperature
Q	Activation energy

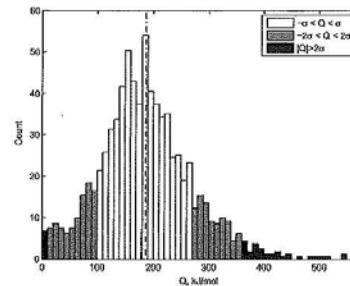
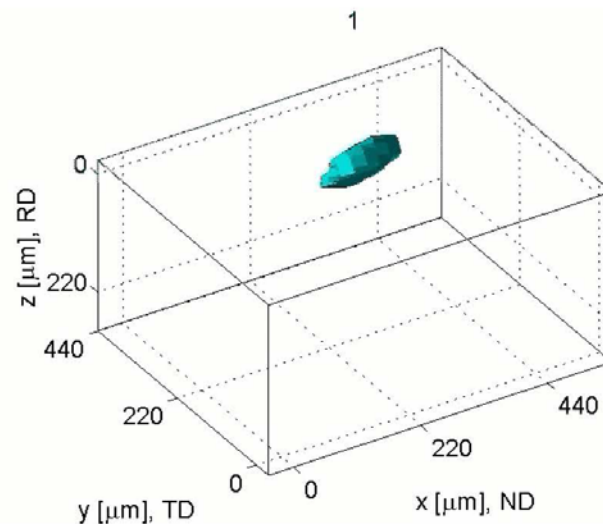


Figure 2. Distribution of grain-averaged activation energies. The mean of the distribution, $\langle Q \rangle = 187 \text{ kJ mol}^{-1}$, is indicated by the vertical line. The standard deviation is $\sigma = 82.9 \text{ kJ mol}^{-1}$, and the 1σ and 2σ confidence intervals are indicated by the colour of the bars.

S.O. Poulsen et al. (2011)
Scripta Mater. **64**, 1003-1006

DTU Wind Energy, Technical University of Denmark

Grain growth during recrystallization in weakly rolled aluminum single crystal



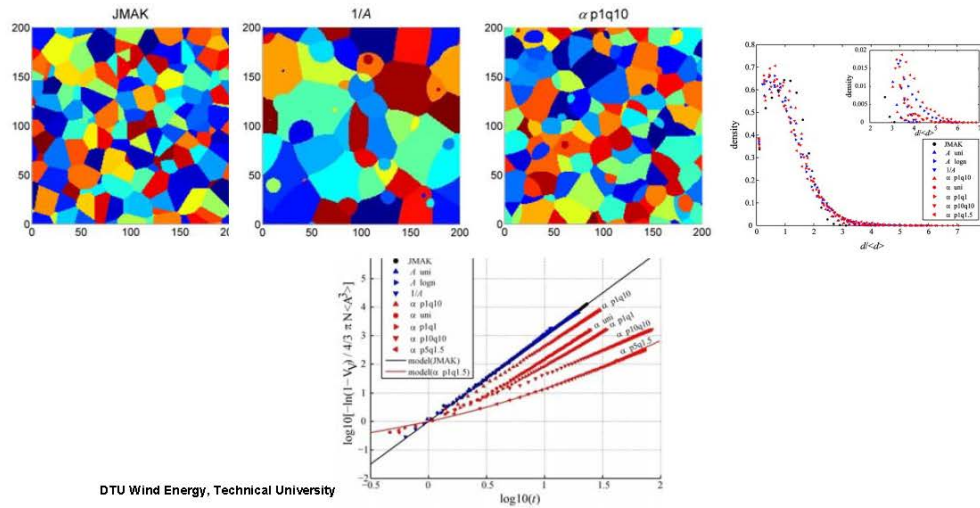
Schmidt, S., Nielsen, S.F., Gundlach, G., Margulies, L., Huang, X., Juul Jensen, D.,
Science, 2004, 229-232.

DTU Wind Energy, Technical University of Denmark

Simulations of effects of distribution of growth rates



$$r = A \cdot t^{1-\alpha}$$



DTU Wind Energy, Technical University



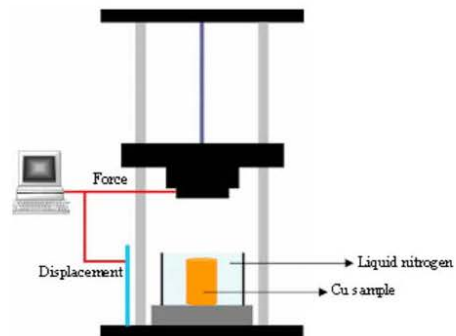
Nanometals

DTU Wind Energy, Technical University of Denmark

Kinetics in nanostructured copper

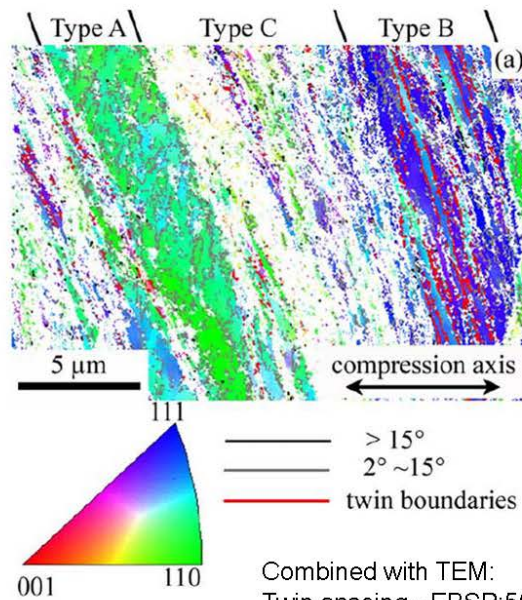


Copper DPD to $\varepsilon = 2.0$



Lin et al., Risø 2012

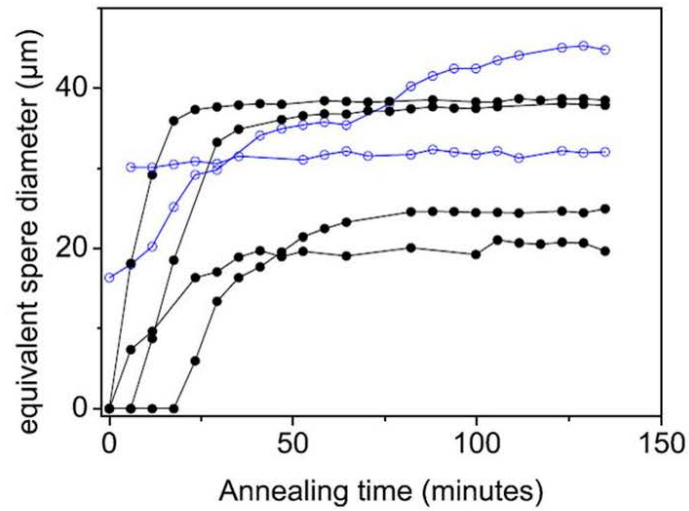
DTU Wind Energy, Technical University of Denmark



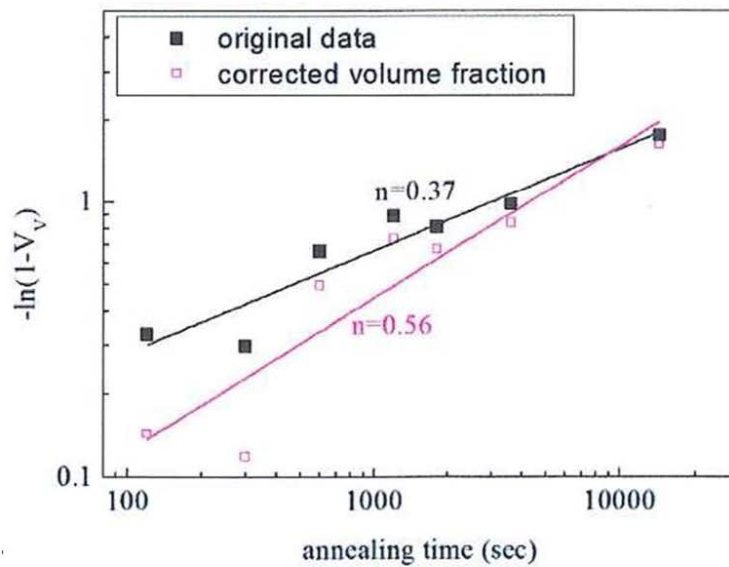
DTU Wind Energy, Technical University of Denmark

Combined with TEM:
Twin spacing - EBSP: 500nm, TEM: 44nm
Type C - TEM: < 100nm

3DXRD measurements anneal at 120C

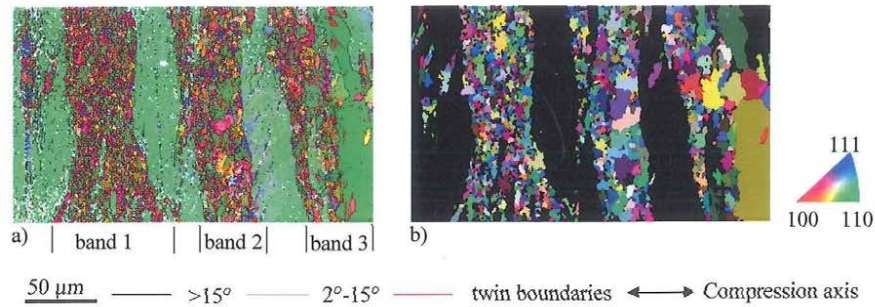


DTU Wind Energy, Technical University of Denmark



DTU

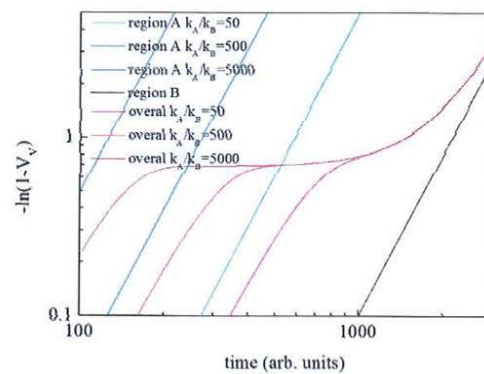
Kinetics in inhomogeneous deformed microstructures



Lin et al., Risø 2012

DTU Wind Energy, Technical University of Denmark

Kinetics in inhomogeneous deformed microstructures



Lin et al., Risø 2012

See also Doherty et al., Risø 1986

DTU Wind Energy, Technical University of Denmark

Conclusions

Recrystallization kinetics is strongly affected by:

- Spatial distribution of nucleation sites
- Time dependent and texture dependent growth rates
- Each recrystallizing grain has its own kinetics
- Wide distribution of activation energies
- Inhomogeneous deformation microstructures

3DXRD combined with electron microscopy are efficient tools to study recrystallization kinetics

Den nyeste generation af røntgen diffraktometre med
tilhørende temperaturcelle

Flemming Grumsen, DTU Mekanik

Den nyeste generation af XRD med tilhørende temperatur celle

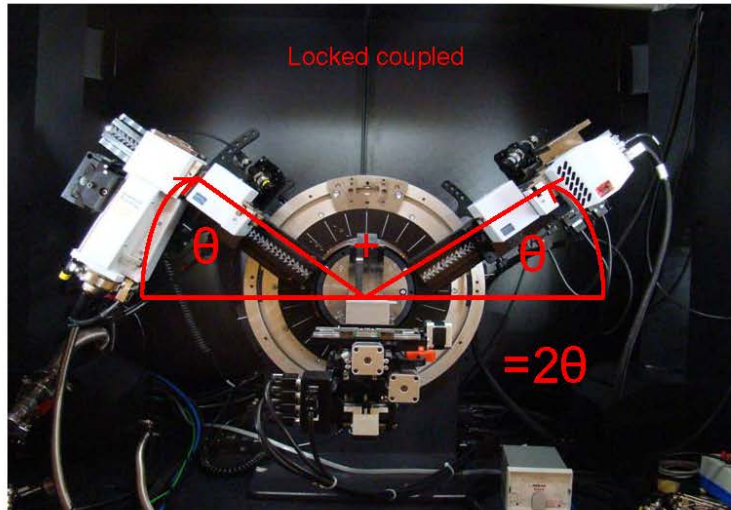
Flemming Bjerg Grumsen

Outline

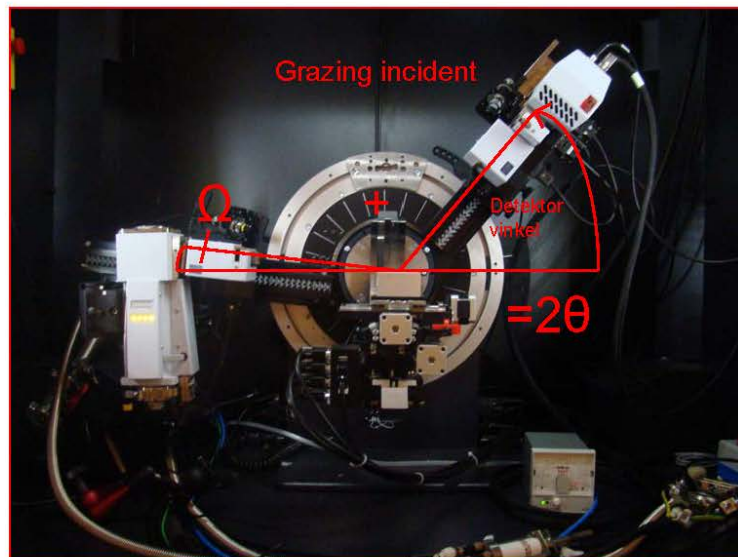
- Hvad er XRD?
- Hvad er nyt?
- Strip detektoren. Hvad kan den?
- Mikrodiffraktion med et eksempel
- Temperatur cellen
- Expanderet austenit
- Varmebehandling af expanderet austenit

Hvad er XRD?

- Braggs lov: $n \lambda = 2 d \sin \theta$

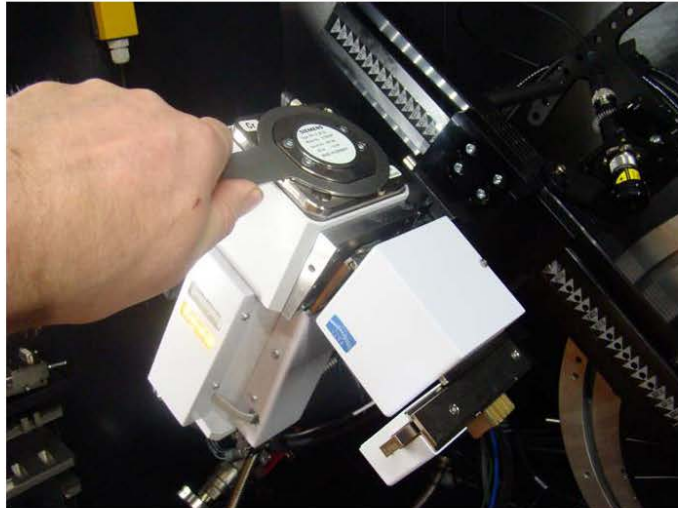


Hvad er XRD?



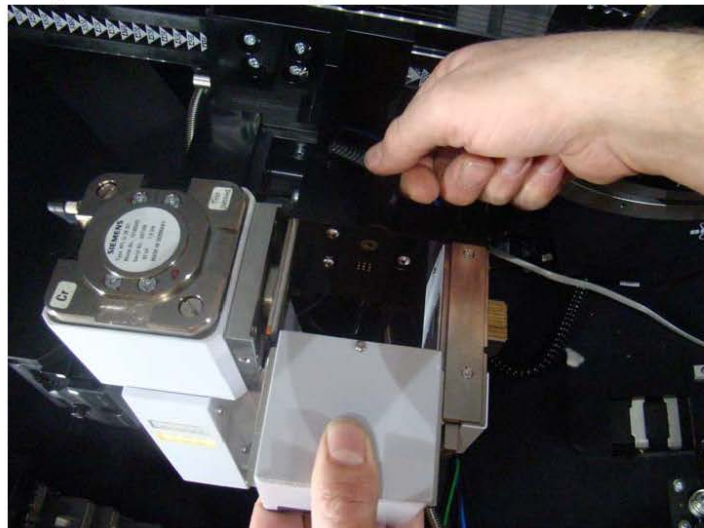
Hvad er nyt?

- Twist tube: linie- og punktfocus



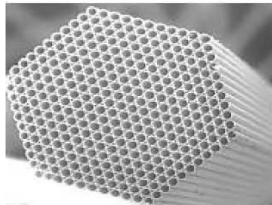
Hvad er nyt?

- Snap lock til skift mellem polycap, göbelspejl og divergence assembly

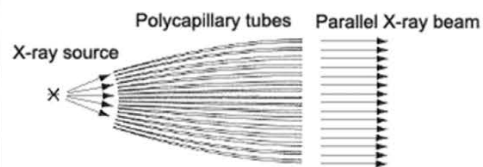


Hvad er nyt?

- Polycap til punkt fokus



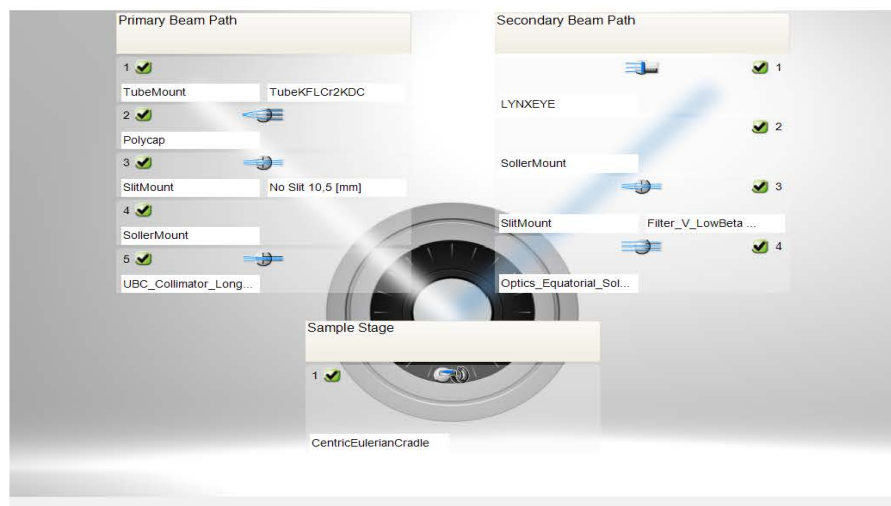
Mikrofibre til guided
Røntgen beam



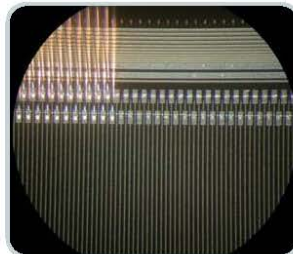
Fra kilde til næsten parrallel beam

Hvad er nyt?

- Automatisk registrering af optik (Da Vinci)

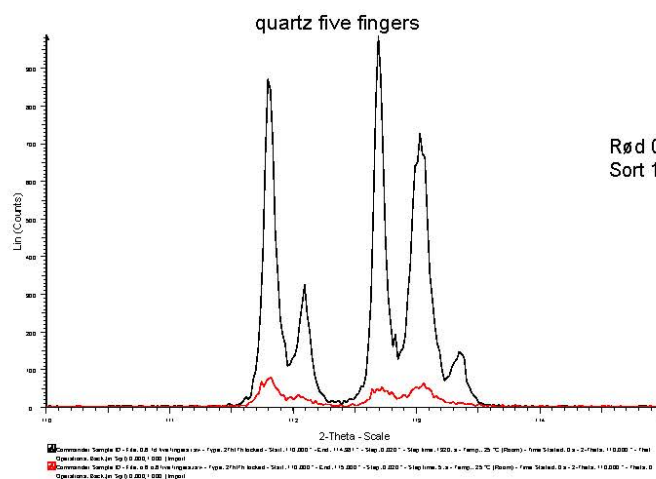


- Silicon strip 1d detektor (lynxeye)



Billede venligst udlånt af Bruker AXS

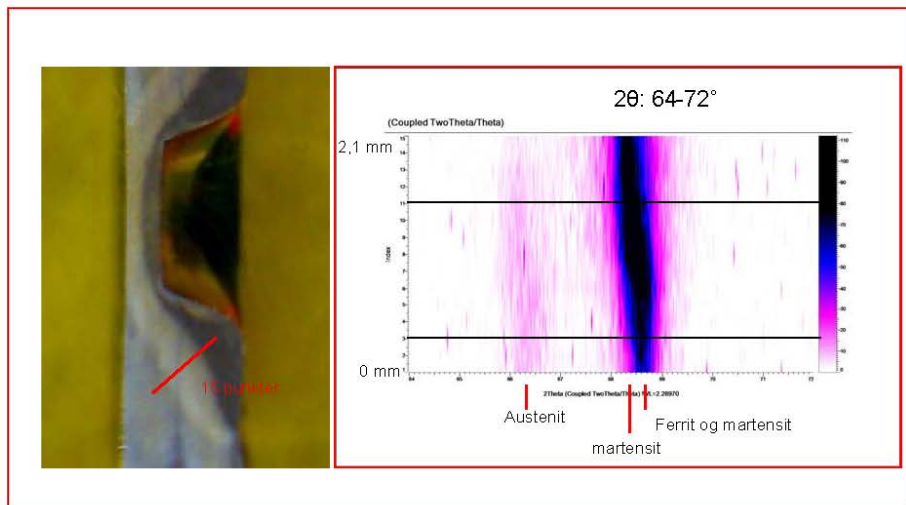
- 0D: sammenlægger alle strips til en detektor
- 1D: hver strip fungerer separat og kompenserer for positionen



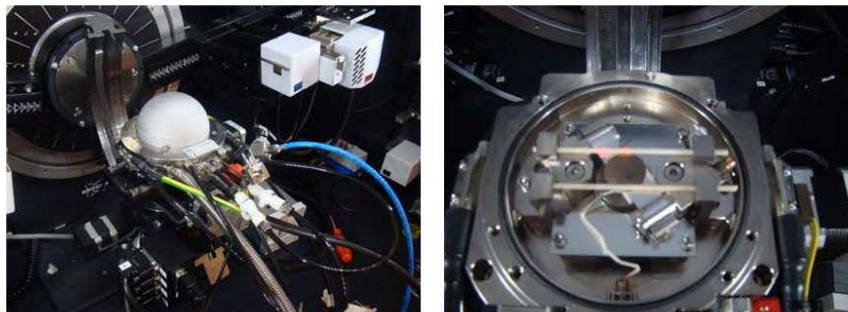
Rød 0D 0.6 mm detektor slit
Sort 1D detektor fuldt åben

Mikrodiffraction på Friction stir welding

Polycap med 0.3 mm collimator



Temperatur cellen

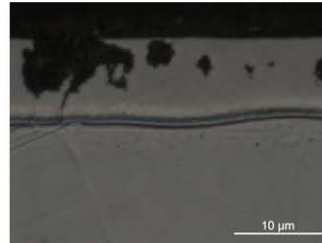
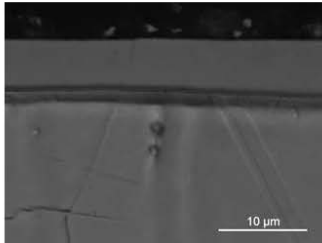


Temperatur spænd: 25-1100 °C eller -180 til 450 °C

Vacuum eller gas flow

Ramping 0,1 – 1 grad pr. sekund

nedbrydning og (Oxidation☹) af ekspanderet austenit

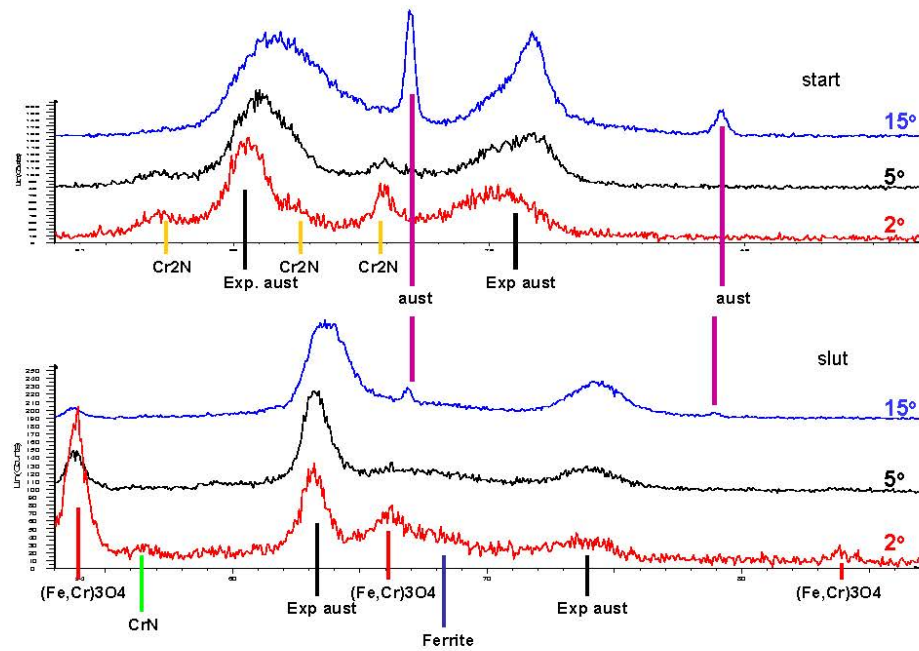


- Expanded austenit is metastabilt
- Ved temperaturer over 450 °C ned brydes den til
 - CrN
 - Ferrit

Forsøgsparametre

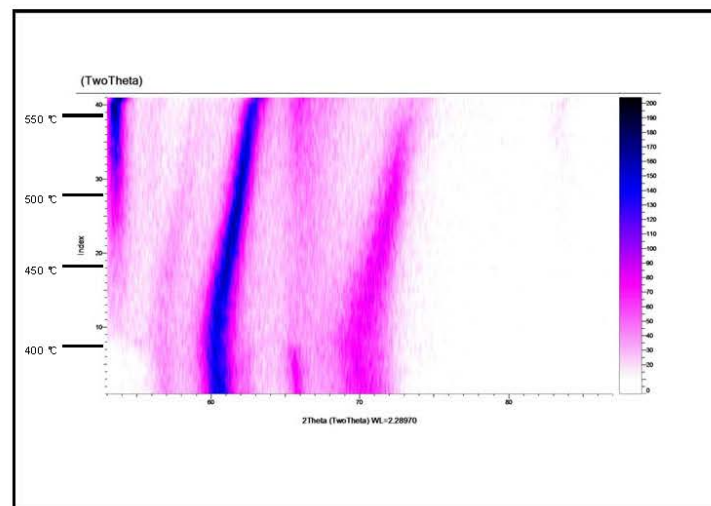
- Grazing incident 2, 5 og 15 grader, 2θ: 53° til 87°
30 min for hvert scan
- 30°C, 100 - 400 °C med 50 °C interval.
Ramping: 1 °C pr s.
- 400 °C til 560 °C med 5 °C interval. Ramping:
0,1 °C pr s.
- Afkøling til 30 °C. ramping: 1 °C pr s.

Resultater



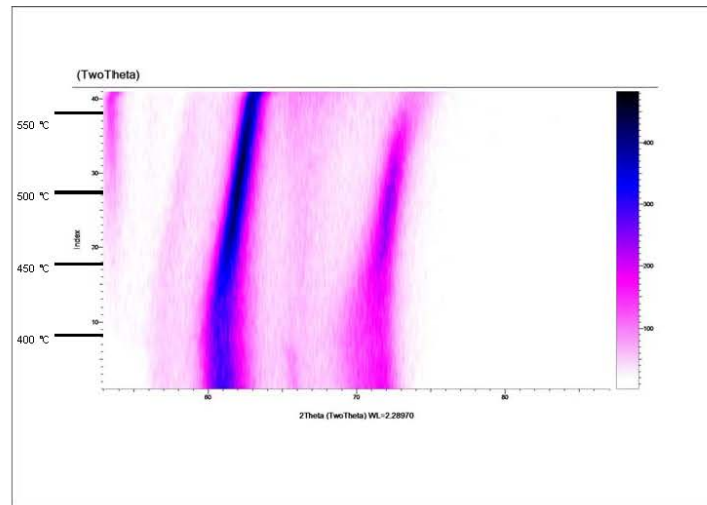
Resultater

2 ° grazing incident



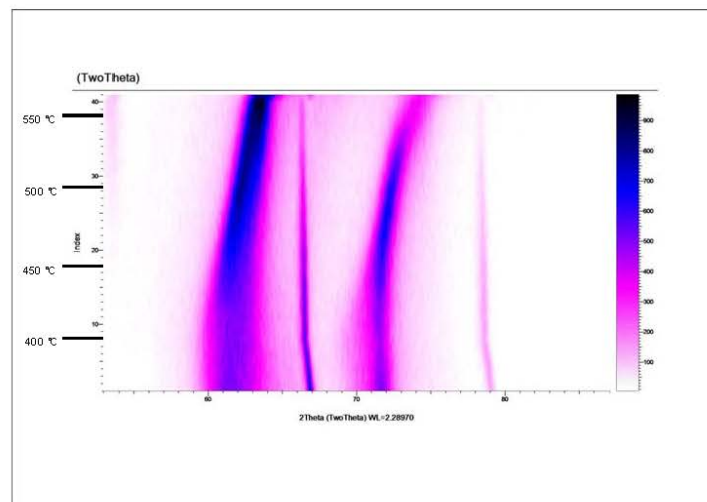
resultater

5 ° grazing incident



Resultater

15 ° grazing incident



Hvad kan man gøre for at undgå oxidation?

- Au eller Pt coating?
 - Ar/H₂ gas?
 - Metal med større affinitet til O₂ end prøven i kammeret?
-
- Og til sidst tak til Christian Hansson fra Bruker for support og til Trine Nybo Lomholt for nye ideer, når problemerne syntes uoverskuelige

NDT – relevant teknikkers muligheder og begrænsninger

Peter Willumsen, Force

NDT af svejsninger

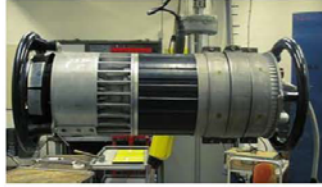


Af Peter Villumsen
DS/EN 473 niveau 3



Metoder:

- Røntgen
- Ultralyd
- Magnetpulverprøvning
- Penetrantprøvning
- Tæthedsprøvning
- Hvirvelstrømsprøvning



Radiografi

Røntgen op til 300 kv.

Isotop (Gamma)

- Selen 75
- Ir 192
- Cobolt 60



Radiografi

Følsomhed 1-2% af godstykkelse



Radiografi bruges på alle emner/svejsninger i alle former for industri både i forbindelse med ny produktion og vedligehold.

Radiografi bruges til af finde fejl i volumen
Radiografi er 2 dimensional.

Fordele:

God til runde fejl eks. Pore
God til tynde godstykkelser

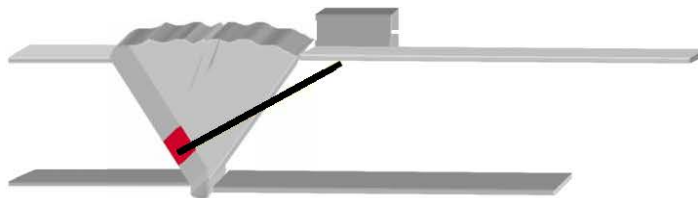


Ulemper:

Stråling
Begrænset godstykkelser

Ultralyd

Manuel eller automatisk



Manuel ultralyd bruges til:

- Tykkelse måling
- Lagdelings kontrol
- Materialefejl
- Svejsekontrol



0.37 mm i mindst 2 retninger

Luftspalte min.
1/10.000 mm



Manuel Ultralyd

Fordele:

God til plane fejl

God til tykke godstykker

Ulemper:

Kræver plads

Ingen dokumentation



Højt ydende automatiseret ultralyd inspektion

- Hurtig automatiseret inspektion
- Optimeret inspektion
- Dokumenteret
- Gentagen inspektion
- Stål, rustfrit stål, etc.



Magnetpulverprøvning

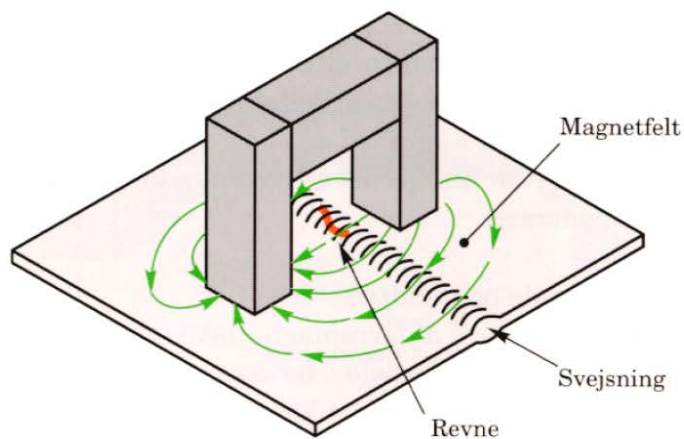
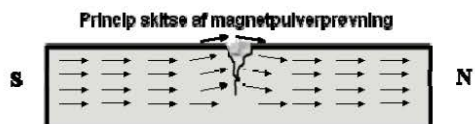
For indikationer åben til overfladen og kun på magnetiske materialer.

Følsomhed
Ca. 0,1 – 1m μ

Magnetpulverprøvning

Kan udføres som prøvning med kontrast farve under alm. belysning.

Eller som fluorescerende prøvning i mørke med ultraviolet belysning



NDT af svejsninger



Fordele:

God til plane fejl åben til overfladen

Hurtig

Ulemper:

Kun overflade fejl

Ingen dokumentation

NDT af svejsninger



Penetrantprøvning (Kapillarprøvning)

Kan udføres som prøvning med kontrast farve under alm.
belysning.

Eller som fluorescerende prøvning i mørke med ultraviolet
belysning
Den mest følsomme metode

NDT af svejsninger



Penetrant bruges på ikke porøse materialer

Primært på umagnetiske som eks, rustfrit stål,
aluminium, magnesium osv.

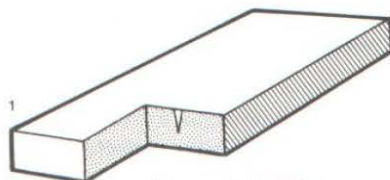
For indikationer åben til overfladen

Følsomhed

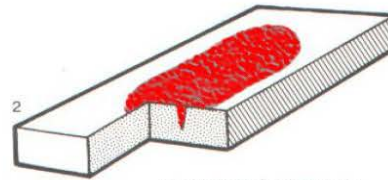
Ca. 0,1 – 1µm



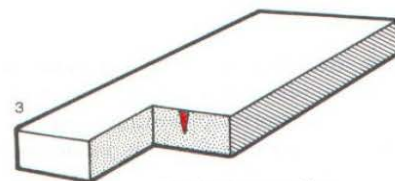
NDT af svejsninger



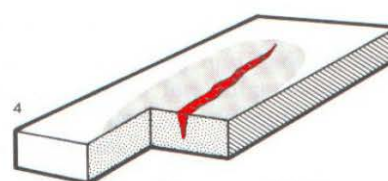
Revnen ikke synlig
på overfladen



Kapillarvæske trænger
ind i evt. revner og
porøsiteter



Hverken revne eller
kapillarvæske er syn-
lig på overfladen



Revnen „synlig“. Frem-
kalderen har suget
væsken ud af revnen
og dannet en bred in-
dikation oven på revnen

Fordele:

God til fejl åben til overfladen
Kan bruges som tætheds prøvning
Let at udføre

Ulemper:

Kun overflade fejl
Ingen dokumentation
Kræver meget rengøring

Tæthedsprøvning

(Lækageprøvning)

Lækageprøvning er ikke bare en, men
mange metoder

De følgende er nogle af de mest
anvendte

Visuelle - Akustiske – Trykforandring –
Sporstoffer - Radioaktive sporstoffer -
Termografi – Hvirvelstrøm -
Farveforandring – Røggasser –
Krydskorrelator – kabilarprøvning

Vakuumboks



Hvirvelstrømsprøvning

Undersøgelse af elektrisk ledende materialer,
primært metaller.

Metoden anvendes bl.a. til revne- og
korrosionsdetektion samt tykkelsesmålinger,
fx til undersøgelse af varmevekslerrør og i
flyindustrien til kontrol af fx turbineblade og
understel.

Slut...

Metrology and Quality Assurance

Maria Holmberg, Teknologisk Institut



THE DANISH TECHNOLOGICAL INSTITUTE


Founded 1906 by Gunnar Gregersen



"To support Danish industry, mainly small enterprises, by providing technical assistance in the form of teaching, advice, testing and technological research"

"Technological research - developed with the necessary scientific approach, but without the means of making science. The purpose is to develop new field for manufacturing "


Gunnar Gregersen



**DANISH
TECHNOLOGICAL
INSTITUTE**

DTI - DIVISIONS AND CENTRES

<p>BUILDING TECHNOLOGY Concrete Building Processes Indoor Climate and Humidity Masonry and Building Components New Industrialization Swimming Pool Technology Timber and Textiles</p> <p>LIFE SCIENCE Food Technology IT Development Chemistry and Water Technology</p>	<p>ENERGY AND CLIMATE Energy Efficiency and Ventilation FEM-Secretariat Installation and Calibration Refrigeration and Heat Pump Technology Pipe Centre Renewable Energy and Transport Automobile Technology</p> <p>MATERIALS Materials Testing Plastics Technology Production Development Tribology Packaging and Transport</p>	<p>PRODUCTION Micro technology and Surface Analysis <u>Metrology and Quality Assurance</u> Robot Technology</p> <p>BUSINESS DEVELOPMENT Policy and Business Development Human Resources Development Creativity and Growth Technology Partnership</p> <p>TRAINING IT Training Conferences Leadership and Management Training</p> <p>INTERNATIONAL CENTRE</p>
---	--	---





**DANISH
TECHNOLOGICAL
INSTITUTE**

METROLOGY & QUALITY ASSURANCE

Geometrical measurements – shape and dimensions of physical objects

Commercial activities
 Pilot production
 Product development
 Subcontractors/customers
 Training and courses

R&D activities
 Trouble shooting
 Product development
 Metrology
 Production and productivity

METROLOGY & QUALITY ASSURANCE



Metrology – DPLL (Danish Primary Laboratory for Length)

Designated institute within length – mechanical calibration of gauge block

Accreditation within geometrical measurements

EURAMET, TC-L (Technical Committee for Length)

CMC (Calibration and Measurement Capabilities)

EMRP projects

Multi-sensor metrology for microparts in innovative industrial projects



Fra programmet:



Dansk industri skal bl.a. overleve på kvalitet, og det er vigtig, at virksomhederne kan **dokumentere denne kvalitet overfor deres kunder**. Vintermødet 2013 har derfor fokus på **karakterisering af materialer, processer og komponenter**, spændende fra nanometer til meterskala og fra **forskning & udvikling** til **monitorering af komponenter i drift**.

Dokumentere kvalitet overfor deres kunder

*Geometrisk opmåling kan kvantificere dette – tolerancer, dimensioner, data
Reproducerbarhed*

Karakterisering af materialer, processer og komponenter

*Kombinere opmåling (dimension, form) med materiale karakterisering (densitet, homogenitet, struktur)
Hvilke parametre repræsenterer hvad?*

Forskning & Udvikling

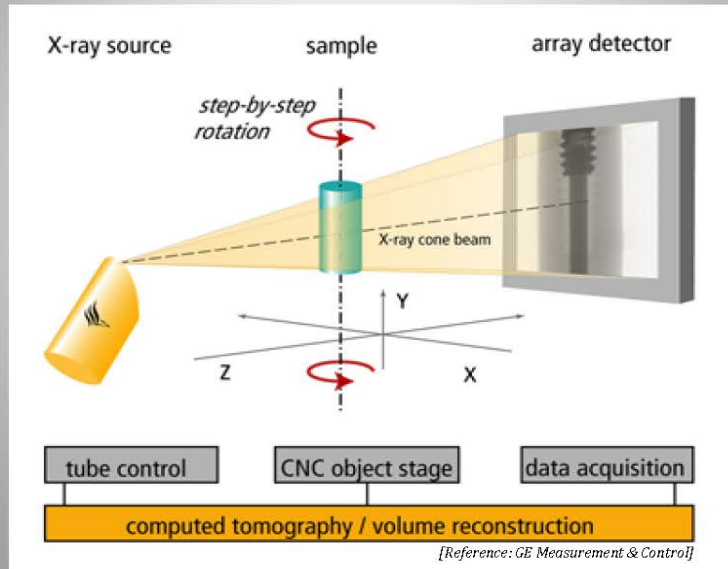
*Trouble shooting – vi ved ikke helt hvad vi kigger efter...
Metrologi & måleteknik i fremtiden – inklusive CT Scanning*

Monitorering af komponenter i drift

CT Scanning som ikke-destruktiv analyse med mulighed for 3D karakterisering

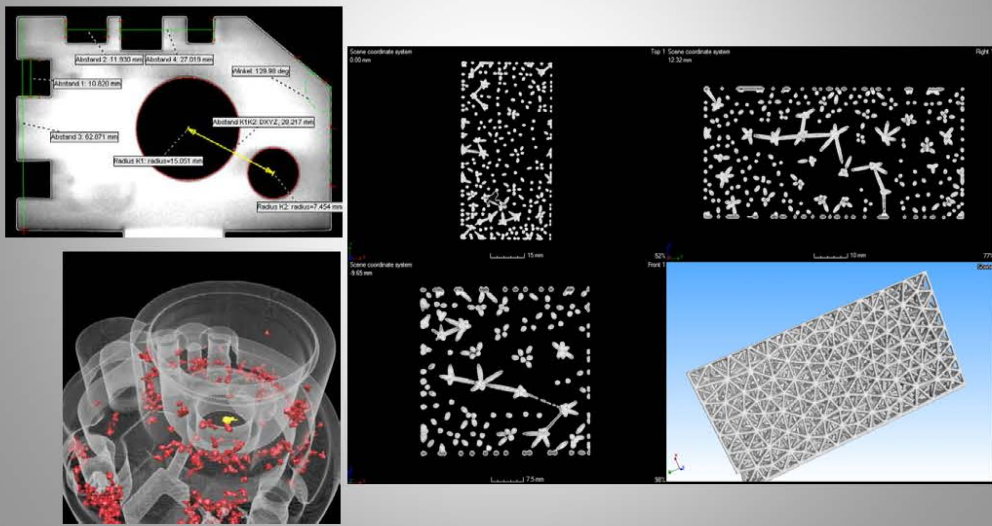
CT SCANNING

CT – Computed Tomography – Scanning



CT SCANNING

- Measuring size, form and position of geometrical features
- Non-destructive analysis of inner structures

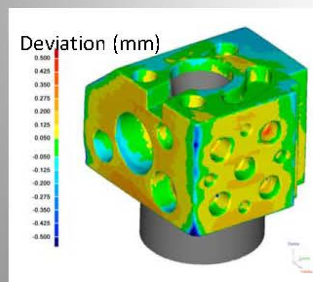


CT SCANNING

Zeiss METROTOM 1500

X-Ray tube: 225 kV
 Detector: 1024 x 1024 pixels
 Sample size: 30 x 30 x 30 cm
 'Detectability': < 10 μ m

Industrial CT Scanner
 Manufacturing, Production,
 In-line Scanning etc.

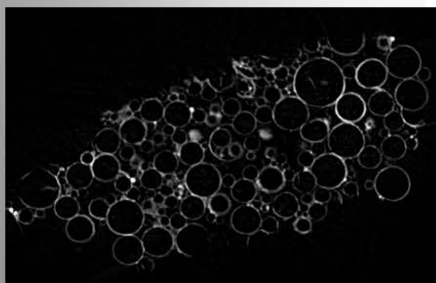


CT SCANNING

Bruker microCT, Skyscan 1172

X-Ray tube: 100 kV
 Detector: 4000 x 2300 pixels
 Sample size: 2 x 2 cm (possibility to combine scans)
 'Detectability': < 1 μ m

μ CT Scanner
 Material characterisation, R&D,
 high resolution etc.



Document quality in regards to customers



Documentation in regards to customers and subcontractors in a supply chain

Often a combination of different technologies, for example CMM and CT Scanning

Manufacturing

‘Quantification of quality’ using geometrical measurements

Example - release of moulds for injection moulding into production



Characterisation of materials, processes and components



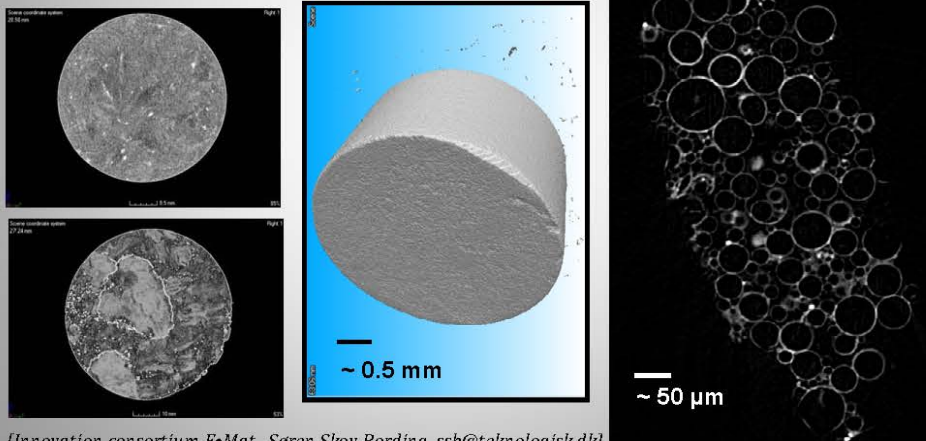
Combining geometrical measurements with material characterisation

How are used processes related to characteristics of resulting component?

Combining data on micro- and macro-scale

Material for use as a matrix aluminium syntactic metal foam

Hollow glass spheres ($\varnothing 20\text{--}80\text{ }\mu\text{m}$) that are bonded chemically to each other by water-based silane coating.



[Innovation consortium F•Mat, Søren Skov Bording, ssb@teknologisk.dk]

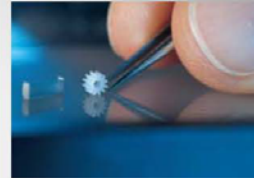
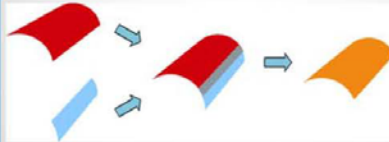
Research and Development



Metrology and geometrical measurements

EMRP project: Multi-sensor metrology for microparts in innovative industrial projects
Transferring new methods, systems, protocols from laboratory to production facilities.

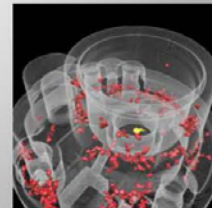
- Influence on uncertainty from parameter X
- Optimization of protocols (tolerances, time etc.)
- Data handling and data fusion



Development together with industry

Product development and trouble shooting
Designed/optimized solution for specific applications

- Automation and multiplying
- Sample holders for CT scan of several items simultaneously
- Software systems (macros) for automatic handling of data



Monitoring components 'in-line'

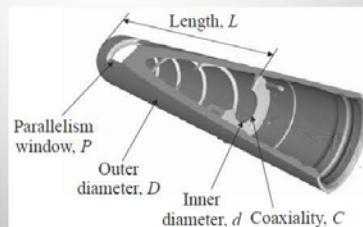
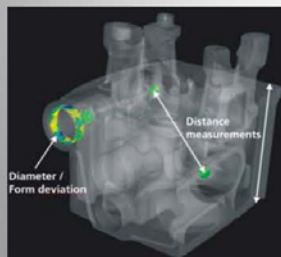


CT Scanning – Possibility to perform non-destructive testing in 3D

'In-line' CT Scanning system

Expensive and time consuming
Necessary to have 3D?
Need to be combined with software solutions

High-end products
Complex technology
Assembled items – components made of different materials etc.

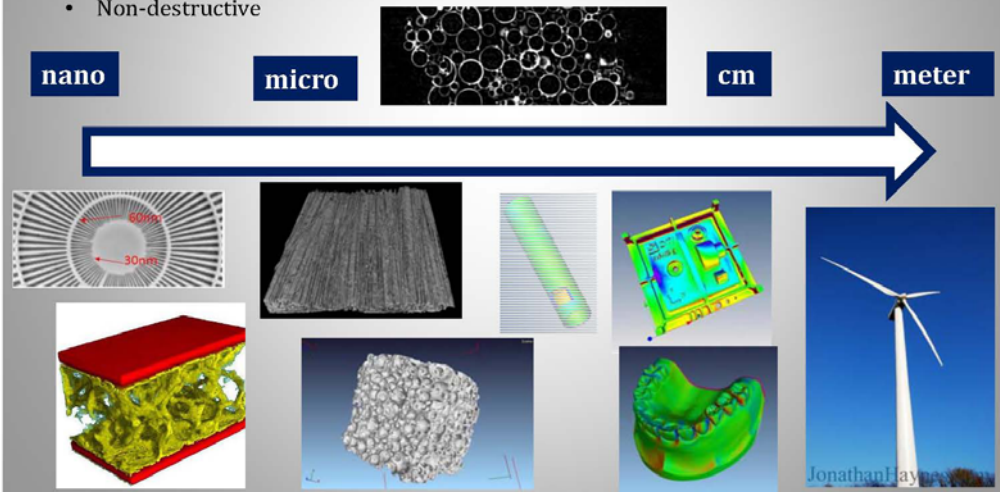


Characterization on all length scales - CT Scanning



Industrial CT Scanning in combination with μ CT

- From micro to cm range
- Low density material
- Complex geometry
- Non-destructive



METROLOGY & QUALITY ASSURANCE



Maria Holmberg

PhD, Senior Consultant

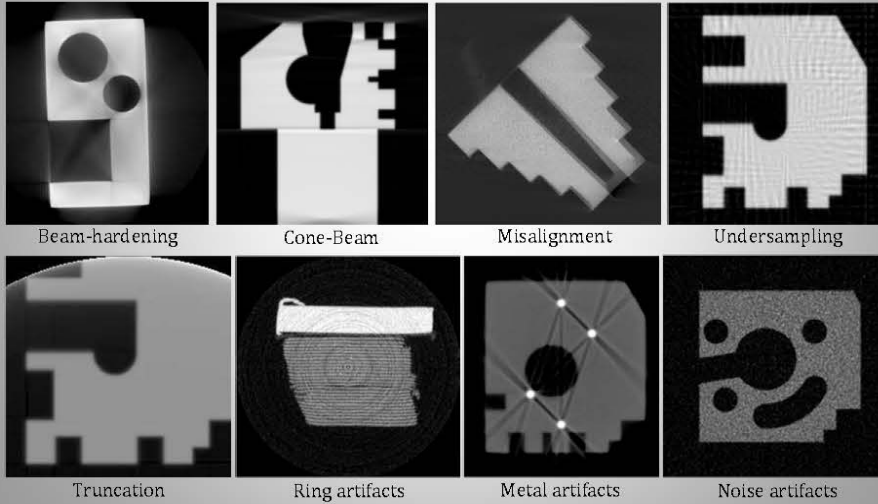
Metrology and Quality Assurance
Production
Danish Technological Institute
Gregersensvej 8B
DK-2630 Taastrup
Denmark

+45 72 20 30 06

mahg@teknologisk.dk
www.teknologisk.dk

CT SCANNING

Image artifacts

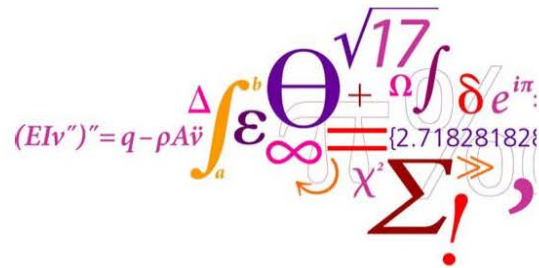


Determining geometrically necessary dislocation densities by EBSD

Philip Littlewood, DTU Mekanik

Determining geometrically necessary dislocation densities by EBSD

Philip Littlewood



DTU Mechanical Engineering
Department of Mechanical Engineering

Overview

- Theoretical basis for determining dislocation density by EBSD
- Cross-correlation method for EBSD patterns
- Application to deformed Ti alloys

DETERMINING DISLOCATION DENSITIES BY EBSD

3 DTU Mechanical Engineering, Technical University of Denmark Determining geometrically necessary dislocation densities by EBSD 17/01/2013

Dislocation and Curvature Tensors

- Dislocation Tensor [1]:

$$\alpha_{ij} = \sum n b_i r_j$$

- Relationship between Dislocation and Curvature Tensors (with/without elastic strain) [1,2]

$$\alpha_{ij} = \kappa_{ji} - \delta_{ij} \kappa_{kk}$$

$$\kappa_{pi} = -\alpha_{ip} + \frac{1}{2} \delta_{pi} \alpha_{kk} + e_{pjk} \epsilon_{ik,j}^{el}$$

[1] J. F. Nye. *Acta Metallurgica*, 1:153-162, 1953.

[2] E. Kröner. *Continuum Theory of Dislocations and Self Stresses*. Springer, Berlin, 1958.

4 DTU Mechanical Engineering, Technical University of Denmark Determining geometrically necessary dislocation densities by EBSD 17/01/2013

Limitations on Determining Dislocation Densities with EBSD

- Only dislocations contributing to lattice curvature (GNDs) can be detected
 - Dipoles, other multipoles are “invisible” (SSD)
- Dislocation tensor gives only nine equations
 - Systems other than simple cubic have too many dislocation types – no unique solution
 - Linear programming can be used to generate lower-bound solutions [1]
- Surface nature of EBSD makes information unavailable
 - Z-components of curvature cannot be measured
 - 5 components of dislocation tensor & difference of two others can be derived [2]
 - Can be overcome by 3D FIB-EBSD [3]

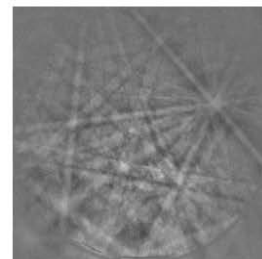
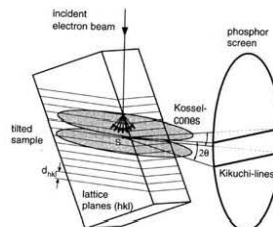
[1] S. Sun, B.L. Adams, C. Shet, S. Saigal, W. King. Scripta Materialia, 39:501-508, 1998.

[2] W. Pantleon. Scripta Materialia 58:994-997, 2008.

[3] E. Demir, D. Raabe, N. Zaafarani, S. Zaefferer. Acta Materialia, 57:559-569, 2009.

Cross-Correlation-Based GND Measurement

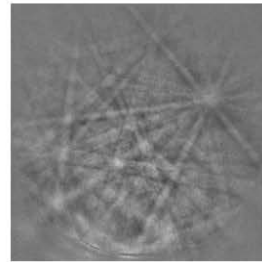
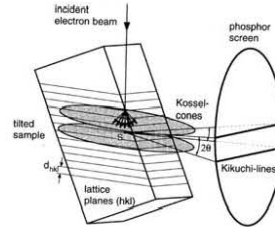
- Standard EBSD error is $\sim 1^\circ$
 - Magnified in calculations of misorientation
 - Cross-correlation method [1] was developed to improve resolution
- Distortion of crystal lattice causes shifts in EBSD patterns
 - Crystal distortion can be measured by measuring the shifts
 - Hydrostatic strains do not realign crystal planes and cannot be detected



[1] A. J. Wilkinson, G. Meaden, D. Dingley. Ultramicroscopy 106:307-313, 2006.

Cross-Correlation-Based GND Measurement

- Standard EBSD error is $\sim 1^\circ$
 - Magnified in calculations of misorientation
 - Cross-correlation method [1] was developed to improve resolution
- Distortion of crystal lattice causes shifts in EBSD patterns
 - Crystal distortion can be measured by measuring the shifts
 - Hydrostatic strains do not realign crystal planes and cannot be detected



[1] A. J. Wilkinson, G. Meaden, D. Dingley. Ultramicroscopy 106:307-313, 2006.

Calculating GND densities from pattern shifts

- A reference pattern is divided into regions
- Shifts of each region are measured at each point
- One region gives two equations:

$$r_1 r_3 \left[\frac{\partial u_1}{\partial x_1} - \frac{\partial u_3}{\partial x_3} \right] + r_2 r_3 \frac{\partial u_1}{\partial x_2} + r_3^2 \frac{\partial u_1}{\partial x_3} - r_1^2 \frac{\partial u_3}{\partial x_1} - r_1 r_2 \frac{\partial u_3}{\partial x_2} = Q_1 r_3$$

$$r_2 r_3 \left[\frac{\partial u_2}{\partial x_2} - \frac{\partial u_3}{\partial x_3} \right] + r_1 r_3 \frac{\partial u_2}{\partial x_1} + r_3^2 \frac{\partial u_2}{\partial x_3} - r_2^2 \frac{\partial u_3}{\partial x_2} - r_1 r_2 \frac{\partial u_3}{\partial x_1} = Q_2 r_3$$

- Measuring 4 regions allows 8 elements of distortion tensor to be derived
 - 9th element must be derived from boundary conditions
 - More than 4 regions allows least-squares fitting to improve accuracy

APPLICATION: FATIGUE IN TITANIUM ALLOYS

9

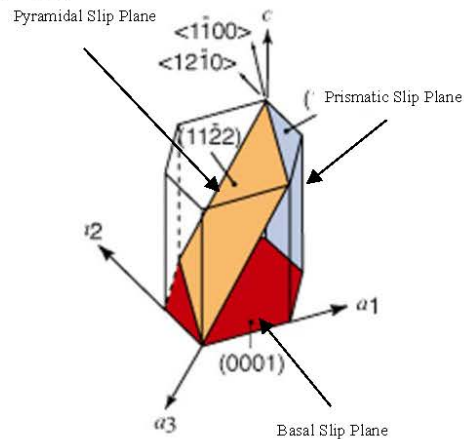
DTU Mechanical Engineering, Technical University of Denmark

Determining geometrically necessary dislocation densities by EBSD

17/01/2013

Crystallography of Ti-6Al-4V

- Two phases: HCP α and BCC β
 - Ti-6Al-4V as received is mostly α
- Three main slip planes in α
 - Slip along \mathbf{a} $\langle 11\bar{2}0 \rangle$ and $\mathbf{c}+\mathbf{a}$ $\langle 11\bar{2}3 \rangle$ directions
 - $\mathbf{c}+\mathbf{a}$ requires higher stress to activate ($\sim 3\text{--}4\times$)



<http://web.earthsci.unimelb.edu.au/wilson/ice1/introduction.html>

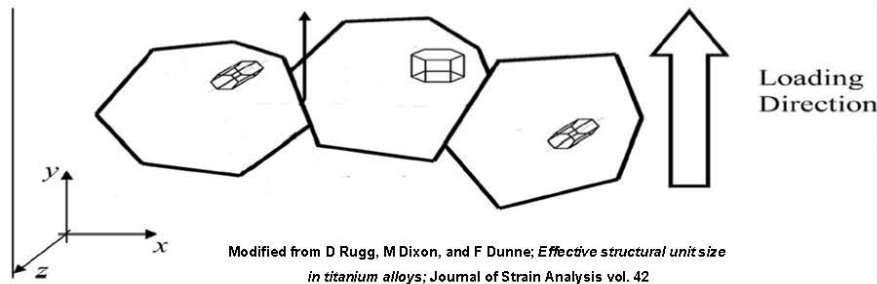
10

DTU Mechanical Engineering, Technical University of Denmark

Determining geometrically necessary dislocation densities by EBSD

17/01/2013

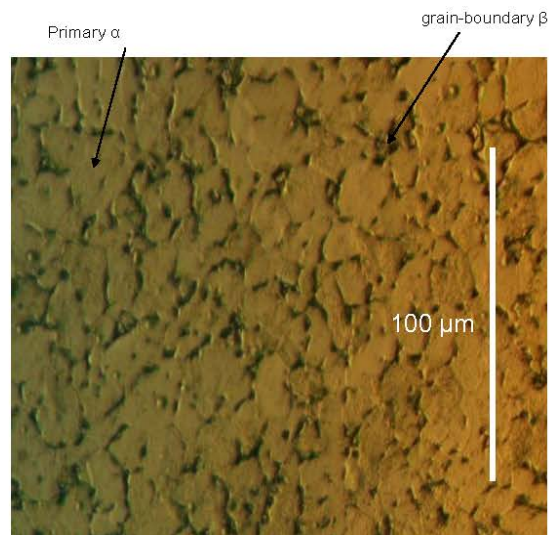
Crystal Anisotropy



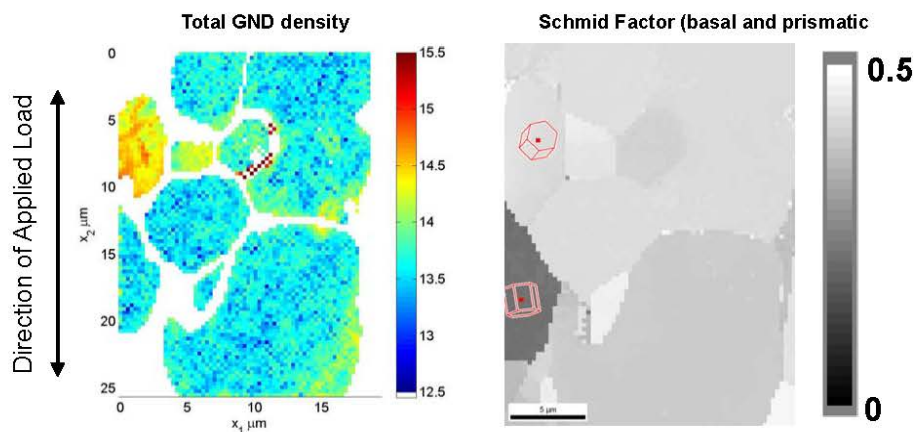
- No resolved shear stress on basal/prismatic planes in center grain
- Grain becomes resistant to plastic deformation relative to others

Fatigue Testing

- Material: Ti-6Al-4V rolled bar stock provided by Rolls-Royce
 - Globular primary α -phase grains, small amount of grain-boundary β phase
 - Average grain size $\sim 12 \mu\text{m}$
- Deformed in fatigue to failure
 - Peak stress 900 MPa, stress ratio 0.1
- Cross-correlation EBSD used to measure GND distributions



Relating GND Densities to Microstructure

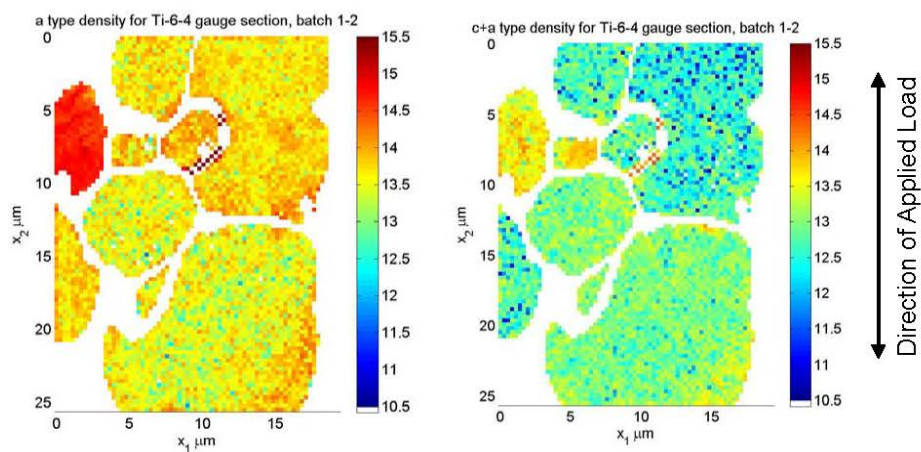


13 DTU Mechanical Engineering, Technical University of Denmark

Determining geometrically necessary dislocation densities by EBSD

17/01/2013

a vs c+a GND densities



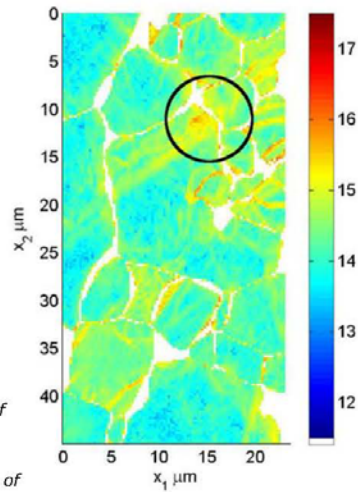
14 DTU Mechanical Engineering, Technical University of Denmark

Determining geometrically necessary dislocation densities by EBSD

17/01/2013

GND Pile-Up

- First proposed as a crack initiation method by Stroh [1]
- Suggested by Bache and Evans as a mechanism in cold-dwell sensitivity [2]



[1] A. N. Stroh. *Proceedings of the Royal Society of London. Series A, Mathematical and Physical Sciences*, 223:404-414, 1954.

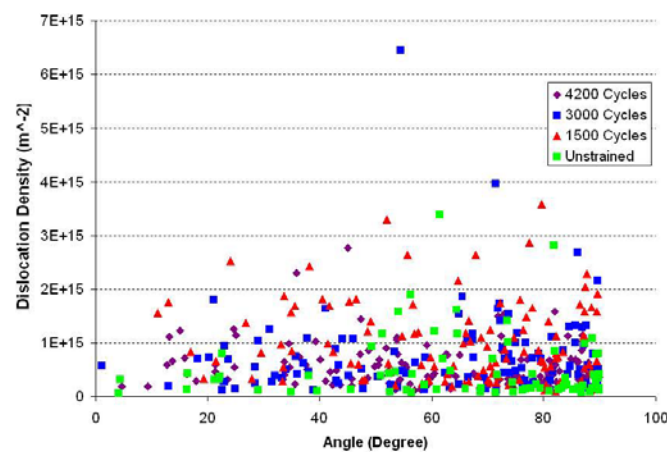
[2] W. J. Evans, M. R. Bache. *International Journal of Fatigue*, 16:443-452, 1994.

15 DTU Mechanical Engineering, Technical University of Denmark

Determining geometrically necessary dislocation densities by EBSD

17/01/2013

GND Statistics

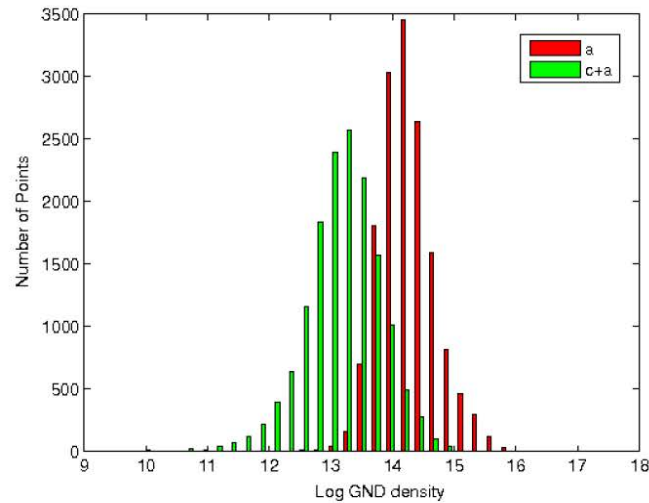


16 DTU Mechanical Engineering, Technical University of Denmark

Determining geometrically necessary dislocation densities by EBSD

17/01/2013

GND Statistics



17 DTU Mechanical Engineering, Technical University of Denmark

Determining geometrically necessary dislocation densities by EBSD

17/01/2013

Conclusions

- Cross-correlation based EBSD can be used to study storage of geometrically necessary dislocations on a microstructural level
- Grain-grain interactions play a significant role in inhomogeneous deformation in Ti-6Al-4V
 - No direct link between crystal orientation and GND density
- Dislocation pile-up along a slip band, and slip penetration into a neighbouring grain, have been observed.

18 DTU Mechanical Engineering, Technical University of Denmark

Determining geometrically necessary dislocation densities by EBSD

17/01/2013

Transformation af udskillelser på atomar skala

Hilmar Danielsen, DTU Mekanik

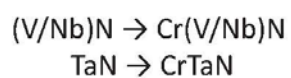
Transformation af udskillelser på atomar skala

Hilmar K. Danielsen
DTU Mekanik



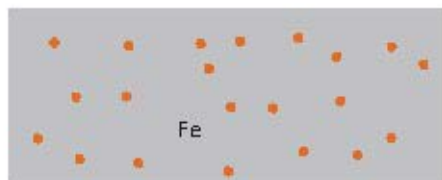
M = V, Nb or Ta

Two different 12%Cr martensitic steels investigated:

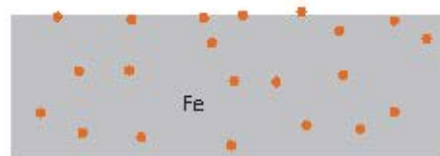


Fremstilling af prøver til TEM (carbon extraction replica)

Udgangspunkt



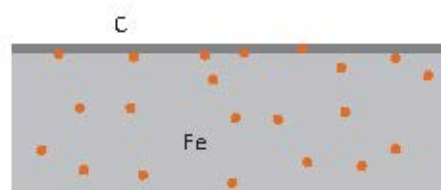
Ætsning



Ætsning

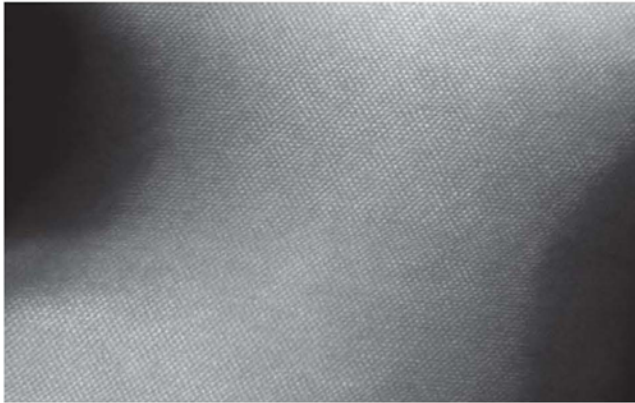


Kulpåddampning

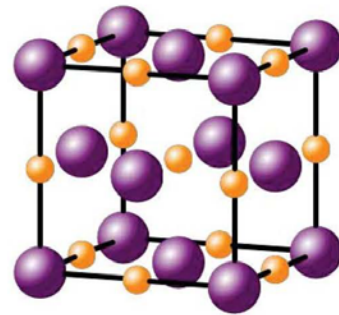


Investigations performed using FEI TITAN 300KV analytical TEM
with High Angle Annular Dark Field (HAADF)

MN (VN, NbN, TaN)

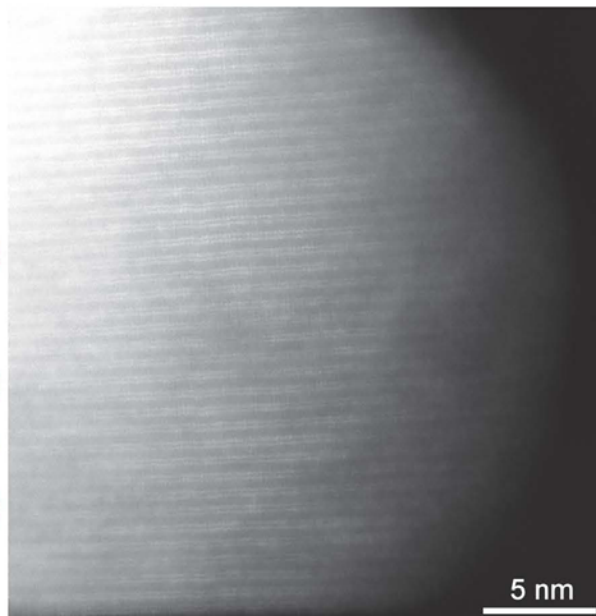
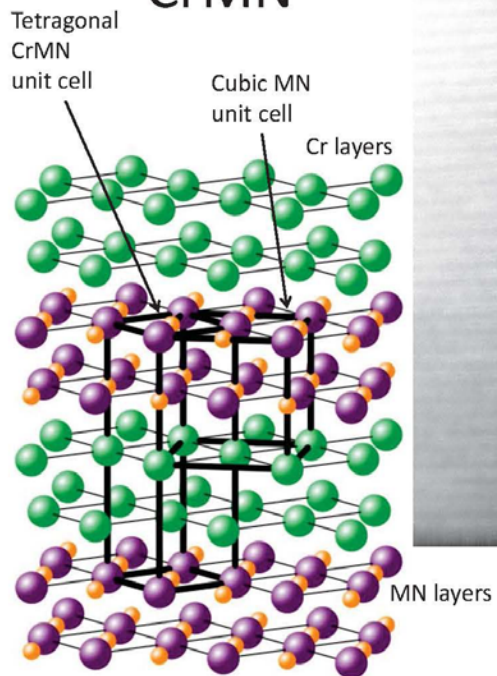


HAADF billede af (V,Nb)N



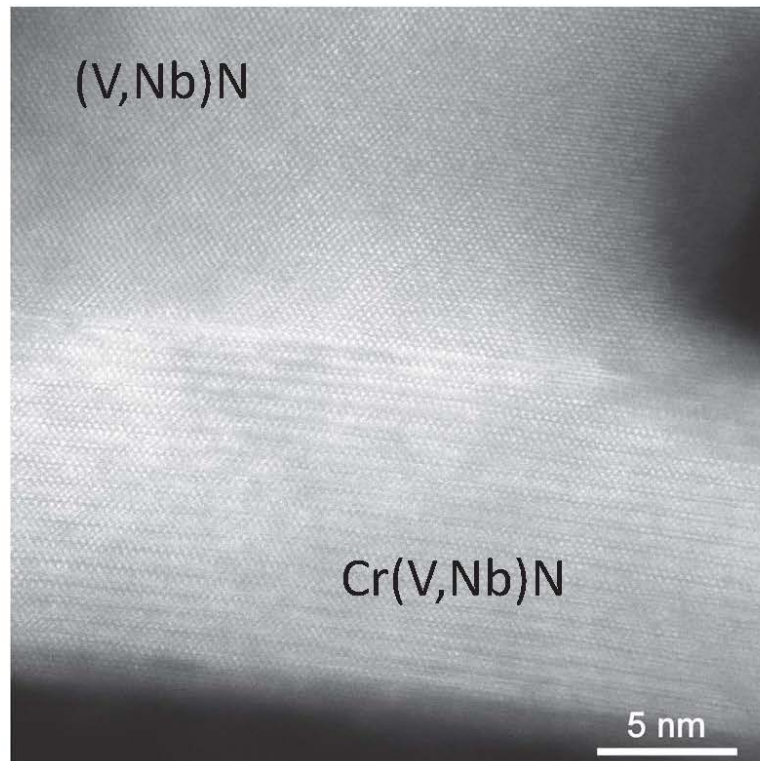
NaCl type enhedscele

CrMN

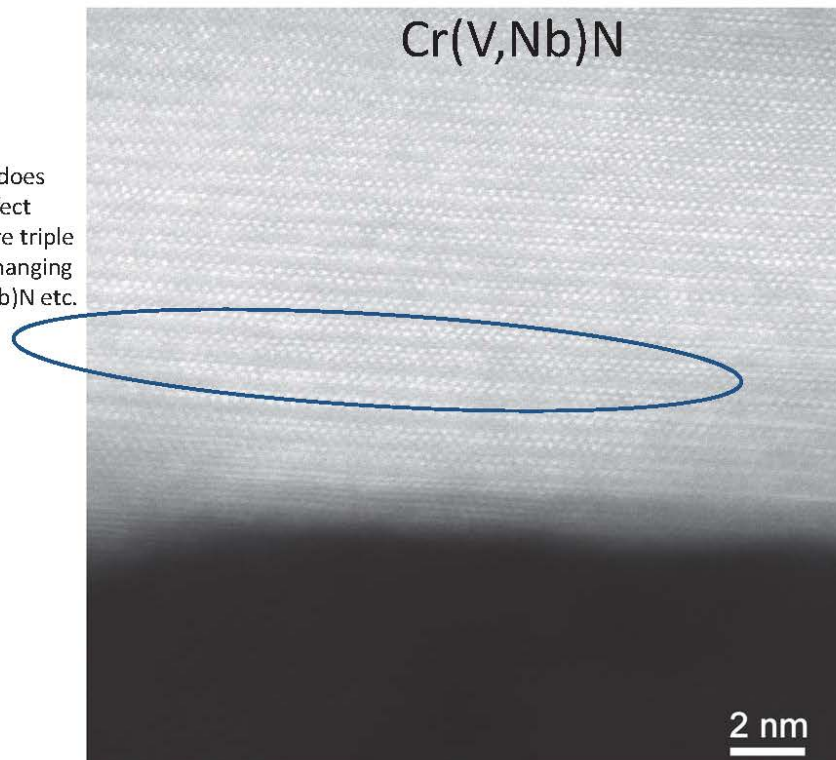


High resolution image of Cr(V,Nb)N showing double layered structure.

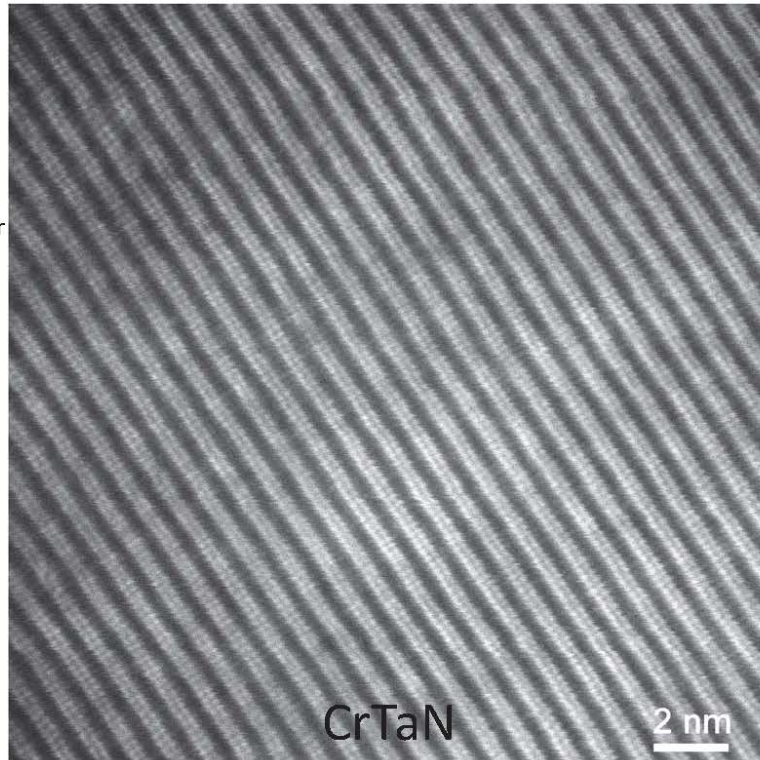
The cubic MN and tetragonal CrMN are bound together as one particle, it is possible to follow the atomic layers through the "interface".



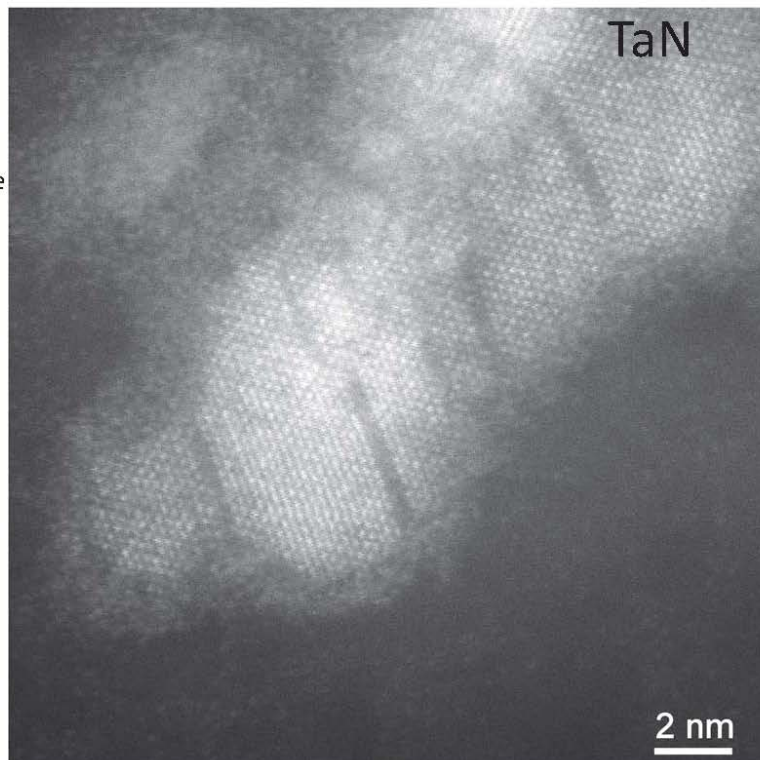
The Cr(V,Nb)N does not have a perfect lattice, there are triple layers, layers changing from Cr to (V,Nb)N etc.

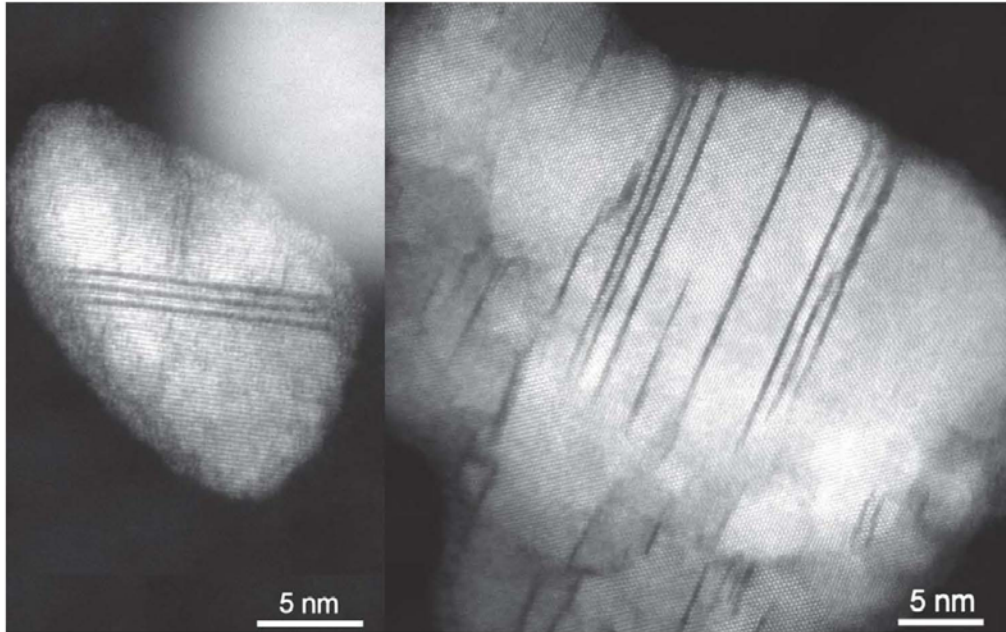


CrTaN has much clearer contrast as Ta atoms are very heavy compared to Cr atoms. Ta atoms are clearly visible while the Cr atoms are very dark.

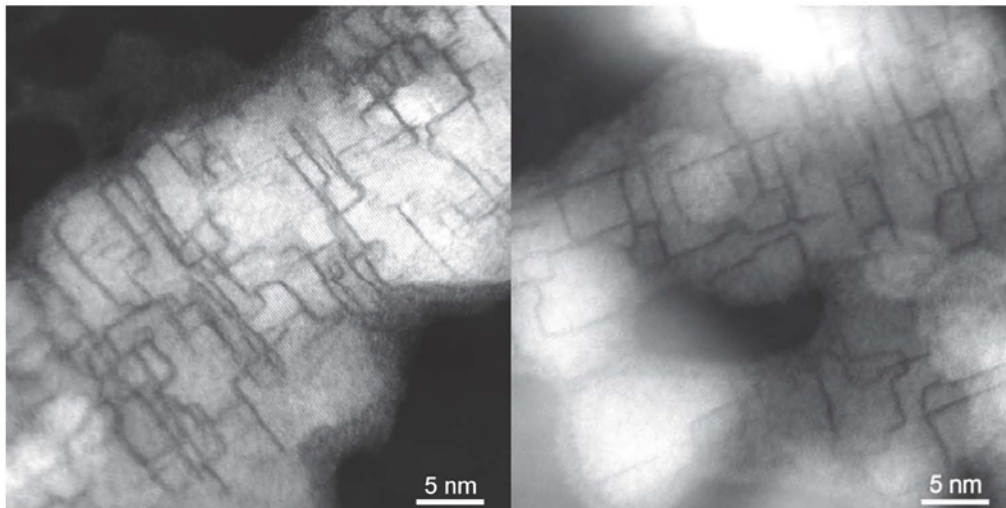


Cr atoms arrange themselves as double layers (dark lines)



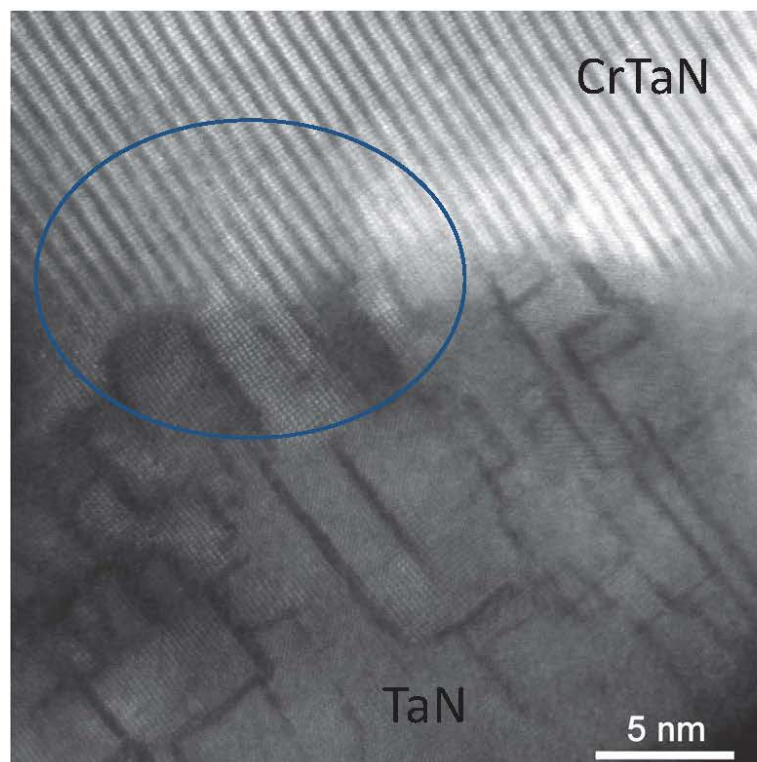


Transformation with a clear orientation relationship
 Cr double layers appear as straight parallel lines through the TaN crystal structure

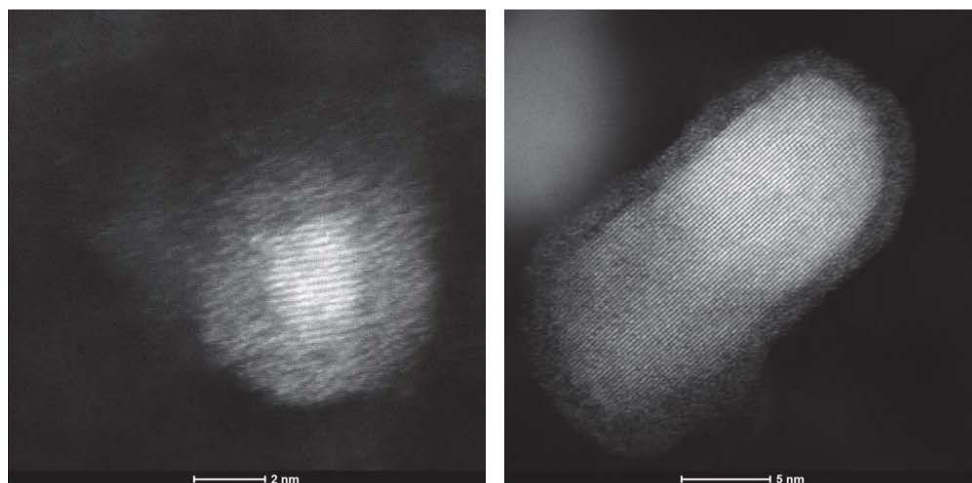


Transformation with a chaotic orientation relationship
 Cr double layers have not decided upon the orientation of the future tetragonal crystal

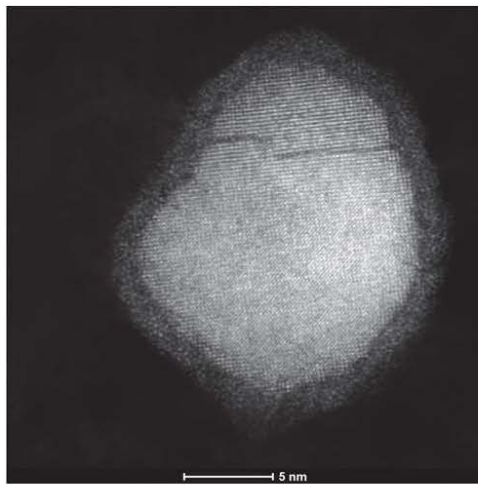
Interface between
CrMN and MN. The
crystal structure can
be followed from one
region to the other.



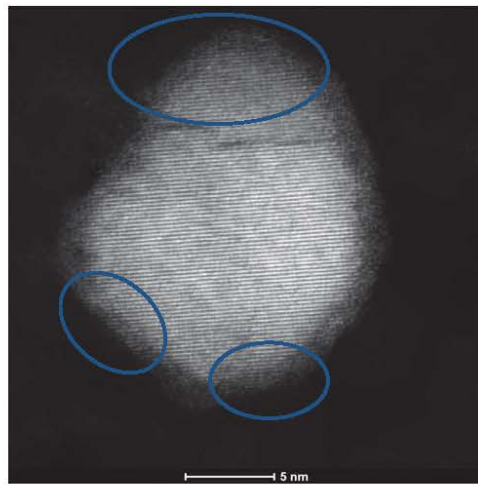
TaN particles with amorphous layer



Areas where the electron beam has been concentrated crystallize

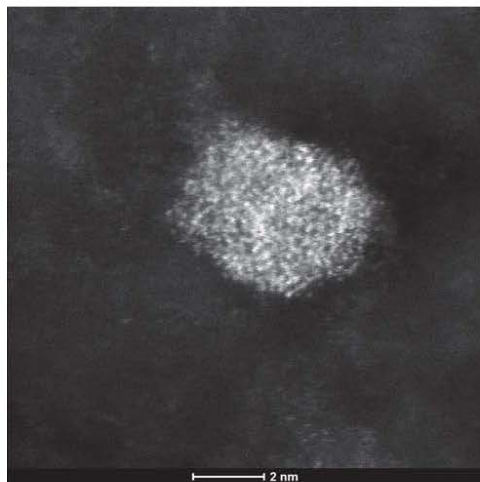


Before

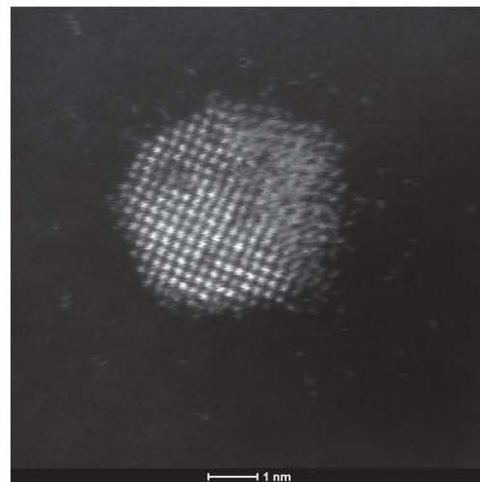


After

Entire interface crystallising after electron beam exposure

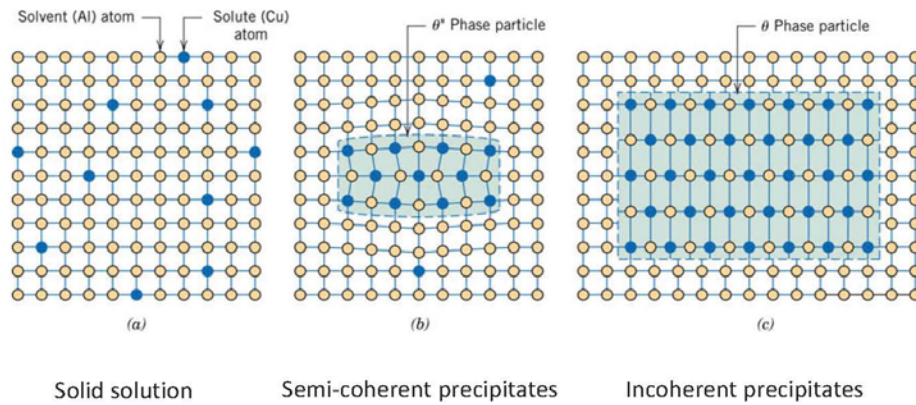


Before

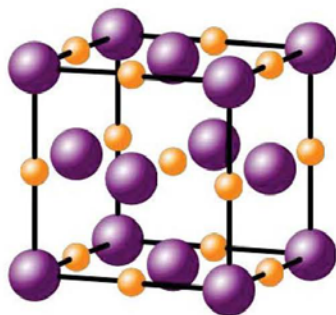


After

Precipitate interfaces



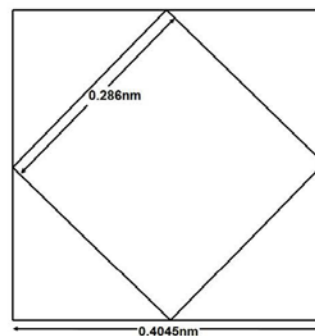
Semi and incoherent MN



Lattice parameters

VN: 0.413 nm	misfit: 2%
NbN: 0.439nm	misfit: 9%
TaN: 0.440nm	misfit: 9%

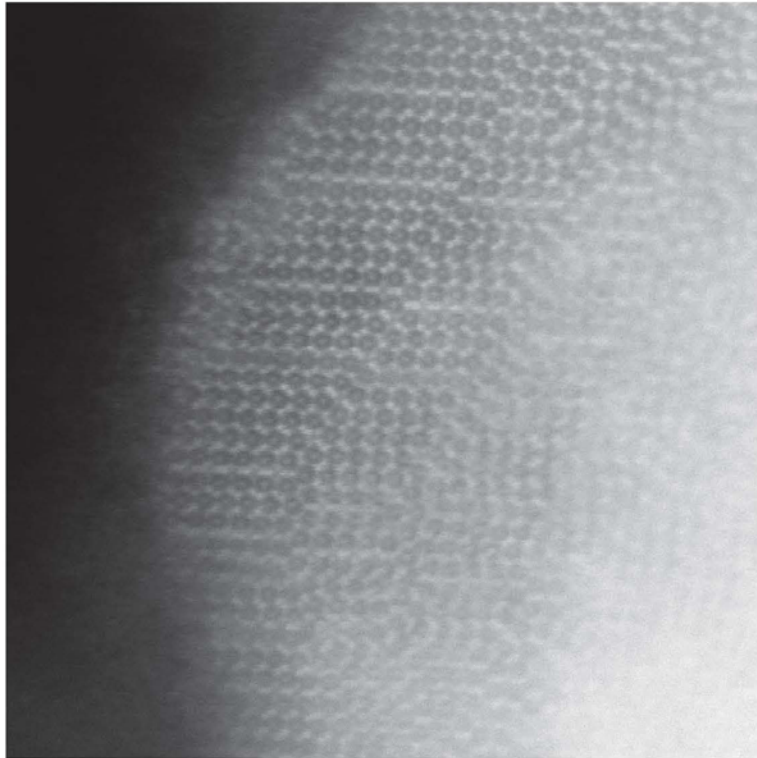
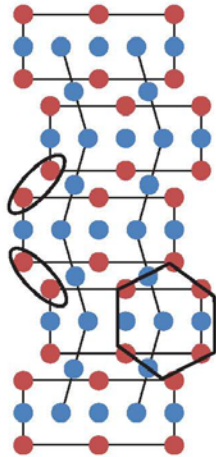
Baker-nutting relationship



no amorphous layer
amorphous layer
amorphous layer

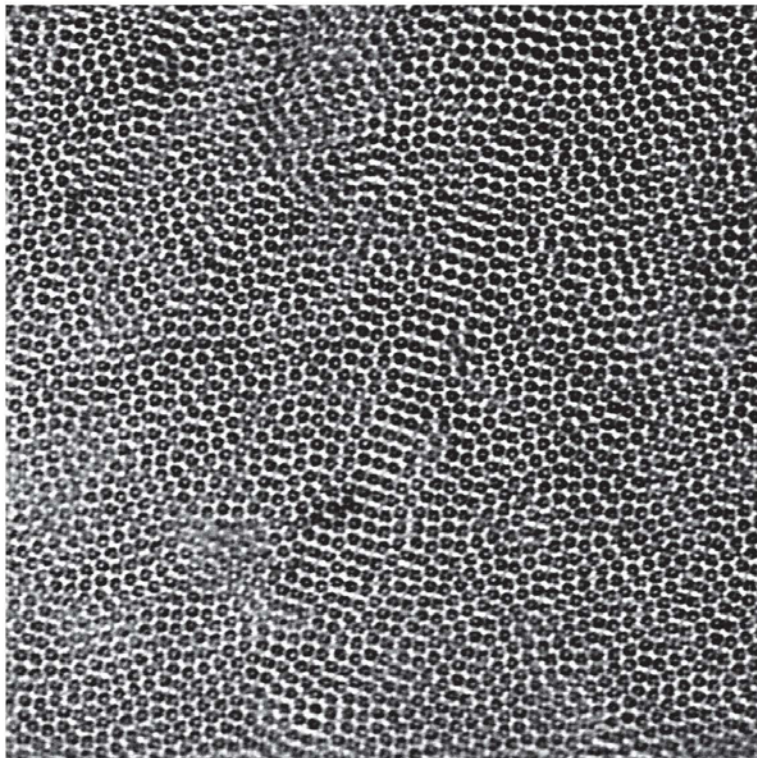
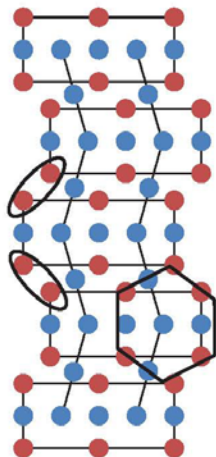
Edge of a large
 Fe_2W particle

● W
● Fe



Small Fe_2W
particle (thin)

● W
● Fe



Konklusion

- TaN kan transformere deres sammensætning og krystalstruktur til en anden type partikler
- Partikler kan have en meget uordnet krystalstruktur
- På atomar skala er vores prøver lette at påvirke (elektron stråle, ætsning osv)

Structure and Chemical Characterization by Electron Microscopy – Spanning the micro and nano regime

Jakob Birkedal Wagner, DTU CEN

Structural and Chemical Characterization by Electron Microscopy – Spanning the micro and nano regime

Jakob B. Wagner

Acknowledgements:

DTU Cen, Technical University of Denmark:
Hossein Alimadadi, Christian D. Damsgaard, Thomas W. Hansen

EPFL:
Quentin Jeangros

FEI:
Jörg Jinschek

DTU Cen
Center for Electron Nanoscopy

1

DTU Cen, Technical University of Denmark

DTU Center for Electron Nanoscopy

- Realized by a generous donation from the A.P. Møller og Hustru Chastine Mc-Kinney Møller's Fond til Almene Formaal
- DKK 100,000,000 ~ €14,000,000
- Grant announced In January 2006
- "Establish a World Class Facility with a unique suite of advanced electron microscopes, in a purpose-built building"
- Inaugurated In December 2007
- Hosting 7 electron microscopes
 - 2 high-end TEM (1 ETEM)
 - 1 work horse TEM
 - 2 dual beam SEM/FIB
 - 2 SEM



2

DTU Cen, Technical University of Denmark

FEI Microscopes at DTU Cen

- SEMs
 - Inspect 'S'
 - Workhorse
 - EDX/WDS
 - Quanta 3D FIB/SEM
 - Sample prep
 - Quanta 200 FEG
 - High res
 - Cryo
 - EDX
 - Helios Nanolab FIB/SEM
 - EBSD
 - EDX
- TEMs
 - Tecnai T20 G2
 - Workhorse
 - EDX/GIF
 - Titan 80-300 probe corrected
 - Holography
 - EDX/GIF
 - Titan 80-300 image corrected
 - ETEM
 - EDX/GIF

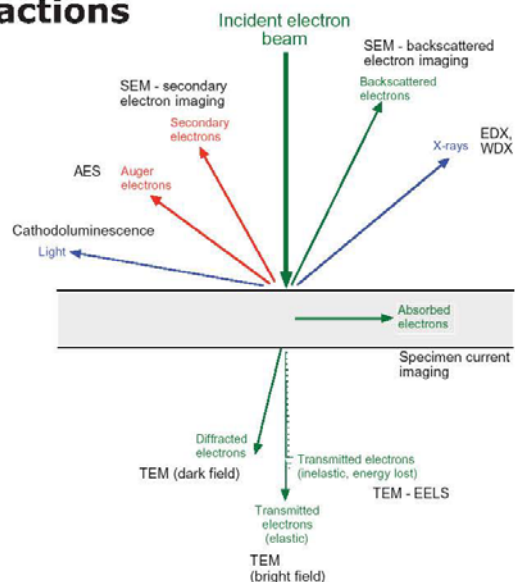
More info on the web: www.cen.dtu.dk

3

DTU Cen, Technical University of Denmark

Image Formation (at all scales) -Beam-specimen interactions

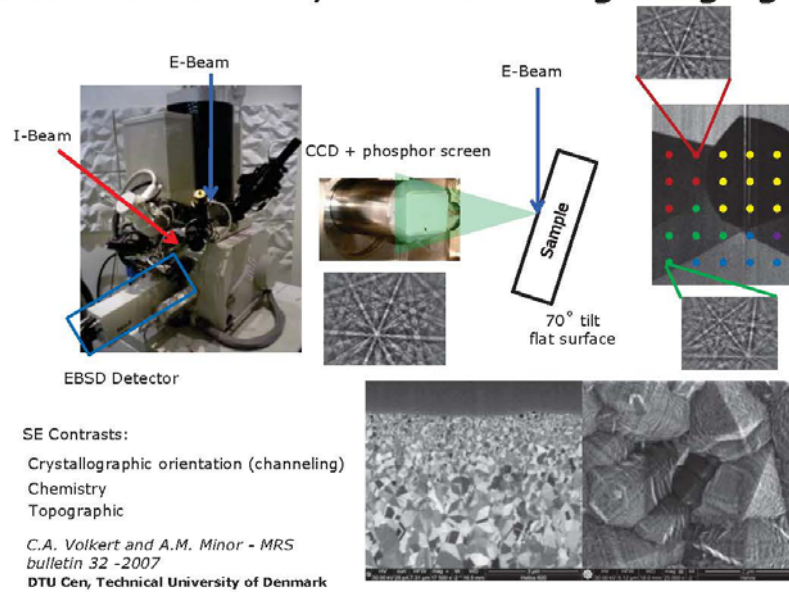
- The fast electrons is focused and controlled easily by electro-magnetic lenses
- Interaction between fast electrons and matter creates a variety of signals



4

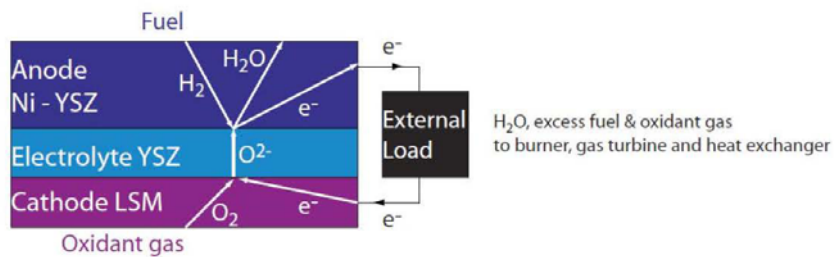
DTU Cen, Technical University of Denmark

Dual Beam: EBSD, ion channeling imaging

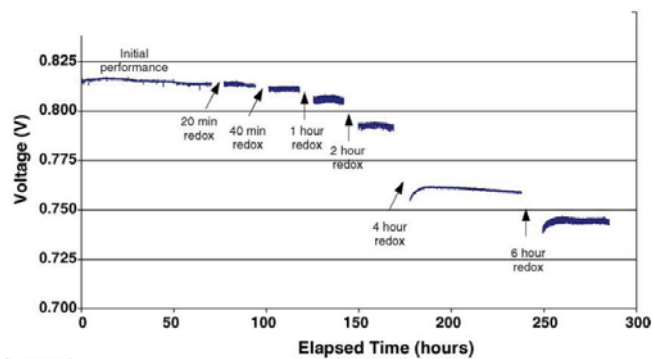


5

Failure of Solid Oxide Fuel Cells



- Fuel Cell Anode Failure
 - Redox stability of NiO/YSZ based anode

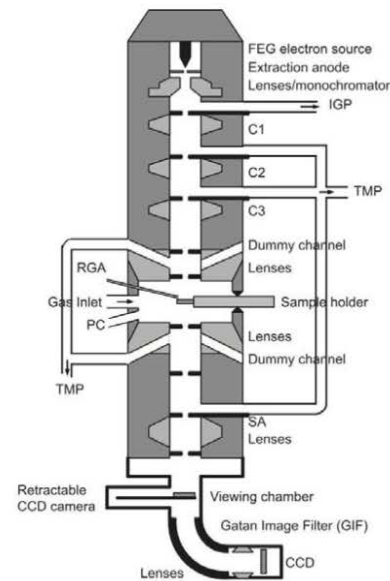


12

DTU Cen, Technical University of Denmark

Environmental TEM

- C_s Image Corrector & Monochromator. E-cell
- Installed gas lines: N_2 , He, Ar, O_2 , H_2 , CO, CO_2 , CH_4 & H_2O
- Possible to attach other (premixed) gases
- Full control of composition using mass flow controllers
- Total pressure in E-Cell: up to 2000Pa
- Temperature depends on heating holder, gas pressure and gas composition (Example: approx. $700^\circ C$ @ 100Pa H_2)
- Dynamic acquisition (at the moment 5 frames/s)
- EELS of gases possible



T. W. Hansen, J. B. Wagner and R. E. Dunin-Borkowski, *Mater. Sci. Technol.*, 26, 1338 (2010)

13

DTU Cen, Technical University of Denmark

Imaging at Different Length Scales

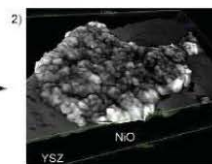
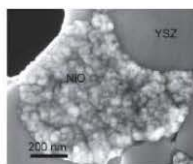
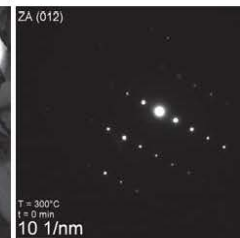
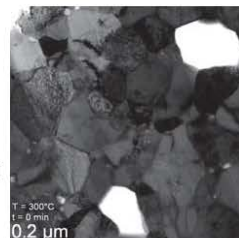
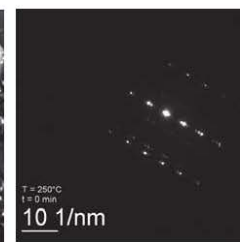
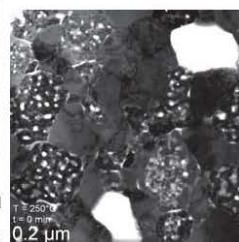
-2D to 3D and irreversible changes

ETEM sample

FIB slice of NiO_x/YSZ based SOFC

Complementary and dynamic information from multiple facilities on the same sample is needed

SEM sample

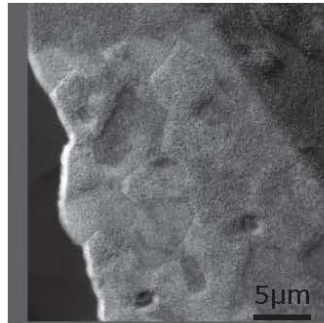
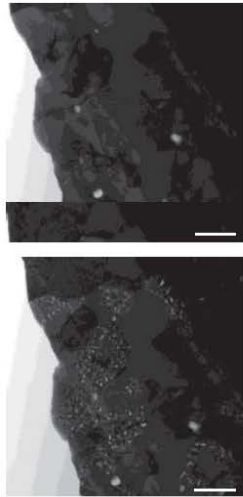

Reduction
150Pa H_2

Oxidation
320Pa O_2


Q. Jeangros et al., *Acta Materialia* 58 (2010) 4578–4589

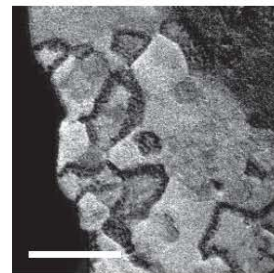
14

DTU Cen, Technical University of Denmark

Elemental mapping (oxygen)



310 °C → 430 °C in 150 Pa H₂

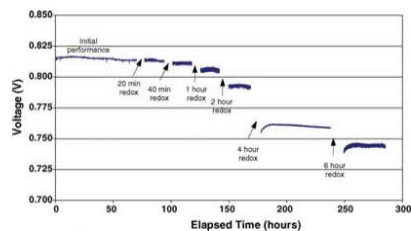
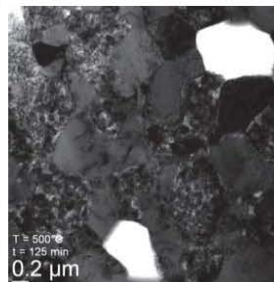
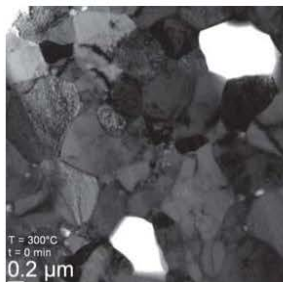


15

DTU Cen, Technical University of Denmark

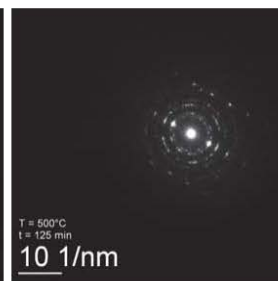
From Structure to Application

Q. Jeangros et al., Acta Materialia 58 (2010) 4578–4589



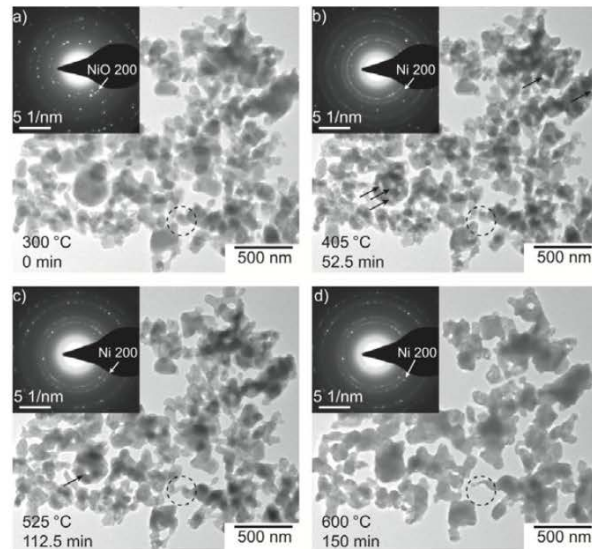
16

DTU Cen, Technical University of Denmark



Deeper insight in Nickel reduction using model system

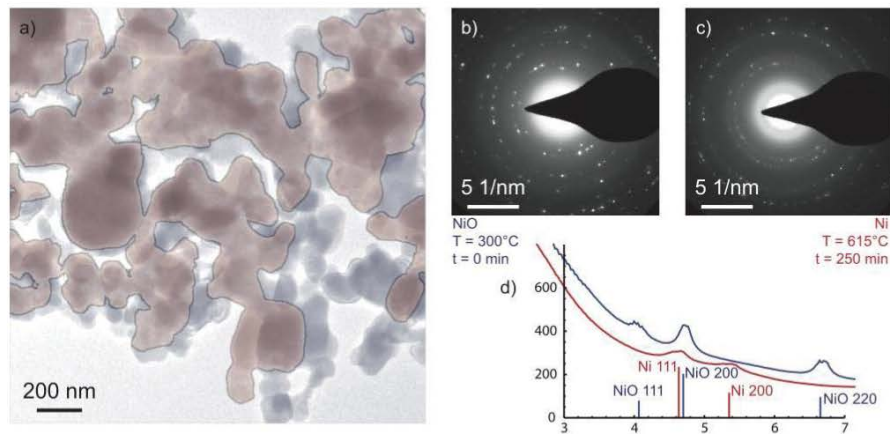
- NiO crystals
- 130Pa H₂



17

DTU Cen, Technical University of Denmark

Evolution during reduction



- In situ reduction in 130Pa H₂

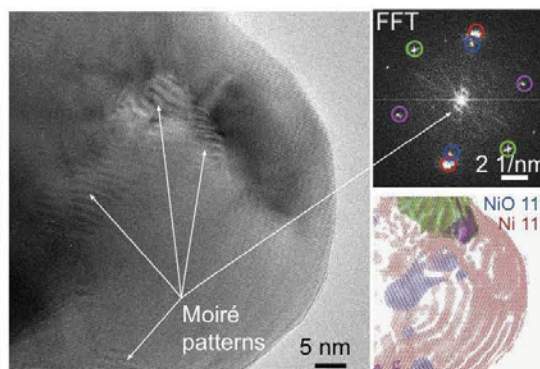
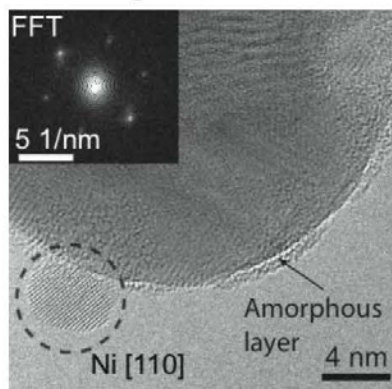
Q. Jeangros et al., J. Mat. Sci. DOI 10.1007/s10853-012-7001-2

18

DTU Cen, Technical University of Denmark

High Resolution ETEM

- Atomic arrangement visualized at 500 °C in 130Pa H₂



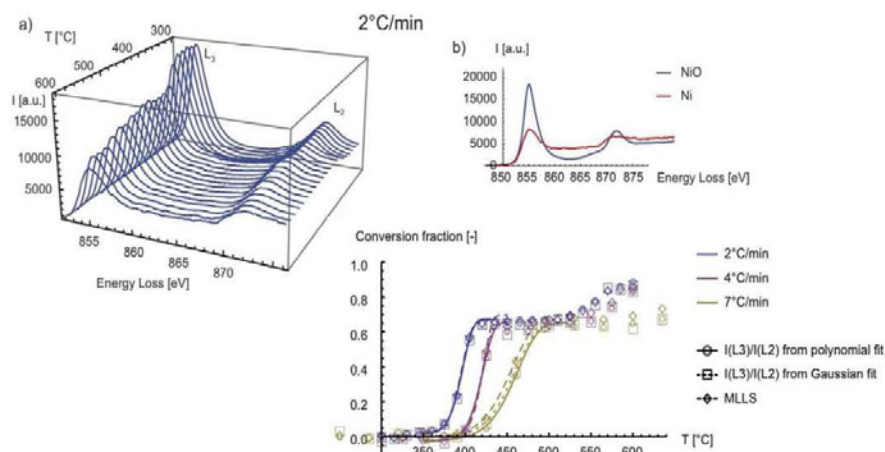
- Moiré and diffraction at 600 °C in 130Pa H₂

Q. Jeangros et al., J. Mat. Sci. DOI 10.1007/s10853-012-7001-2

19

DTU Cen, Technical University of Denmark

Determination of Activation Energies - Spectroscopical Analysis



E_a (NiO to Ni) = 70 ± 5 kJ/mol

Similar results obtained from diffraction analysis

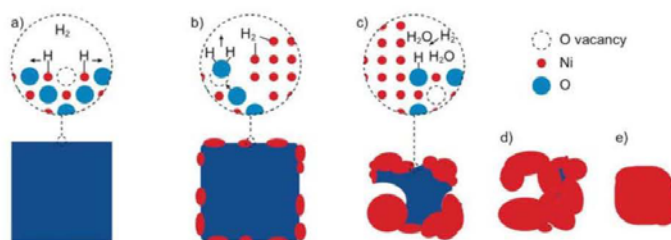
Q. Jeangros et al., J. Mat. Sci. DOI 10.1007/s10853-012-7001-2

20

DTU Cen, Technical University of Denmark

Methodology

- A complete dataset using different tools and techniques can be acquired
 - Different length scales
 - Different types of information (crystallographic, morphology, chemical, etc.)
- From analysis of such a dataset a coherent understanding of the process can be obtained

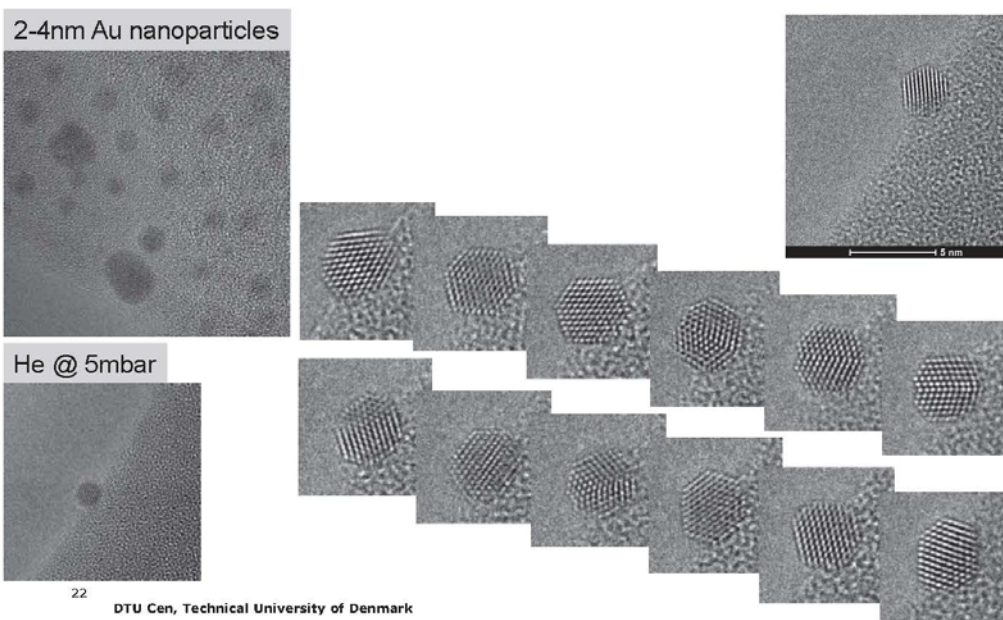


Q. Jeangros et al., J. Mat. Sci. DOI 10.1007/s10853-012-7001-2

21

DTU Cen, Technical University of Denmark

Nanoparticle mobility

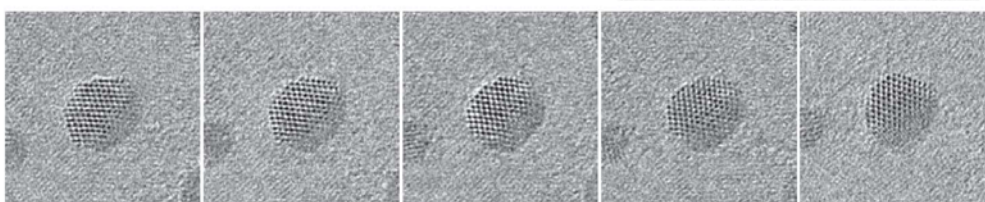
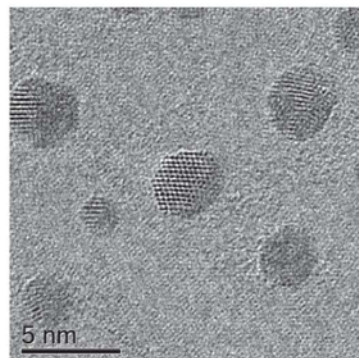


22

DTU Cen, Technical University of Denmark

Au/Graphene

- Ca. 4x real time
- RT, Vacuum: Particles are mainly immobile
- Slight rotations are observed
- Coalescence events occur, but equilibrium shapes are only slowly obtained
- Surface reconstruction occurs
- All movies recorded at same beam current density (ca. 1A/cm²)

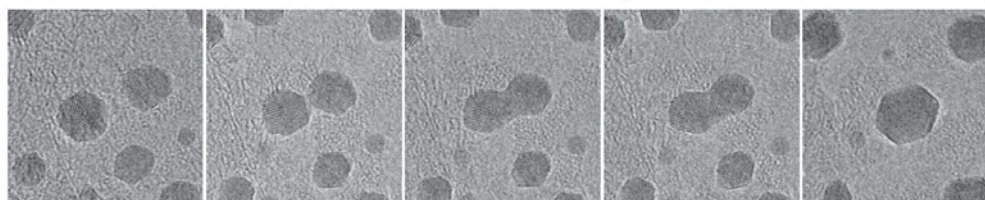
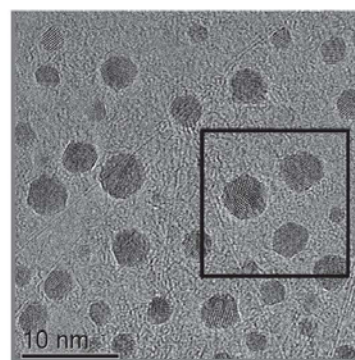


23

DTU Cen, Technical University of Denmark

Au/Graphene

- Ca. 8x real time
- 104°C, 200Pa H₂
- Cross correlation used for image alignment
- At low temperatures, particles wobble around equilibrium positions, but do not tend to migrate long distances
- Particles in close proximity can coalesce into single particles, but do not readily form single crystalline structures

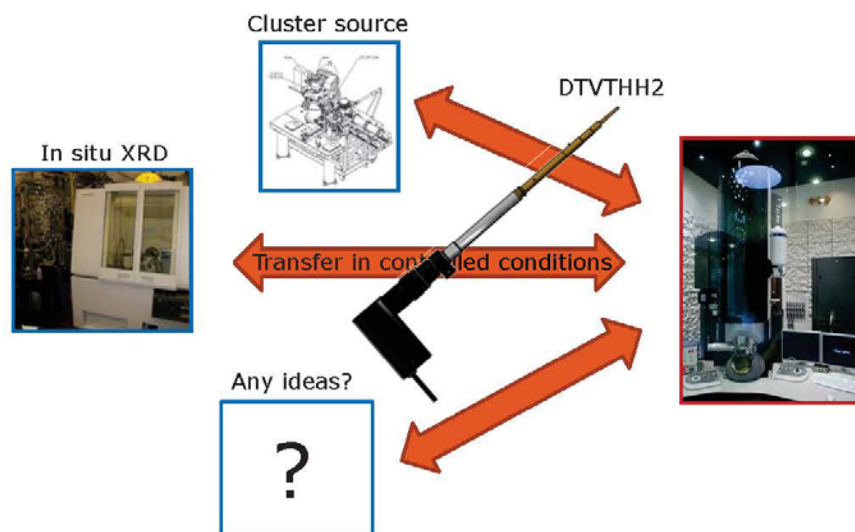


24

DTU Cen, Technical University of Denmark

Outlook – longer term

Combining complimentary characterization and sample prep. techniques with TEM

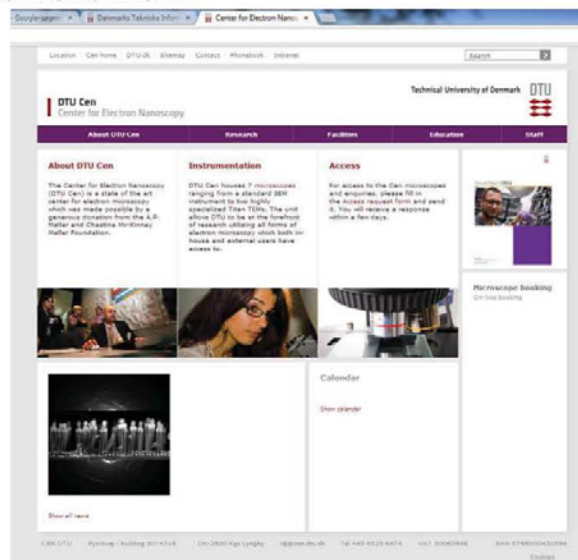


25

DTU Cen, Technical University of Denmark

Interested in collaboration?

- Please contact us at [cen.dtu.dk](mailto:cen@dtu.dk)



26

DTU Cen, Technical University of Denmark

Nanostruktur og styrke af stål deformeret ved valsning og med shot peening

Niels Hansen, DTU Vindenergi

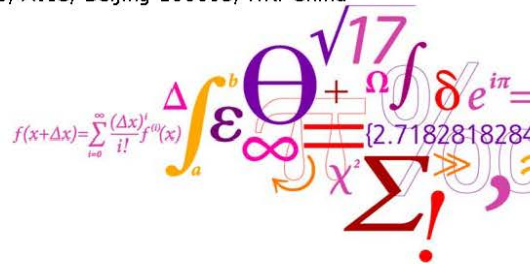
Dansk Metallurgisk Selskabs Vintermøde 2013

Nanostruktur og styrke af stål deformeret ved valsning og ved shot peening

N. Hansen¹, X.D. Zhang¹, Y. Gao², X. Huang¹

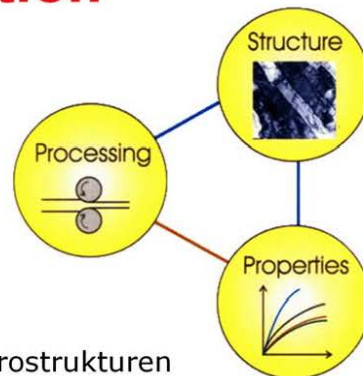
¹Danish-Chinese Center for Nanometals, Wind Energy Department, Technical University of Denmark, Campus Risø, DK-4000 Roskilde, Denmark

²Beijing Institute of Aeronautical Materials, AVIC, Beijing 100095, P.R. China



DTU Wind Energy
Department of Wind Energy

Plastisk deformation



Generelle principper

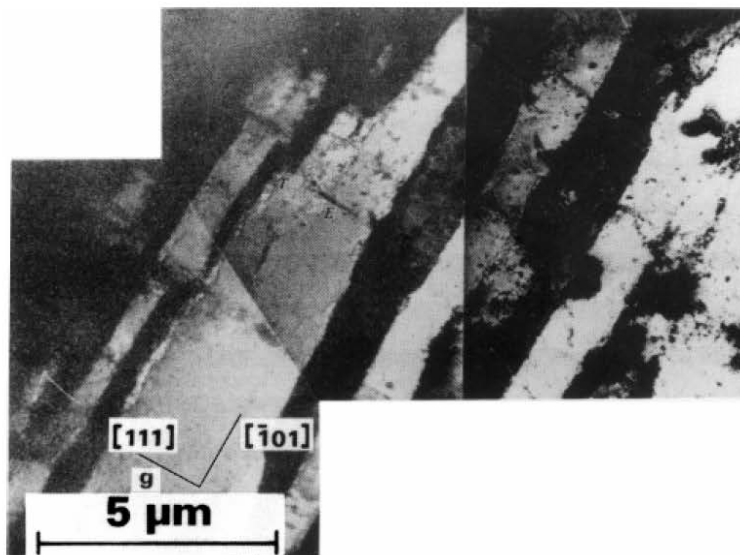
- Plastisk deformation forfiner mikrostrukturen
- En finere mikrostruktur følges af højere styrke
- Høj styrke kan opnås gennem kraftig plastisk deformation

Evolution of deformation microstructures

Subdivision of grains/crystals by dislocation boundaries in characteristic 2D and 3D configurations.

3 DTU Wind Energy, Technical University of Denmark

Carpet structure in Cu



4 DTU Wind Energy, Technical University of Denmark

Cell structure in Fe



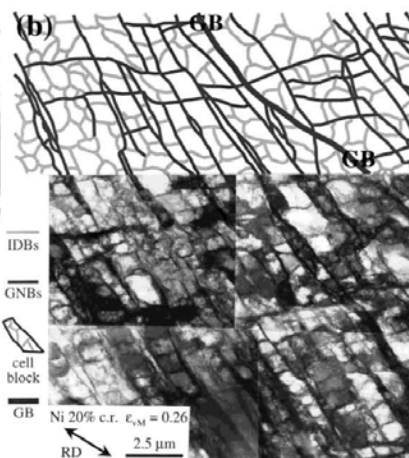
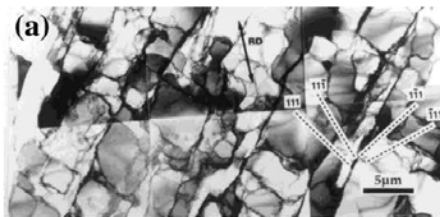
5 DTU Wind Energy, Technical University of Denmark

Cold deformed structures subdivided by extended almost planar boundaries (carpets) and short cell boundaries forming cell blocks



99.96% Al $\epsilon_{VM} = 0.12$

99.99% Ni $\epsilon_{VM} = 0.26$



6 DTU Wind Energy, Technical University of Denmark

Structural evolution during plastic deformation



Grains/crystals subdivide by formation of dislocation and high angle boundaries, creating hierarchical structures in a finer and finer scale down to the nanometer dimension as the strain and stress increased to a high level.

7 DTU Wind Energy, Technical University of Denmark

Large strain deformation



Structural length scale > 100 – 300 nm

Process examples are:

Rolling

Torsion

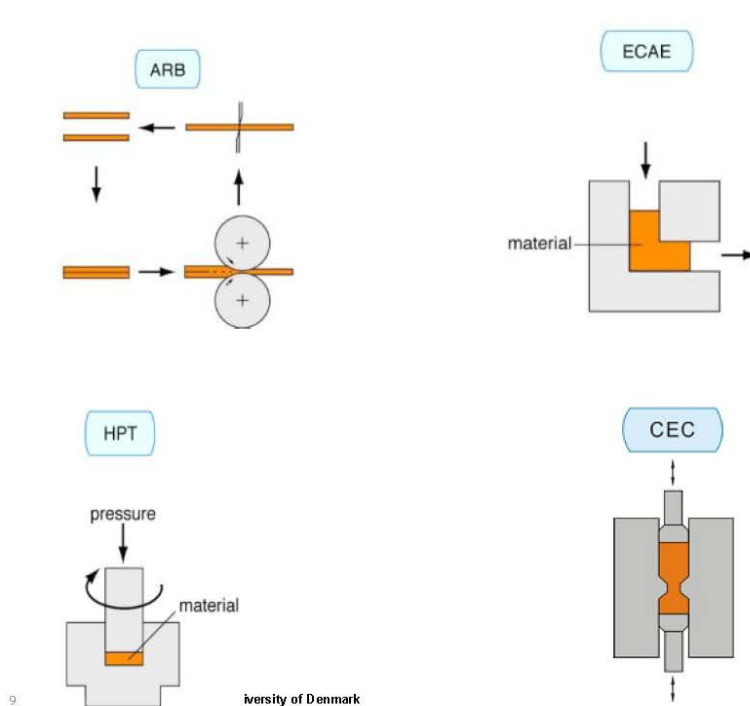
Drawing

Accumulative roll bonding

Equal channel angular extrusion

Multidirectional deformation

8 DTU Wind Energy, Technical University of Denmark

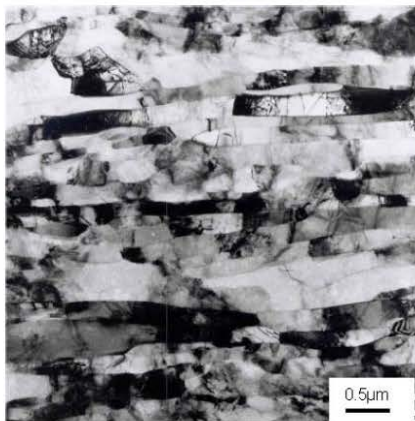


9

iversity of Denmark

Al and Ni cold rolled to large strain

Al, $\epsilon_{VM}=6$



Ni, $\epsilon_{VM}=3.5$



10 DTU Wind Energy, Technical University of Denmark

Large strain deformation



Structural length scale > 50 nm

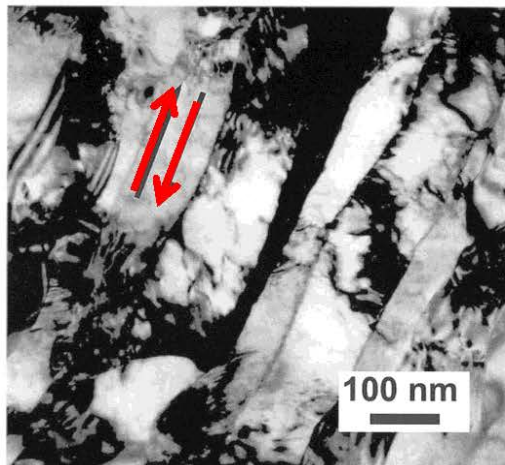
Process examples are:
High pressure torsion
Dynamic plastic deformation

Structural length scale > 5 nm

Process examples are:
Ball milling
Surface mechanical attrition
Friction

11 DTU Wind Energy, Technical University of Denmark

TEM of 99.99% Ni cold-deformed by high pressure torsion to ϵ_{VM} 12. The shear direction is marked.

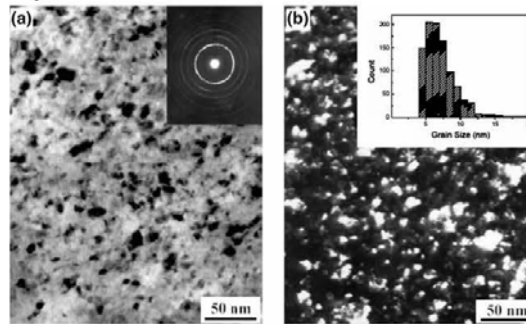


12 DTU Wind Energy, Technical University of Denmark

Surface mechanical attrition treatment (SMAT) of iron



- The surface layer is nanostructured with a boundary spacing about 10 nm.
- The subsurface layer is graded and extend to about 50 μm below the surface.



Bright field image (a) and dark field image (b) of 99.95% pure iron – surface layer

13 DTU Wind Energy, Technical University of Denmark



Analysis of structure and strength
of low carbon steel deformed by
shot peening and by cold rolling

14 DTU Wind Energy, Technical University of Denmark

Applications

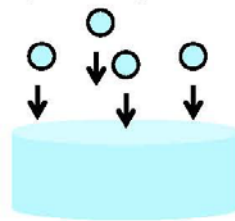


15 DTU Wind Energy, Technical University of Denmark

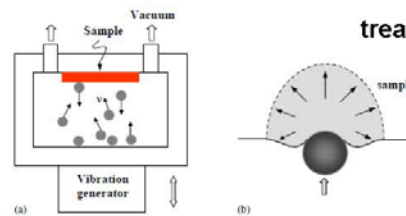
Particle Impact



Shot-peening



SMAT (surface mechanical attrition treatment)

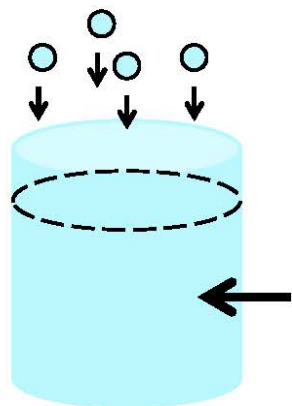


	Shot-peening	SMAT
Shot size	0.05 ~ 1 mm	1 ~ 10 mm
Shot velocity	~ 100 m/s	1 ~ 20 m/s
Shot direction	Single direction (~ 90°)	Multi-direction (vibration frequency: 20 ~ 50 HZ)
Temperature increase	50-100 °C	50-100 °C
Thickness of graded nanostructures	~ 20 μm	~ 40 μm

DTU Wind Energy, Technical University of Denmark

16

Shot Peening (1)



0.8 mm high-carbon steel balls
High shot velocity: 260-300 m/s

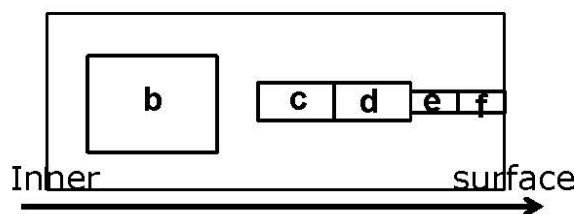
Cold rolling: low to high strain
Strain rate: about 0.3 s^{-1}

Material

Pure industrial iron: Fe-0.004C-0.44Al-0.017Ni-0.13Mn-0.0066P

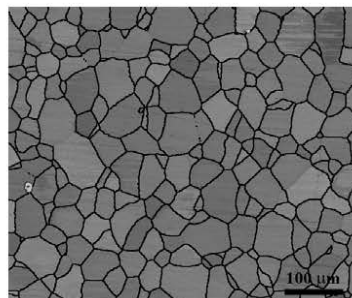
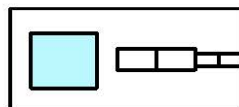
17 DTU Wind Energy, Technical University of Denmark

Shot-peening (2)



- b)** 1200 - 600 μm from surface
- c)** 460 - 260 μm from surface
- d)** 260 - 60 μm from surface
- e)** 60 - 30 μm from surface
- f)** 30 - 0 μm from surface

b): 1200 - 600 μm from surface



Inner

surface

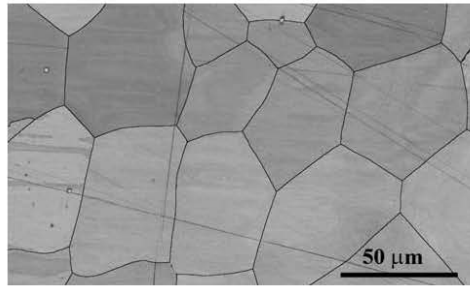
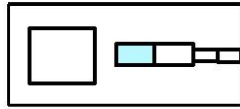
Black line: high angle boundary (Misorientation angle $> 15^\circ$)

18 DTU Wind Energy, Technical University of Denmark

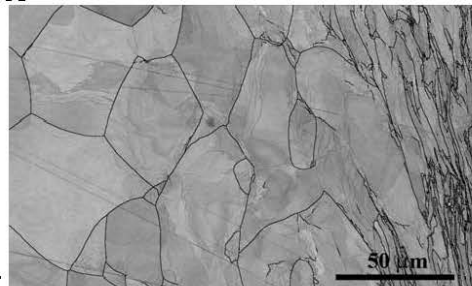
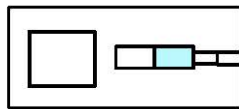
Shot-peening (3)



c: 460 - 260 μm from surface



d: 260 - 60 μm from surface



Inner

surface

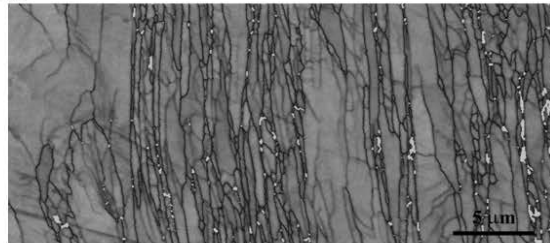
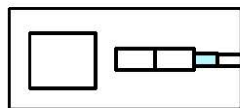
DTU Wind Energy, Technical University of Denmark
Black line: high angle boundary (Misorientation angle $> 15^\circ$)



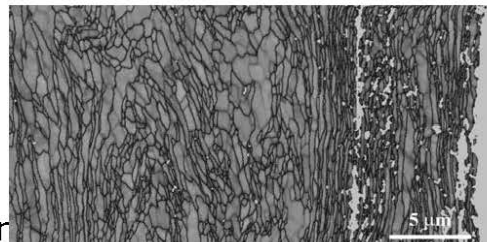
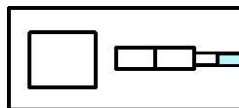
Shot-peening (4)



e: 60 - 30 μm from surface



f: 30 - 0 μm from surface



Inner

surface

DTU Wind Energy, Technical University of Denmark
Black line: high angle boundary (Misorientation angle $> 15^\circ$)

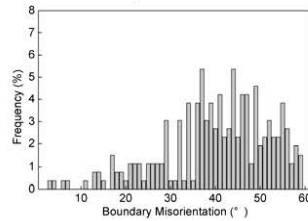


Shot-peening (5)

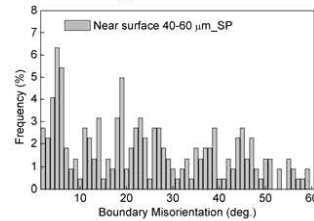


Lamellar boundary misorientation angle (EBSD)

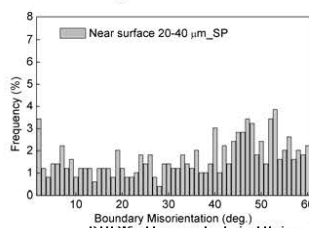
1200 - 600 μm from surface



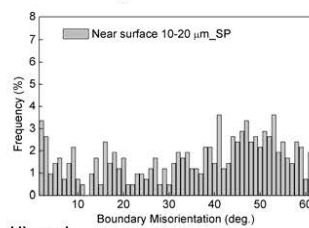
60 - 40 μm from surface



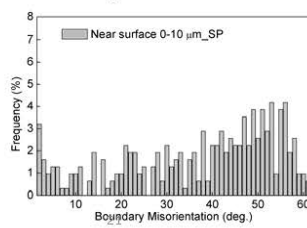
40 - 20 μm from surface



20 - 10 μm from surface



10 - 0 μm from surface



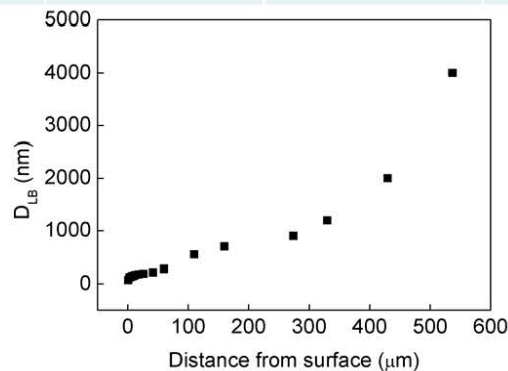
DTU Wind Energy, Technical University of Denmark

Shot-peening (6)



Structural parameters in a lamellar surface

	$\theta_{LB}(\text{deg.})$	$D_{LB}(\text{nm})$	Fraction of HABs (%), F_{HAB}
Near surface 0-20 μm_{SP}	35.4	223	80.6
Near surface 20-40 μm_{SP}	34.9	301	80.7
Near surface 40-60 μm_{SP}	24.6	515	65.2

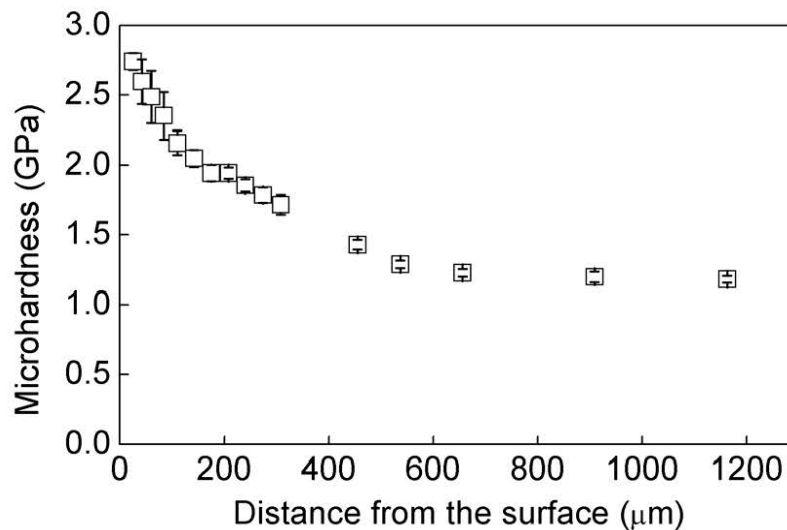


22 DTU Wind Energy, Te

Shot-peening (7)



Hardness vs distance from surface

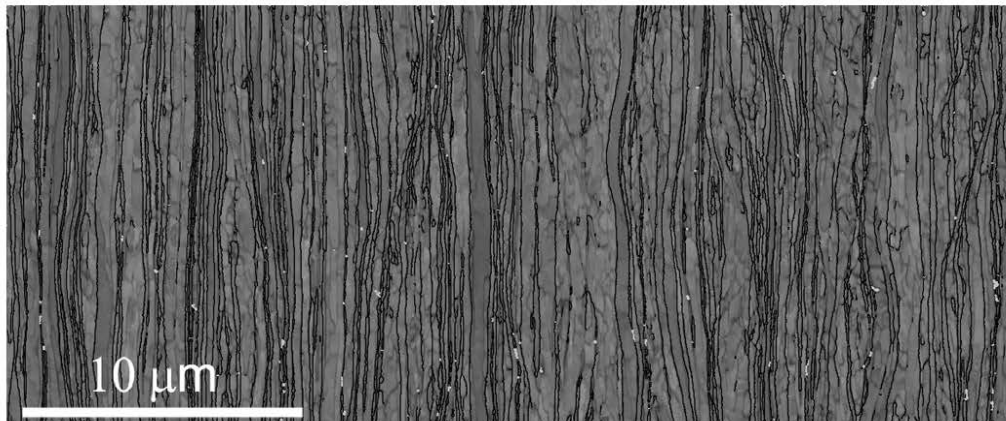


23 DTU Wind Energy, Technical University of Denmark



The microstructure in a shot-peened surface and subsurface is a graded lamellar structure, also observed in a friction and wear sample. The lamellar morphology also characterizes samples cold rolled to high strain.

24 DTU Wind Energy, Technical University of Denmark

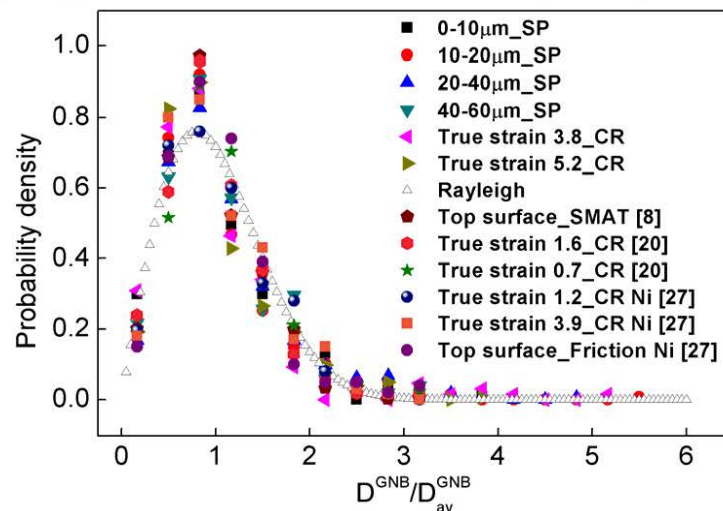


Microstructure of cold-rolled pure iron_Strain 4.26

25 DTU Wind Energy, Technical University of Denmark

Scaling of D^{GNB}

In samples deformed by shot peening (SP), cold rolling (CR), surface mechanical attrition (SMAT) and friction



26 DTU Wind Energy, Technical University of Denmark

Relationships between microstructural parameters and the stress and strain state in a graded surface layer as a basis for constitutive equations



- **Stress estimate:** microhardness, nanoindentation, miniature test samples.
- **Strain estimate:** displacement of structural markers as grain boundaries, twin boundaries and embedded pins.

Structure property relationships are difficult to obtain as surface layers are thin ($< 50 \sim 100 \mu\text{m}$) and the microstructure is graded at a nanostructural scale.

27 DTU Wind Energy, Technical University of Denmark

Indirect estimate of structure-property relationships in a graded structure



The deformed structures in shot-peened, friction and cold-rolled samples have similar characteristics, and it is suggested to use the structure-property relationships for rolled (bulk) samples as a baseline for the analysis of graded surface structures.

28 DTU Wind Energy, Technical University of Denmark

Structure property relationships for cold-rolled samples



Establish master curves for the relationships:

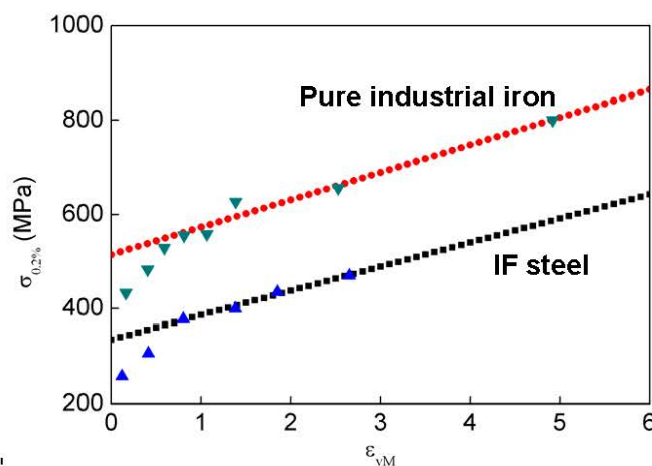
- Stress (σ) and strain (ε)
- Stress (σ) and boundary spacing (D_{av})
- Strain (ε) and boundary spacing (D_{av})

29 DTU Wind Energy, Technical University of Denmark

Flow stress (σ) as a function of the rolling strain (ε)

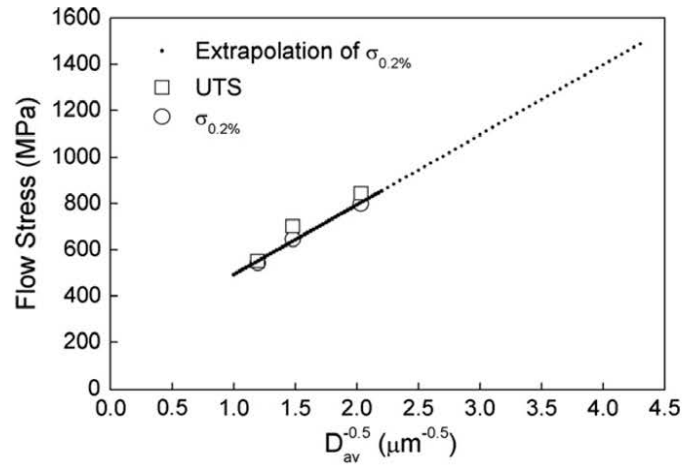


Parabolic hardening (Stage III)
Linear hardening (Stage IV)



30 DTU Wind En

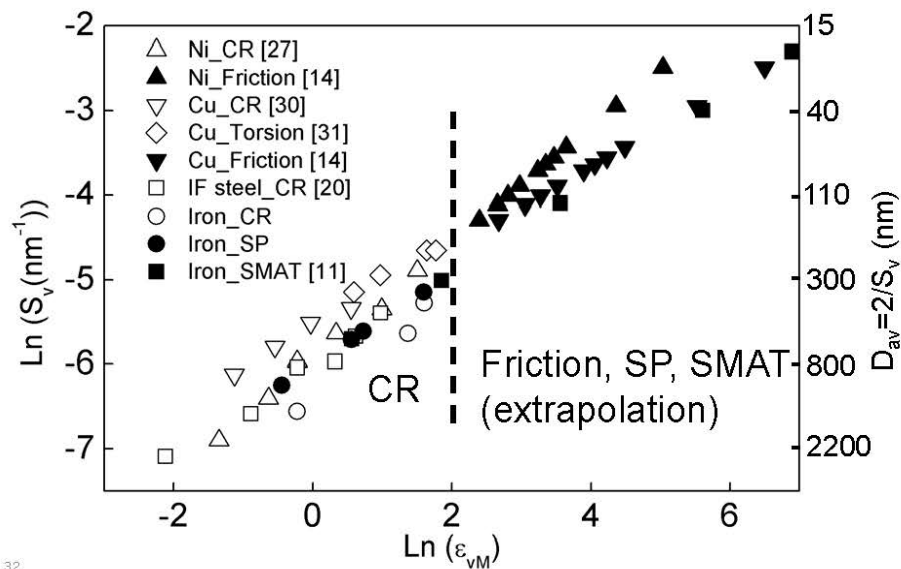
Flow stress (σ) as a function of boundary spacing (D_{av})



$$\sigma = 190.74 + 301.36 \times D_{av}^{-0.5}$$

31. DTU Wind Energy, Technical University of Denmark

Relationship between boundary spacing D_{av} ($=2/S_v$) and strain (ϵ)



32.

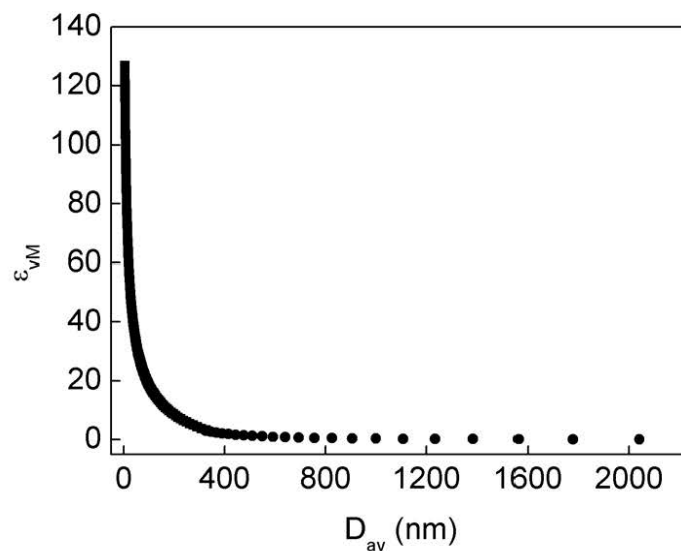
Stress and strain state in graded structures



Based on master curves for rolled samples the local stress and strain state in a graded surface structure can be estimated by a measurement of D_{av} as a function of the distance from the surface.

33 DTU Wind Energy, Technical University of Denmark

Strain (ϵ) as a function of boundary spacing (D_{av})

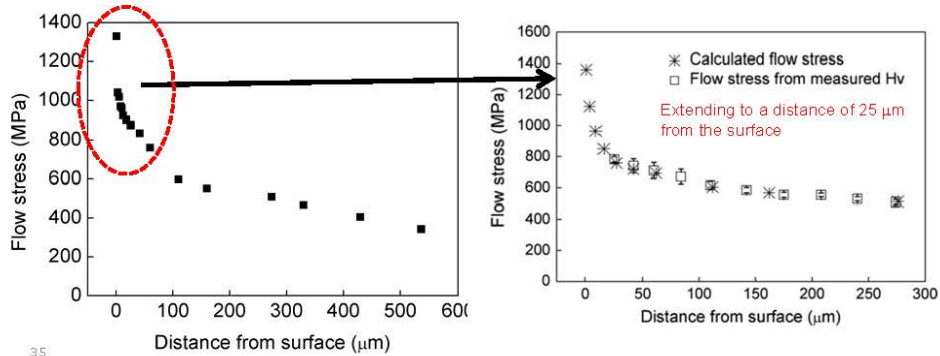


34.

Stress distribution in a graded surface / subsurface layer

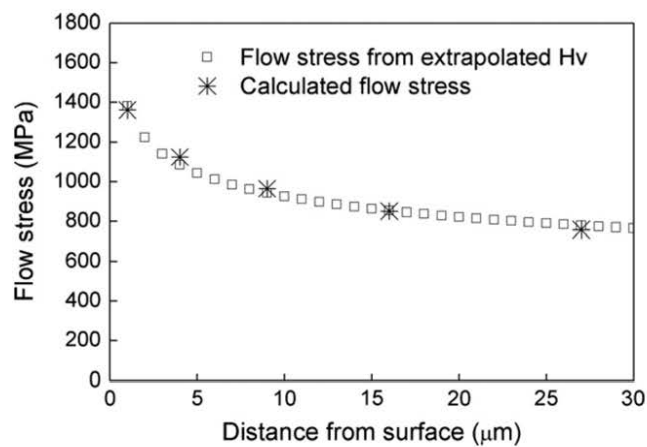


- Determined by microhardness, approx. 1/3 the flow stress
- Determined indirectly based on a master curve for the relationship between σ and D_{av}



35

Stress distribution in the top surface layer (0-25 μm) of a SP sample



36 DTU Wind Energy, Technical University of Denmark

Konklusion

- Et hårdt overfladelag dannet ved plastisk deformation som f.eks. shot peening har en gradueret nanostruktur, der strækker sig 50-100 μm ind i materialet.
- Spændings- og tøjningstilstanden i overfladelaget kan analyseres ved lokalt at bestemme afstanden mellem dislokationsgrænser og korngrenser, D_{av} , der relaterer til styrken, σ , gennem ligningen

$$\sigma = K \cdot D_{av}^{-0.5}$$

K er en konstant for hårdt deformeret materiale, der kan bestemmes ved at måle sammenhørende værdier for D_{av} og σ for grundmaterialet deformeret f.eks. ved valsning til en høj deformationsgrad.

- Den foreslåede mikroskopiske metode til analyse af en lokal spændings- og tøjningstilstand i et deformeret materiale kan anvendes generelt ved analyse af deformationszoner, f.eks. nær revner, partikler og korngrenser.

Homogen og lokaliseret tøjningsudvikling af
nanostruktureret aluminium

Jacob Kidmose, DTU Vindenergi

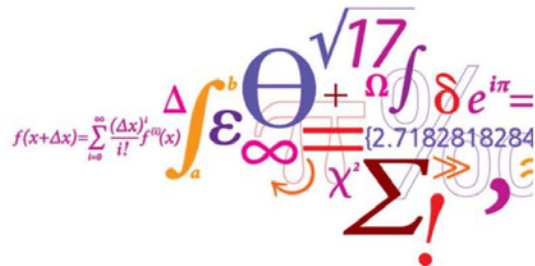
Homogen og lokaliseret tøjningsudvikling af nanostruktureret aluminium

Fordele ved brugen af ARAMIS

Jacob Kidmose

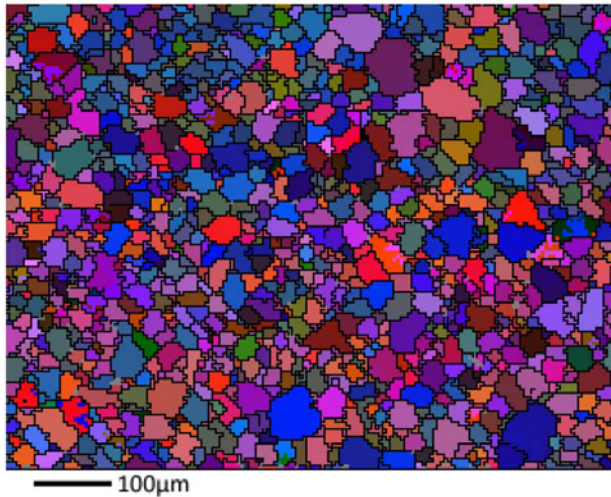
vejledere:

N. Hansen, G. Winther and X. Huang



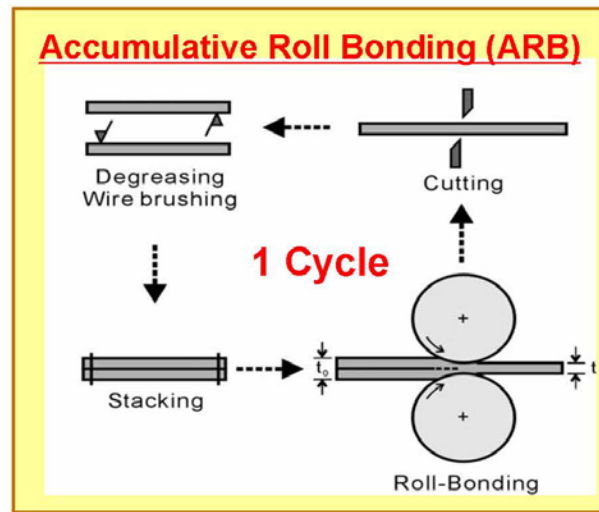
DTU Wind Energy
Department of Wind Energy
1

Start materiale



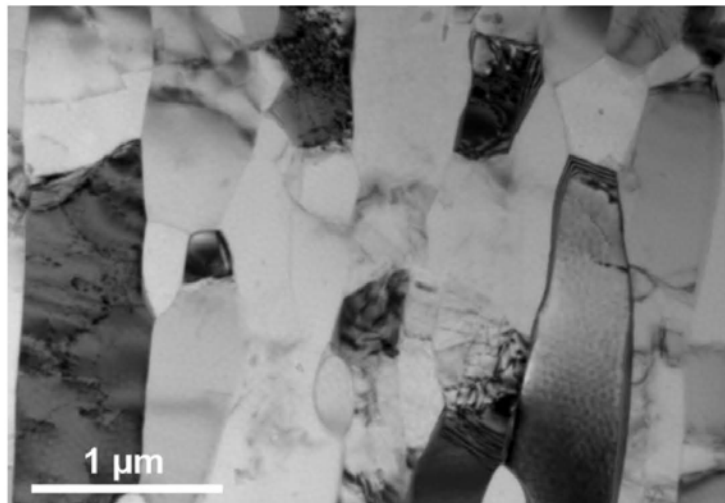
- Al1050
–99.5%
- Kornstørrelse
30 μm.

Accumulative Roll Bonding



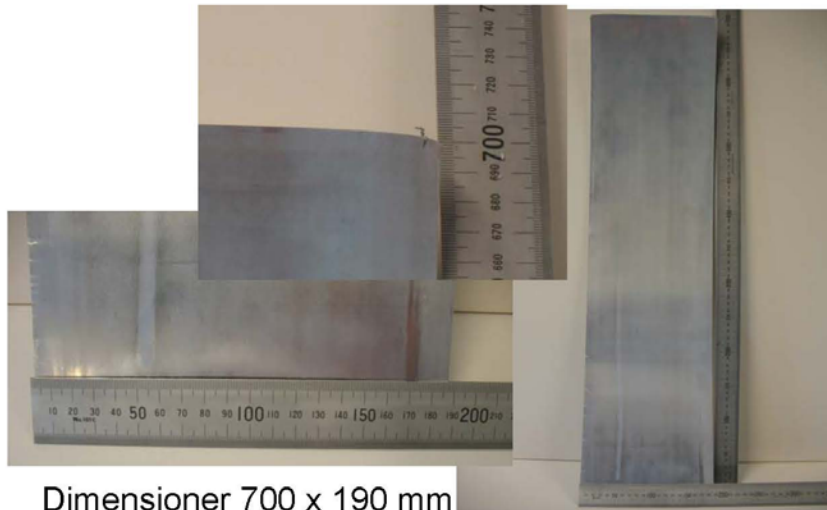
3 DTU Wind Energy, Technical University of Denmark

6C-ARB Microstruktur



4 DTU Wind Energy, Technical University of Denmark

6C-ARB1050Al plade



Dimensioner 700 x 190 mm

5 DTU Wind Energy, Technical University of Denmark

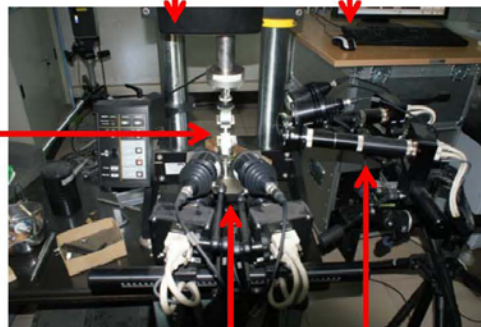
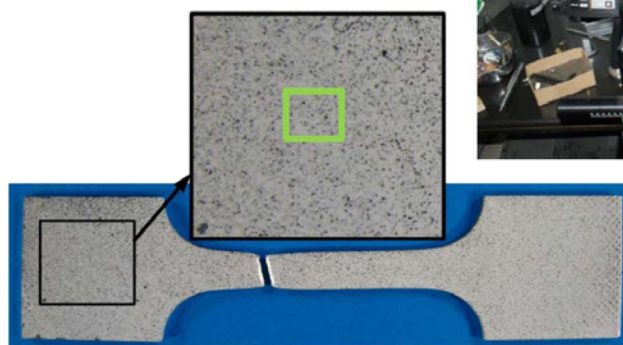
ARAMIS

- Dot pattern
- Facet size 0,75 mm

Tensile machine

ARAMIS software

Sample



Side camera system
(not used)

Front camera system

DTU Wind Energy, Technical University of Denmark

Mechanical properties

• AA1050



• 6C-ARB



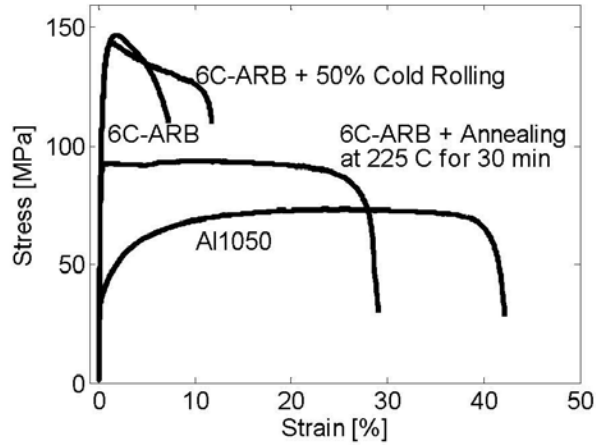
• Varmbehandling

• 6C-ARB-225



• Valsning

• 6C-ARB-CR50



7 DTU Wind Energy, Technical University of Denmark

Homogen deformation

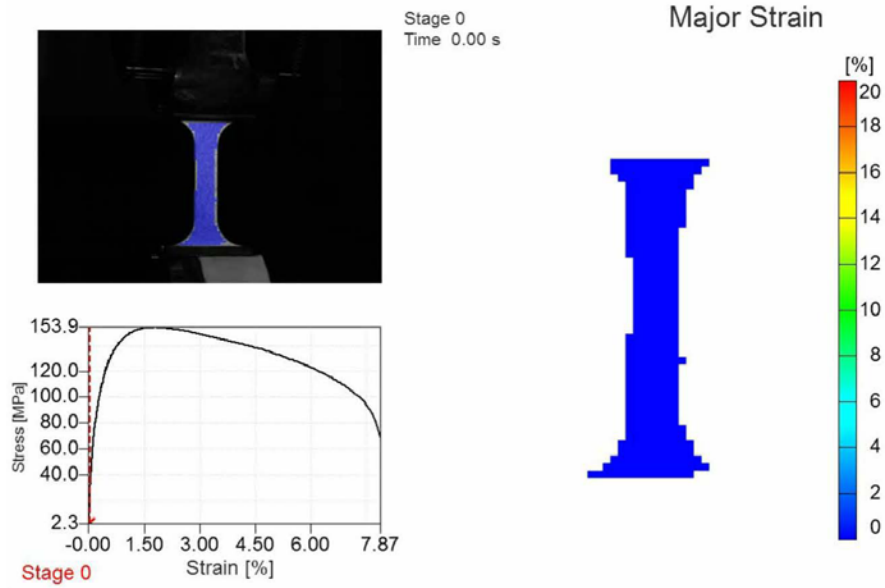
$$f(x+\Delta x) = \sum_{i=0}^{\infty} \frac{(\Delta x)^i}{i!} f^{(i)}(x)$$

$$\Delta \int_a^b \epsilon \Theta + \Omega \int \delta e^{i\pi} = \{2.7182818284$$

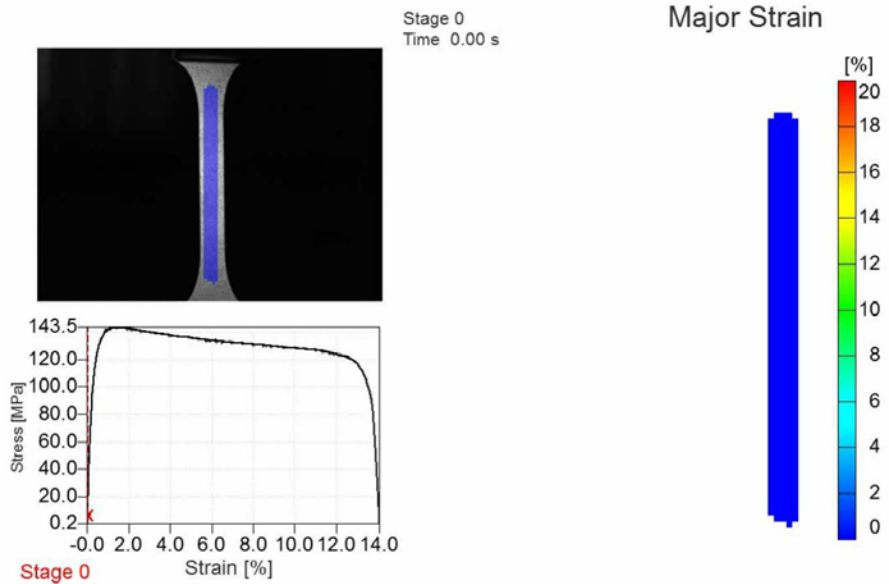
$$\infty \chi^2 \Sigma ! \gg \}$$

DTU Wind Energy
Department of Wind Energy

6C-ARB

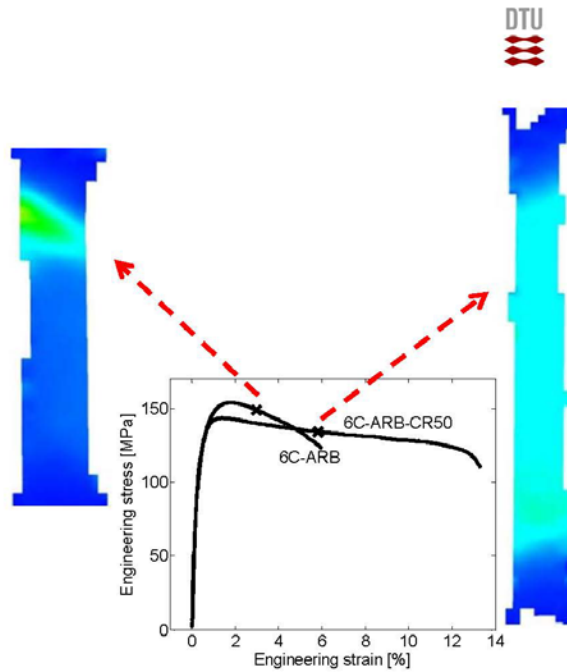


6C-ARB-CR50



Results

- 6C-ARB udvikler shear band lige efter brud styrken
- 6C-ARB-CR50 har homogene deformation flere procent efter brud styrke



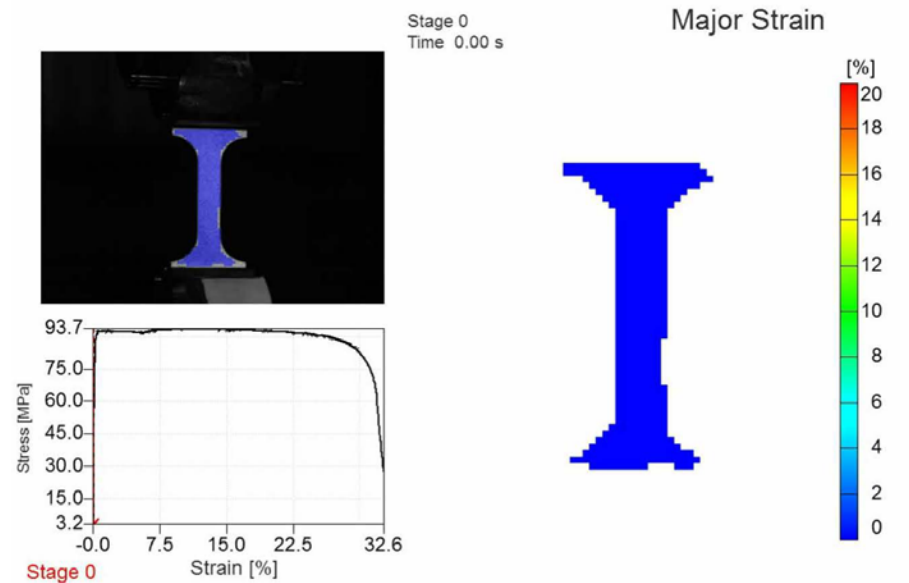
DTU Wind Energy, Technical University of Denmark

Varmbehandling

$$f(x+\Delta x) = \sum_{i=0}^{\infty} \frac{(\Delta x)^i}{i!} f^{(i)}(x) = \int_a^b \epsilon \Theta + \Omega f \delta e^{i\pi} = \{2.7182818284\}$$

DTU Wind Energy
Department of Wind Energy

6C-ARB-225



ARAMIS

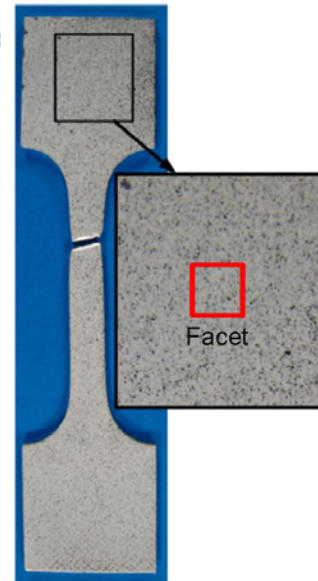
- En-akset træk prøve
 - tøjnings-spændings kurve
 - Sand tøjnings-spændings kurve (også gældende efter UTS)
 - Anisotropi

Sand tøjnings-spændings kurve

Volume konstant $\Rightarrow \epsilon_{\text{Tykkelse}} = -\epsilon_{\text{bredde}} - \epsilon_{\text{træk}}$

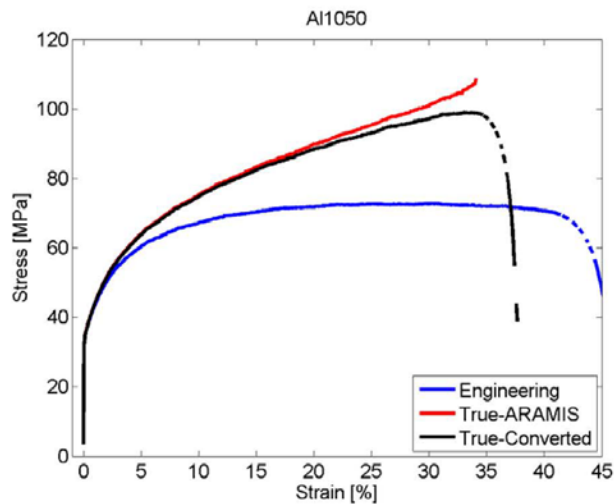
Udregning af tykkelses tøjningen over bredden af indsnævringens zonen

Derved fås det aktuelle tværsnits areal af indsnævringens zonen



DTU Wind Energy, Technical University of Denmark

Sand tøjnings-spændings kurve

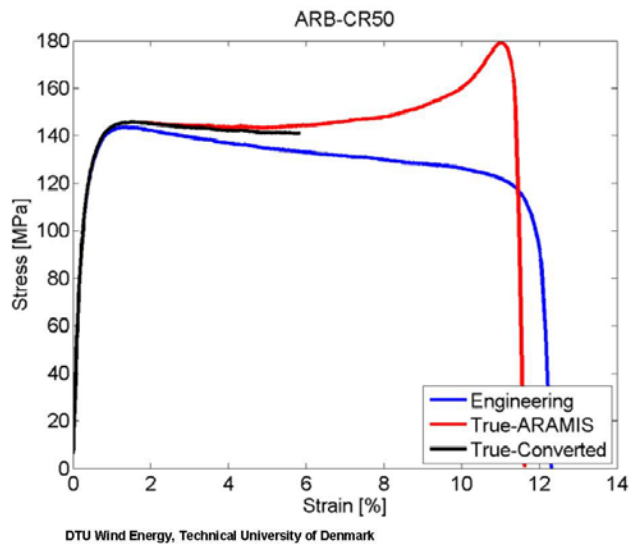


DTU Wind Energy, Technical University of Denmark

$$\sigma_t = \sigma_E (1 + \epsilon_E)$$

$$\epsilon_t = \ln(1 + \epsilon_E)$$

Sand tøjnings-spændings kurve

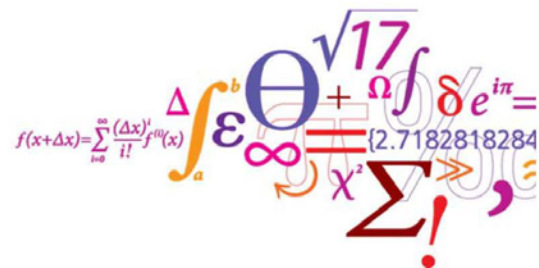


ARAMIS

- En-akset træk prøve
 - tøjnings-spændings kurve
 - Sand tøjnings-spændings kurve (også gældende efter UTS)
 - Anisotropi

Spørgsmål?

Tak for jeres opmærksomhed.



DTU Wind Energy
Department of Wind Energy

Baggrund for Innovationskonsortiet REEgain om magnetiske materialer

Jens Christiansen, Teknologisk Institut

Baggrund for Innovationskonsortiet REEGain om magnetiske materialer

Jens Christiansen og Martin Brorholt Sørensen

Indhold

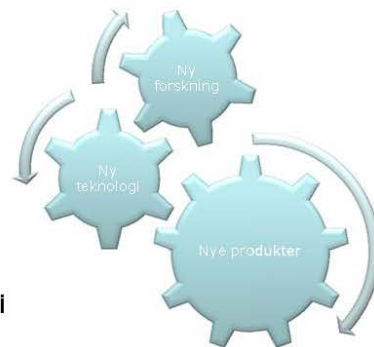
- Hvad er innovationskonsortier?
- Baggrunden for REEGain
- Virksomhedernes interesser
- Aktiviteterne REEGain

Hvad er et innovationskonsortium?

- Konkrete samarbejdsprojekter mellem virksomheder, forskningsinstitutioner og teknologiske serviceinstitutter
- Formålet er, at parterne i fællesskab udvikler viden eller teknologi, som ikke blot gavner enkelte virksomheder, men hele brancher indenfor dansk erhvervsliv
- Mindst 2 virksomheder, en forskningsinstitution og et teknologisk serviceinstitut
- Varighed på mellem 2 og 4 år

Hvad er et innovationskonsortium også?

- 'Kortslutning' mellem forskning, teknologiudvikling og produktudvikling
- Støtten til universiteterne og Teknologisk Institut balanceres med virksomhedernes indsats
- Ingen temaer, men vurderes ud fra virksomhedernes og samfundets behov
- Meget lidt bureaukrati, når projektet er i gang

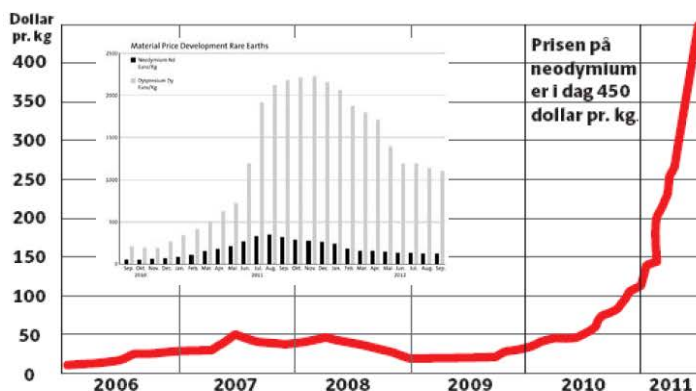


Artikler om magneter og sjældne jordarter



Skyhoje priser på vigtige råvarer

Priserne på **neodymium** er i denne måned røget helt op på en pris på **450 dollar eller knap 2.400 kr. pr. kilo**, der er den vigtigste af disse eftertragtede, strategisk vigtige råvarer. Det er en tidobling i forhold til prisen i slutningen af 2010. Samtidig svinger priserne meget, så de gør det svært og uforudsigeligt at indkøbe råvarer fra Kina. I dag betaler europæiske magnetproducenter over 30 procent mere for neodymium end de kinesiske konkurrenter.



Berlingske Business, august 2011

De Sjældne jordarter

Periodic table of elements showing color-coded groups and a red oval highlighting the rare earth elements (lanthanides and actinides).

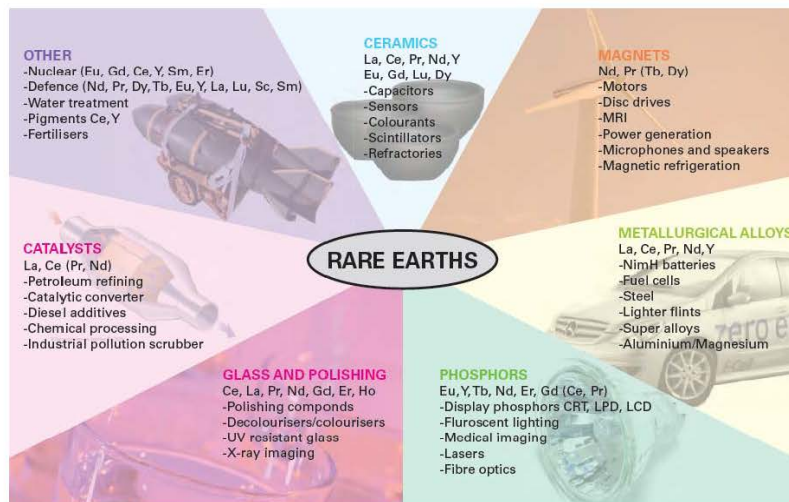
Legend:

- Alkalimetaller
- Alkaliske jordmetaller
- Overgangsmetaller
- Lantanider
- Actinider
- Andre metaller
- Ikke-metaller
- Ædelgasser
- Solid
- Liquid
- Gas
- Synthetic

Note: The subgroup numbers 1-10 were added in 1988 to the International Union of Pure and Applied Chemistry. The number of elements 112-118 are the Latin equivalent of those numbers.

Atomic masses in parentheses are those of the most stable or common isotope.

Sjældne jordarters anvendelser



Kilde: mineralsUK



TEKNOLOGISK
INSTITUT

Sjældne jordarter i Toyota Prius



Kilde: mineralsUK



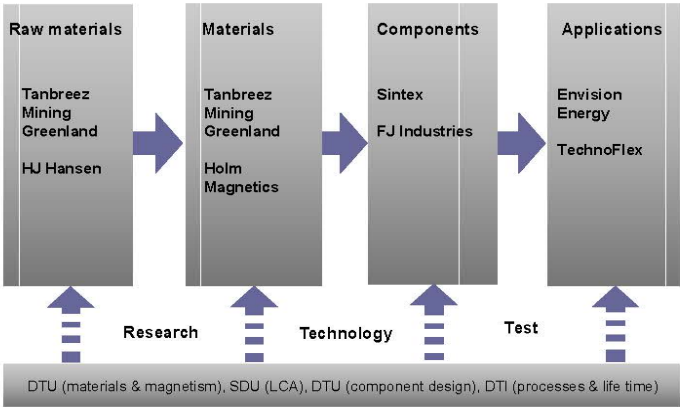
DANISH
TECHNOLOGICAL
INSTITUTE

REEgain konsortiet

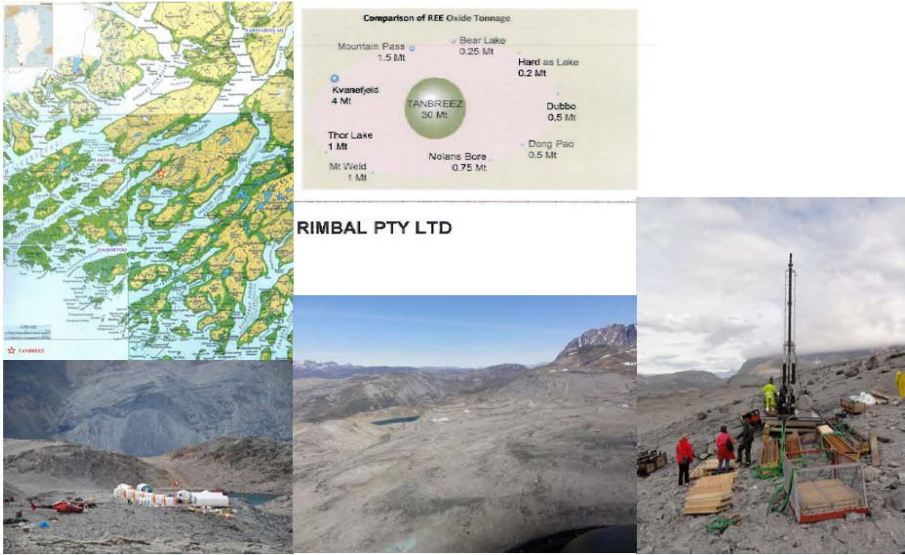
- DTU
- Syddansk universitet
- Teknologisk Institut
- Envision Energy APS
- FJ Industries A/S
- HJ Hansen A/S
- Holm Magnetics APS
- Sintex A/S
- Tanbreez Mining Greenland A/S
- Technoflex APS



Konsortium med fødekæde



TANBREEZ Mining Greenland A/S



Ta-Nb-REE-Z(r) - malm

Tre fraktioner:

1. Eudialyt (20%)

- REE
- Zirkonium
- Niob
- Tantal



2. Feldspat – nepheline (40%)

- Kan sælges som byggemateriale

3. Arfvedsonit (40%)

- Uudnyttet

Eudialyt	
Zirkonium oxide	1.8%
Niobium oxide	0.2%
Lette REE	0.5%
Tunge REE	0.15%

Arfvedsonit - uudnyttet fraktion (40%)

Udnyttelse

- Indeholder stor forekomst af litium
- Magnetisk
- Udvikle metode til at udvinde litium fra arfvedsonit



Mulige anvendelser af arfvedsonit

- "Sort sand"
- Sorte mursten?
- Salget skal kun dække omkostninger ved transporten - deponeringsomkostninger udgås

Lithium-anvendelser:

- Li-ion-batterier
- Produktion af glas (Li_2CO_3)
- Smøremidler (LiOH)
- Medicin
- Organisk kemi (LiAlH_4)

Genvinding af permanente magneter fra affald – *urban mining*



Magnetseparation fra kompressorer hos HJ Hansen





DANISH
TECHNOLOGICAL
INSTITUTE



H.J. HANSEN
Udvikling gennem generationer



DANISH
TECHNOLOGICAL
INSTITUTE

Shredder: 100 biler i timen



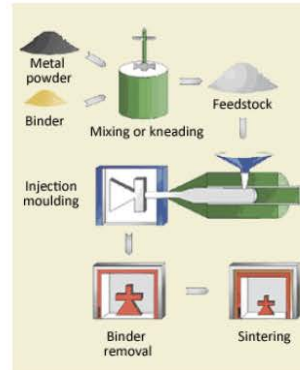
Formgivning af NdFeB magneter med *Metal Injection Moulding*

Styrker

- Kan automatiseres
- Mulighed for kompleks form
- Lavt spild
- snævre tolerancer i forhold til støbeprocesser

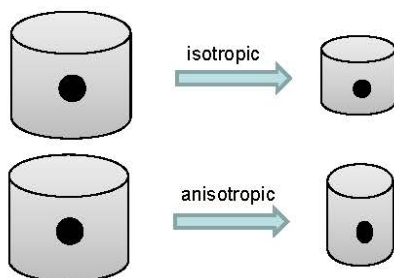
Svagheder

- Begrænsning på dimensioner
- Kræver stort styktal – eller høj stykpris



Udfordringer for MIM fremstillet NdFeB magneter

- Forhindring af oxidation
- Kontrol af karbon - legering reagerer med bindemidler ved forhøjet temperatur
- Kontrol med kornstruktur
- Anisotropisk krympning af aligned NdFeB
- Ingen komprimeringstryk



Magnetens evne til at modstå afmagnetisering

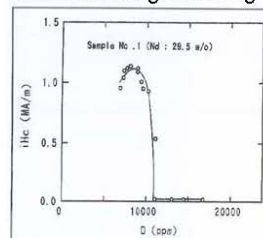


Figure 2. Dependence of H_c on oxygen content; residual carbon 530-730ppm.

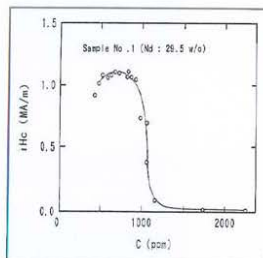


Figure 3. Dependence of H_c on carbon content; residual oxygen 7400-8500ppm.

Osamu Yamashita, 1998

Magneter til vindmøller

- Kan magneterne designes, så de blot skal remagnetiseres?
- Kan mængden af magnetisk materiale reduceres?
- Hvor store magneter kan vi lave?
- Har vi sjældne jordarter nok?
- Kan simple blandinger af sjældne jordarter benyttes?



Foto: ing.dk

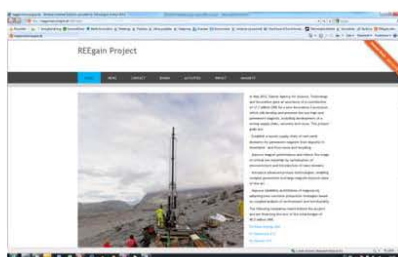
Pilotudstyr og analyselaboratorier Teknologisk Institut



Delprojekter i REEgain

- Mixed Rare-Earth-Fe-B sintered magnets – DTU Energy Conversion (manager), Holm Magnetics (exploitation manager)
- Minimizing Magnetic Materials by design and recycling - DTU Elektro (manager), SDU, Envision Energy (Exploitation manager), HJ Hansen, Sintex
- Minerals chemistry, separation and recycling - Tanbreez (manager), DTI, HJ Hansen
- Materials investigation and processing - Sintex (manager), DTI, FJ Industries
- Operational magnetic systems - reliability and surface protection - Technoflex (manager), DTI, Envision Energy, Sintex

Følg med i projektet på www.reegain.dk





Superleder tapes karakteriseret fra nanometer pinning
til meter store spoler

Asger Bech Abrahamsen, DTU Vindenergi

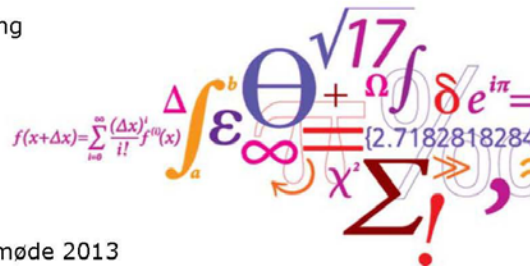
Superconductors characterized from nanometer pinning sites to meter size coils for direct drive wind generators

Asger B. Abrahamsen¹ and Bogi Bech Jensen²

¹Department of Wind Energy

²Department of Electrical Engineering

Technical University of Denmark



Dansk Metallurgisk Selskab, Vintermøde 2013
January 16-18, Kolding, Denmark

DTU Wind Energy
Department of Wind Energy

Outline

- **Motivation**
- **Scaling laws of turbines**
- **Superconductors**
- **Generators**
- **Conclusion**

Cost Of Energy (COE)

$$COE = \frac{CAPEX + OPEX}{Energy\ production}$$

CAPEX: Capital Expenditure

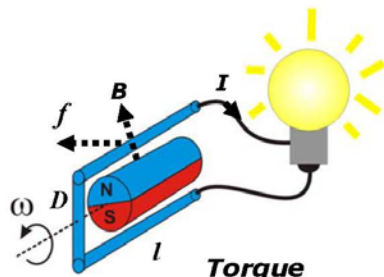
1.5 MEuro/MW* →

7.5 MEuro for 5 MW

OPEX: Operational Expenditure

*EU 2030 target for offshore wind

Motivation for superconducting generator



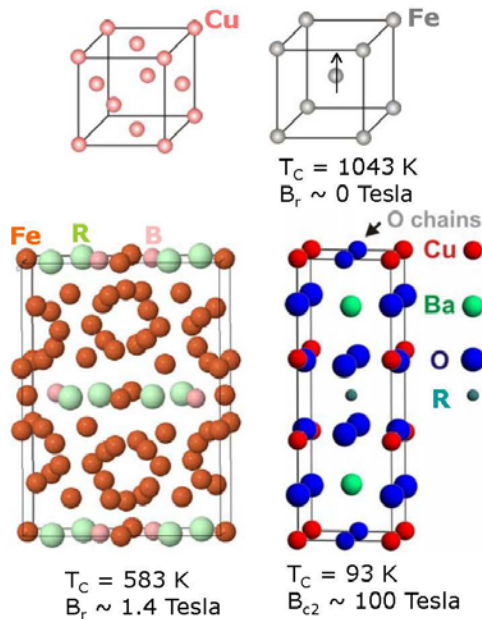
$$\text{Power} \propto B I D^2 l \omega$$

1G : Copper + Iron

2G : $R_2Fe_{14}B$ magnets+Fe
10 MW ~ 6 tons PM

3G : $RBa_2Cu_3O_{6+x}$ HTS + Fe
10 MW ~ 10 kg RBCO

DTU Wind Energy, Technical University of Denmark

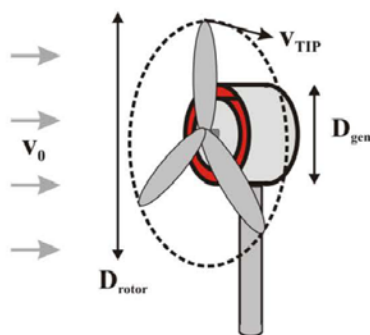


Motivation: Up-scaling the turbine power

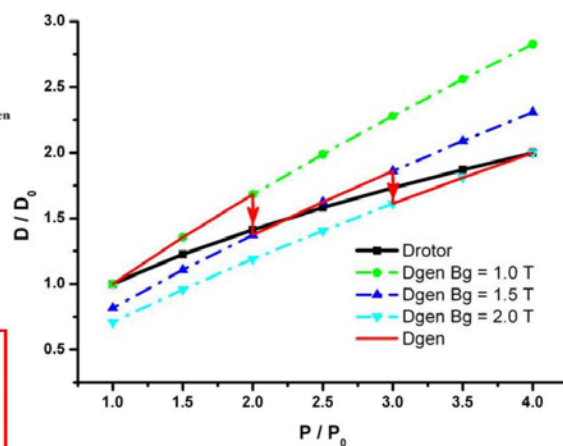


Constant tip speed \rightarrow Rotor diameter
Torque
Generator diameter

$$\begin{aligned} D_{\text{rotor}} &\sim P^{1/2} \\ T &\sim P^{3/2} \\ D_{\text{gen}} &\sim (BI)^{-1/2} P^{3/4} \end{aligned}$$



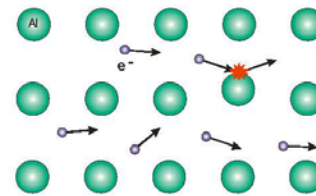
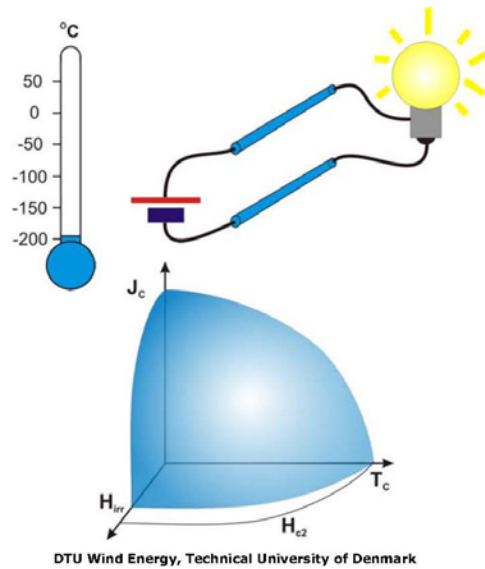
$$\begin{aligned} P &= T\omega = \frac{1}{2} \rho D_{\text{rotor}}^2 v_0^3 C_p \\ &= B_g I D_{\text{gen}}^2 L_{\text{gen}} \omega \end{aligned}$$



Abrahamsen et. al., ASC 4LF-04 (2012)

Superconductivity

DTU

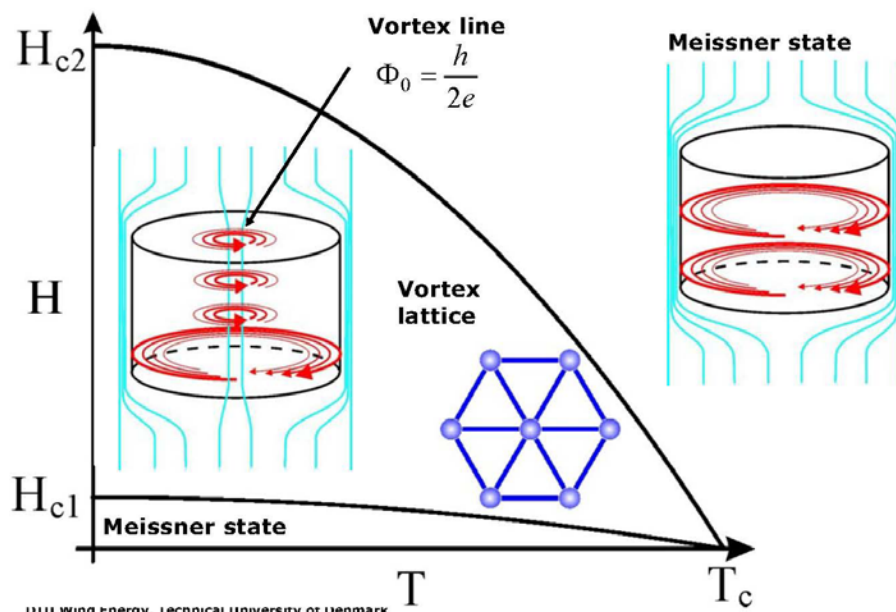


$$P = R I^2$$

$$R = 0 \, \Omega \rightarrow P = R I^2 = 0 \, \text{Watt}$$

Critical fields

DTU



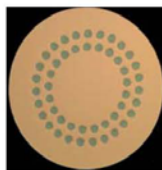
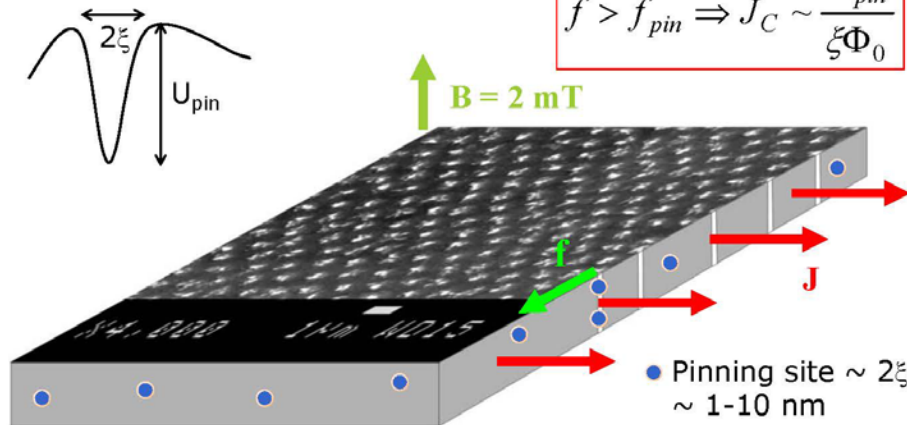
Critical current density

- Lorentz force on vortex line
- Pinning force
- Vortex movement when:

$$\vec{f} = \vec{J} \times \Phi_0 \vec{z}$$

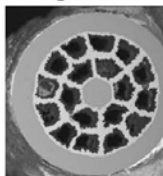
$$f_{pin} = \frac{dU}{dx} \sim \frac{U_{pin}}{\xi}$$

$$f > f_{pin} \Rightarrow J_C \sim \frac{U_{pin}}{\xi \Phi_0}$$

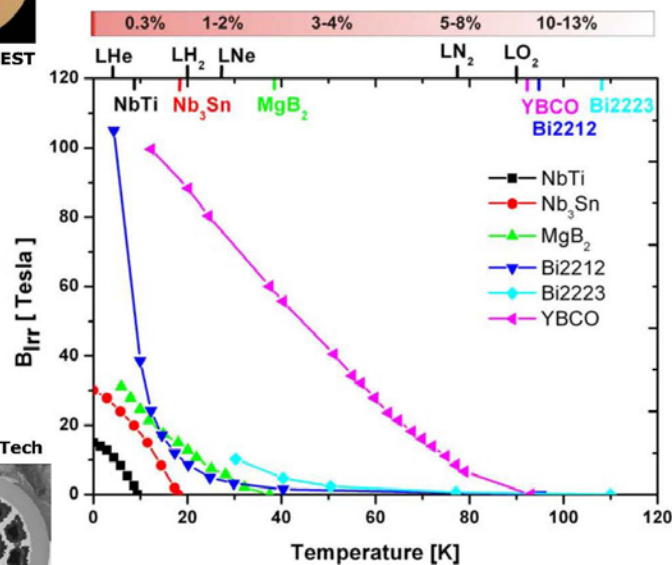


NbTi Bruker EST
0.4 €/m

1-4 €/m
MgB₂ HyperTech



Choice of superconductor



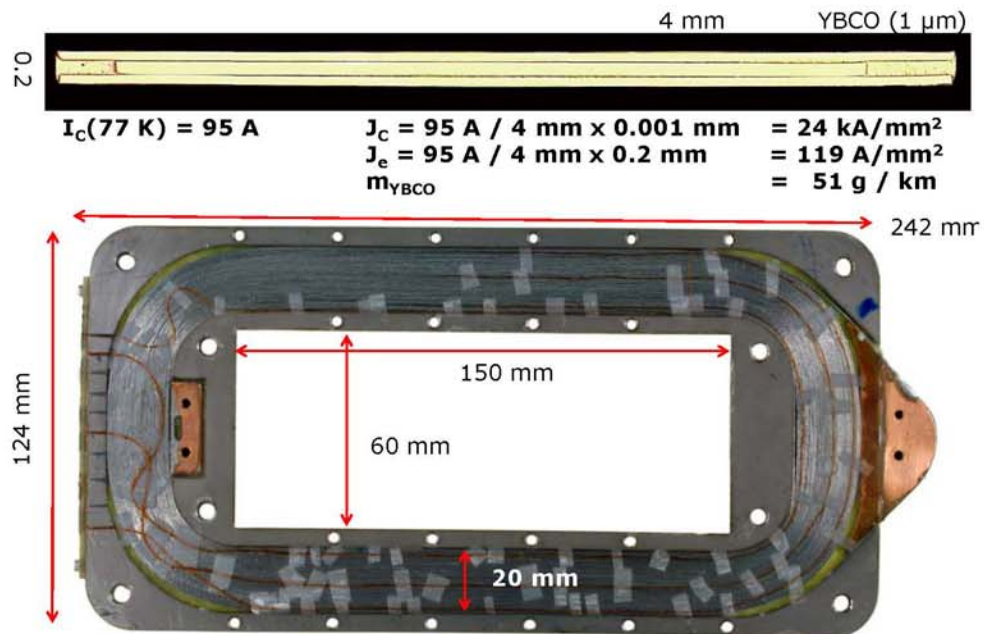
30 €/m 20 €/m



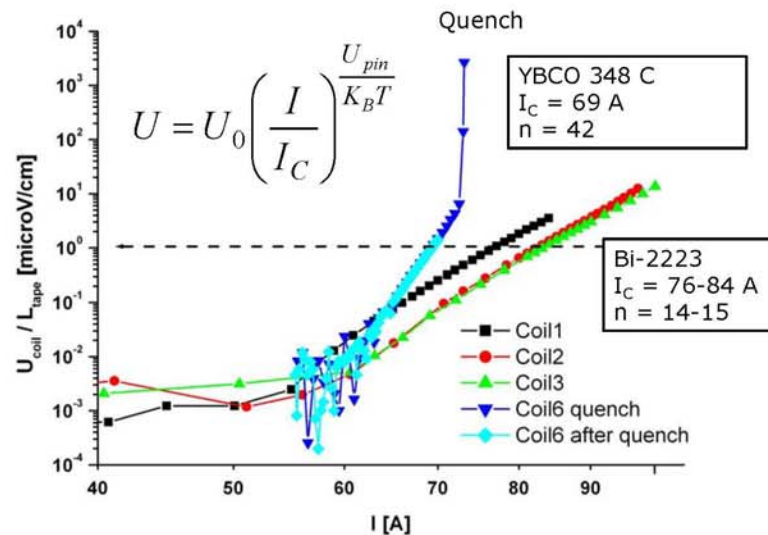
YBCO Bi-2223

Jensen, Mijatović & Abrahamsen, EWEA 2012

HTC tapes and coils

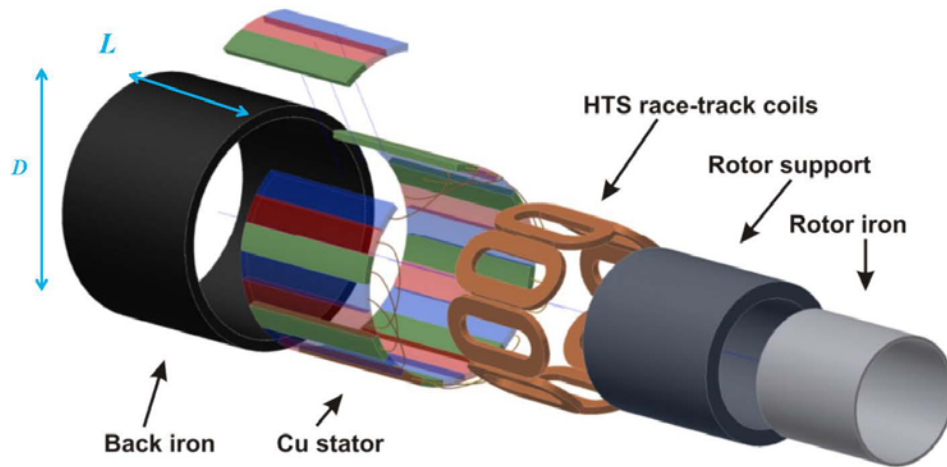


IV curves of coils @ 77 K in liquid nitrogen



DTU Wind Energy, Technical University of Denmark Abrahamsen et. al., "Feasibility of 5 MW superconducting wind turbine generator", Physica C471, 1464 (2011)

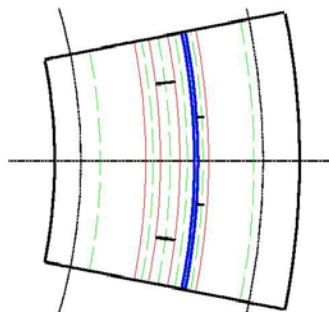
Radial flux machine



DTU Wind Energy, Technical University of Denmark

Abrahamsen et. al., SUST23,034019 (2010)

Superconducting generator and J_e



$$D = 4.2 \text{ m}$$

$$L = 1.4 \text{ m}$$

$$t_r = 0.25 \text{ m}$$

$$t_{ic} = 0.04$$

$$t_s = 0.053$$

$$t_{oc} = 0.04$$

$$t_g = 0.01$$

$$t_{cu} = 0.029$$

$$t_{os} = 0.25$$

$$T = 4.2 \text{ MNm}$$

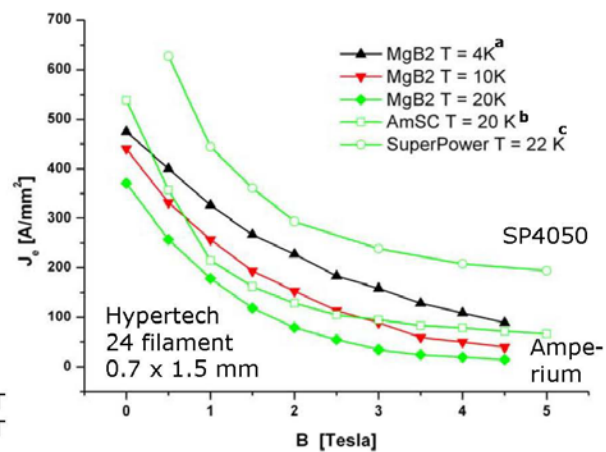
$$B_{Fe} = 2.5 \text{ T}$$

$$B_{airgap} = 2.4 \text{ T}$$

$$\text{Cu loss} = 5 \%$$

$$B_{sup} \sim 3.3 \text{ T (FE)}$$

$$J_e = 70 \text{ A/mm}^2$$



^aS. Mine et al., *IEEE Trans. Appl. Supercond.* 22, 2012, p. 4400604.

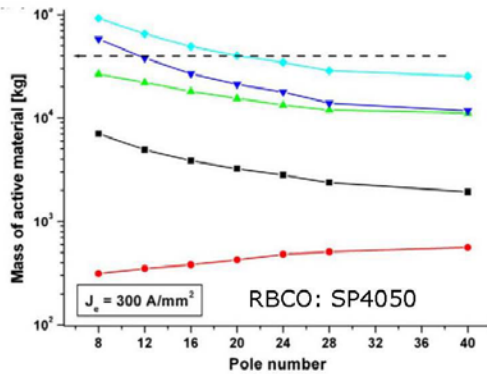
^bAmSC Amperium application note

^cD.W. Hazelton and V. Selvamianickam, *Proceedings of the IEEE*, Vol. 97, 2009, p. 1831.

Coated conductor

vs.

MgB₂



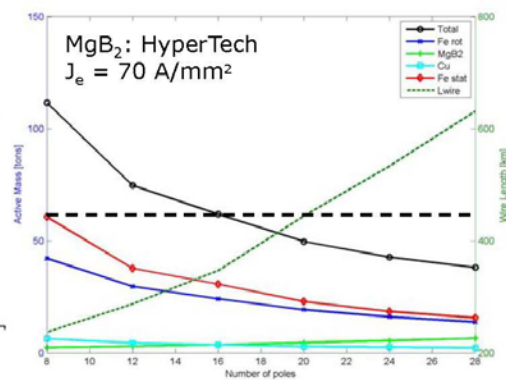
24 poles $m \sim 40$ tons

$L = 134 \text{ km}$ 30 Euro/m

Tape cost \sim 4.0 MEuro

CAPEX fraction 53 % $> 1/3$

Abrahamsen et. al., Physica C471, 1464 (2011)



16 poles $m \sim 60$ tons

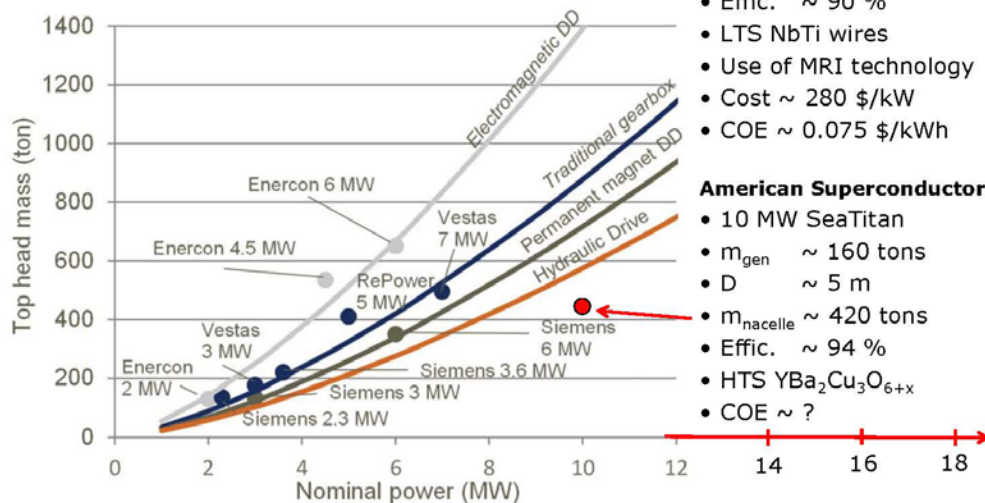
$L = 347 \text{ km}$ 1-3 Euro/m

Wire cost \sim 0.4-1.0 MEuro

CAPEX fraction 5-13 % $< 1/3$

Abrahamsen et. al., ASC 4LF-04 (2012)

Top head mass (nacelle + rotor)



DTU Wind Energy, Technical University of Denmark

GE Global Research

- 10 MW DE-EE0005143
- $m_{\text{gen}} \sim 142$ tons
- $D \sim 5 \text{ m}$
- Effic. $\sim 90 \%$
- LTS NbTi wires
- Use of MRI technology
- Cost $\sim 280 \text{ \$/kW}$
- COE $\sim 0.075 \text{ \$/kWh}$

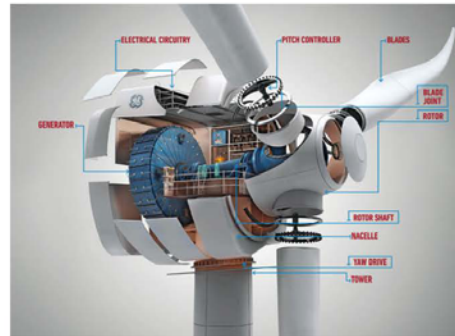
American Superconductors

- 10 MW SeaTitan
- $m_{\text{gen}} \sim 160$ tons
- $D \sim 5 \text{ m}$
- $m_{\text{nacelle}} \sim 420$ tons
- Effic. $\sim 94 \%$
- HTS $\text{YBa}_2\text{Cu}_3\text{O}_{6+x}$
- COE $\sim ?$

Source: www.btm.dk

World market update 2011

Conclusion



Magneto Resonant Imaging + Wind =

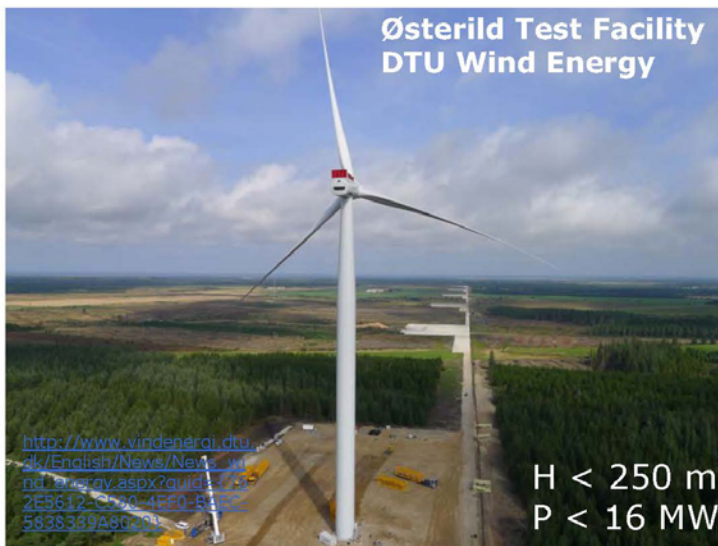
Superconducting direct drive generator

NbTi & MgB₂ almost cost competitive now. HTC in the long run.

DTU Wind Energy, Technical University of Denmark

Source: GE

Thank you for your attention



Acknowledgement

Superwind.dk
DTU Globalization

INNWIND.EU
FP7 Energy
2012-2017

Superconducting
generators
P = 10-20 MW

Copyright Siemens Denmark

DTU Wind Energy, Technical University of Denmark

Mikrostruktur karakterisering af SG-støbejern

Karl-Martin Pedersen, Siemens Wind Power A/S



Karakterisering af mikrostruktur i SG-jern

DMS Vintermøde 2013

Karl Martin Pedersen
Siemens Wind Power A/S

© Siemens AG 2013

Outline

- Mikrostrukturevaluering i SG jern
 - Visuel evaluering
 - Billedanalyse
- Grafit størrelsesfordeling i 2D og 3D
- Grafit på brudflader

Hvorfor SG jern

Ved st rkning

- Metaller svinder (=por siteter i centrum af emnet)
- Kulstof udvider sig ved dannelse af grafit (modvirker por siteter)
- Kulstof s nker st rkne-temperaturen ca. 350 C i forhold til st l

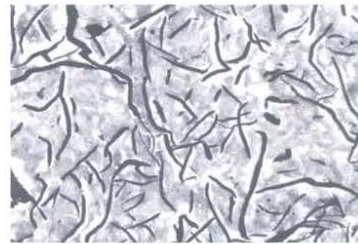
Grafit-kugler i stedet for grafit-flager

- H jere styrke og sejhed

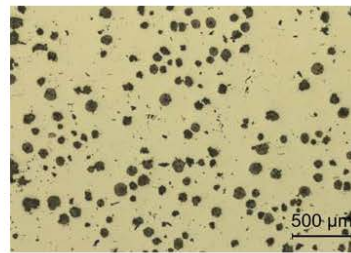
Processen

- Stor geometrisk frihed

Pris



Gr t st bejern



SG jern

  Siemens AG 2013

Siemens Wind Power A/S

Karakterisering af mikrostruktur (Visuelt)

Grafitten

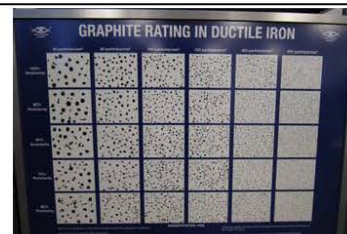
- Form og st rrelse
- ISO 945-1

Matrixen

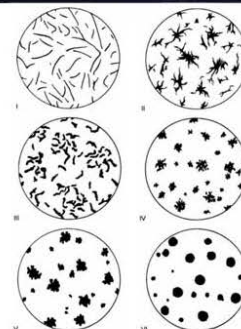
- Perlit/Ferrit indhold
- Evt. Karbider eller andet



Poster fra Ductile Iron Society



Poster fra Ductile Iron Society

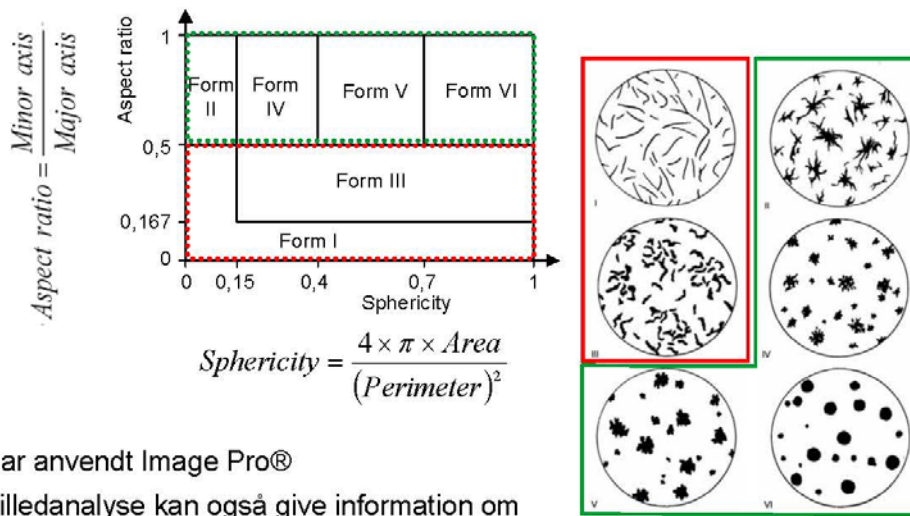


ISO 945-1

  Siemens AG 2013

Siemens Wind Power A/S

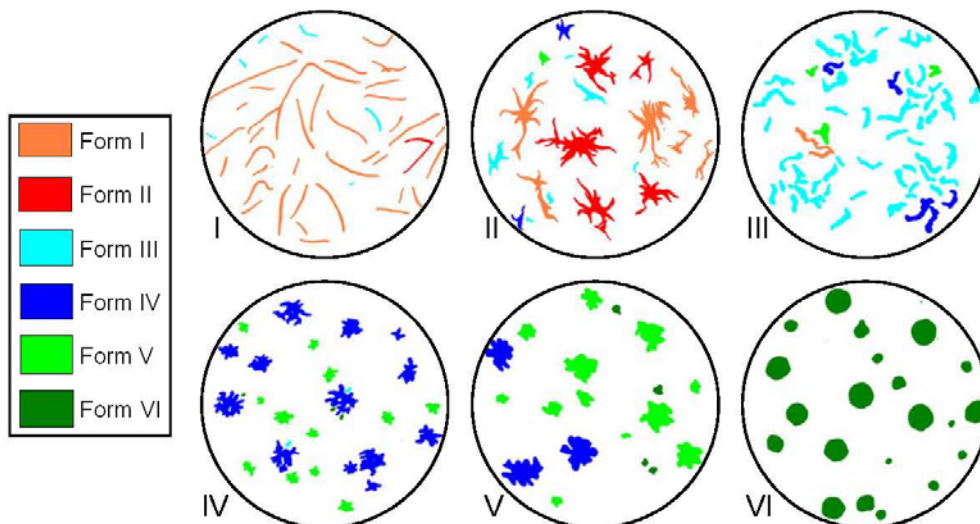
Karakterisering af grafitform (Billedanalyse)



Har anvendt Image Pro®

Billedanalyse kan også give information om nodulantal pr areal, samt størrelsesfordeling.

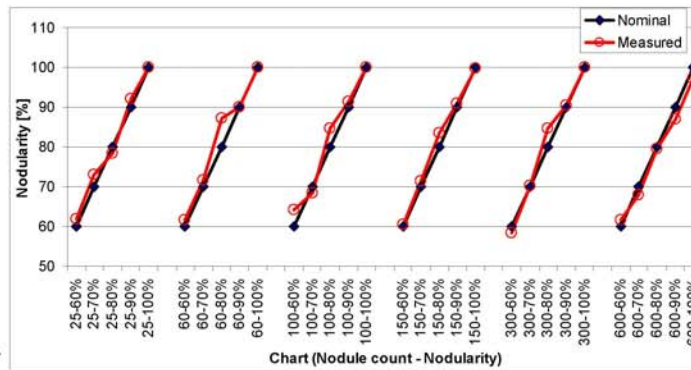
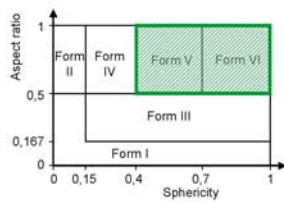
Validering af billedanalyse (ISO 945-1)



Validering af billedanalyse (ISO 945-1)

Målt	Charts i Figur 1 i ISO 945-1					
	Form I	Form II	Form III	Form IV	Form V	Form VI
Form I	90.6	38.5	3.8	0	0	0
Form II	3.9	46.7	0	0	0	0
Form III	5.5	9.4	80.1	0.9	0	0
Form IV	0	4.1	11.5	74.7	36.1	0
Form V	0	1.3	4.7	23.4	60.0	0
Form VI	0	0	0	1.0	4.0	100.0

Validering af billedanalyse
(Poster fra Ductile Iron Society)



Både Form V og VI
er acceptable

$$Nodularity = \frac{\text{Area of acceptable graphite}}{\text{Total graphite area}} \times 100\%$$

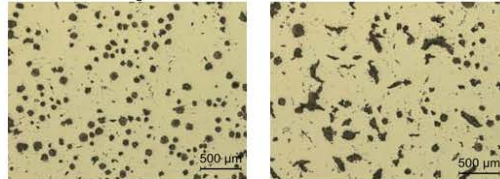
Nogle praktiske erfaringer om billedanalyse

Præparering meget vigtig

Krav om flere billeder (bruger typisk 10 billeder)

Opgør fordeling af grafitform ud fra areal, ikke ud fra antal

Taget med få millimeters afstand

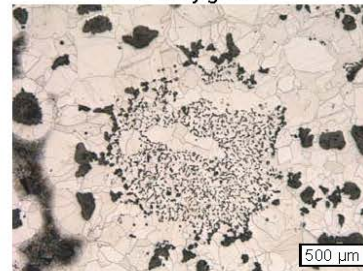


Ofte lige så hurtig at gøre det visuelt, men billedanalyse kan virke mere overbevisende.

Visuel evaluering kan udføres på ætsede emner eller på replica (sammen med vurdering af ferrit/perlit indhold). Billedanalyse skal udføres på polerede emner.

Billedanalyse har svært at tage højde for dårlig grafitform, f.eks. Chunky grafit (tilbage melding til produktion)

Chunky grafit



© Siemens AG 2013
Siemens Wind Power A/S

Page 9

18-01-2013

Karl Martin Pedersen

ISO/TR 945-2 Mikrostruktur i støbejern. Del 2: Grafitklassifikation ved billedanalyse

Har ikke anvendt den endnu, men nogle få kommentarer:

Omhandler IKKE matematiske beskrivelser af grafitformer
Ikke anvendelig for fordeling af grafit i gråt støbejern.

Beskriver nogle krav eller ting til overvejelse (listen er ikke komplet):

- Præparering
- Billedtagning
 - Lysstyrke, skarphed, gråskala
 - Pixelstørrelse (1µm/pixel)
- Minimum 20 grafitpartikler pr billede
- Analysere mindst 400 til 1000 partikler
- Ikke grafit partikler/porer skal ekskluderes
- Opdel sammenhængende grafitpartikler
- Validering ved sammenligne med visuelle målinger

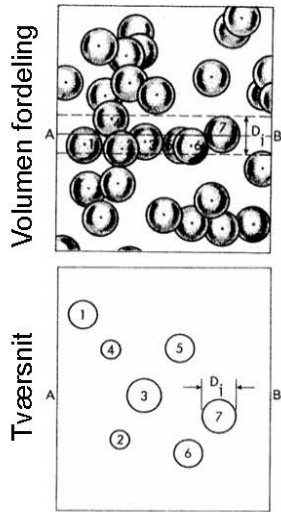
© Siemens AG 2013
Siemens Wind Power A/S

Page 10

18-01-2013

Karl Martin Pedersen

Konvertering fra 2D til 3D



Forudsætning: Ensartet nodule størrelse

$$\left. \begin{aligned} N_A &= d \cdot N_V \\ d &= \left(\frac{6f^\xi}{\pi N_V} \right)^{1/3} \end{aligned} \right\} N_V = \left(\frac{\pi}{6f^\xi} \right)^{1/2} (N_A)^{3/2}$$

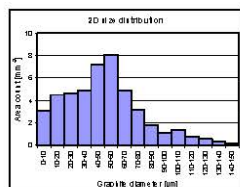
$N_A = \text{Area count } [\text{mm}^{-2}]$
 $N_V = \text{Volume count } [\text{mm}^{-3}]$
 $d = \text{Diameter } [\text{mm}]$
 $f^\xi = \text{Fraction of graphite}$

Variierende nodule størrelser:

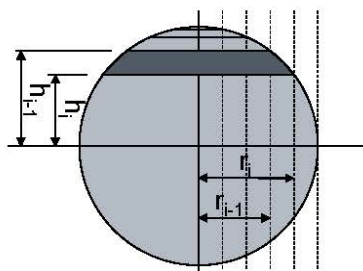
$$N_V = \left(\frac{\pi}{6f^\xi} \right)^{1/2} (\alpha N_A)^{3/2}$$

$\alpha = \text{size distribution parameter } (\approx 1.2)$

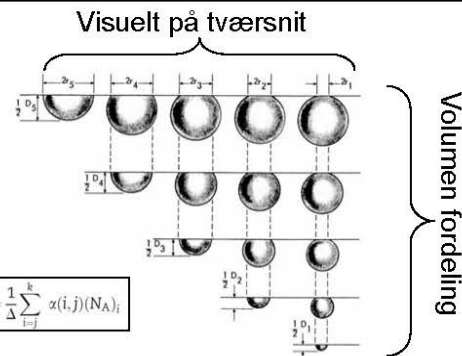
3D størrelsesfordeling



3D?



Vandret snit i grafitnodul
5 størrelsesintervaller



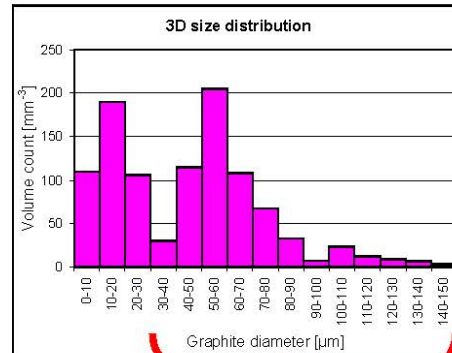
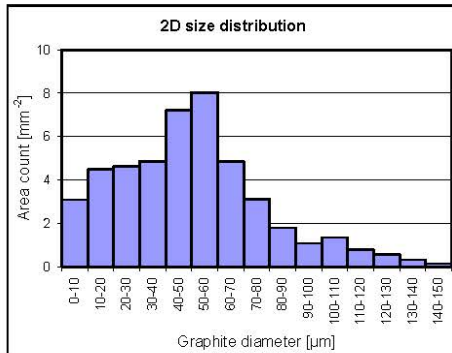
$$(N_V)_i = \frac{1}{\Delta} \sum_{j=1}^k x(i,j) (N_A)_j$$

$$x(i,i) = 1 \quad \text{for } i = 1$$

$$x(i,i) = \frac{2}{\pi} \ln \left(\frac{i + \sqrt{i^2 - (i-1)^2}}{i-1} \right) \quad \forall i > 1$$

$$x(i,j) = \frac{2}{\pi} \ln \left(\frac{i + \sqrt{i^2 - (j-1)^2}}{i + \sqrt{i^2 - j^2}} \times \frac{i-1 + \sqrt{(i-1)^2 - j^2}}{i-1 + \sqrt{(i-1)^2 - (j-1)^2}} \right) \quad \forall i > j$$

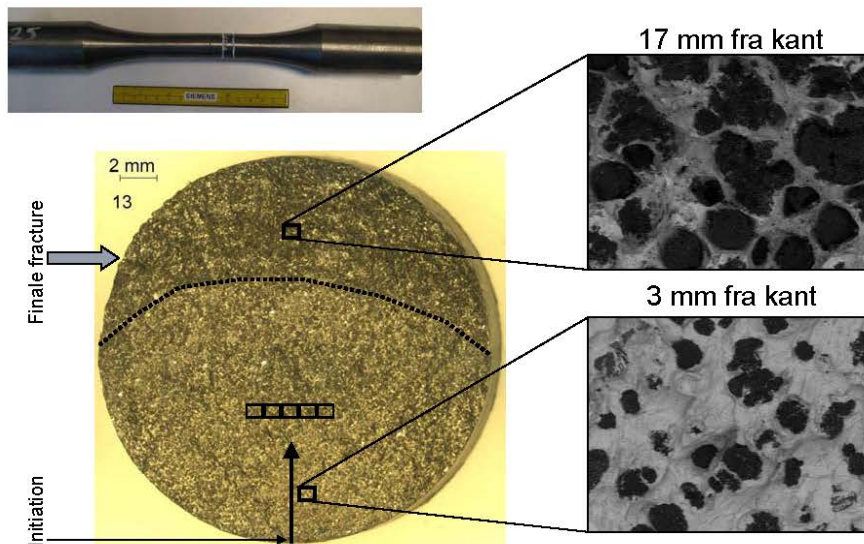
3D størrelsesfordeling



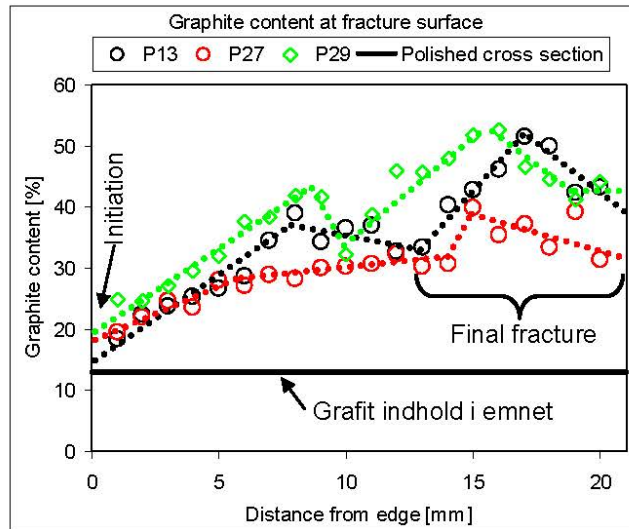
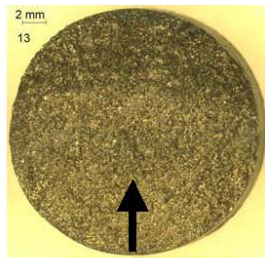
Grafit noder

	2D	3D
Count (<30μm)	12,3 mm ⁻²	405 mm ⁻³
Count (>30μm)	34,2 mm ⁻²	621 mm ⁻³

Grafitindhold på brudflade (Udmattelsestest, R = -1)



Grafitindhold på brudflade



© Siemens AG 2013

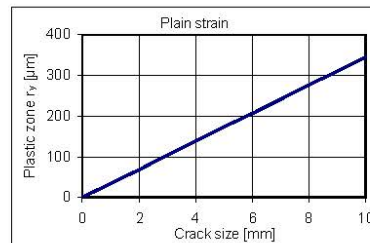
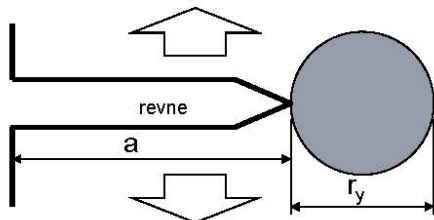
Siemens Wind Power A/S

Page 15

18-01-2013

Karl Martin Pedersen

Plastic zone at crack tip



$$r_y = \frac{1}{2\pi} \left(\frac{K_{\max}}{\sigma_{YS}} \right)^2 \quad (\text{Plain stress})$$

$$r_y = \frac{1}{6\pi} \left(\frac{K_{\max}}{\sigma_{YS}} \right)^2 \quad (\text{Plain strain})$$

$$K_{\max} = Y\sigma_{\max}\sqrt{\pi a}$$

$$r_y = \frac{a}{6} \left(\frac{Y\sigma_{\max}}{\sigma_{YS}} \right)^2 \quad (\text{Plain strain})$$

K = spændings intensity factor

σ_{\max} = max spænding

σ_{YS} = flydespænding

a = revnelængde

r_y = plastisk zone

Y = Form faktor

© Siemens AG 2013

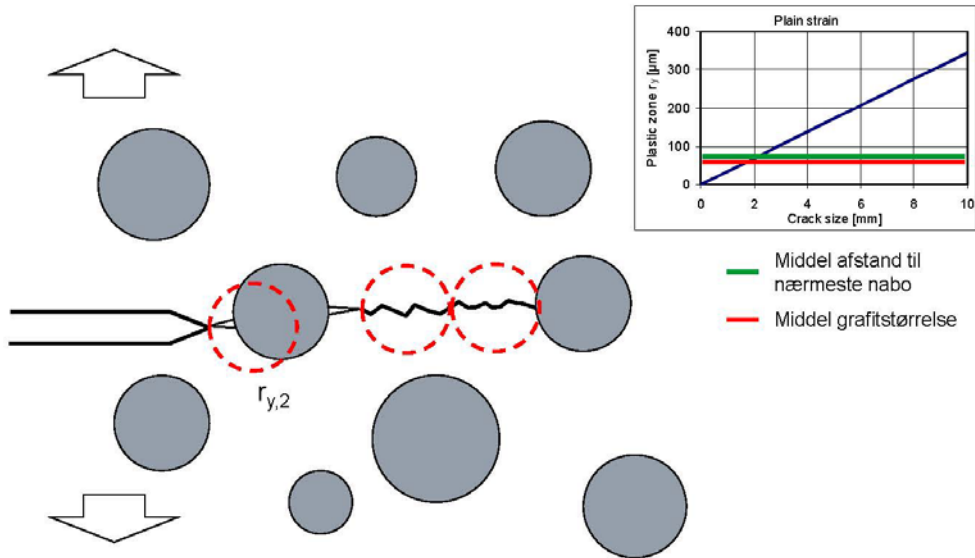
Siemens Wind Power A/S

Page 16

18-01-2013

Karl Martin Pedersen

Plastisk zone og grafit noduler (lille zone)



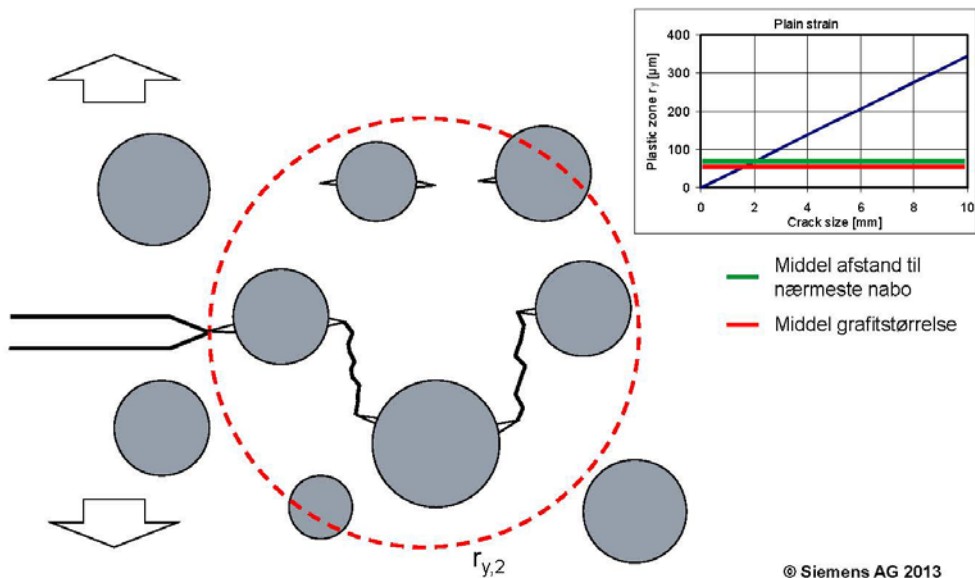
Page 17

18-01-2013

Karl Martin Pedersen

© Siemens AG 2013
Siemens Wind Power A/S

Plastisk zone og grafit noduler (stor zone)



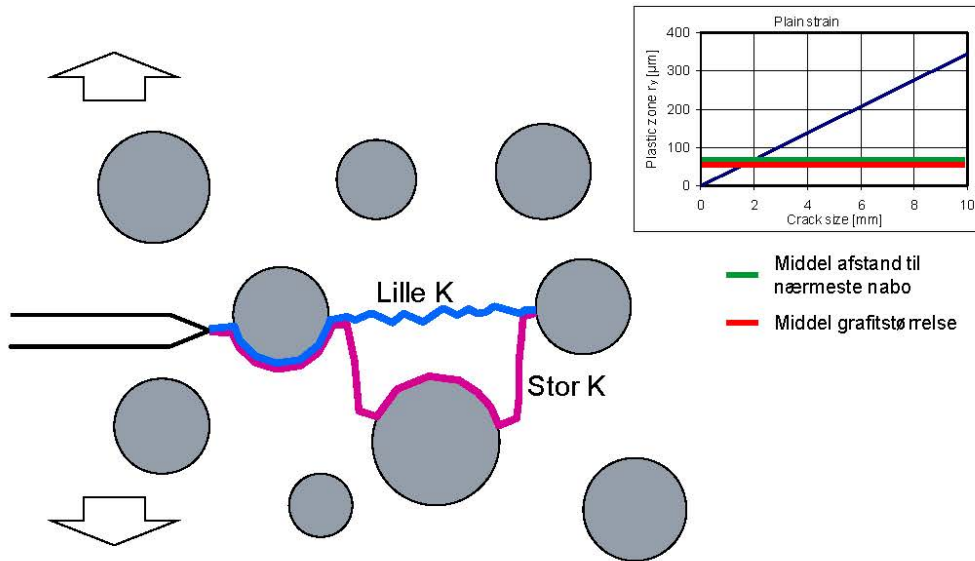
Page 18

18-01-2013

Karl Martin Pedersen

© Siemens AG 2013
Siemens Wind Power A/S

Plastisk zone og grafit noduler



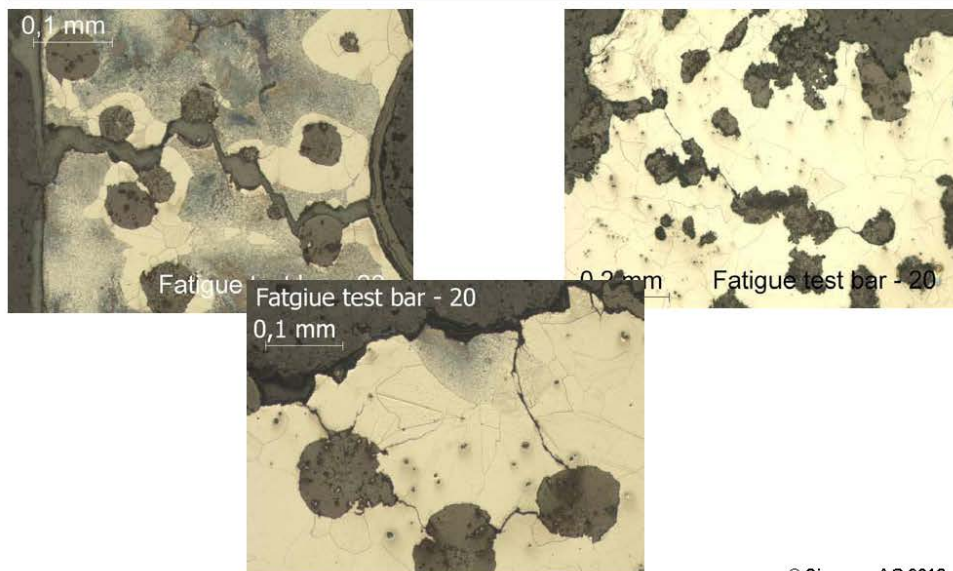
Page 19

18-01-2013

Karl Martin Pedersen

© Siemens AG 2013
Siemens Wind Power A/S

Cross section of fracture surface



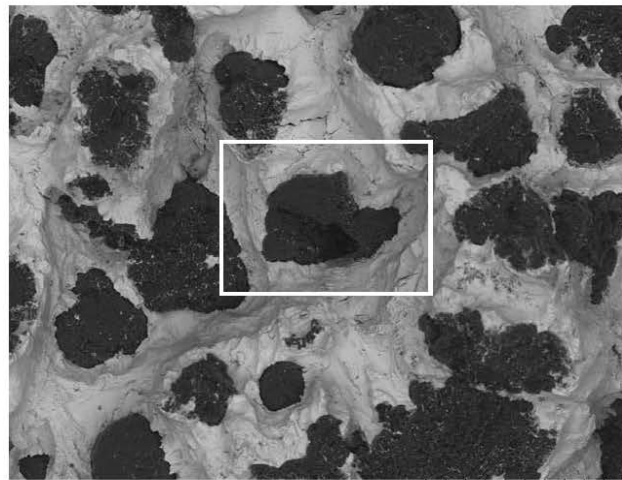
Page 20

18-01-2013

Karl Martin Pedersen

© Siemens AG 2013
Siemens Wind Power A/S

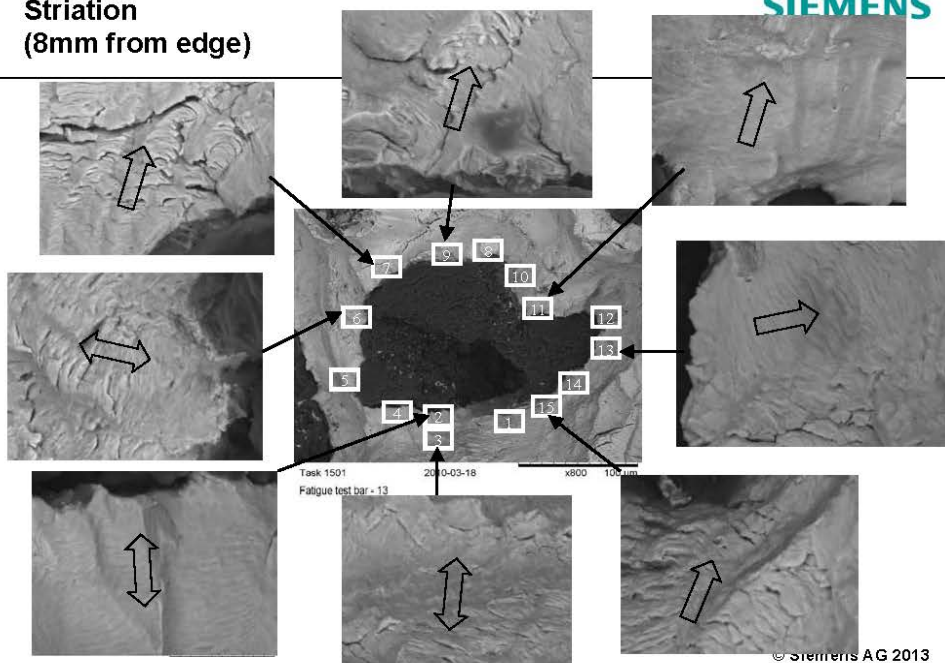
Striation (8mm from edge)



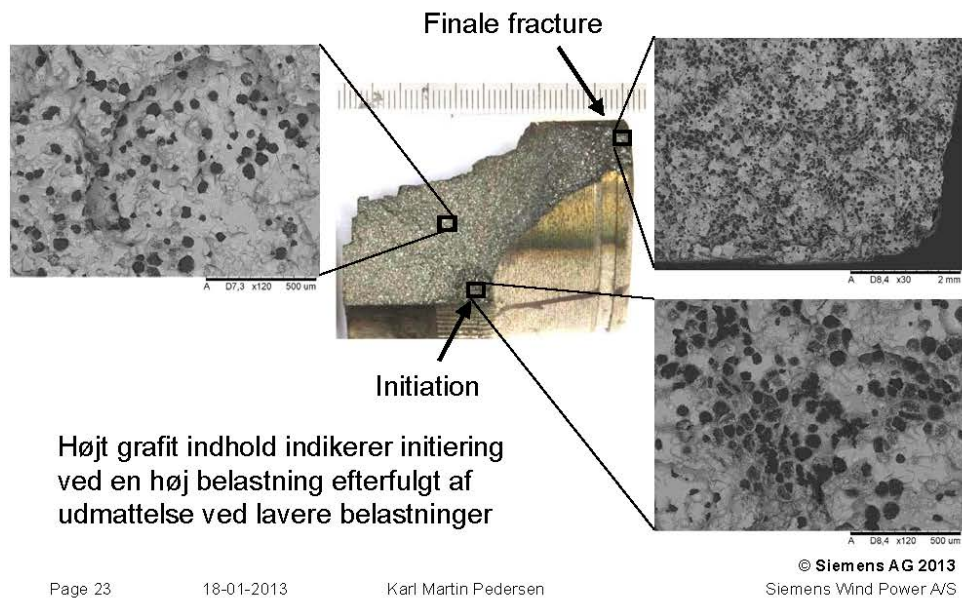
Task 1501 2010-03-18 x250 300 μm

Fatigue test bar - 13

**Striation
(8mm from edge)**



Eksempel på fejlet komponent



Tak for jeres opmærksomhed



Page 24

18-01-2013



Karl Martin Pedersen



© Siemens AG 2013
Siemens Wind Power A/S

Kilder

Grafit noder i 2D og 3D:

- K.M. Pedersen and N.S. Tiedje: Graphite nodule count and size distribution in thin-walled ductile cast iron, Materials Characterization, Vol 8, p 1111-1121, 2008
- E.E. Underwood: Quantitative Stereology. Addison-Wesley Publishing Company; 1970. p. 109–145
- C.B. Basak and A.K. Sengupta: Development of a FDM based code to determine the 3-D size distribution of homogeneously dispersed spherical second phase from microstructure: a case study on nodular cast iron. Scripta Materialia, Vol 51, p. 255–260, 2004

Kvalitetssikring af støbegods i MAN B&W motorer

Knud Strande, MAN

Kvalitetssikring af Støbegods i MAN B&W Motorer



Knud Strande
Production Support
Engineering
Marine Low Speed

Kvalitetssikring - MAN B&W Motorer



- MAN Diesel & Turbo – København
- Typiske støbte komponenter i MAN B&W motorer; Gråjern, Stål, SG jern og Kompakt grafit jern.
- Kvalitetssikring – Controlled Component Concept.
- "Dagligt arbejde" i Production Supports støbegruppe.
- Tekniske udfordringer foranlediget af design og af produktion – eksempler.
- Indløb og efterføding – "god latin".
- Sammenfatning, kvalitetssikring - "Værktøjskassens" indhold.

MAN DIESEL & Turbo



Company Logo



Company Brand

MAN Diesel & Turbo

Product Brand



Service Brands

MAN | PrimeServ

MAN | PowerManagement

Product /Type
Designations
(Examples)

51/60DF B&W K98ME-C TCA88 SaCoS_{one}
VBS1180 MARC6 DWE THM turbolog

MAN Diesel & Turbo

Knud Strand

Production Support

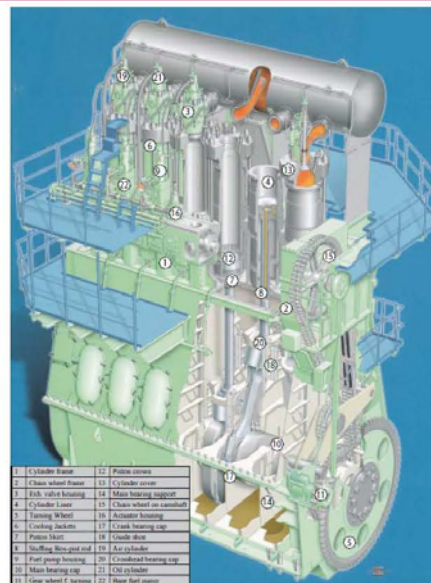
Januar 2013



MAN B&W Motoren



- Størrelser: 26-98 cm cylinder diameter
- Effekt: 450 kW – 87.000 kW
- Typiske støbte komponenter: Gråjern, Stål, SG jern og CGI jern
- Ca. 30% af motorens vægt består af støbegods
- På en 6S60MC-C motor (~15 MW) svarer det til ~ 100t
- På 15 GW svarer det til ~ 100.000t



1 Cylinder frame	12 Piston crown
2 Chain wheel frame	13 Cylinder cover
3 Pist. valve housing	14 Main bearing support
4 Cylinder cover	15 Chain wheel on crankshaft
5 Turning Wheel	16 Actuator housing
6 Cooling jackets	17 Crank bearing cap
7 Piston skirt	18 Piston skirt
8 Scuffing Ring and	19 Air cylinder
9 Fuel pump housing	20 Crankshaft bearing cap
10 Main bearing cap	21 Air cylinder
11 Crank wheel & bearing	22 Chain belt pump

MAN Diesel & Turbo

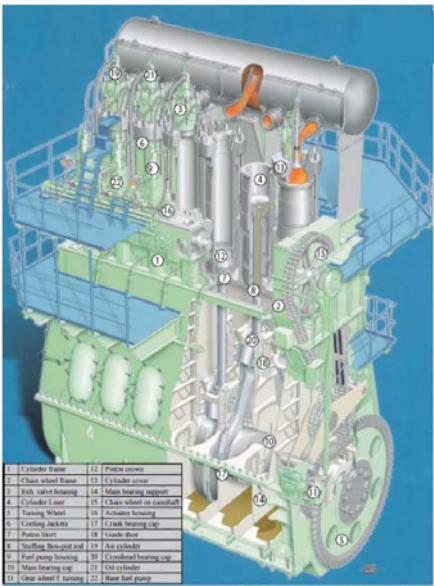
Knud Strand

Production Support

Januar 2013



Støbegods i MAN B&W motorer



1	Cylinder frame	12	Piston crown
2	Chain wheel frame	13	Cylinder cover
3	Pin valve bearing	14	Chain wheel support
4	Cylinder liner	15	Chain wheel air duct
5	Turning wheel	16	Armature bearing
6	Cooling jacket	17	Crank bearing cap
7	Piston head	18	Crank pin
8	Stuffing box/piston rod	19	Air cylinder
9	Fuel pump bearing	20	Condensed bearing cap
10	Main bearing cap	21	Oil cylinder
11	Clear wheel & turning	22	Rear fuel pump



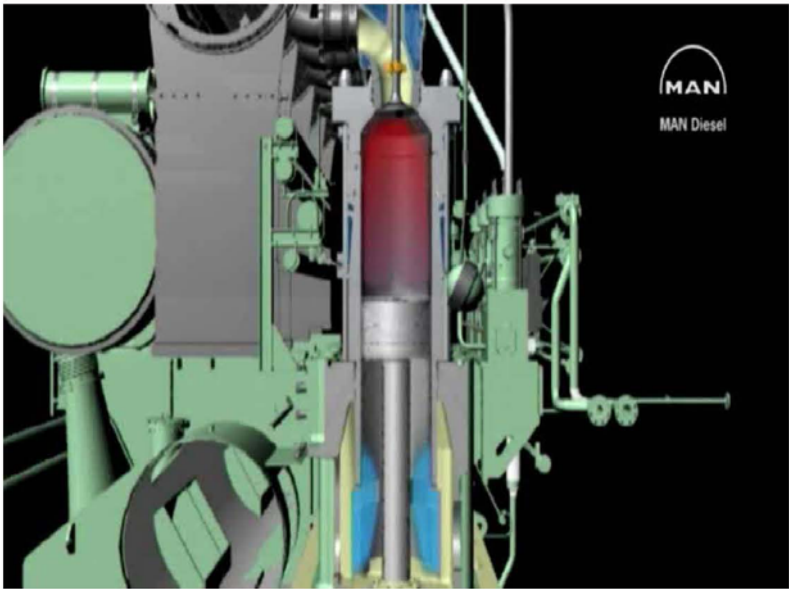
MAN Diesel & Turbo

Knud Strande

Production Support

Januar 2013 < 6 >

MAN B&W Motoren



MAN Diesel & Turbo

Knud Strande

Production Support

Januar 2013 < 6 >

Kvalitetssikring – Controlled Components



- **Simple Components**

Requirements to material properties (alloy), geometrical tolerances and surface tolerances stated on drawings and in general accepted standards.

- **Controlled Components**

Components with certain functional requirements and/or components considered difficult to manufacture.

- **Quality Specification**

States quality requirements, which always are based on expected component performance set by the designer (and experience).

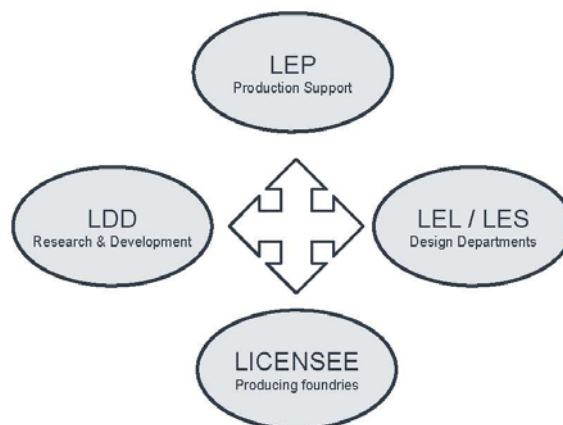
- **First Time Approval Test (FTA)**

Supplier has to show his technical ability before being approved.

- **Production Recommendation**

Special process knowledge required.

Støbegruppens samarbejdspartnere



Eksempel på kvalitets specifikation



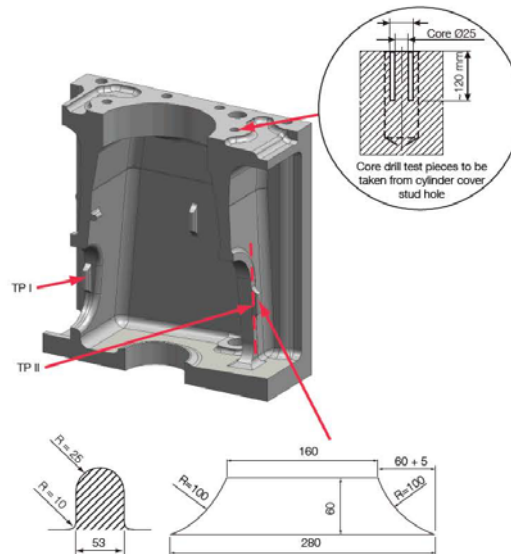
Cylinder Frames

Cylinder Frames, Grey Cast Iron

This document is valid for existing engine types on order as of the date of this document:

Engine types:

All two-stroke engine types
(Specified with C3Cu Cylinder Frames).



MAN Diesel & Turbo

Knud Strande

Production Support

Januar 2013

< 9 >

B&W Støberi 1885 – P. S. Krøyer



MAN Diesel & Turbo

Knud Strande

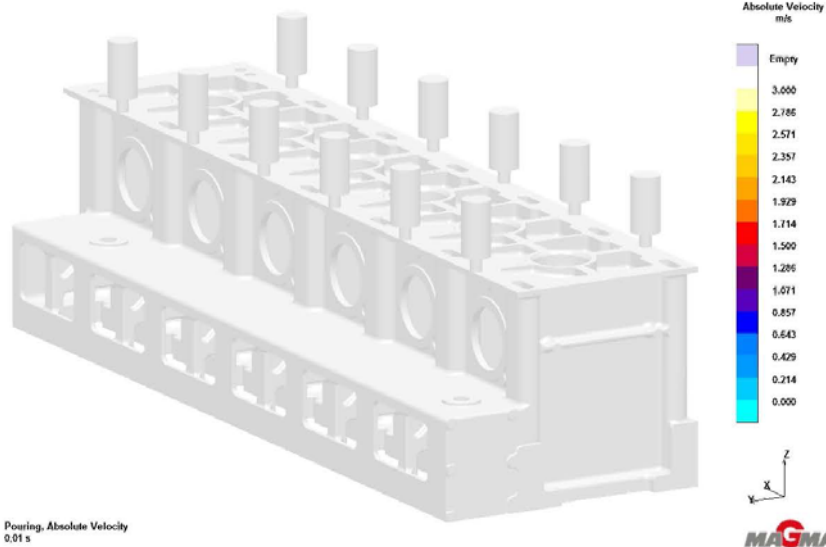
Production Support

Januar 2013

< 10 >

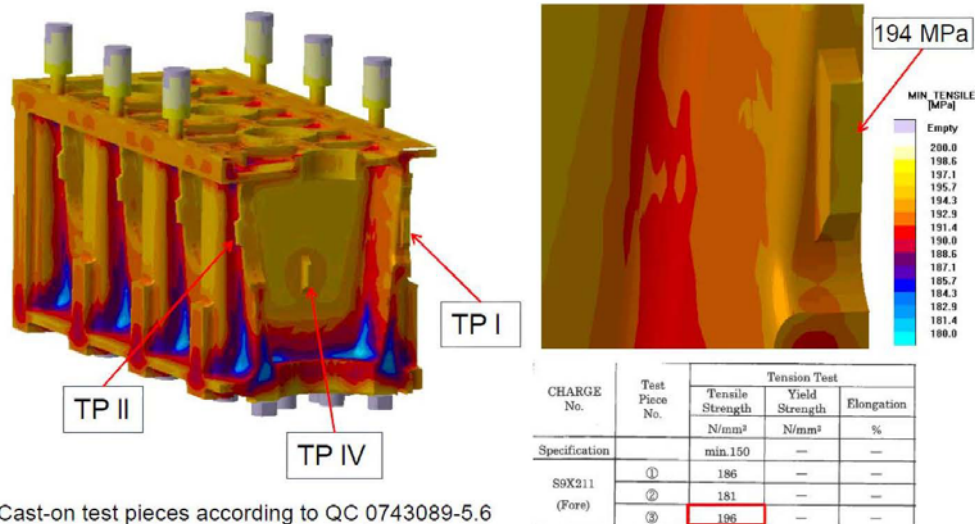
Casting Simulation

Filling, Absolute Velocity



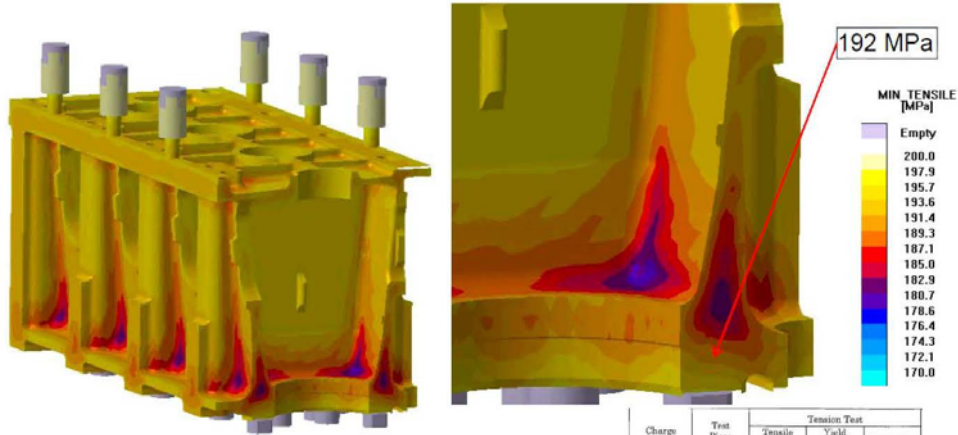
Feed back from "real life"

Cylinder frame castings – material strength



Feed back from "real life"

Cylinder frame castings – material strength



Core drilled test pieces in according to QC 0743089-5.6

Charge No.	Test Piece No.	Tension Test		
		Tensile Strength	Yield Strength	Elongation
		N/mm ²	N/mm ²	%
Specification		≥ 140	—	—
	1	161	—	—
90K211	5	158	—	—
(For)	9	161	—	—
	10	160	—	—

MAN Diesel & Turbo

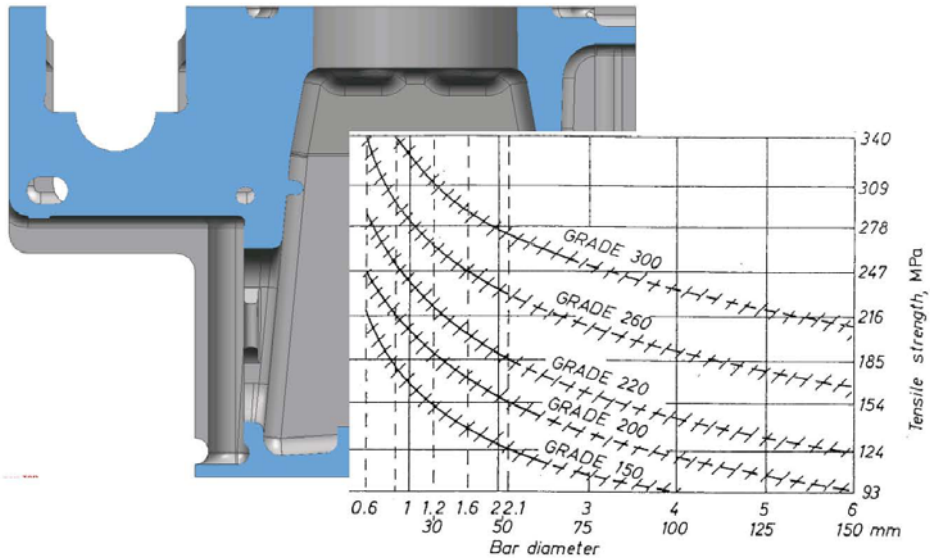
Knud Strande

Production Support

Januar 2013 < 13 >

Feed back from "real life"

Cylinder frame castings – too low material strength



MAN Diesel & Turbo

Knud Strande

Production Support

Januar 2013 < 14 >

Feed back from "real life"

Cylinder frame castings – too low material strength



MAN Diesel & Turbo

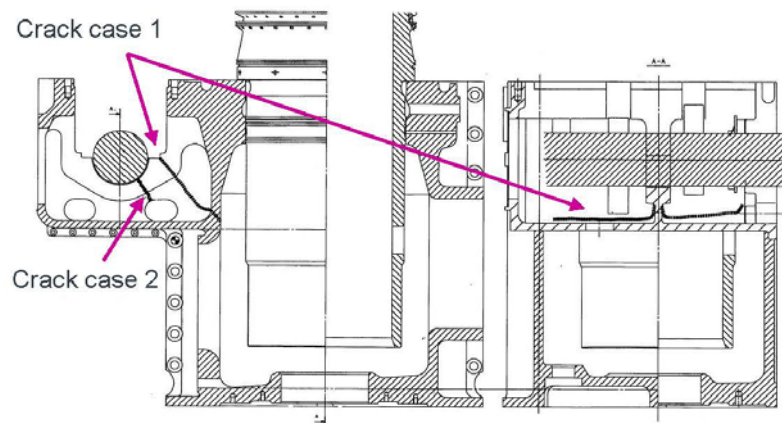
Knud Strande

Production Support

Januar 2013 < 15 >

Feed back from "real life"

Cylinder frame castings – too low material strength



MAN Diesel & Turbo

Knud Strande

Production Support

Januar 2013 < 16 >

Feed back from "real life"

Cylinder frame castings – shrinkage defects



MAN Diesel & Turbo

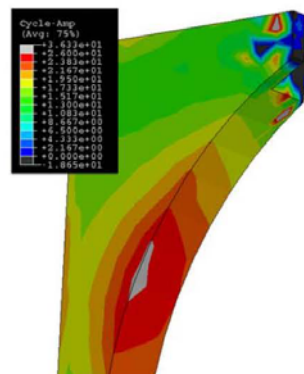
Knud Strande

Production Support

Januar 2013 < 17 >

Feed back from "real life"

Cylinder frame castings – residual stresses



Stresses caused by engine operation

MAN Diesel & Turbo

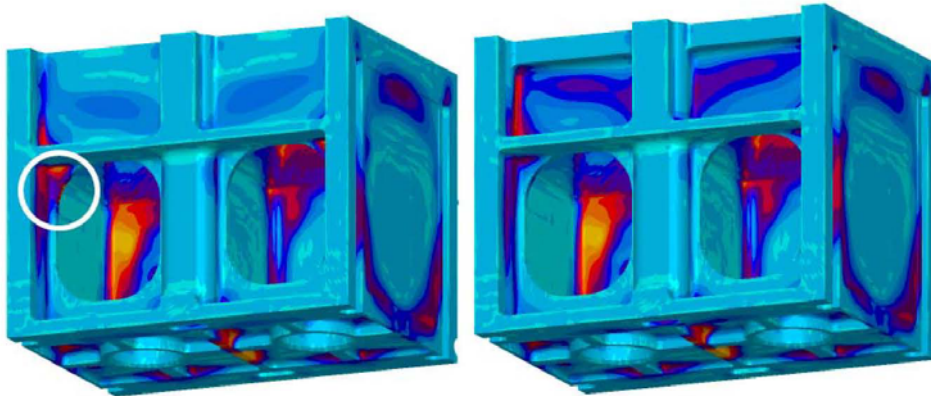
Knud Strande

Production Support

Januar 2013 < 18 >

Feed back from "real life"

Cylinder frame castings – residual stresses



Reducing residual stresses by design modifications

MAN Diesel & Turbo

Knud Strande

Production Support

Januar 2013 < 19 >

Feed back from "real life"

Indeslutninger/overfladefejl



MAN Diesel & Turbo

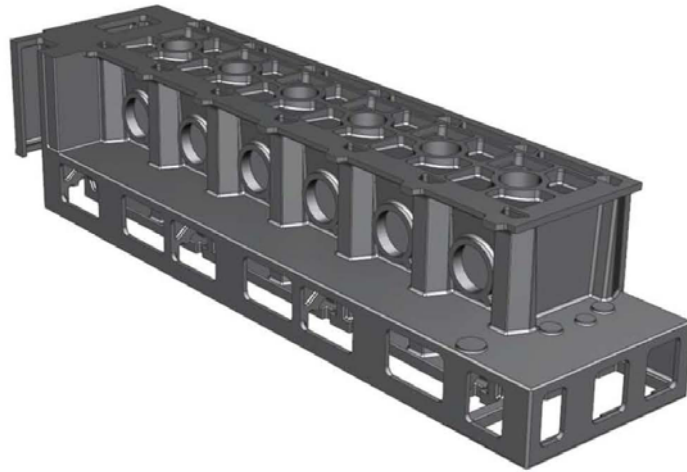
Knud Strande

Production Support

Januar 2013 < 20 >

6S50ME-B9 cylinder frame

KPF, nodular cast iron



MAN Diesel & Turbo

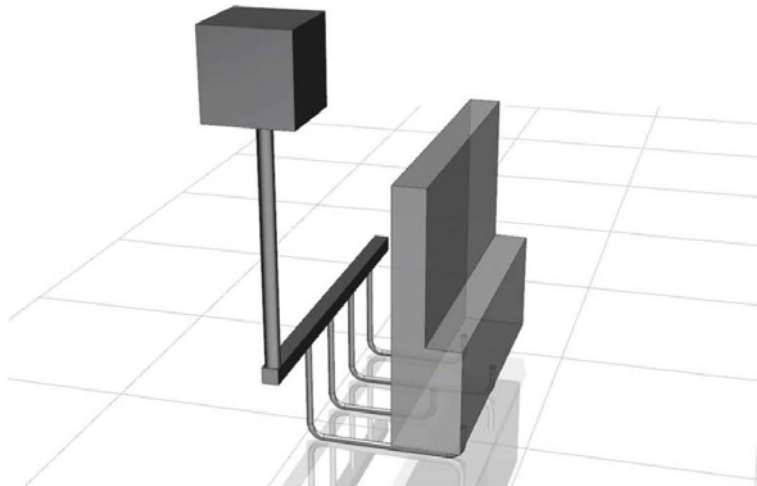
Knud Strände

Production Support

Januar 2013 < 21 >

Dummy filling, layout 1

Vertical sprue, Ø90



MAN Diesel & Turbo

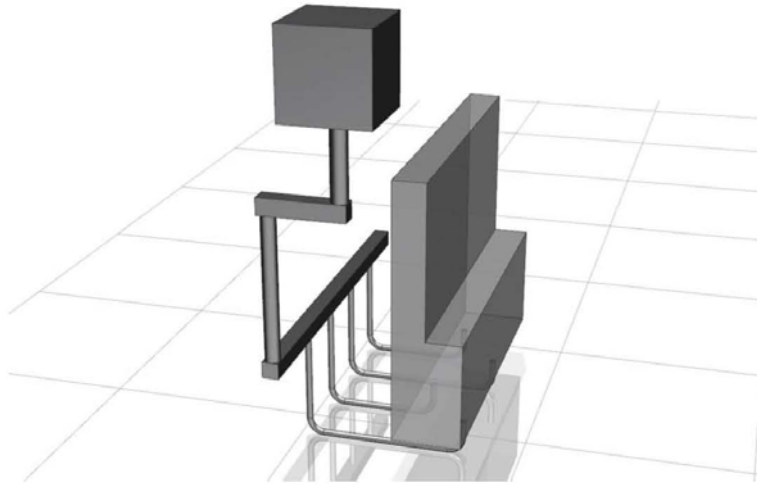
Knud Strände

Production Support

Januar 2013 < 22 >

Dummy filling, layout 2

Split sprue, Ø100 & Ø90



MAN Diesel & Turbo

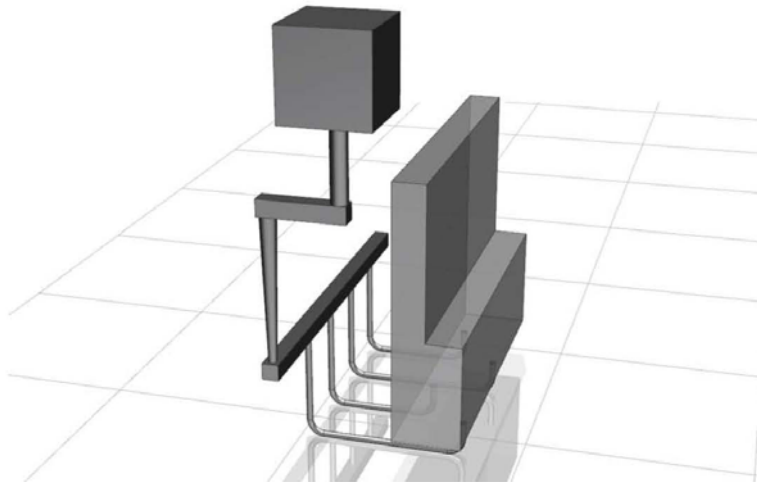
Knud Strande

Production Support

Januar 2013 < 23 >

Dummy filling, layout 3

Split sprue, Ø100 & Ø90 - Ø50



MAN Diesel & Turbo

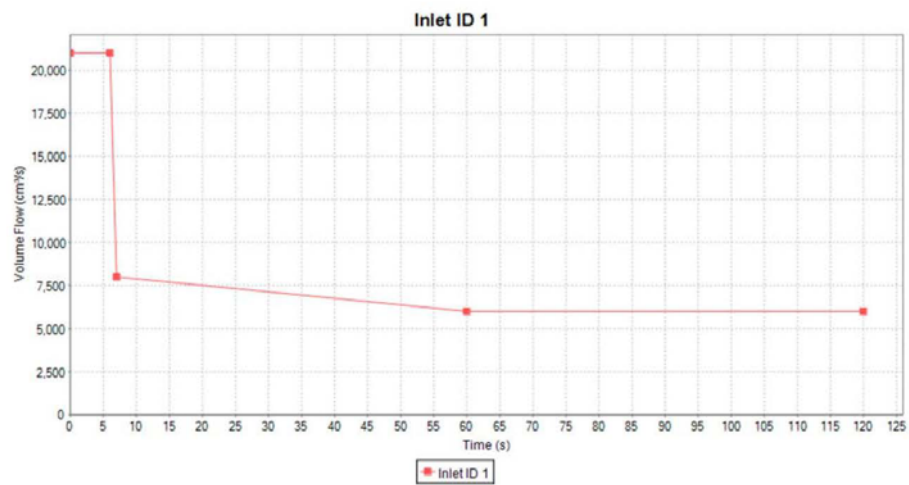
Knud Strande

Production Support

Januar 2013 < 24 >

Dummy filling

Same pouring rate for all three layouts



MAN Diesel & Turbo

Knud Strande

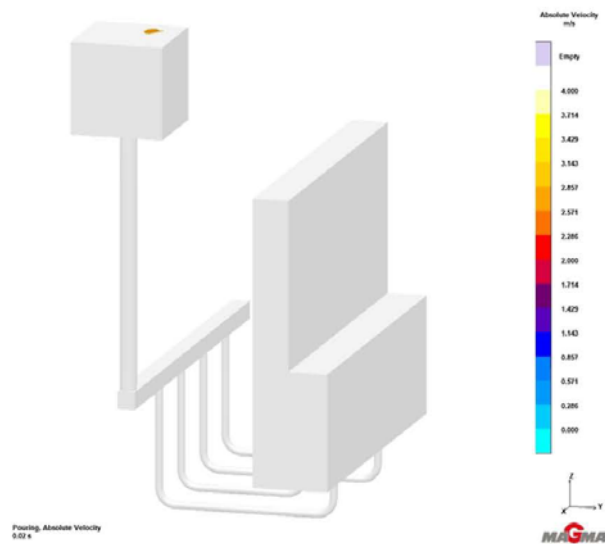
Production Support

Januar 2013

< 25 >

Layout 1

Absolute Velocity, fill time ~128s



MAN Diesel & Turbo

Knud Strande

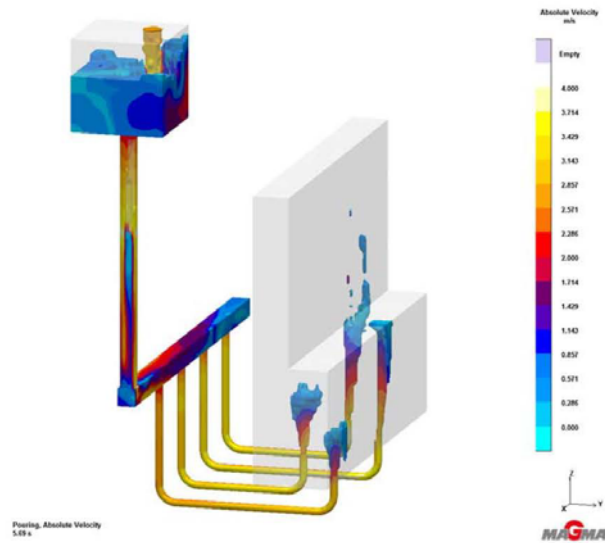
Production Support

Januar 2013

< 26 >

Layout 1

Absolute Velocity



MAN Diesel & Turbo

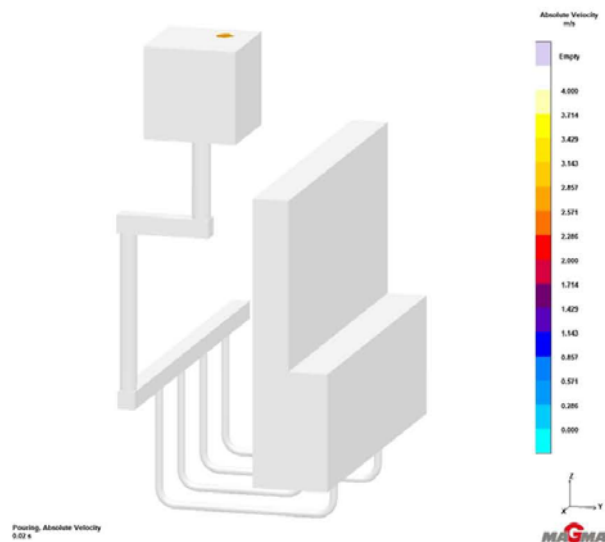
Knud Strande

Production Support

Januar 2013 < 27 >

Layout 2

Absolute Velocity, fill time ~130s



MAN Diesel & Turbo

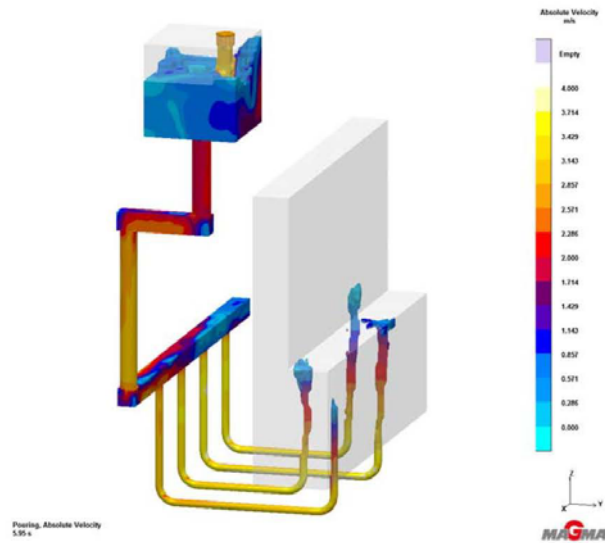
Knud Strande

Production Support

Januar 2013 < 28 >

Layout 2

Absolute Velocity



MAN Diesel & Turbo

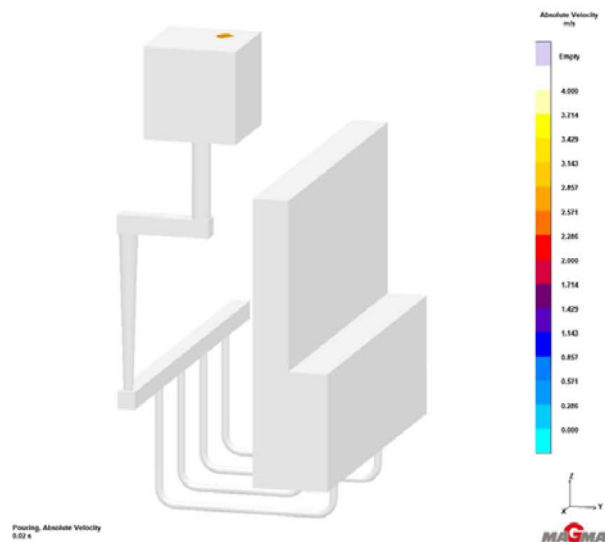
Knud Strande

Production Support

Januar 2013 < 29 >

Layout 3

Absolute Velocity, fill time ~140s



MAN Diesel & Turbo

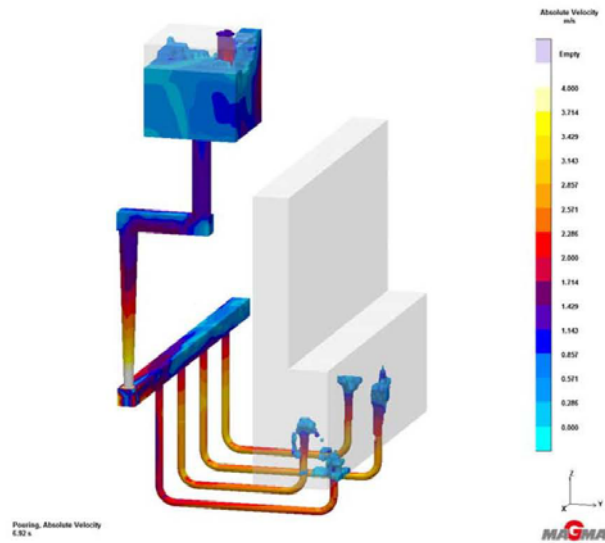
Knud Strande

Production Support

Januar 2013 < 30 >

Layout 3

Absolute Velocity



MAN Diesel & Turbo

Knud Strande

Production Support

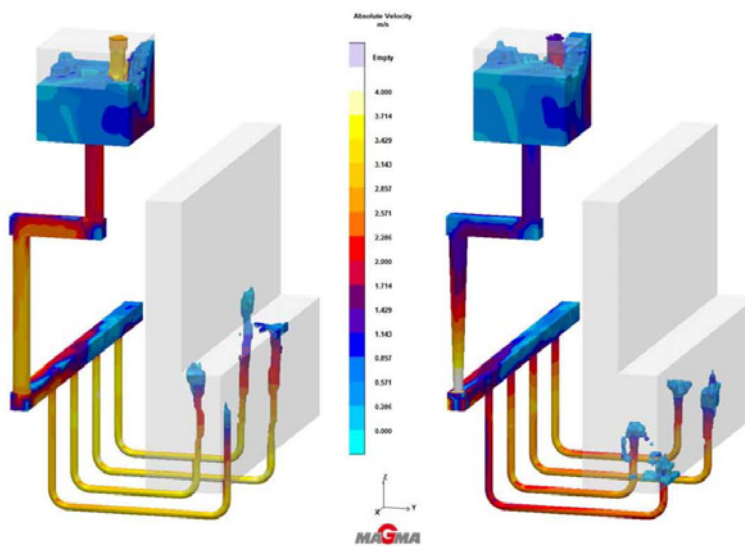
Januar 2013

< 31 >

Comparison, ~6 sec.

Layout 2

Layout 3



MAN Diesel & Turbo

Knud Strande

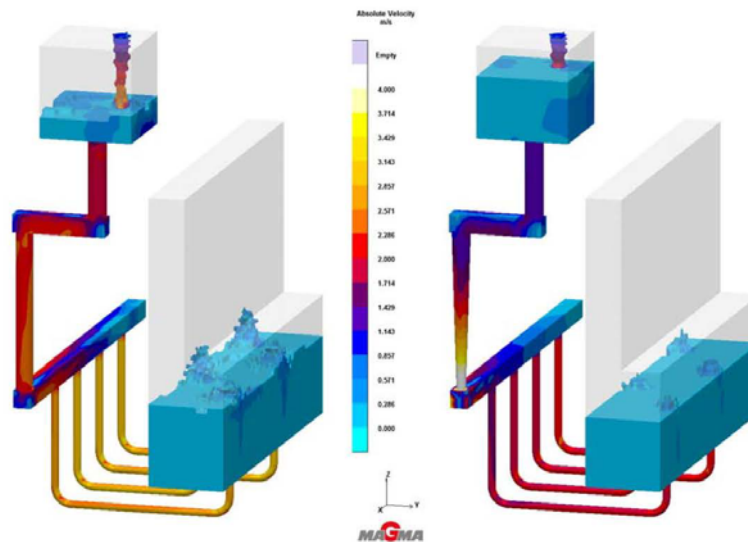
Production Support

Januar 2013

< 32 >

Comparison, ~45 sec. Layout 2

Layout 3



MAN Diesel & Turbo

Knud Strande

Production Support

Januar 2013

< 33 >

Cylinder liner G50ME-C Grey cast iron – Tarkalloy A



MAN Diesel & Turbo

Knud Strande

Production Support

Januar 2013

< 34 >

Kvalitets sikring – internt & eksternt

Værktøjsskassens indhold



- Optimere designet, så det er støbevenligt
- **støbesimulering.**
- Udarbejde specifikationer og rekommandationer
- **designkrav + erfaring + tilbagemeldinger fra producenter.**
- Hjælpe specifikke producenter med at optimere støbe layoutet
- **støbesimulering.**
- Hjælpe specifikke producenter med at optimere smeltebehandlingen
- **smeltemetallurgisk viden.**
- Hjælpe specifikke producenter med at optimere formmaterialerne
- **viden om formsand og bindemidler.**

Ny metode til kvantificering af grafitstørrelse og – morfologi i støbejern

Steen Krogh Jensen, MAN

Ny metode til kvantificering af grafitstørrelse og -morfologi i støbejern



Dansk Metallurgisk Selskab,
Vintermøde 16-18/1-2013



Steen Krogh Jensen

Manager
Material Technology and Research
Research & Development
/ Marine Low Speed

Disclaimer



All data provided on the following slides is for information purposes only, explicitly non-binding and subject to changes without further notice.

Agenda



- 1 Cylinderforing – gammel materialspecifikation
- 2 ISO 945 – graphite classification
- 3 Cylinderforing – eksempler på grafit struktur, matrix and hårdfase
- 4 Grafitstørrelse – en ny definition
- 5 Hårdfase – mængde og fordeling
- 6 Ferrit – mængde?
- 7 Cylinderforing – ny materialespecifikation
- 8 Eksempler fra støberier
- 9 Stempelring – materialespecifikation – nodularitet
- 10 ISO 16 112 – Compacted (vermicular) graphite cast irons - Classification

MAN Diesel & Turbo

Steen Krogh Jensen

Kvantificering af grafitstørrelse og -morfologi i støbejern



18.01.2012



Cylinderforing Gammel materialspecifikation



MAN B&W Diesel A/S

Cast Iron

Cast Iron for Cylinder Liners

Tarkall-C

Mechanical Properties

• Tensile Strength	R_m	MPa	min. 245 ¹⁾
• Elongation	A_{50}	%	min. 5.2 ¹⁾
• Brinell Hardness (ISO 6506:1981)	HBS	10/3000/15	185-230 ²⁾

¹⁾ In the upper part of the cylinder liner.

²⁾ Total elongation at fracture, i.e. elastic + plastic elongation. See Q.C. 74 18 99-0.

³⁾ Measured on the inside of the cylinder liner, 100 mm from the top.

Microstructure

• Graphite (ISO 945-1975): I A 2/3/4.

• Matrix: Lamellar pearlite. Max. 3% ferrite, 3-7% cementite + steadite.

Microstructure

• Graphite (ISO 945-1975): I A 2/3/4.

• Matrix: Lamellar pearlite. Max. 3% ferrite, 3-7% cementite + steadite.

• Figures and text in bold type denote imperative demands.
All other information - including Similar Standards - is given for guidance only. (See General Note).

• According to Quality Control No. 74 14 12-0 the foundry must carry out a first time casting and obtain the approval of MAN B&W Diesel A/S as supplier of cylinder liners made of Tarkall-C.

Similar Standards

ISO

EN

JIS

These standards do not include any Cast Iron similar to the above quality.

Supply Form

Finished cylinder liner. Tarkall-C is an abbreviation of the trade name Tarkalloy C.

Tribologi/Styrke/
Varmeledningsevne

Slidstyrke

Scuffing resists

Styrke/Tribologi



Copyright © MAN B&W Diesel A/S, November 1996

Material Sheet P 676-2

MAN Diesel & Turbo

Steen Krogh Jensen

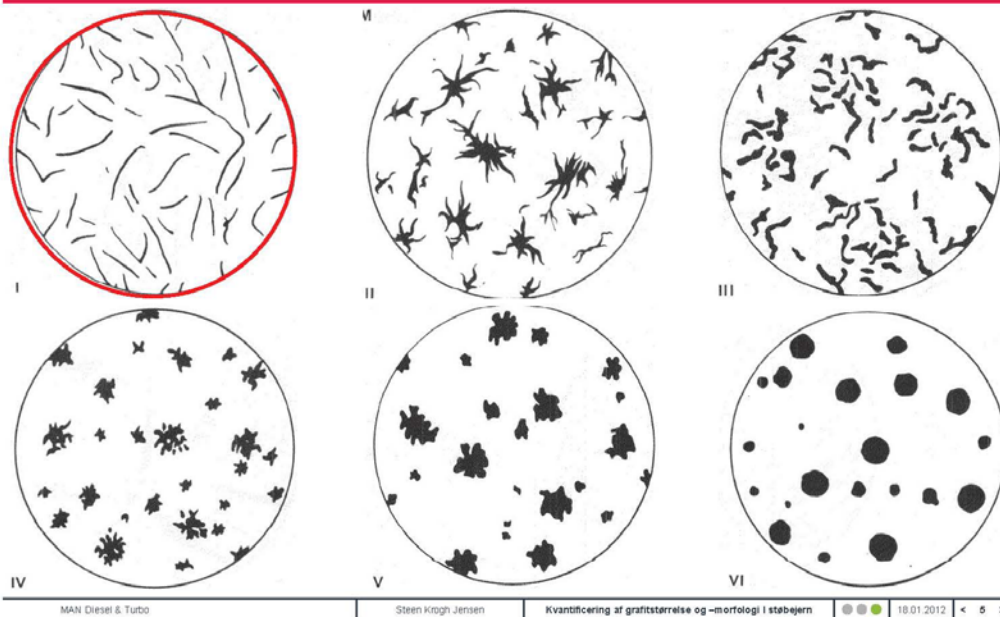
Kvantificering af grafitstørrelse og -morfologi i støbejern



18.01.2012



Grafitform ifølge ISO 945



MAN Diesel & Turbo

Steen Krogh Jensen

Kvantificering af grafitstørrelse og -morfologi i støbejern



10.01.2012

< 5 >

Grafitstørrelse ifølge ISO 945



Table 1 — Dimensions of graphite particle forms I to VI

Dimensions in millimetres

Size range reference number	Indication of the particle size observed at $\times 100$ magnification	Actual dimension
1	≥ 100	≥ 1
2	50 to < 100	0,5 to < 1
3	25 to < 50	0,25 to $< 0,5$
4	12 to < 25	0,12 to $< 0,25$
5	6 to < 12	0,06 to $< 0,12$
6	3 to < 6	0,03 to $< 0,06$
7	1,5 to < 3	0,015 to $< 0,03$
8	$< 1,5$	$< 0,015$

NOTE 1 When determining size ranges 1 and 2, a lower magnification ($\times 25$ or $\times 50$) may be used.
 NOTE 2 When determining size ranges 6 to 8, a higher magnification ($\times 200$ or $\times 500$) may be used.
 NOTE 3 For determining size ranges, the largest visible graphite particle size is used.

MAN Diesel & Turbo

Steen Krogh Jensen

Kvantificering af grafitstørrelse og -morfologi i støbejern



10.01.2012

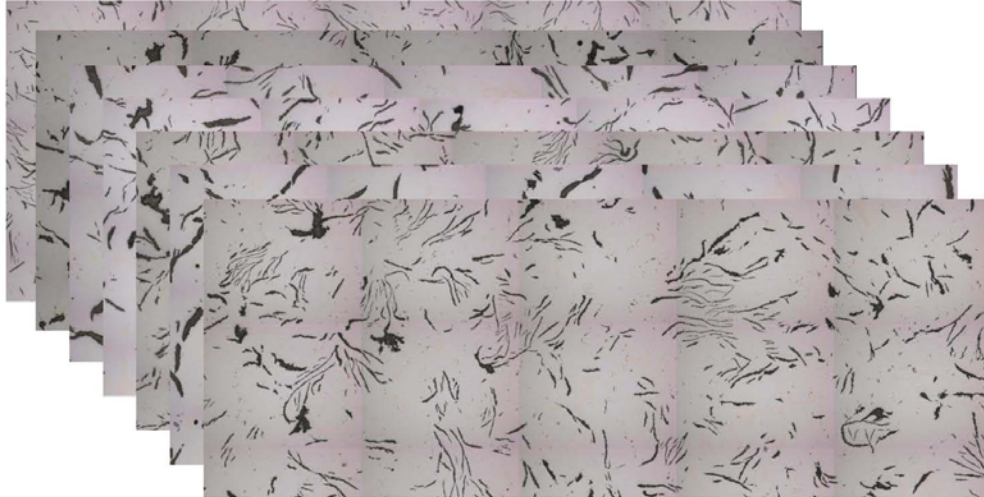
< 6 >

Grafiteform - 7 støberier



Graphite (ISO 945-1975): I A 2/3/4.

1 mm



MAN Diesel & Turbo

Steen Krogh Jensen

Kvantificering af grafitstørrelse og -morfologi i støbejern



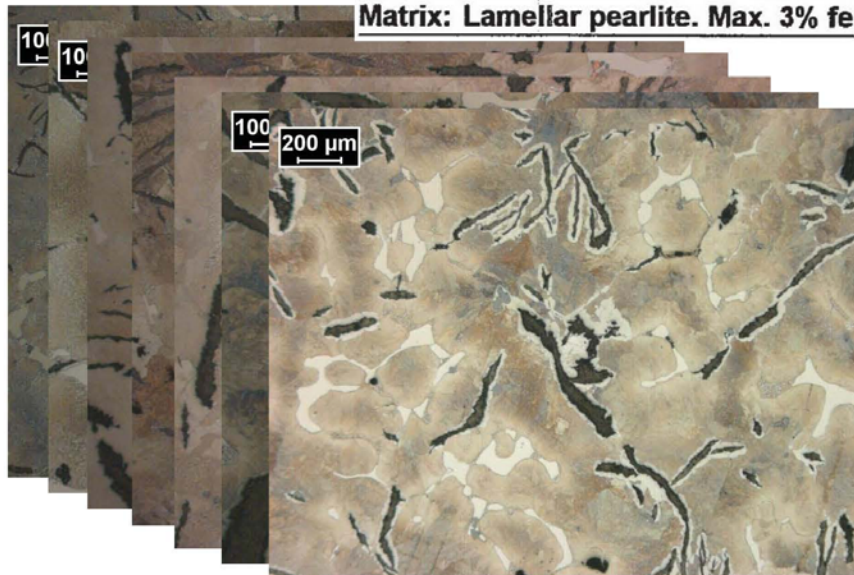
18.01.2012

< 7 >

Matrix (perlit/ferrit)- 7 støberier



Matrix: Lamellar pearlite. Max. 3% ferrite.



MAN Diesel & Turbo

Steen Krogh Jensen

Kvantificering af grafitstørrelse og -morfologi i støbejern



18.01.2012

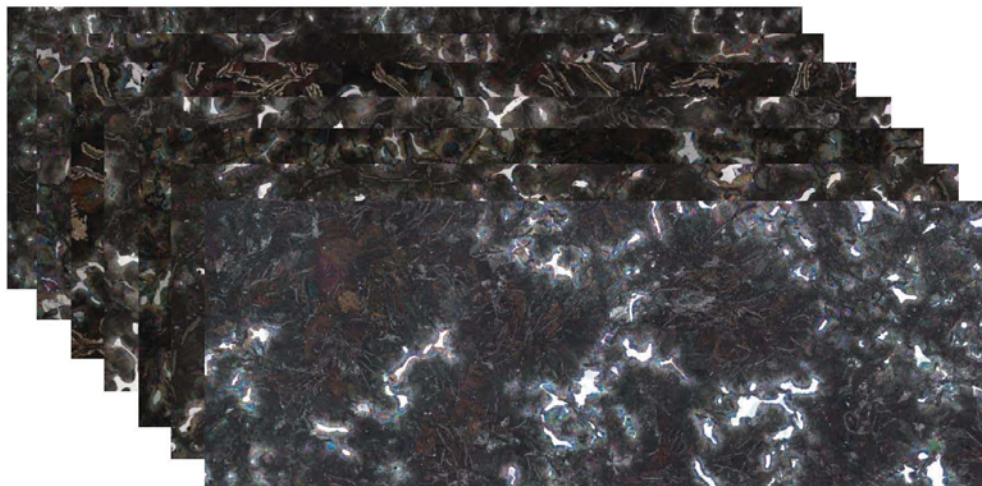
< 8 >

Hårdfase - 7 støberier



3-7% cementite + steadite.

1 mm



MAN Diesel & Turbo

Steen Krogh Jensen

Kvantificering af grafitstørrelse og -morfologi i støbejern

18.01.2012

< 9 >

Samlet vurdering af Mikrostruktur 7 støberier



Position	Matrix	Graphite type			% Cementite + Steadite			% Ferrite		
		inside	centre	outside	inside	centre	outside	inside	centre	outside
MAN Diesel A/S	Pearlite	IA3/4/5	IA3/4/5	IA3/4/5	2.13	1.52	1.88	< 1	< 1	< 1
Leverandør nr. 1	Pearlite	A4			< 2			-		
MAN Diesel A/S	Pearlite	IA3/4/5	IA3/4/5	IA3/4/5	3.82	2.97	3.36	< 1	< 1	< 1
Leverandør nr. 3	Pearlite	A2-4			3 - 4			< 3		
MAN Diesel A/S	Pearlite	IA3/4/5	IA3/4/5	IA3/4/5	2.76	2.49	3.60	< 1	< 1	< 1
Leverandør nr. 4	Pearlite	A2-4			3 - 4			< 3		
MAN Diesel A/S	Pearlite	IA2/3/4	IA2/3/4/5	IA2/3/4/5	5.91	6.95	7.08	< 1	< 1	< 1
Leverandør nr. 2	Pearlite	IA3/4			4.2 - 6.4			Max. 1		
MAN Diesel A/S	Pearlite	IA2/3/4	IA2/3/4	IA2/3/4	4.48	5.50	5.88	~1	~1	~1
Leverandør nr. 6	Pearlite	-			-			-		
MAN Diesel A/S	Pearlite	IA2/3/4	IA2/3/4	IA3/4/5	4.46	4.27	3.29	< 1	< 1	< 1
Leverandør nr. 5	Pearlite	IA3	IA3	IA3	5.0	5.3	4.6	0	0	0
MAN Diesel A/S	Pearlite	IA2/3/4	IA2/3/4	IA2/3/4	5.7	5.3	6.1	< 1	< 1	< 1
Leverandør nr. 7	Pearlite	IA3/4	IA3/4	IA3/4	5.2	4.8	4.5	< 2	< 2	< 2
Spec. Takalloy-C	Pearlite	IA2/3/4			3-7			Max. 3		

- Ud fra ovenstående tabel er det svært at differentiere mellem forskellige leverandører
- Vurderingen af specielt grafitstørrelsen er delvis subjektiv
- Ikke særlig god overensstemmelse mellem vurderinger fra leverandører og MDT

MAN Diesel & Turbo

Steen Krogh Jensen

Kvantificering af grafitstørrelse og -morfologi i støbejern

18.01.2012

< 10 >

Serviceerfaringer



Serviceerfaringer:

- Højere slid på nogle foringer end andre
- Større tilbøjelighed til scuffing på nogle foringer
- Revnede foringer

Observationer i mikrostrukturen:

- Stor forskel på grafitstørrelse (Længde/Bredde/Areal)
- Kæmpe forskel på mængden af hårdfase og fordelingen af denne
- Store variationer på mængden af ferrit
- Derudover fandtes store variationer på trækstyrken/udmattelsesstyrken

Brug for et generelt løft i kvaliteten:

- Målemetode til ensartet bestemmelse af grafitstørrelsen
- Bedre fordeling af hårdfasen – primære cellestørrelse
- Bestemmelse af ferritmængden

MAN Diesel & Turbo

Steen Krogh Jensen

Kvantificering af grafitstørrelse og -morfologi i støbejern



10.01.2012

< 11 >

Grafitstørrelse – ISO 945 Forstørrelse: 100x



Repræsentativt?
Statistik?
Primær cellestørrelse?

Løsningen er
Mosaik!



MAN Diesel & Turbo

Steen Krogh Jensen

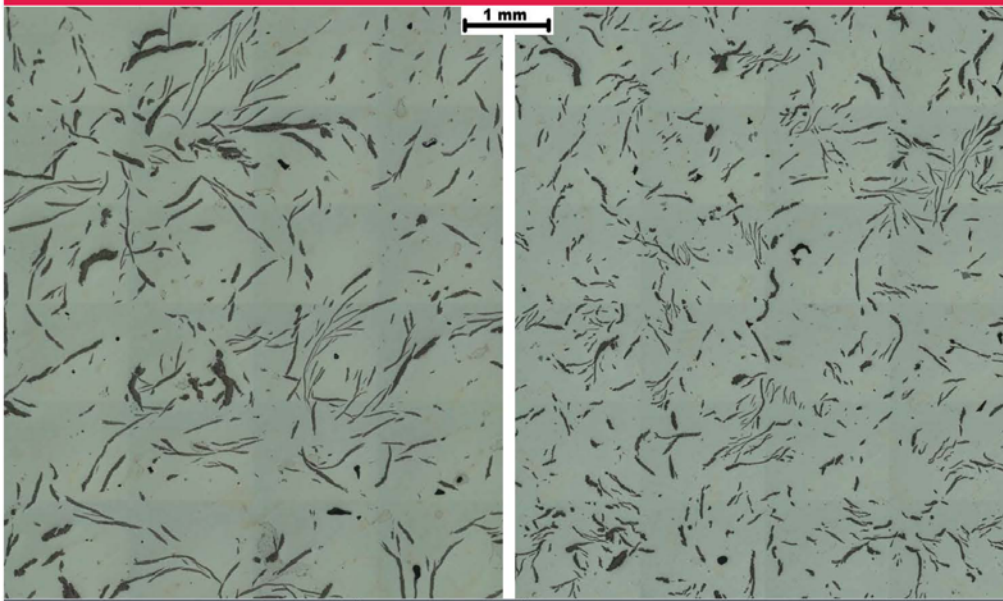
Kvantificering af grafitstørrelse og -morfologi i støbejern



10.01.2012

< 12 >

Grafitstørrelse - Så er det jeres tur!



MAN Diesel & Turbo

Steen Krogh Jensen

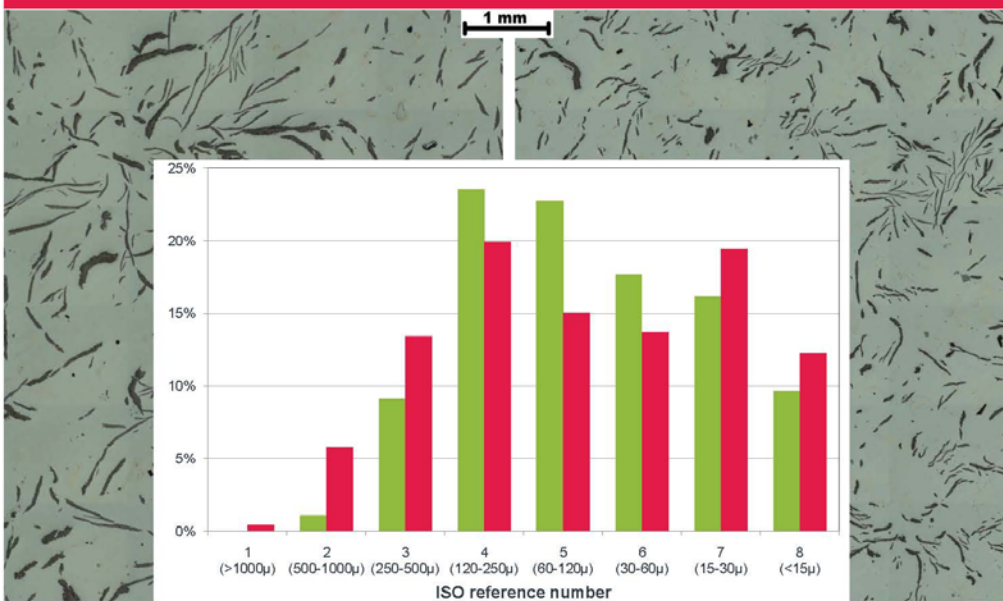
Kvantificering af grafitstørrelse og -morfologi i støbejern



10.01.2012

< 13 >

Grafitstørrelse - Lidt Hjælp



MAN Diesel & Turbo

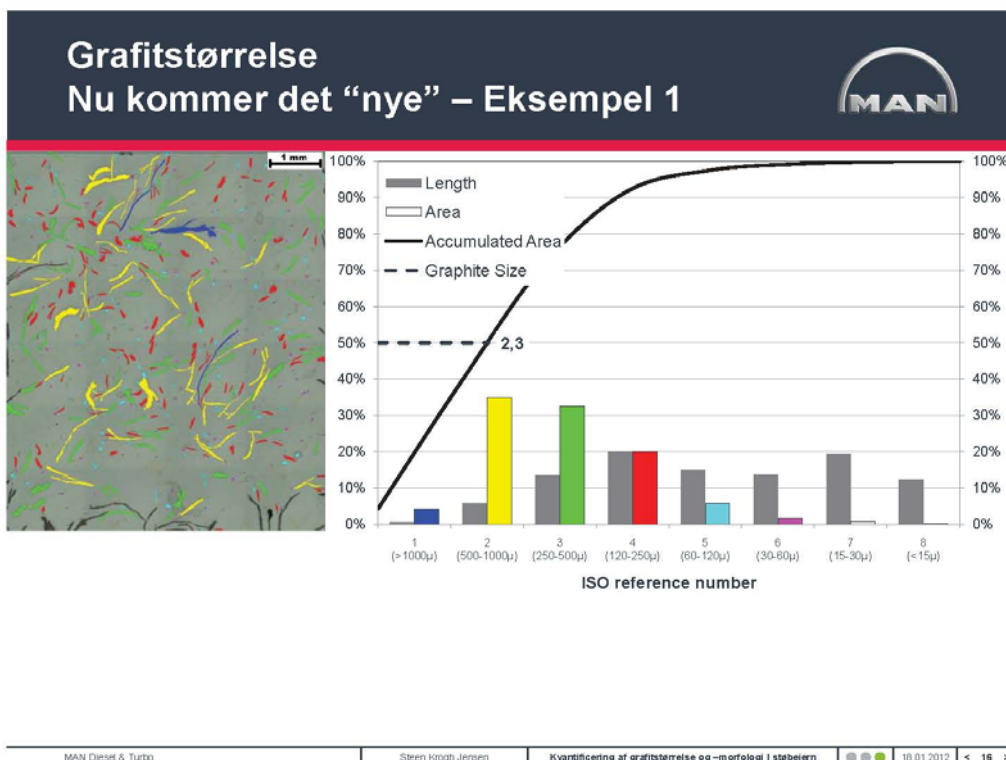
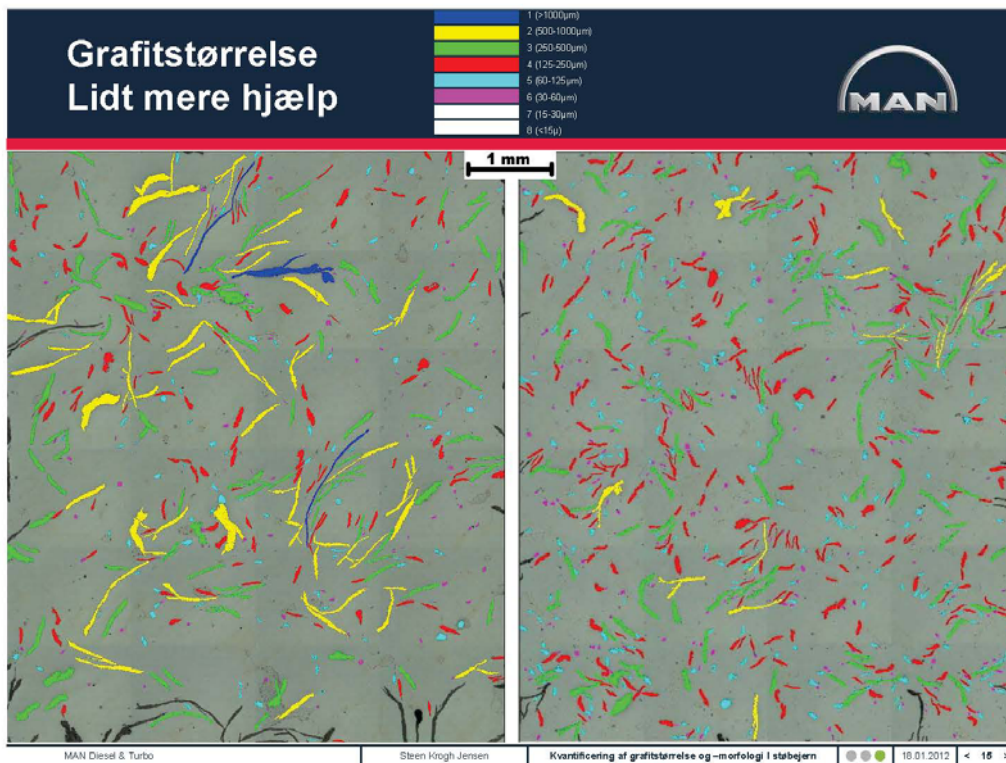
Steen Krogh Jensen

Kvantificering af grafitstørrelse og -morfologi i støbejern

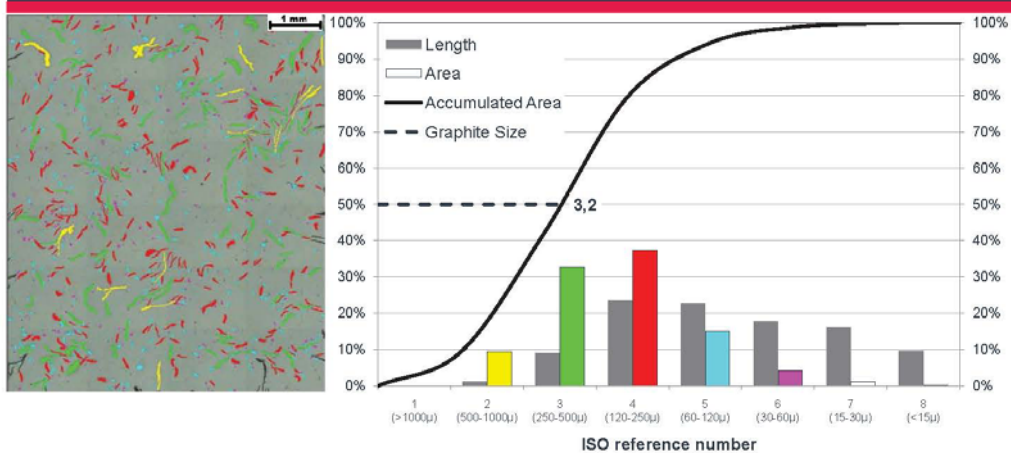


10.01.2012

< 14 >



Grafitstørrelse Nu kommer det “nye” – Eksempel 2



MAN Diesel & Turbo

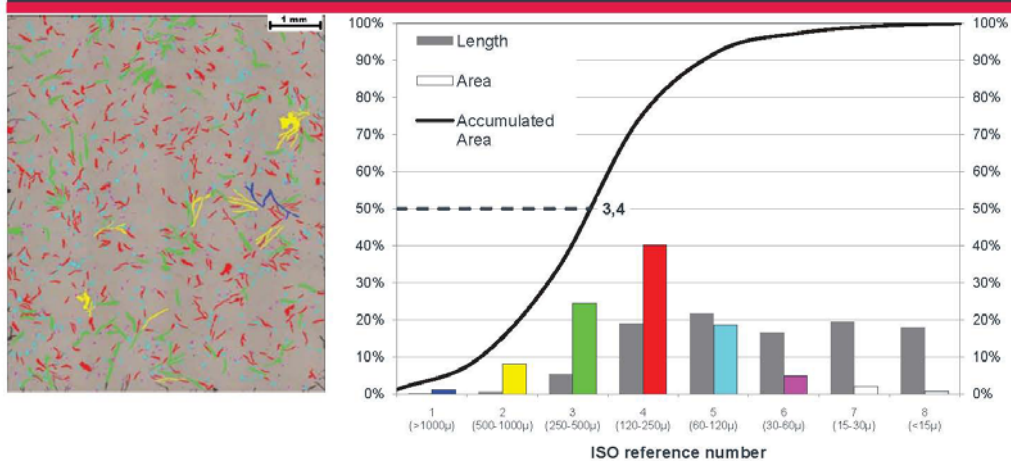
Steen Krogh Jensen

Kvantificering af grafitstørrelse og -morfologi i støbejern

10.01.2012

< 17 >

Grafitstørrelse Nu kommer det “nye” – Eksempel 3



MAN Diesel & Turbo

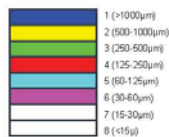
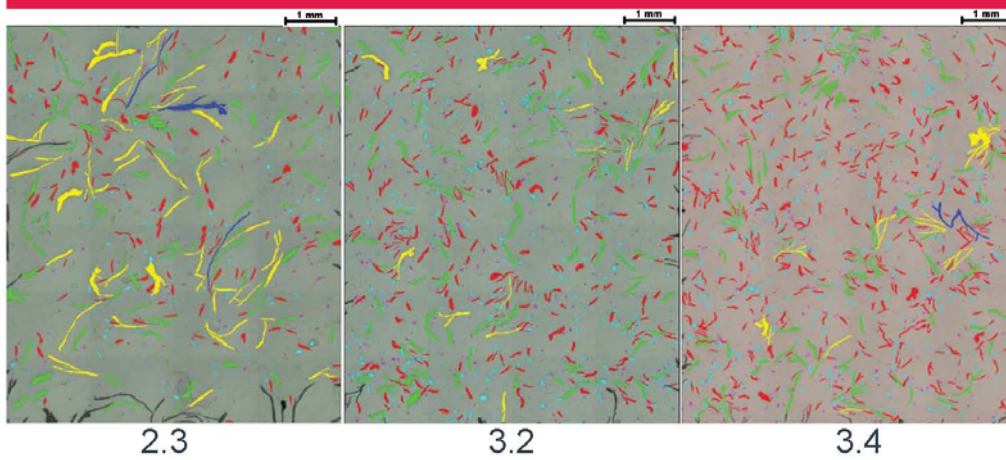
Steen Krogh Jensen

Kvantificering af grafitstørrelse og -morfologi i støbejern

10.01.2012

< 18 >

Grafitstørrelse - sammenfatning



MAN Diesel & Turbo

Steen Krogh Jensen

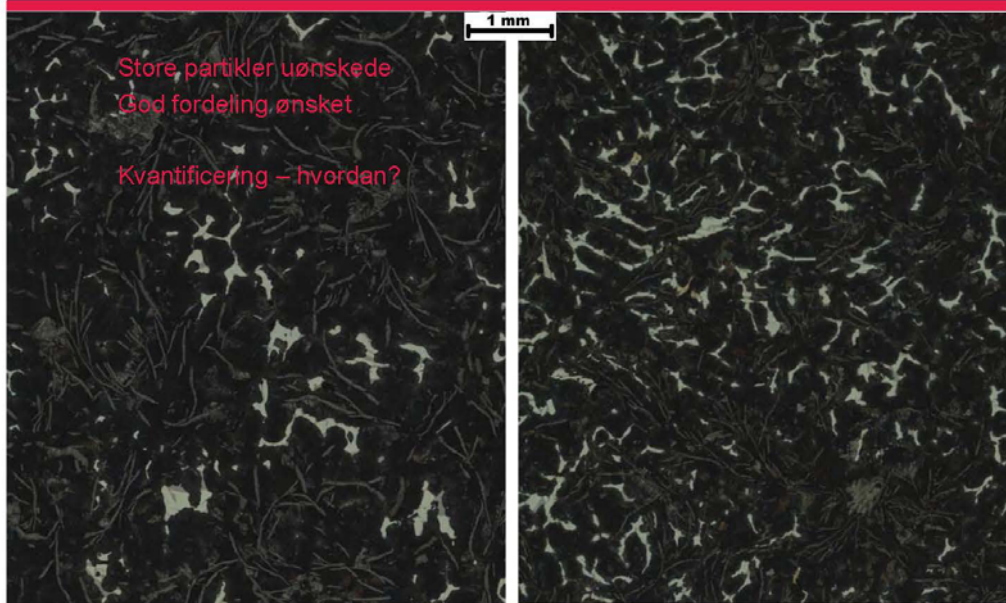
Kvantificering af grafitstørrelse og -morfologi i støbejern



10.01.2012

< 19 >

Hårdfase – Mængde og fordeling?



MAN Diesel & Turbo

Steen Krogh Jensen

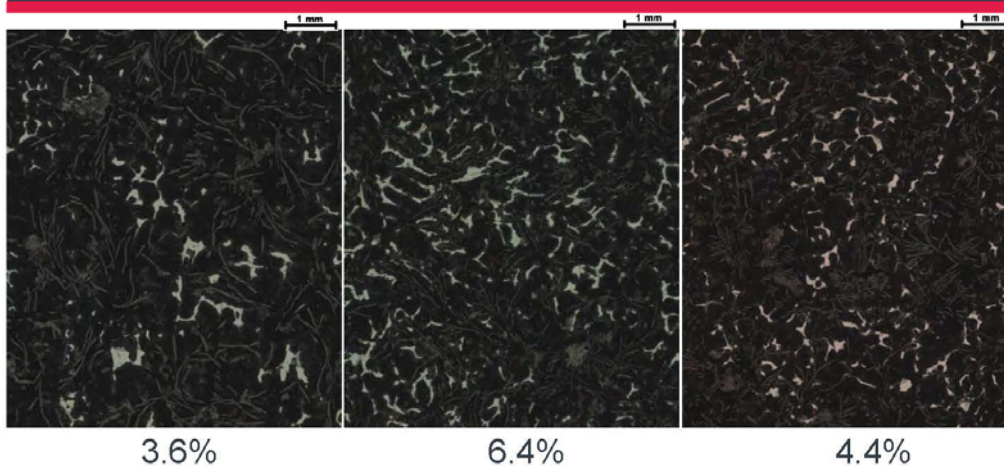
Kvantificering af grafitstørrelse og -morfologi i støbejern



10.01.2012

< 20 >

Hårdfase - Eksempler



MAN Diesel & Turbo

Steen Krogh Jensen

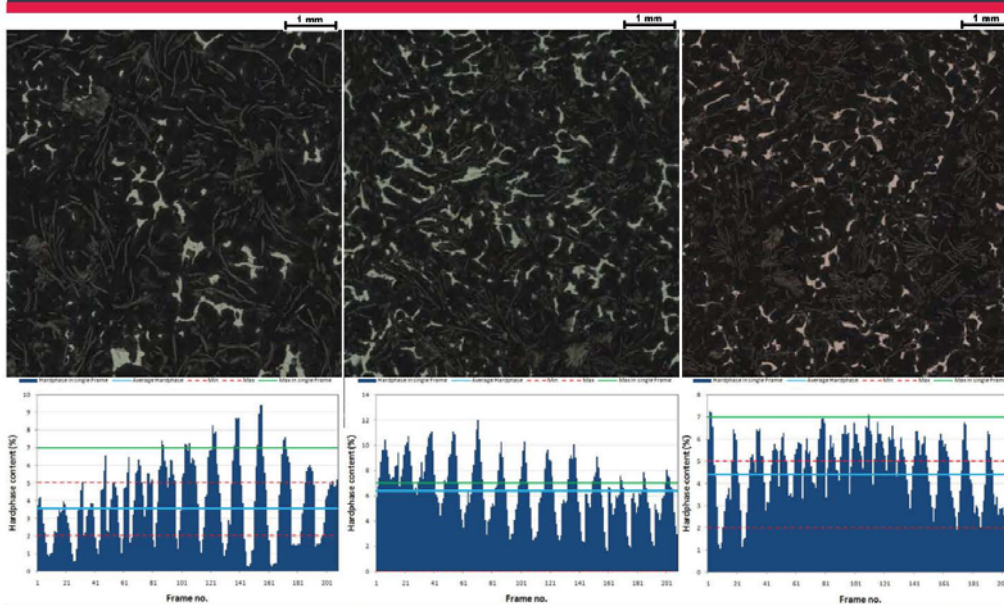
Kvantificering af grafistørrelse og -morfologi i støbejern



10.01.2012

< 21 >

Hårdfase - Sammenfatning



MAN Diesel & Turbo

Steen Krogh Jensen

Kvantificering af grafistørrelse og -morfologi i støbejern



10.01.2012

< 22 >

Ferrit?



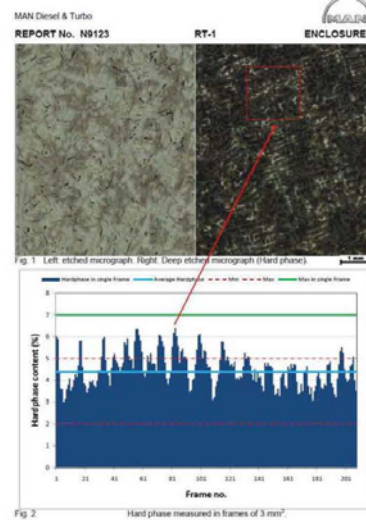
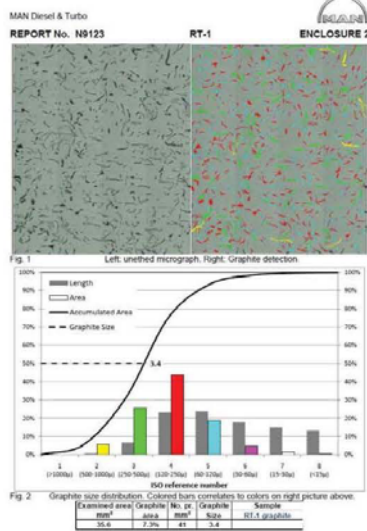
MAN Diesel & Turbo

Steen Krogh Jensen

Kvantificering af grafitstørrelse og -morfologi i støbejern

10.01.2012 < 23 >

Cylinderforing “Komplet” beskrivelse af mikrostrukturen



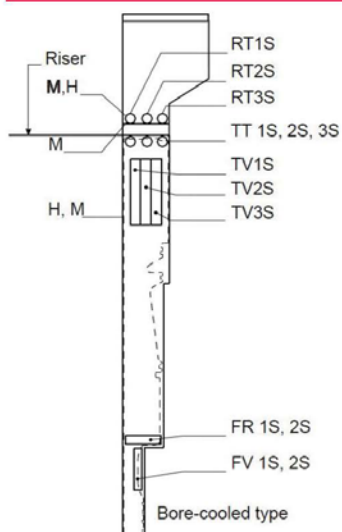
MAN Diesel & Turbo

Steen Krogh Jensen

Kvantificering af grafitstørrelse og -morfologi i støbejern

10.01.2012 < 24 >

Cylinder foring Samlet mikrostruktur evaluering



MDT	Matrix	Graphite				Cementite + Steadite		Ferrite		Enclosure
		Form	Distribution	Size	Area	Average	Max	Average	Max	
RT 1	Pearlite	I	A	3.0	8.3	6.1	12.6	<1	-	2 and 3
RT 2	Pearlite	I	A	3.2	7.8	6.7	12.6	<1	-	4 and 5
RT 3	Pearlite	I	A	3.1	7.2	5.4	9.6	<1	-	6 and 7
TT 1	Pearlite	I	A	2.9	8.0	5.1	9.2	<1	-	8 and 9
TT 2	Pearlite	I	A	3.0	8.6	4.9	9.7	<1	-	10 and 11
TT 3	Pearlite	I	A	2.9	7.6	4.9	8.0	<1	-	12 and 13
TV 1	Pearlite	I	A	3.0	8.6	4.4	9.0	<1	-	14 and 15
TV 2	Pearlite	I	A	2.9	7.9	5.1	8.8	<1	-	16 and 17
TV 3	Pearlite	I	A	3.0	8.2	4.6	9.1	<1	-	18 and 19
FR 1	Pearlite	I	A	3.2	7.5	6.8	12.5	<1	-	20 and 21
FR 2	Pearlite	I	A	3.1	7.4	4.1	6.8	<1	-	22 and 23
FV 1	Pearlite	I	A	3.2	7.9	5.6	9.0	<1	-	24 and 25
FV 3	Pearlite	I	A	3.4	6.2	5.6	10.0	<1	-	26 and 27
Spec. for Tarkalloy C	Pearlite	IA2/3/4			-	<7	-	<3	-	

MAN Diesel & Turbo

Steen Krogh Jensen

Kvantificering af grafitstørrelse og -morfologi i støbejern



18.01.2012

< 25 >

Cylinderforing Ny materialespecifikation



Gammel



MAN B&W Diesel A/S

Cast Iron

Cast Iron for Cylinder Liners

Tarkall-C

Mechanical Properties

• Tensile Strength	R_m	N/mm ²	min. 245 ¹⁾
• Elongation	A_{50}	%	min. 0.3 ¹⁾
• Brinell Hardness (ISO 6506-1:1981)	HBS	10/3000/15	180-230 ²⁾

- ¹⁾ In the upper part of the cylinder liner.
- ²⁾ Total elongation at fracture (%), elastic + plastic elongation. See Q.C. 74 18 99-0.
- ³⁾ Measured on the inside of the cylinder liner, 100 mm from the top.

Microstructure

- Graphite (ISO 945-1:1975): I A 23/4.
- Matrix: Lamellar pearlite. Max. 3% ferrite, 3-7% cementite + steadite.

Chemical Composition

	C%	Si%	Mn%	P%	S%	Bi%	Cu%	V%
• Min.	3.0	0.2	0.2	0.02	1.0			
• Nominal	3.2	1.1	0.8					
• Max.				0.4	0.10	0.04	1.5	0.22

Heat Treatment

In case of demand for stress relieving: Heat max. 90°C/hour to 550°C, hold for 4 hours. Cool in furnace max. 50°C/hour to max. 150°C.

- Figures and text in bold type denote imperative demands.
- All other information - including similar standards - is given for guidance only. (See General Note).

- According to Quality Control No. 74 14 12-0 the Foundry must carry out a first-time casting and obtain the approval of MAN B&W Diesel A/S as supplier of cylinder liners made of Tarkall-C.

Similar Standards

ISO
EN
JIS
These standards do not include any Cast Iron similar to the above quality.

Supply Form

Finished cylinder liners. Tarkall-C is an abbreviation of the trade name Tarkalloy C.

Copyright © MAN B&W Diesel A/S, November 1996

Material Sheet P 676-2

MAN Diesel & Turbo

Steen Krogh Jensen

Kvantificering af grafitstørrelse og -morfologi i støbejern



18.01.2012

< 26 >

MAN Diesel & Turbo

Iron, Cast
Cast Iron for Cylinder Liners

Ny



See marked with "w" are imperative demands.

All other information, including "Guidance - Standards - References", are given for guidance only.

MDT SPECIFICATIONS
Q.C. 74 14 12-0 Cylinder Liners - Tarkalloy C. First-Time Production Approval
Q.C. 74 14 12-0 Evaluation of microstructures based on image analysing equipment/software for Tarkalloy C. Cylinder Liners
Q.C. 74 14 12-0 Quality specification for two-piece cylinder liners

APPLICATION

Cylinder Liners

NOTES

New suppliers of TARKALL-C CYLINDER LINERS must be approved by MDT, see the Q.C. mentioned in the MDT Specifications.

Material	Condition	Position	Dimension (mm)	Temperature (°C)	Rebound (mm)	Rebound (mm)	Rebound (mm)	Rebound (mm)	Rebound (mm)	Rebound (mm)
• Tarkall-C	ISO 945-1:1975	Line Material	1	20	20	20	20	20	20	20

MECHANICAL PROPERTIES - NOTES

- In the upper part of the cylinder liner.
- Total elongation at fracture (%), elastic + plastic elongation. See the Q.C. mentioned in the MDT Specifications.

HARDNESS - ROOM TEMPERATURE

Condition	Condition	Position	Dimension (mm)	HB	HB	HB	HB	HB	HB	HB
• Tarkall-C	ISO 945-1:1975	Line Material	1	180	180	180	180	180	180	180

HARDNESS NOTES

Measured on the inside of the cylinder liner, 100 mm from the top.

CHEMICAL COMPOSITION

Line	Dimension (mm)	C%	Si%	Mn%	P%	S%	Bi%	Cu%	V%	Bi%	Cu%	V%
• Min.	1	3.0	0.2	0.2	0.02	1.0						
• Nominal	1	3.2	1.1	0.8								
• Max.	1				0.4	0.10	0.04	1.5	0.22			

COMPOSITION - NOTES

Normal for elemental composition means "average". Normally a deviation of a 1% is fully acceptable, but this is not an imperative demand as long as the mechanical properties are fulfilled.

STRUCTURE - IRON - ACCORDING TO ISO 945-1:1975

Line	Dimension (mm)	Graphite Form	Graphite Distribution	Reference Size	Cementite Steadite %	Ferrite %	Ferrite %
• Tarkall-C	1	A	A	2.5/4	2.5%	6.1%	12.6%
• Tarkall-C	1	A	A	2.5/4	2.5%	6.1%	12.6%

STRUCTURE - NOTES

- The notes are valid only for group 3 cylinder liners - 0-40 mm from fresh machined inside surface.
- Max. 1% Ferrite - measured within a test area of approx. 2 mm², where highest concentration is observed.
- Max. 1% Carbon - measured within a test area of approx. 2 mm², where highest concentration is observed.

HEAT TREATMENT

Stress Relieving in case of demand.

HEAT TREATMENT - NOTES

Process	Temperature (°C)	Heating Rate (°C/h)	Soaking Time (h)	Cooling Rate (°C/h)	Soaking Time (h)	Application
• Stress Relieving	550	10	4	10	1	-

© MAN Diesel & Turbo
MAN Diesel & Turbo
Revised By: E18
Approved By: E18
Revised Date: March 2011
New details for group 3 liners
Revision No. P 676-4
Page 1 of 2

Cylinderforing Ny materialespecifikation



Gammel

Microstructure

- **Graphite (ISO 945-1975): I A 2/3/4.**
- **Matrix: Lamellar pearlite. Max. 3% ferrite. 3-7% cementite + steadite.**

Ny

STRUCTURE - IRON ACCORDING TO ISO 945 (1975)

Dimension (mm)	Graphite Form	Graphite Distribution	Reference Size	Cementite+ Steadite %	Ferrite %	Pearlite %
■ < 800 mm	I	A	2-3-4	< 7%	< 3%	Rest
■ ≥ 800 mm	I	A	2-3-4	2-5%	≤ 1%	Rest

STRUCTURE - NOTES

The notes are valid only for group 3 cylinder liners - 0-40 mm from finish machined inside surface:

- Max 3% Ferrite - measured within a test area of app. 2 mm², where highest concentration is observed
- Max 7% Cem+Ste - measured within a test area of max 3 mm², where highest concentration is observed

- Øget ensartethed
- Generelt kvalitetsløft
- "Ny" omgang FTA
- Fundet "aktive" leverandører
- Ferritmåling er endnu ikke automatiseret!
- Indkøb af billedbehandlingsudstyr hos underleverandører

MAN Diesel & Turbo

Steen Krogh Jensen

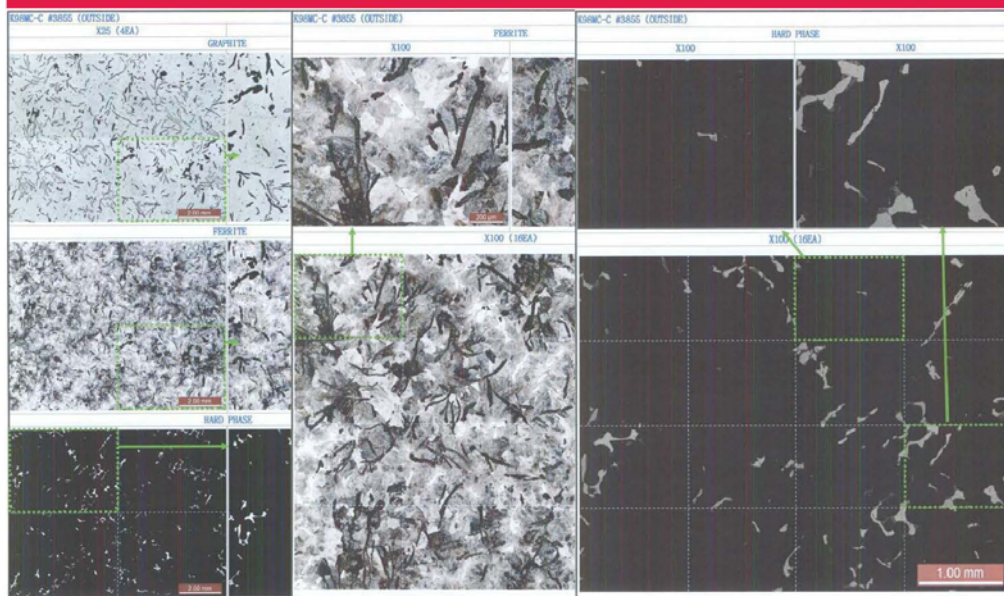
Kvantificering af grafitstørrelse og -morfologi i støbejern



18.01.2012

< 27 >

Cylinderforing Eksempler fra underleverandører



MAN Diesel & Turbo

Steen Krogh Jensen

Kvantificering af grafitstørrelse og -morfologi i støbejern



18.01.2012

< 28 >

Cylinderforing Eksempler fra underleverandører



No.	Microstructure	Hard Phase				Porosity		
		Centrifugal		Steady		Foam		
		Area	Porosity	Area	Porosity	Area	Porosity	
Cylinder foring i 25% - 25%								
1		Studs	Area	Porosity	Area	Porosity	Area	Porosity
		Area	Area	Area	Area	Area	Area	
		Area	Area	Area	Area	Area	Area	
		Area	Area	Area	Area	Area	Area	
		Area	Area	Area	Area	Area	Area	
		Area	Area	Area	Area	Area	Area	
2		Studs	Area	Porosity	Area	Porosity	Area	Porosity
		Area	Area	Area	Area	Area	Area	
		Area	Area	Area	Area	Area	Area	
		Area	Area	Area	Area	Area	Area	
		Area	Area	Area	Area	Area	Area	
		Area	Area	Area	Area	Area	Area	
3		Studs	Area	Porosity	Area	Porosity	Area	Porosity
		Area	Area	Area	Area	Area	Area	
		Area	Area	Area	Area	Area	Area	
		Area	Area	Area	Area	Area	Area	
		Area	Area	Area	Area	Area	Area	
		Area	Area	Area	Area	Area	Area	
4		Studs	Area	Porosity	Area	Porosity	Area	Porosity
		Area	Area	Area	Area	Area	Area	
		Area	Area	Area	Area	Area	Area	
		Area	Area	Area	Area	Area	Area	
		Area	Area	Area	Area	Area	Area	
		Area	Area	Area	Area	Area	Area	
5		Studs	Area	Porosity	Area	Porosity	Area	Porosity
		Area	Area	Area	Area	Area	Area	
		Area	Area	Area	Area	Area	Area	
		Area	Area	Area	Area	Area	Area	
		Area	Area	Area	Area	Area	Area	
		Area	Area	Area	Area	Area	Area	
6		Studs	Area	Porosity	Area	Porosity	Area	Porosity
		Area	Area	Area	Area	Area	Area	
		Area	Area	Area	Area	Area	Area	
		Area	Area	Area	Area	Area	Area	
		Area	Area	Area	Area	Area	Area	
		Area	Area	Area	Area	Area	Area	
7		Studs	Area	Porosity	Area	Porosity	Area	Porosity
		Area	Area	Area	Area	Area	Area	
		Area	Area	Area	Area	Area	Area	
		Area	Area	Area	Area	Area	Area	
		Area	Area	Area	Area	Area	Area	
		Area	Area	Area	Area	Area	Area	
8		Studs	Area	Porosity	Area	Porosity	Area	Porosity
		Area	Area	Area	Area	Area	Area	
		Area	Area	Area	Area	Area	Area	
		Area	Area	Area	Area	Area	Area	
		Area	Area	Area	Area	Area	Area	
		Area	Area	Area	Area	Area	Area	

No.	Microstructure	Hard Phase				Porosity		
		Centrifugal		Steady		Foam		
		Area	Porosity	Area	Porosity	Area	Porosity	
Cylinder foring i 25% - 25%								
1		Studs	Area	Porosity	Area	Porosity	Area	Porosity
		Area	Area	Area	Area	Area	Area	
		Area	Area	Area	Area	Area	Area	
		Area	Area	Area	Area	Area	Area	
		Area	Area	Area	Area	Area	Area	
		Area	Area	Area	Area	Area	Area	
2		Studs	Area	Porosity	Area	Porosity	Area	Porosity
		Area	Area	Area	Area	Area	Area	
		Area	Area	Area	Area	Area	Area	
		Area	Area	Area	Area	Area	Area	
		Area	Area	Area	Area	Area	Area	
		Area	Area	Area	Area	Area	Area	
3		Studs	Area	Porosity	Area	Porosity	Area	Porosity
		Area	Area	Area	Area	Area	Area	
		Area	Area	Area	Area	Area	Area	
		Area	Area	Area	Area	Area	Area	
		Area	Area	Area	Area	Area	Area	
		Area	Area	Area	Area	Area	Area	
4		Studs	Area	Porosity	Area	Porosity	Area	Porosity
		Area	Area	Area	Area	Area	Area	
		Area	Area	Area	Area	Area	Area	
		Area	Area	Area	Area	Area	Area	
		Area	Area	Area	Area	Area	Area	
		Area	Area	Area	Area	Area	Area	
5		Studs	Area	Porosity	Area	Porosity	Area	Porosity
		Area	Area	Area	Area	Area	Area	
		Area	Area	Area	Area	Area	Area	
		Area	Area	Area	Area	Area	Area	
		Area	Area	Area	Area	Area	Area	
		Area	Area	Area	Area	Area	Area	
6		Studs	Area	Porosity	Area	Porosity	Area	Porosity
		Area	Area	Area	Area	Area	Area	
		Area	Area	Area	Area	Area	Area	
		Area	Area	Area	Area	Area	Area	
		Area	Area	Area	Area	Area	Area	
		Area	Area	Area	Area	Area	Area	
7		Studs	Area	Porosity	Area	Porosity	Area	Porosity
		Area	Area	Area	Area	Area	Area	
		Area	Area	Area	Area	Area	Area	
		Area	Area	Area	Area	Area	Area	
		Area	Area	Area	Area	Area	Area	
		Area	Area	Area	Area	Area	Area	
8		Studs	Area	Porosity	Area	Porosity	Area	Porosity
		Area	Area	Area	Area	Area	Area	
		Area	Area	Area	Area	Area	Area	
		Area	Area	Area	Area	Area	Area	
		Area	Area	Area	Area	Area	Area	
		Area	Area	Area	Area	Area	Area	

MAN Diesel & Turbo

Steen Krogh Jensen

Kvantificering af gråstøbelse og -morfologi i støbejern

10.01.2012

< 25

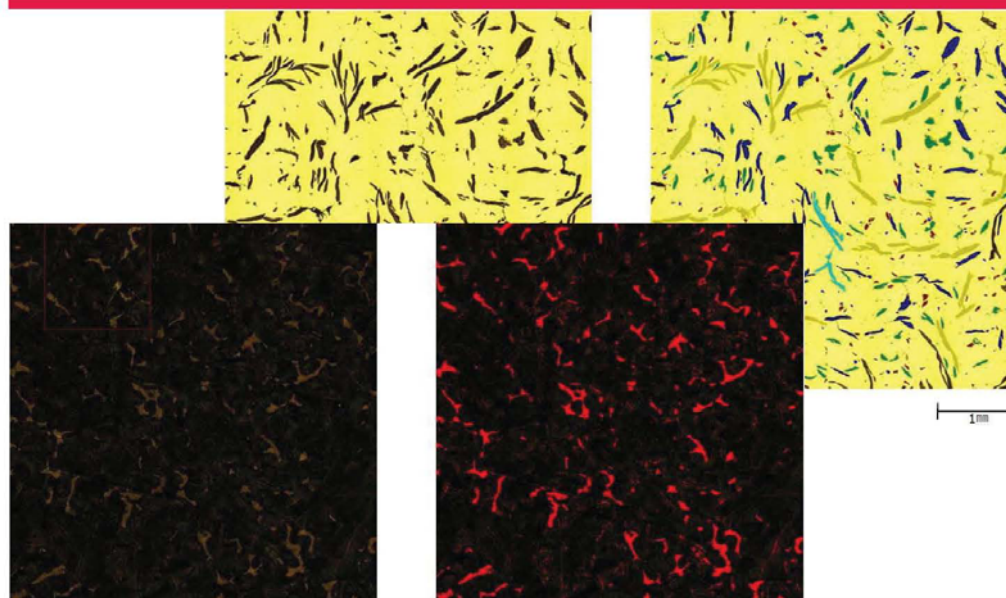
MAN Diesel & Turbo

Steen Krogh Jensen

Kvantificering af grafittørrelse og -morfologi i støbejern

10.01.2012 < 29 >

Cylinderforing Eksempler fra underleverandører



MAN Diesel & Turbo

Steen Krogh Jensen

Kvantificering af grafittørrelse og -morfologi i støbejern

10.01.2012 < 30 >

Cylinderforing Eksempler fra underleverandører



Fig. 1 Left: Unetched micrograph. Right: Graphite detection. Detection area is totally 83mm².

Length	1	2	3	4	5	6	7	8
Length	>1000µm	300-1000µm	250-300µm	120-250µm	60-120µm	30-60µm	15-30µm	<15µm
Area	0.29%	7.05%	27.20%	35.15%	16.49%	5.79%	4.10%	4.93%
Accumulated area	0.29%	7.34%	34.54%	69.69%	86.18%	91.97%	96.07%	100.00%

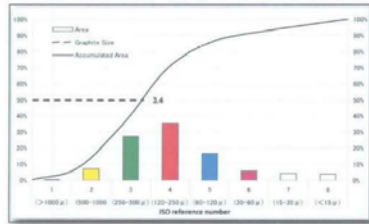
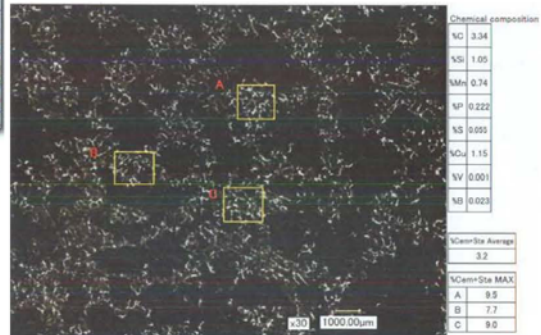


Fig. 2 Graphite size distribution. Colored bars correlates to colors on right picture above.



MAN Diesel & Turbo

Steen Krogh Jensen

Kvantificering af grafitstørrelse og -morfologi i støbejern

18.01.2012 < 31 >

Stempelring Materialespecifikation



MAN Diesel & Turbo

Iron, Cast

Cast Iron for Piston Rings (Vermicular graphite)



Data marked with "a" are imperative demands.

All other information, including "Guidance - Standards - References", are given for guidance only.

MDT SPECIFICATIONS

G.C. 142050-4 Piston Rings - First Time Production Approval

APPLICATION

Finished piston rings.

The piston ring maker MUST be approved by MDT.

NOTES

Previous part of datasheet: R/VK-C - Revision 10 P 649-2 issued January 2003

Standard	Material	Condition	Dimension	Temperature	Reference	Reference	Reference	Reference	Reference	Reference
ISO 682/2000	Cast Iron	Ring	mm	°C	mm	mm	mm	mm	mm	mm
ISO 682/2000	Cast Iron	Ring	mm	°C	mm	mm	mm	mm	mm	mm

MECHANICAL PROPERTIES - NOTES

• Elongation (A): $\geq 0.5\%$ (long dimension ≥ 500 mm)

STRUCTURE - IRON ACCORDING TO ISO 945 (1975)

Dimension (mm)	Graphite Form	Graphite Distribution	Reference Size	Cementite+ Steadite %	Ferrite %	Pearlite %
$\geq \phi 900$	III; nodularity $< 20\%$	A	4/6	1-3	≤ 3	Rest
$< \phi 900$	III; nodularity $< 20\%$	A	4/6	3-7	≤ 3	Rest

STRUCTURE - NOTES

• The nodularity must be determined according to ISO16112 or JIS5502 respectively

• The approved piston ring maker must produce piston rings in full agreement with own material specification, known and approved by MDT.

• Any changes of the chemical composition already approved for the actual piston ring maker will result in a demand for a new approval test.

Structure	Graphite Form	Graphite Distribution	Reference Size	Cementite+ Steadite %	Ferrite %	Pearlite %
ISO 945	III; nodularity $< 20\%$	A	4/6	1-3	≤ 3	Rest
ISO 945	III; nodularity $< 20\%$	A	4/6	3-7	≤ 3	Rest

STRUCTURE - NOTES

• The nodularity must be determined according to ISO16112 or JIS5502 respectively

Temperature	Density	Modulus of Elasticity	Thermal Conductivity	Modulus of Elasticity	Modulus of Elasticity
°C	kg/m³	GPa	W/mK	GPa	GPa
20	7.1	130	40	130	130

PHYSICAL - NOTES

For Modulus of Elasticity specified as "Nominal" a deviation of $\pm 10\%$ is acceptable. Must be verified during the "First Time Approval".

MAN Diesel & Turbo

Steen Krogh Jensen

Kvantificering af grafitstørrelse og -morfologi i støbejern

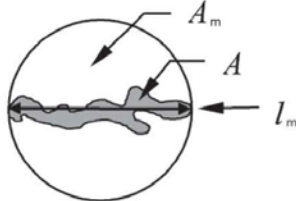
18.01.2012 < 32 >



Nodularity according to ISO 16112



$$\text{Roundness} = \frac{A}{A_m} = \frac{4 \times A}{\pi \times l_m^2}$$



A_m area of circle of diameter l_m

A area of the graphite particle in question

l_m maximum axis length of the graphite particle in question = maximum distance between two points on the graphite particle perimeter

Roundness-shape factor	Graphite form
0,625 to 1	Nodular (ISO form VI)
0,525 to 0,625	Intermediate (ISO forms IV and V)
< 0,525	Compacted (ISO form III)

Flake graphite particles and graphite particles with maximum axis length less than 10 µm are not included in the analysis.

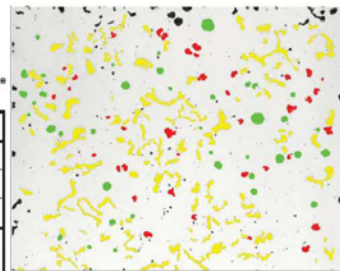
Percent nodularity is calculated on an area basis as follows:

$$\text{Percent nodularity} = \frac{\sum A_{\text{nodules}} + 0,5 \times \sum A_{\text{intermediates}}}{\sum A_{\text{all particles}}} \times 100$$

A_{nodules} is the area of particles classified as spheroidal (nodular) graphite;

$A_{\text{intermediates}}$ is the area of particles classified as intermediate forms of graphite;

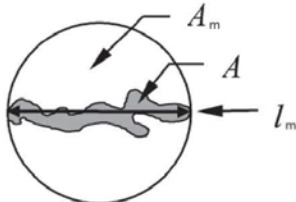
$A_{\text{all particles}}$ is the area of all graphite particles greater than 10 µm.



Nodularity according to JIS 5502



$$\text{Roundness} = \frac{A}{A_m} = \frac{4 \times A}{\pi \times l_m^2}$$



5. Image analysis (calculation of nodularity) procedure

- (1) Import the image data of graphite structure ----- 3. - a)
- (2) Digitalization: split into black particles (graphite) and white part (matrix)
- (3) Correction of digitalized images: eliminate graphite which size is not over 15 µm ----- 3. - b)
- (4) Calculation of nodularity (automatic calculation)

- i) Classification of graphite: divide graphite shape into I -IV and V-VI

*Classification method;

If a graphite area ratio against the minimum circumscribed circle of the graphite

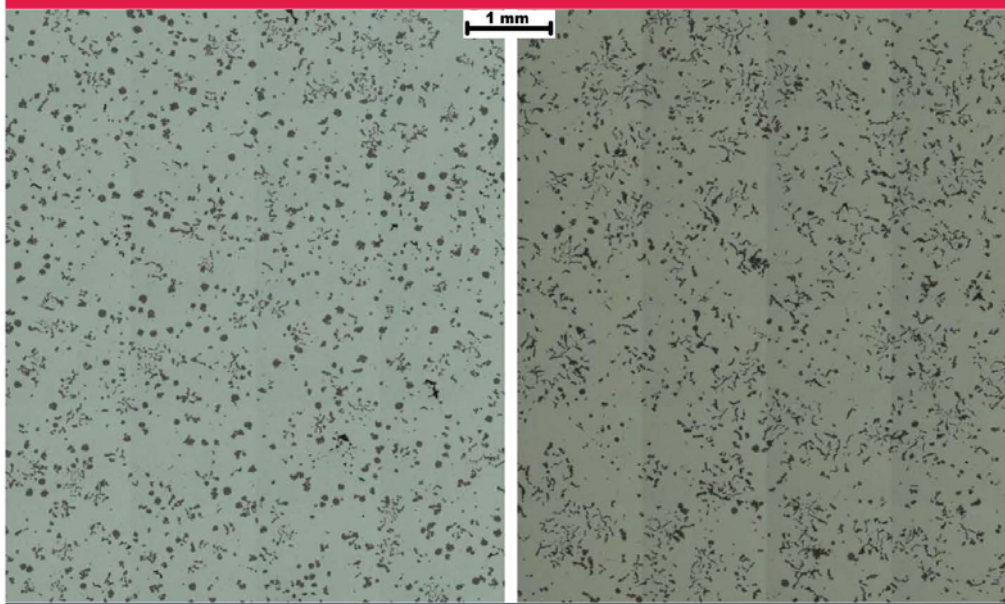
$$\left(= \frac{(\text{Area of graphite}) \times 100}{\text{Area of minimum circumscribed circle}} \right) \text{ is:}$$

- under 55% => I -IV
- over 55% => V-VI

- ii) Calculation of nodularity of graphite ----- 3. - c)

$$\frac{\text{Figure of shape V-VI graphite}}{\text{Figure of all graphite}} \times 100 = \text{Nodularity (\%)}$$

Nodularitet - Eksempler



MAN Diesel & Turbo

Steen Krogh Jensen

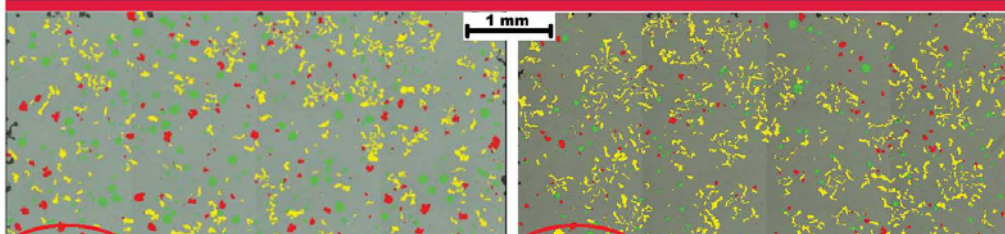
Kvantificering af grafitstørrelse og -morfologi i støbejern



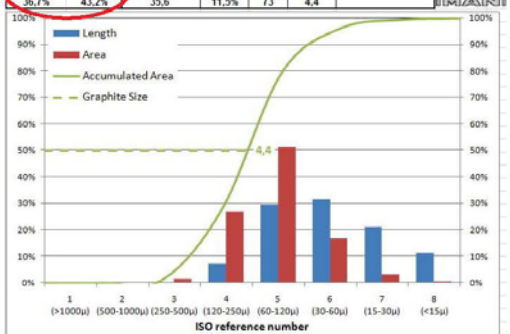
10.01.2012

< 35 >

Nodularitet - Eksempler



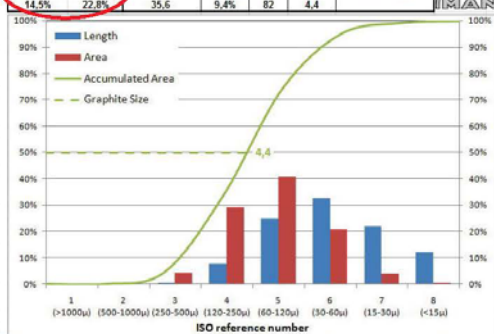
Nodularity (ISO 16112)	Nodularity (JIS5502)	Examined area mm ²	Graphite area mm ²	No. pr. mm ²	Graphite Size mm	Sample
36.7%	43.2%	35,6	11,5%	73	4,4	N9041-29.2 Graphite



MAN Diesel & Turbo

Steen Krogh Jensen

Nodularity (ISO 16112)	Nodularity (JIS5502)	Examined area mm ²	Graphite area mm ²	No. pr. mm ²	Graphite Size mm	Sample
14.5%	22.8%	35,6	9,4%	82	4,4	N9192 #84 Graphite



Kvantificering af grafitstørrelse og -morfologi i støbejern



10.01.2012

< 36 >

Stempelring "Komplet" beskrivelse af mikrostrukturen



MAN Diesel & Turbo

REPORT No. N9192

#94-4

ENCLOSURE 4

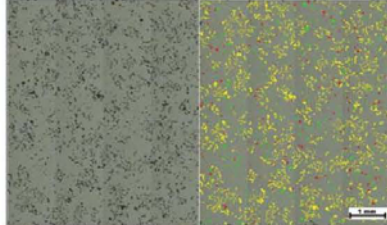


Fig. 1 Left: unetched micrograph. Right: Graphite detection

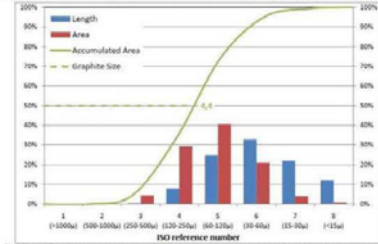


Fig. 2 Graphite size distribution. Colored bars correlates to colors on right picture above.

Modularity (ISO 15112)	Modularity (ISO 15112)	Examined area (mm²)	Graphite area (mm²)	No. of graphite (mm²)	Graphite Size
14.5%	22.8%	35.5	9.4%	62	5.4

MAN Diesel & Turbo

Steen Krogh Jensen

Kvantificering af grafistørrelse og -morfologi i støbejern

10.01.2012 < 37 >

MAN Diesel & Turbo

REPORT No. N9192

#81-4

ENCLOSURE 3



Fig. 1 Left: etched micrograph. Right: Deep etched micrograph (Hard phase)

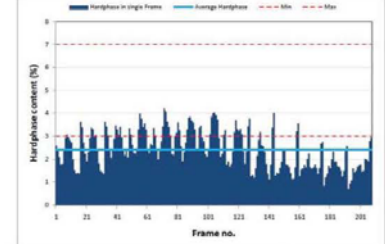
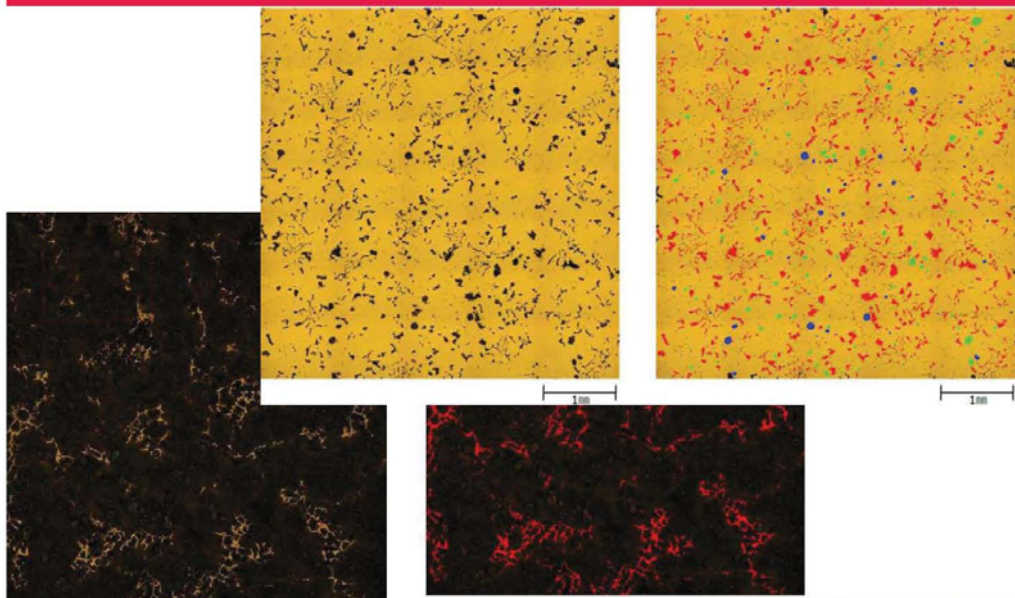


Fig. 2 Hard phase measured in frames of 3 mm²

Nodularitet - underleverandører



MAN Diesel & Turbo

Steen Krogh Jensen

Kvantificering af grafistørrelse og -morfologi i støbejern

10.01.2012 < 38 >

Disclaimer



All data provided in this document is non-binding.

This data serves informational purposes only and is especially not guaranteed in any way. Depending on the subsequent specific individual projects, the relevant data may be subject to changes and will be assessed and determined individually for each project. This will depend on the particular characteristics of each individual project, especially specific site and operational conditions.

Tak for opmærksomheden!

Materialvalg/Stålfremstilling

Stig Rubæk, Metal-Consult

Materialevalg/Stålfremstilling

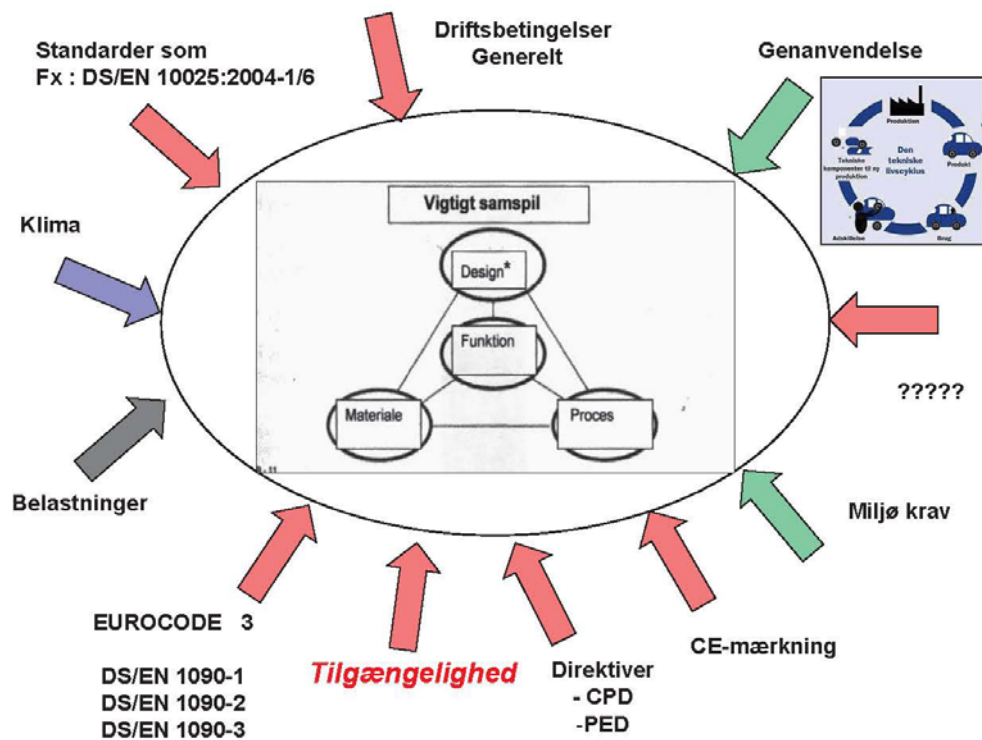
Særligt indlæg ved DMS's Vintermøde 2013

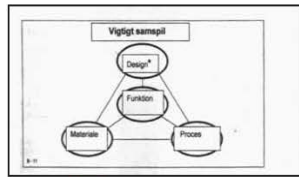
på

Hotel Koldingfjord

16.-18 Januar 2013

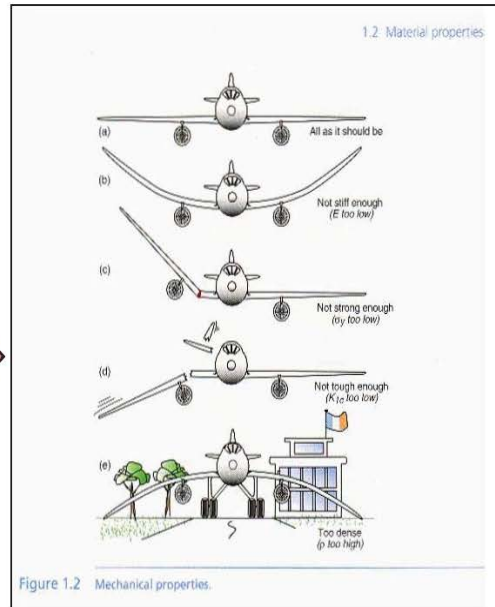
Stig Rubæk /Metal-Consult





Materiernes egenskaber er altid det centrale element ved materialevalg. Eksempler på design-begrænsende egenskaber kan ses i nedenstående skema.

Klasse	Egenskab
Generel	Pris
	Densitet (massfylde)
Mekanisk	Elasticitetsmodul (stivhed)
	Styrke (fx elasticitetsgrænse)
	Sjæld
	Brudsejhed
	Dæmpningskapacitet
	Udmattelsesstyrke
Termisk	Termisk ledningsevne
	Specifik varmekapacitet
	Smeltepunkt
	Glastemperatur
	Termisk udvidelseskoefficient
	Krybemodstand
Slid	Slid-konstant
	Korrosionshastighed



DMS



DS/EN 10025



DS/EN 10025 del 1 til 6

Del 1 Generelle tekniske leveringsbetingelser

Del 2 Tekniske leveringsbetingelser for ulegerede konstruktionsstål
(S235 -, S275 -, S355 - og S450- med undergrupperne JR, J0, J2 og K2,
samt tillægsbetegnelserne +AR, +N og +M (kun lange produkter))

Del 3 Tekniske leveringsbetingelser for (ovn)normaliserede/valsede normaliserede
svejselige finkornskonstruktionsstål
(S275 N/NL, S355N/NL, S420N/NL, S460N/NL)

Del 4 Tekniske leveringsbetingelser for termomekanisk valsede
svejselige finkornskonstruktionsstål
(S275M/ML, S355M/ML, S420M/ML -, S460M/ML)

Del 6 Tekniske leveringsbetingelser for flade produkter af
højstyrke konstruktionsstål i sejhærdet tilstand
(S460Q/QL/QL1, S500Q/QL/QL1, S550Q/QL/QL1, S620Q/QL/QL1, S690Q/QL/QL1,
S890Q/QL/QL1, 960QQL)

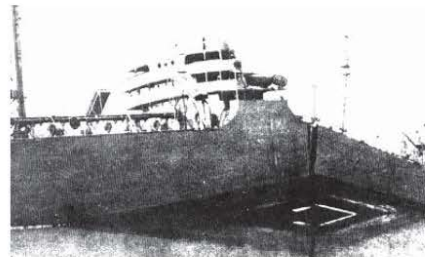
Del 5 Tekniske leveringsbetingelser for konstruktionsstål med forøget atmosfærisk
korrosionsbestandighed (korrosionstræge stål)
(S235 -W, S355 -WP, S355 -W med undergrupperne JR, J0, J2 og K2)



DMS

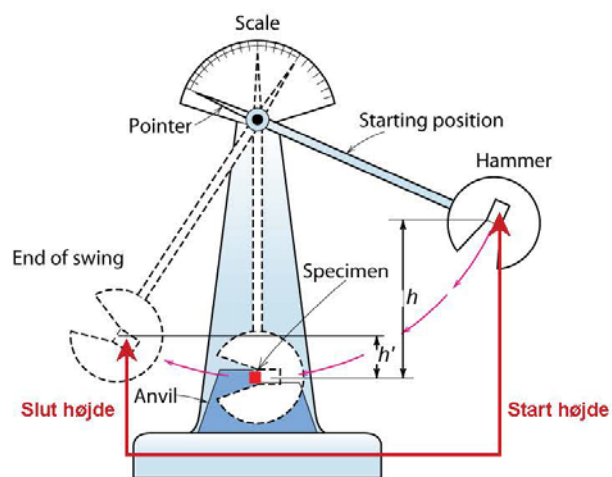
Design Strategi: Hold dig over DBTT!

- Pre-WWII: Titanic
- WWII: Liberty skibe



- Problem: Anvendelse af ståltyper med omslagstemperatur omkring rumtemperatur.

Slagprøvning

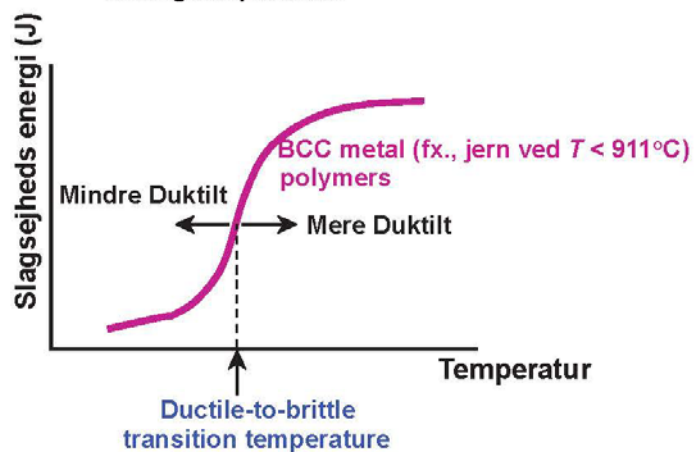


7

DMS

Omslags-Temperaturen

- Ductile-to-Brittle Transition Temperature (DBTT) ...
= Omslagstemperaturen



8

$$CEV (\%) = C + Mn/6 + (Cr+Mo+V)/5 + (Ni+Cu)/15$$

DS/EN 10025-2:2004

Tabel 6 – Maksimalt CEV baseret på chargeanalysen*

Betegnelse		Decarburiseringsmetode *	Maks. CEV i % for nominal produkttykkelse i mm				
Ifølge EN 10027-1 og CR 10260	Ifølge EN 10027-2		≤ 30	> 30 ≤ 40	> 40 ≤ 150	> 150 ≤ 250	> 250
S235JR	1.0038	FN	0,35	0,35	0,35	0,40	-
S235J0	1.0114	FN	0,35	0,35	0,35	0,40	-
S235J2	1.0117	FF	0,35	0,35	0,35	0,40	0,40
S275JR	1.0044	FN	0,40	0,40	0,42	0,44	-
S275J0	1.0143	FN	0,40	0,40	0,42	0,44	-
S275J2	1.0145	FF	0,40	0,40	0,42	0,44	0,44
S355JR	1.0045	FN	0,45	0,47	0,47	0,49 ^b	-
S355J0	1.0553	FN	0,45	0,47	0,47	0,49 ^b	-
S355J2	1.0577	FF	0,45	0,47	0,47	0,49 ^b	0,49
S355J2C	1.0596	FF	0,45	0,47	0,47	0,49 ^b	0,49
S460J2 ^c	1.0590	FF	0,47	0,49	0,49	-	-

* For valgt forpagelse af elementer, der påvirker CEV, se 7.2.4 og 7.2.5.
^a FN = benyttet stål ikke slak, FF = slak benyttet stål (se 6.2.2).
^b For lange produkter gælder maksimalt CEV på 0,54.
^c Gælder kun for lange produkter.

DS/EN 10025-3:2004

Tabel 4 – Maksimalt CEV baseret på chargeanalysen for (ovr)normaliseret stål

Betegnelse		Maks. CEV i % for nominal produkttykkelse i mm
Ifølge EN 10027-1 og CR 10260	Ifølge EN 10027-2	
S275N*	1.0490*	≤ 63 0,40
S275NL*	1.0491*	> 63 ≤ 100 0,40
S355N*	1.0545*	> 100 ≤ 250 0,42
S355NL*	1.0546*	
S420N	1.8902	
S420NL	1.8912	0,48 0,50 0,52
S460N	1.8901	
S460NL	1.8903	0,53 0,54 0,55

* For valgt forpagelse af elementer, der påvirker CEV, se 7.2.3.

DS/EN 10025-4:2004

Tabel 4 – Maksimalt CEV baseret på chargeanalysen for termomekanisk valset stål^a

Betegnelse		Maks. CEV i % for nominal produkttykkelse i mm				
Ifølge EN 10027-1 og CR 10260	Ifølge EN 10027-2	≤ 16	> 16 ≤ 40	> 40 ≤ 63	> 63 ≤ 120	> 120 ≤ 150 ^b
S275M	1.8818					
S275ML	1.8819	0,34	0,34	0,35	0,38	0,38
S355M	1.8823					
S355ML	1.8834	0,39	0,39	0,40	0,45	0,45
S420M	1.8825					
S420ML	1.8836	0,43	0,45	0,46	0,47	0,47
S460M	1.8827					
S460ML	1.8838	0,45	0,46	0,47	0,48	0,48

^a For valgt forpagelse af elementer, der påvirker CEV, se 7.2.3.
^b Tallene gælder kun for lange produkter.

DS/EN 10025-6:2004

Tabel 4 – Maksimalt CEV baseret på chargeanalysen for søjlebetonet stål^a

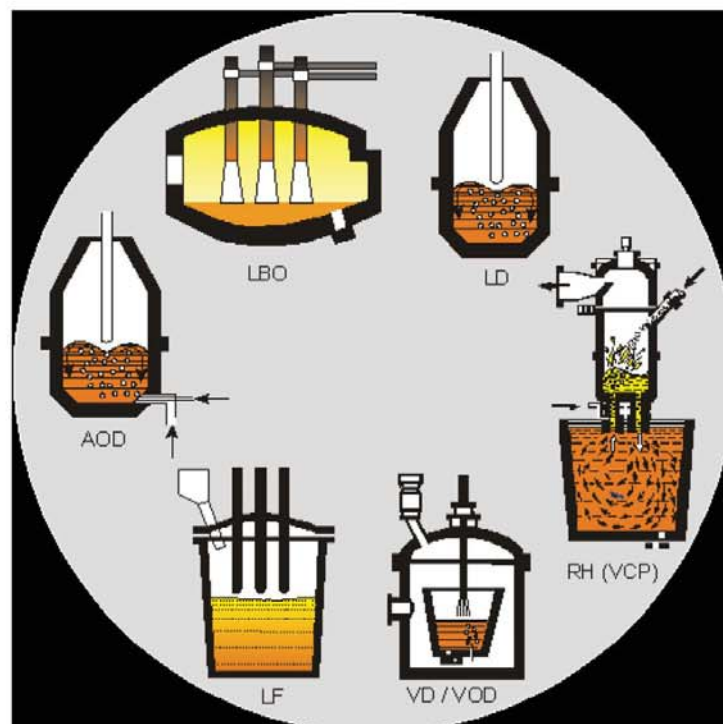
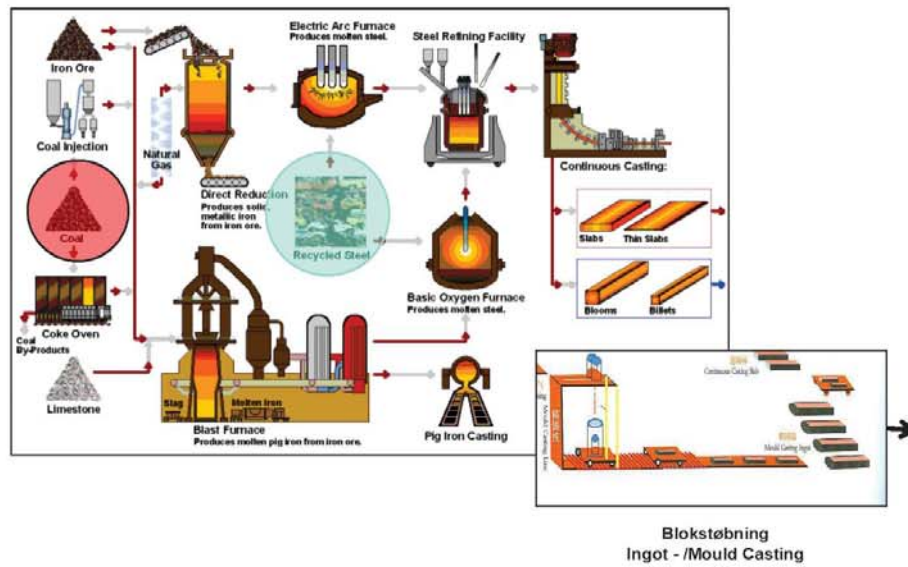
Betegnelse		Maks. CEV i % for nominal produkttykkelse i mm		
Ifølge EN 10027-1 og CR 10260	Ifølge EN 10027-2	≤ 50	> 50 ≤ 100	> 100 ≤ 150
S460C	1.8908			
S460CL	1.8906	0,47	0,48	0,50
S460CL.1	1.8910			
S500C	1.8924			
S500CL	1.8928	0,47	0,70	0,70
S500CL.1	1.8944			
S500C	1.8904			
S500CL	1.8908	0,65	0,77	0,83
S500CL.1	1.8988			
S620C	1.8914			
S620CL	1.8927	0,65	0,77	0,83
S620CL.1	1.8997			
S690C	1.8931			
S690CL	1.8928	0,65	0,77	0,83
S690CL.1	1.8988			
S890C	1.8940			
S890CL	1.8983	0,72	0,82	-
S890CL.1	1.8933			
S960C	1.8941			
S960CL	1.8933	0,82	-	-

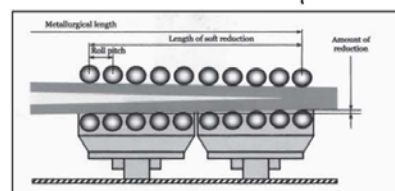
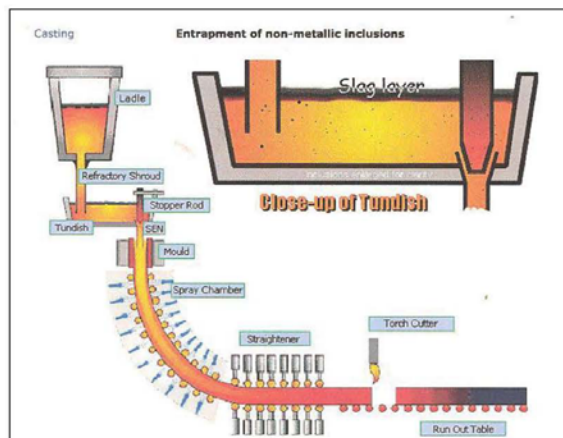
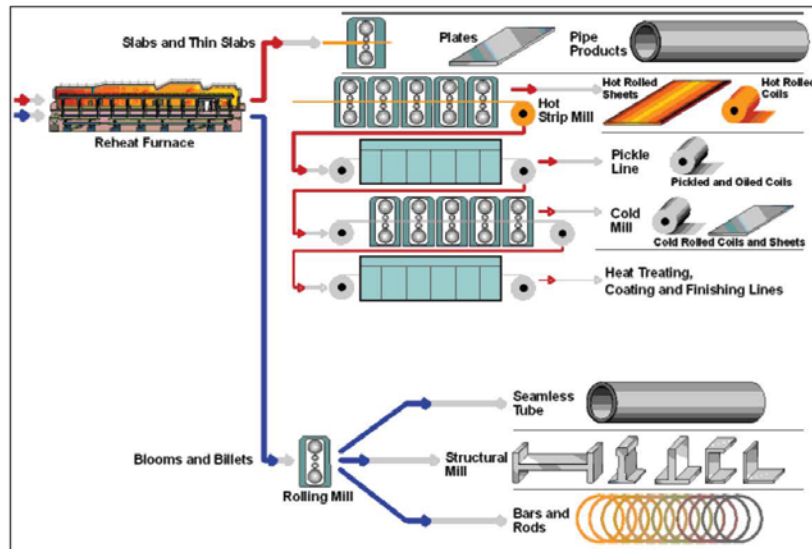
* For valgt forpagelse af elementer, der påvirker CEV, se 7.2.3.

DMS

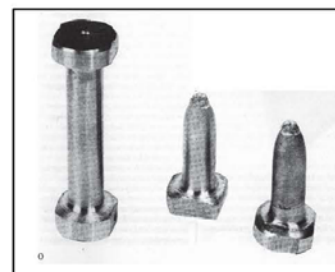
Fremstilling af svejseelige konstruktionsstål med udgangspunkt i :

EN 10025:2004 del 1-6





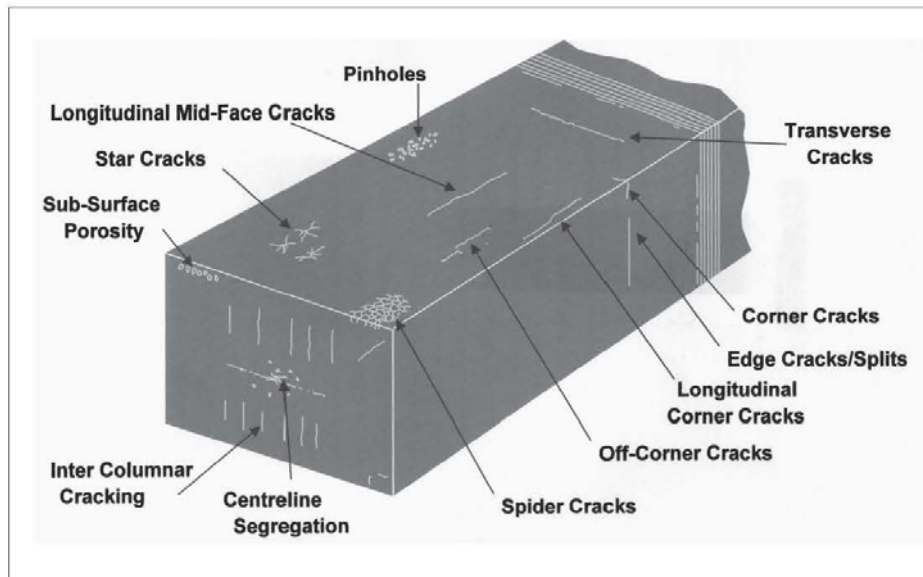
"Soft reduction"



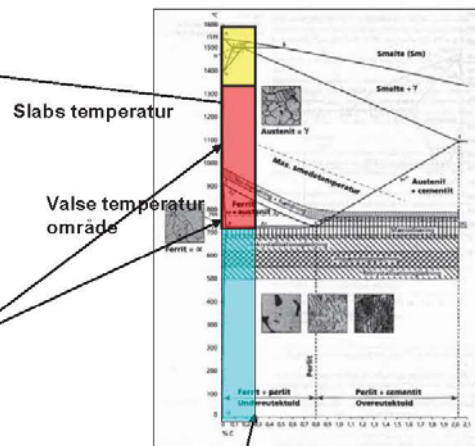
Z-prøvning (Z = 70%)



Slabs tværsnit

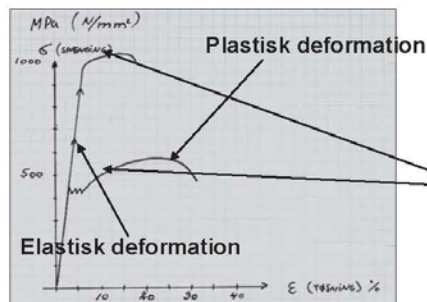


Varmvalsning

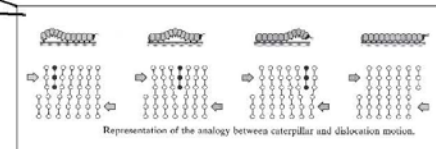
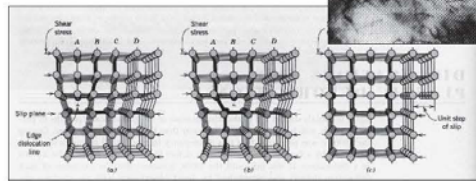


Max. kulstof(carbon) indhold for svejselige konstruktionsstål i overensstemmelse med DS/EN 10025: $C_{\max} = 0,24 \%$

Styrkeøgning



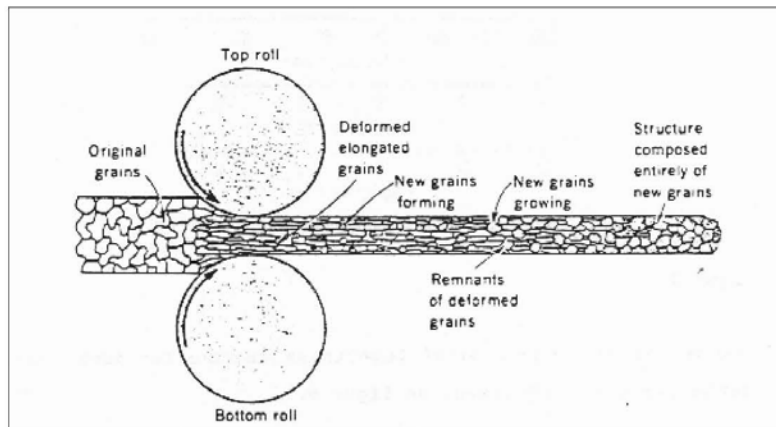
Dislokation



Dislokationbarrierer/-bremser \rightarrow udvidelse af det elastiske område \rightarrow Styrkeøgning:

- Fremmedatomer (fx C og Mn)
- Korngrænser (ved kornforfining)
- Dislokationsforøgelse (deformationshærdning)
- Fremmede faser (ved modningshærdning)

DMS



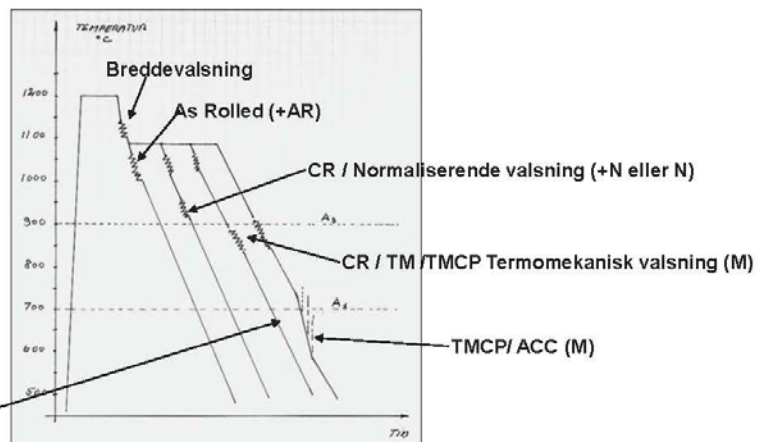
Valseprocesser



Kvarto- valseværk

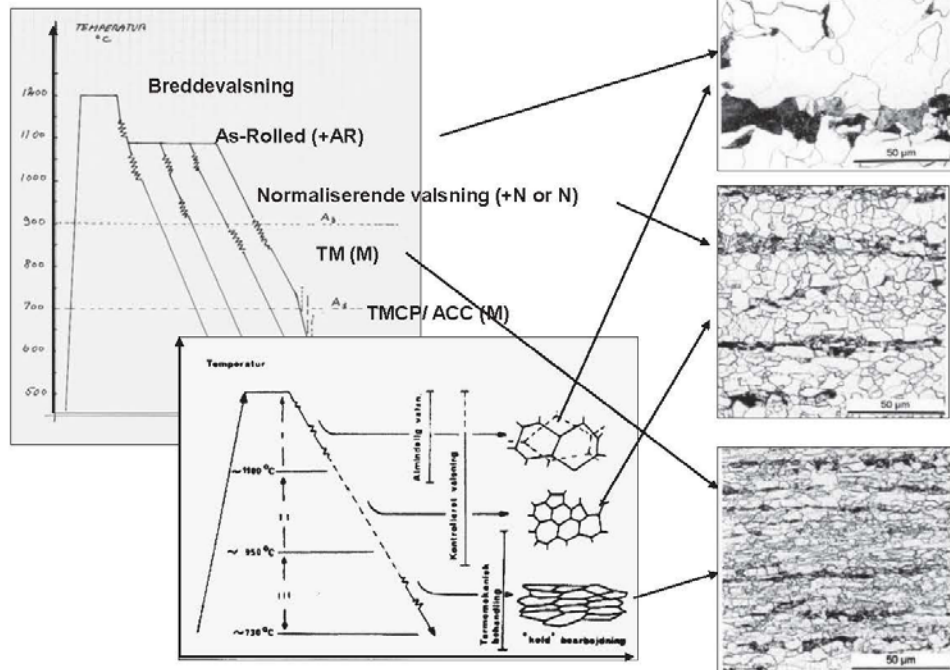


ACC-udstyr

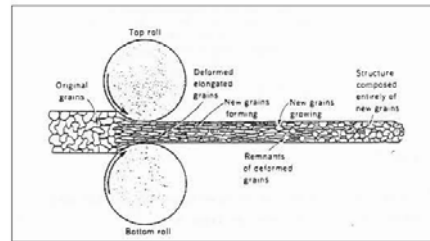


CR-valsning = Controlled Rolling

Valseprocesser



Egenskaber frembragt ved en valseproces.



Varmvalsning

I) Normal varmvælsning (Leveringstilstand as-rolled)

En evt. breddevalsning udføres umiddelbart efter, at slabs/blokken er udtaget af slabs/blokovnen. Slabs/bloktemperatur er typisk 1250 °C. Herefter vendes den breddevalsedes slabs/blok, og længdevalsningen påbegyndes umiddelbart.

Længderetningen på pladen omtales som "hovedvalseretningen"

Det varmvalsedes ståls struktur er relativt grovkornet (ASTM-kornstørrelse omkring 5-6, alt efter pladedimension).

II) Kontrolleret (styret) vælsning (CR-vælsning = Controlled Rolling)

Siden 30'erne er der udviklet kontrollerede (styrede) valseprocesser, som går under fællesbetegnelsen »Kontrolleret vælsning, forkortet CR (Controlled Rolling).

CR-processerne omfatter en række processer, der som fælleskendetegn har det ene, at de sidste 20 %'s deformation foregår under nøje temperaturkontrol, dvs. i et bestemt temperaturinterval.

II.a) Normaliserende vælsning

Vælsningen udføres næsten som beskrevet under varmvælsning, men de sidste stik (tykkelsesreduktionen) udføres i det temperaturinterval, hvor stålet normalt (ovn)normaliseres, altså lige over A_3 .

De resulterende mekaniske egenskaber skal modsvare det (ovn)normaliserede produkt. Det er væsentligt at påpege, at stålstandarderne ikke skelner imellem de to processer. Dette betyder derfor, at en forbruger ikke i certifikatet, uanset type, kan få oplyst, hvilken type normaliseret stål forbrugeren har modtaget.

II.b) TMCP-stål (Thermo Mechanical controlled Process)

TMCP-vælsning dækker over et antal forskellige valseprocesser.

For de fleste af disse processer findes flere betegnelser, hvilket fra et forbrugersynspunkt kan være meget forvirrende. Det vil derfor altid i tvivlstilfælde være en god ide at gennemlæse specifikationen efter standarden for det aktuelle stål.

II.b.1) TM-stål (Thermo Mechanical Rolling)

Startvælsstemperaturen er normalt, men ikke nødvendigvis, en del lavere end for varmvælsning. Endvidere udføres slutvælsningen ved så lave temperaturer, at austenitten ikke rekrystalliserer, dvs. ved en temperatur lige over A_3 eller i tofaseområdet imellem A_3/A_1 , og der dannes derfor en finkornet struktur.

I sidstnævnte tilfælde kan de højeste styrkeegenskaber opnås, idet der lidt populært sker en form for »kolddeformation» af de enkelte korn, som sammen med den finkornede struktur giver en mærkbar styrkeforøgelse, samt en god sejhed.

II.b.2) ACC-stål (Accelerated Controlled Cooling)

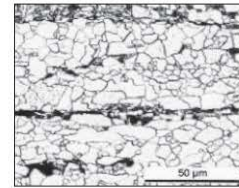
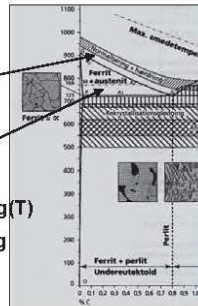
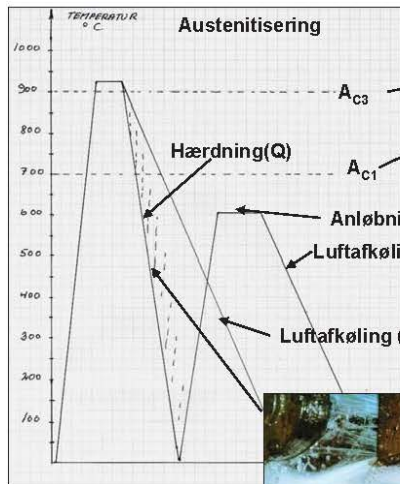
En japansk udviklet proces til fremstilling af højstyrkestål med særdeles gode egenskaber, hvad angår lav kulstofækvivalent (CEV), omslagstemperatur mm.

Udgangspunktet er et normaliseret valset/TM-stål. Den endnu varme plade føres igennem et langt køleanlæg (typisk 40-50 m), hvori pladen afkøles styret fra ca. 800 °C til ca. 600 °C, alt efter ønskede egenskaber. Derefter afkøles i luft.

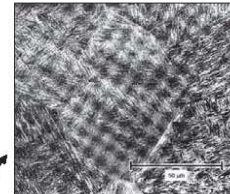
Strukturen er ferritisk/finperlitisk/bainitisk

Varmebehandling

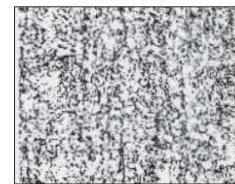
(Ovn) Normalisering og sejhærdning



Normalisering (N)
Fin kornet perlit/ferrit



Hærdet (Q)
Martensit



Sejhærdet (Q/T)
Anløbet martensit

Basis materiale: Varmvalset produkt (As-rolled)



"Roll quenching" udstyr

Egenskaber frembragt ved varmebehandling

DMS

I) (Ovn) Normalisering

Processen udføres ved at opvarme emnet til temperaturen over A_{c3} -linien (til austenitområdet) i en ovn. Efter en kort holdetid, afkøling i luft.

Den opnåede struktur er finkornet ferritisk/perlitisk (ASTM-kornstørrelse 9-11, alt efter pladedimension).

Man opnår herved en forbedring af flydespændingen såvel som en sænkning af omslagstemperaturen (en forbedring af slagsejhedsegenskaberne).

De opnåede egenskaber er ækvivalente med egenskaber opnået ved normaliserende valsing.

II) Q/T-stål (Quench/Tempering = (Martensit)hærdning/anløbning) På dansk er betegnelsen sejhærdning.

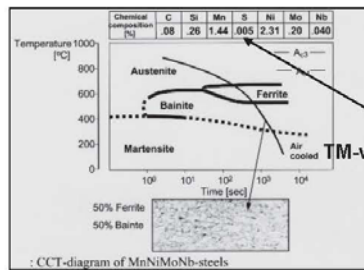
Som den engelske forkortelse antyder, er der her tale om to varmebehandlingsprocesser. En hærdning til martensit (quenching) efterfulgt af en anløbning (tempering). Hærdningen udføres ved at opvarme et varmvalset produkt til en temperatur over A_{c3} -linien (til austenitområdet). Efter en kort holdetid sendes pladen igennem et hærdeanlæg, hvor selve brat-køling-gen og dermed martensitdannelsen finder sted.

Vær opmærksom på, at martensithårdheden udelukkende er et spørgsmål om kulstofindholdet, hvilket indebærer, at stærkere stål har et højere kulstof indhold.

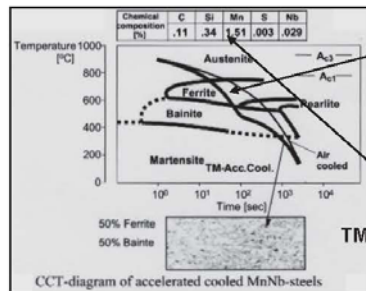
Anløbningen udføres fx i en normaliseringsovn, og temperaturintervallet imellem 600 °C og 660 °C. Forbrugeren bør være opmærksom på, at producenten normalt angiver anløbningstemperaturen i certifikatet, idet en overskridelse af denne temperatur fx i forbindelse med en varmbearbejdning kan føre til en reduktion af stålets styrkeegenskaber.

ACC-treatment ("alloying with water") Accelerated Continuous/Controlled Cooling

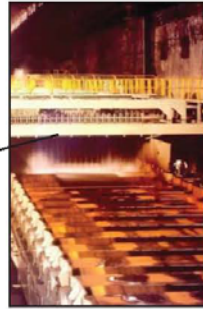
DMS



TM-valset lavt legeret stål



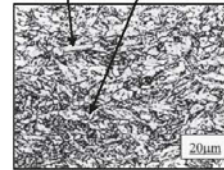
TM/ACC - behandlet u-legeret stål



DS/EN 10025-4-S420M



Ferritisk/bainitisk struktur



DS/EN 10025-4-S460ML

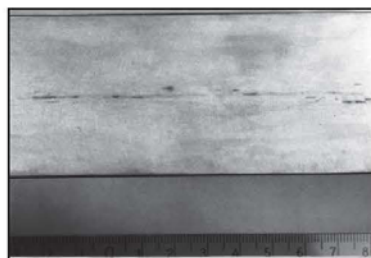
Hydrogen inducerede revner (ca. 1980)

DMS

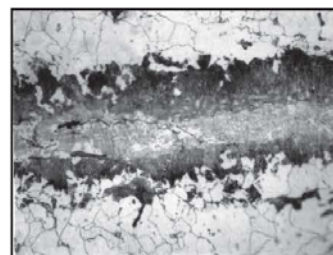
Ståltipe : St 52-3 Svovl : S 0,008 % Hydrogen : H < 0,0010 % ?



Slabs tværsnit



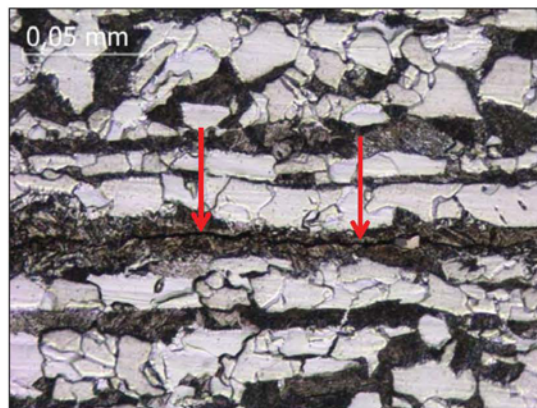
Plade tværsnit



Microstruktur : 400 x

Hydrogen inducerede revner (ca. 2010)

Ståltipe : S 355 J2 Svovl : S 0 0,002 % Hydrogen : H < 0,0002 % ?



Revnen løber i det perlitiske bånd i den sejrede zone i pladens center

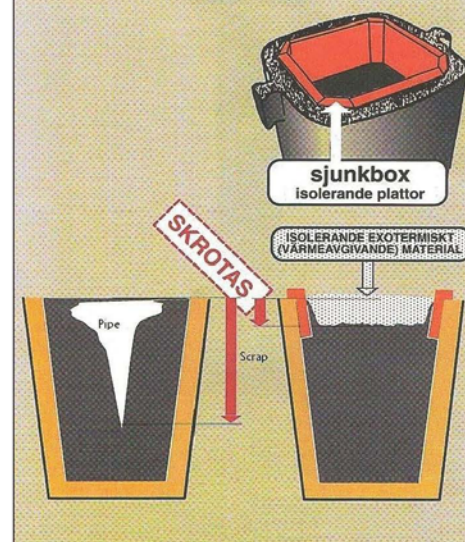
Blokstøbning

Ingot Casting

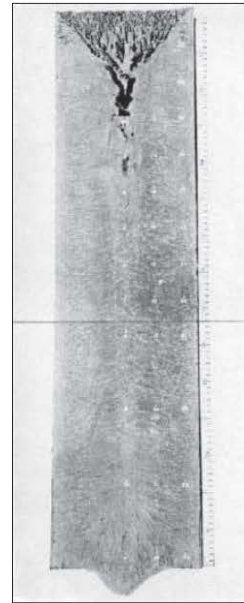
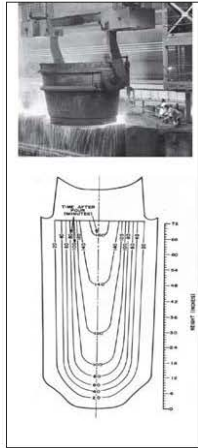
- o Production of material for rolling of e.g. rod, pipe, wire or sheet metal .
- o The Mould:
 - o Usually made of cast iron.
 - o Different shapes (conical)
- o Metoder:
 - Downhill casting.
 - Centering is very important
 - problems : splashes, waves, oxidation, low productivity/slow process
 - Uphill casting
 - More preparation steps
 - Higher produktivity
 - Higher quality.



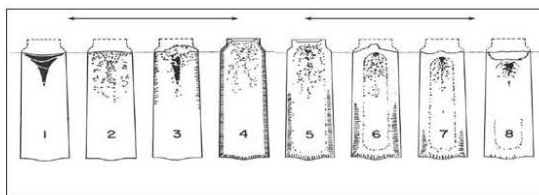
MED OCH UTAN SJUNKBOX



DMS



Makrostruktur



Moderne blokstøbning med vandkølet kobberkokille



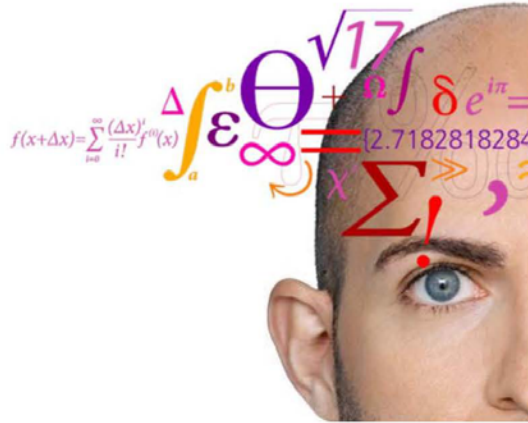
Varmebehandling og karakterisering af nye udskilningshærdbare superlegeringer

Uffe Bihlet, MAN og DTU Mekanik

Varmebehandling og karakterisering af nye udskilningshærdbare superlegeringer

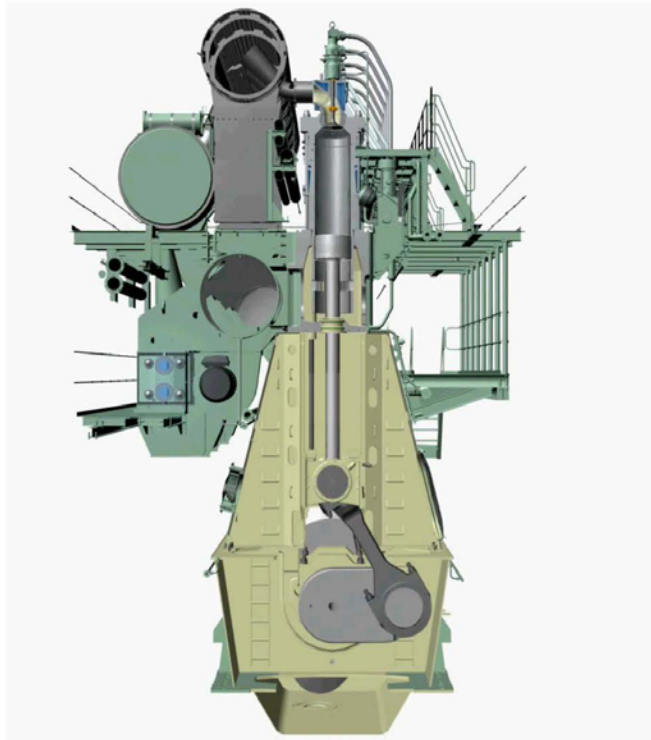
DMS Vintermøde 2013

Uffe D. Bihlet
ErhvervsPhD studerende
MAN Diesel & Turbo
DTU MEK



Agenda

- To-takts motoren og udstødningsventilen
- Udskilningshærdning i Inconel 718
- Ny legering
- Verificering af hærtningsmekanismen i ny legering
 - Røngtendiffraktion (XRD)
 - Focused Ion Beam Imaging (FIB)
 - TEM
- Wrap-up



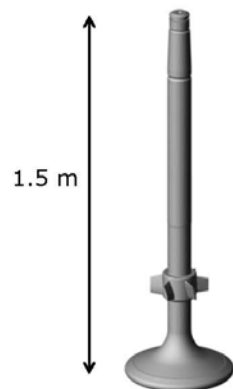
3

4.05.2013

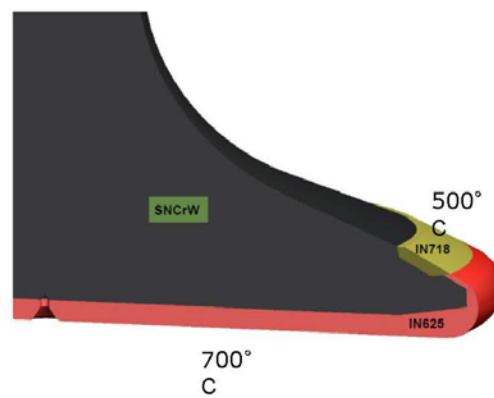


Ventilspindlen

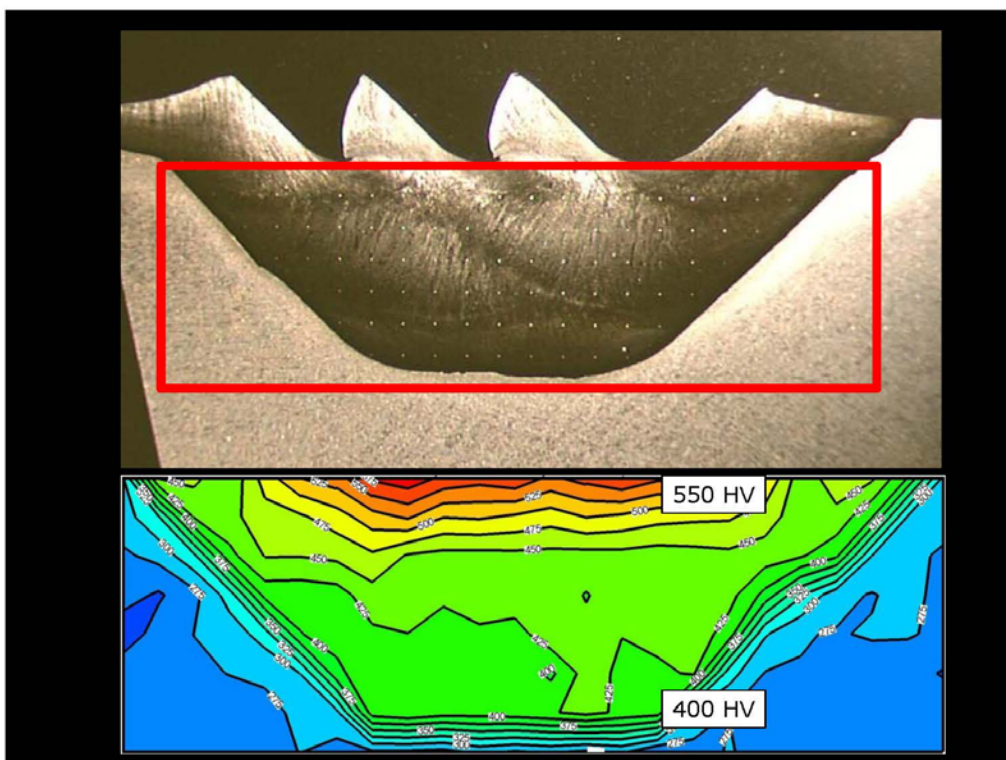
Legering	Cr	Nb	Ti	Al	Fe	Mo	Ni
IN718	19	5	0.9	0.5	18	3	Bal



4

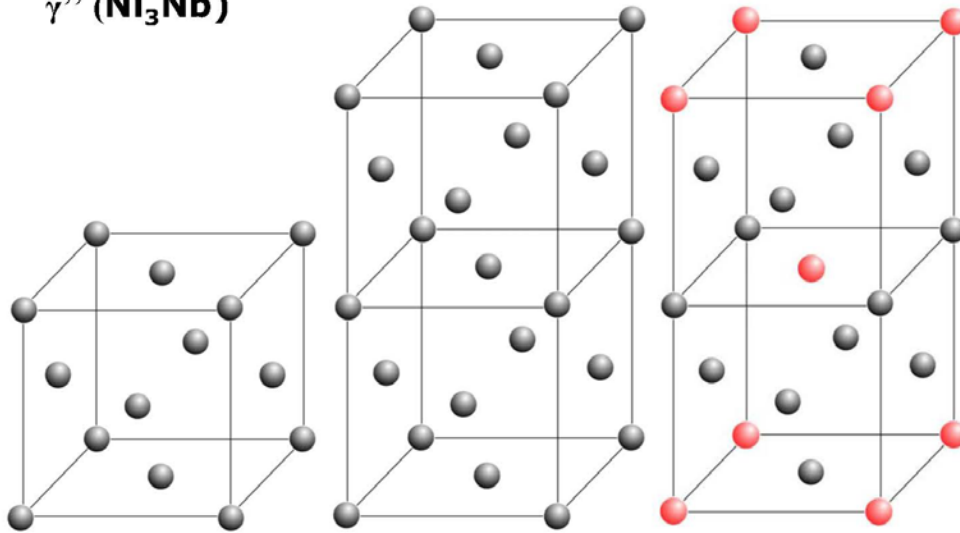


24.05.2013



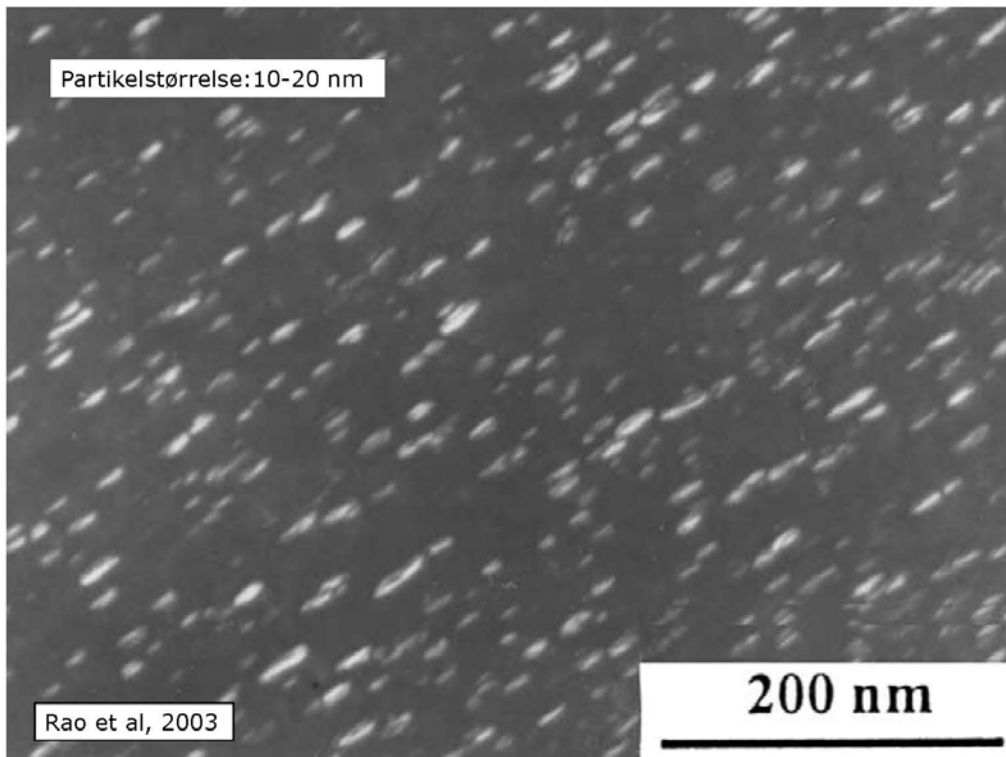


γ'' (Ni_3Nb)



7

24.05.2013



Agenda

- To-takts motoren og udstødningsventilen
- Udskilningshærdning i Inconel 718
- Ny legering
- Verificering af hærdningsmekanismen i ny legering
 - Røngtendiffraktion (XRD)
 - Focused Ion Beam Imaging (FIB)
 - TEM
- Wrap-up

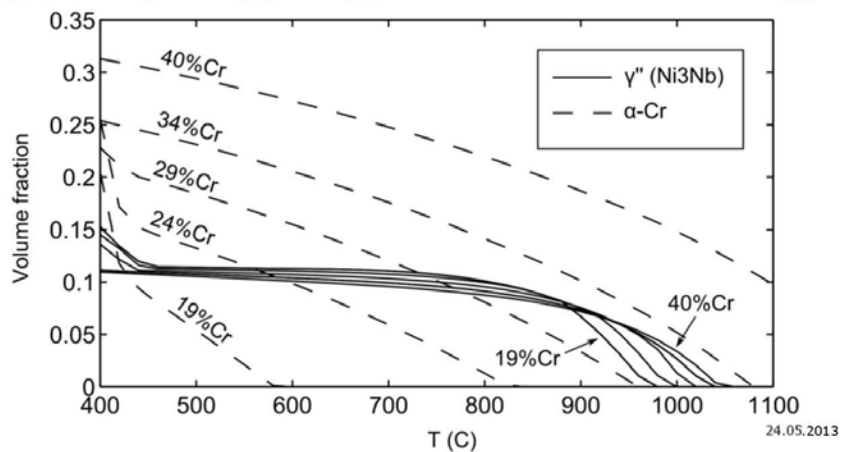
9

24.05.2013



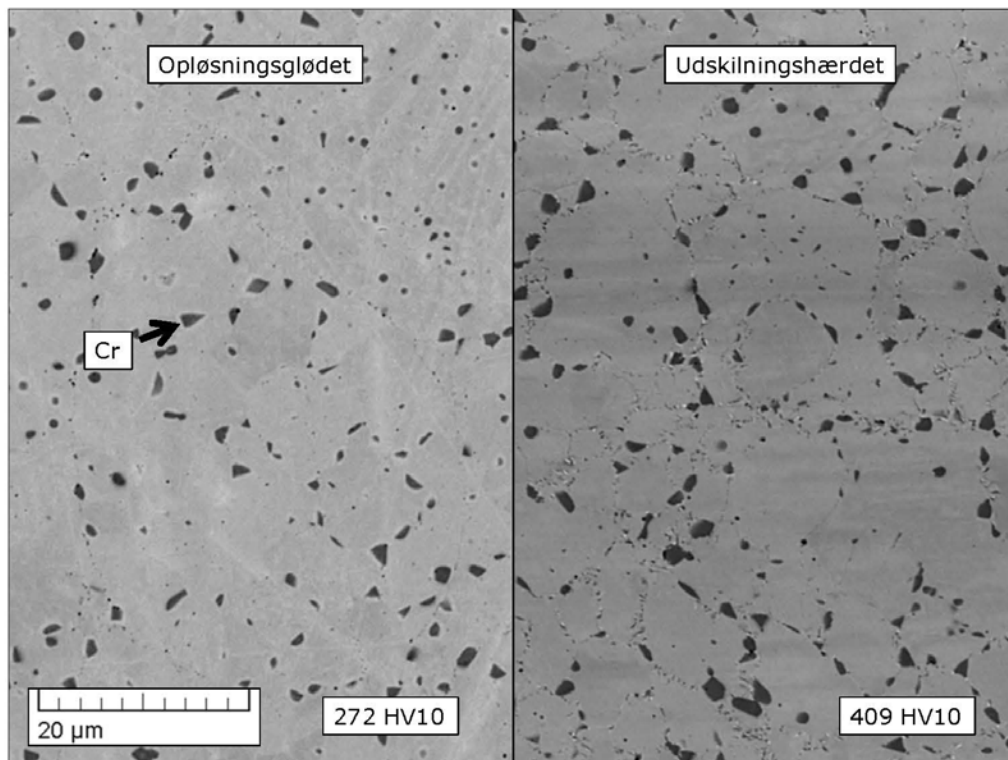
Fra Inconel 718 -> ?

Legering	Cr	Nb	Ti	Al	Fe	Mo	Ni
IN718	19	5	0.9	0.5	18	3	Bal
No. 6	40	3.5	0.5	-	-	-	Bal



10

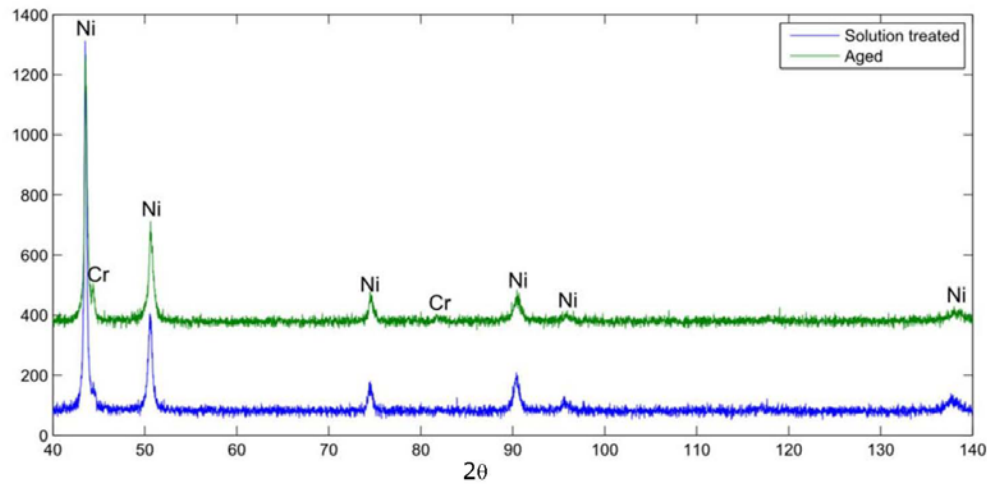
24.05.2013



Agenda

- To-takts motoren og udstødningsventilen
- Udskilningshærdning i Inconel 718
- Ny legering
- Verificering af hærtningsmekanismen i ny legering
 - Røngtendiffraktion (XRD)
 - Focused Ion Beam Imaging (FIB)
 - TEM
- Wrap-up

Røngtendiffraktion (XRD)



13

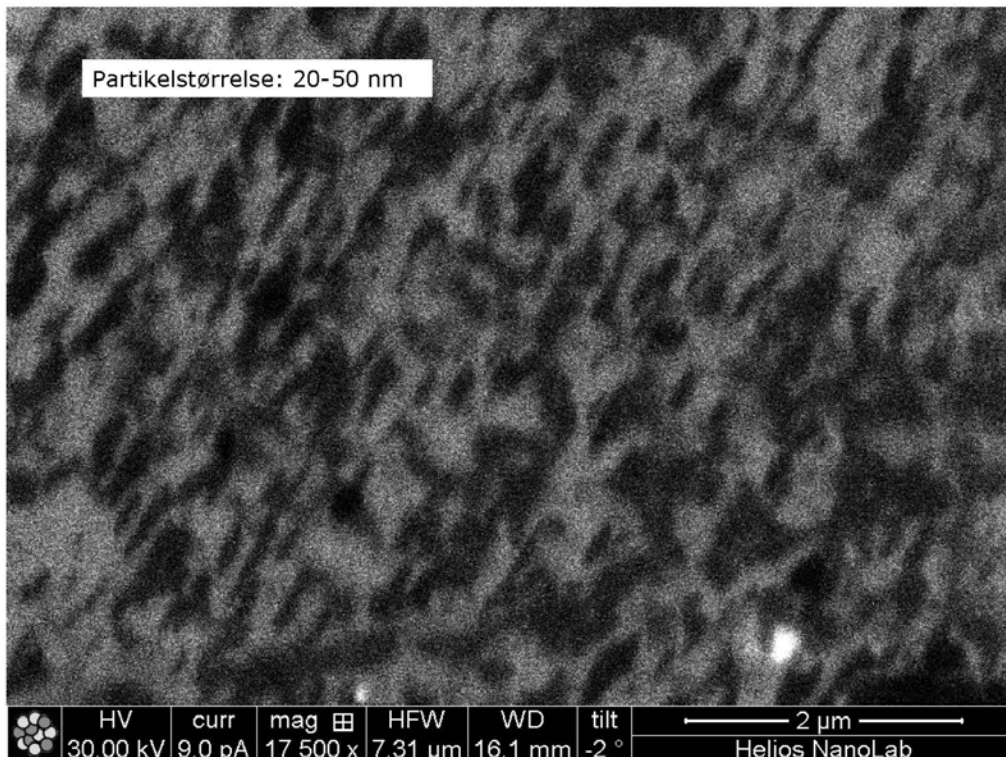
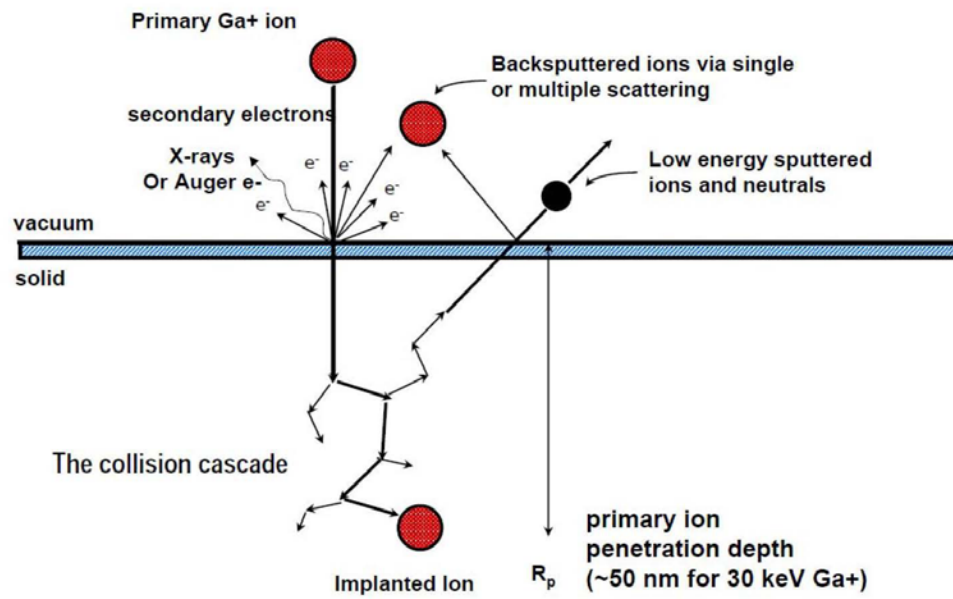
24.05.2013

Agenda

- To-takts motoren og udstødningsventilen
- Udskilningshærdning i Inconel 718
- Ny legering
- Verificering af hærtningsmekanismen i ny legering
 - Røngtendiffraktion (XRD)
 - Focused Ion Beam Imaging (FIB)
 - TEM
- Wrap-up

14

24.05.2013

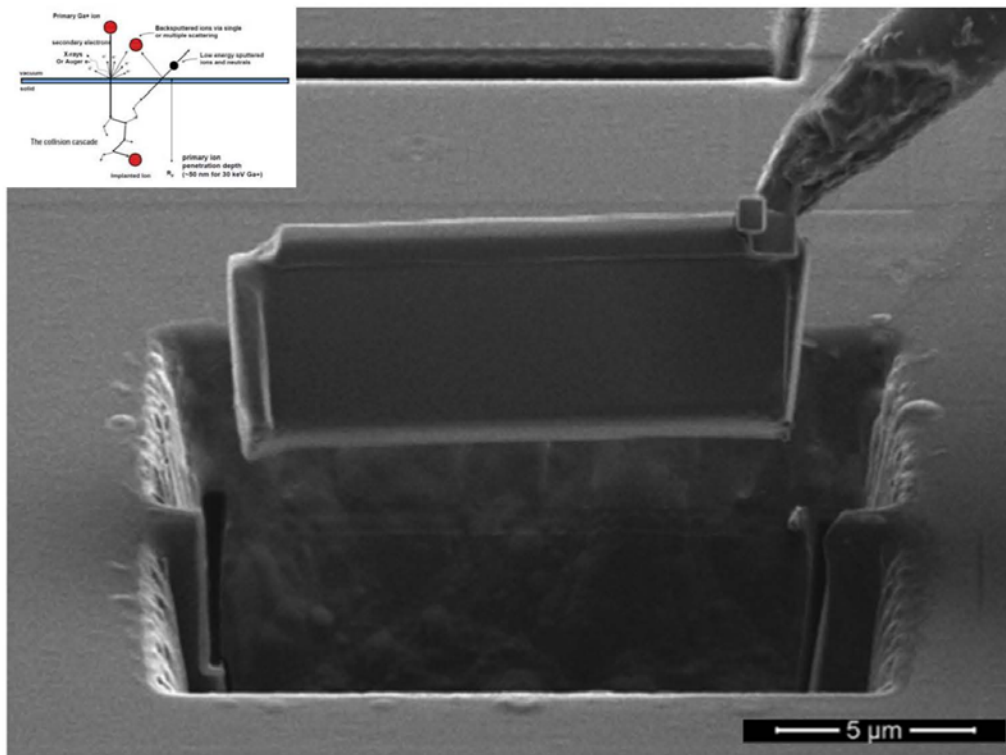


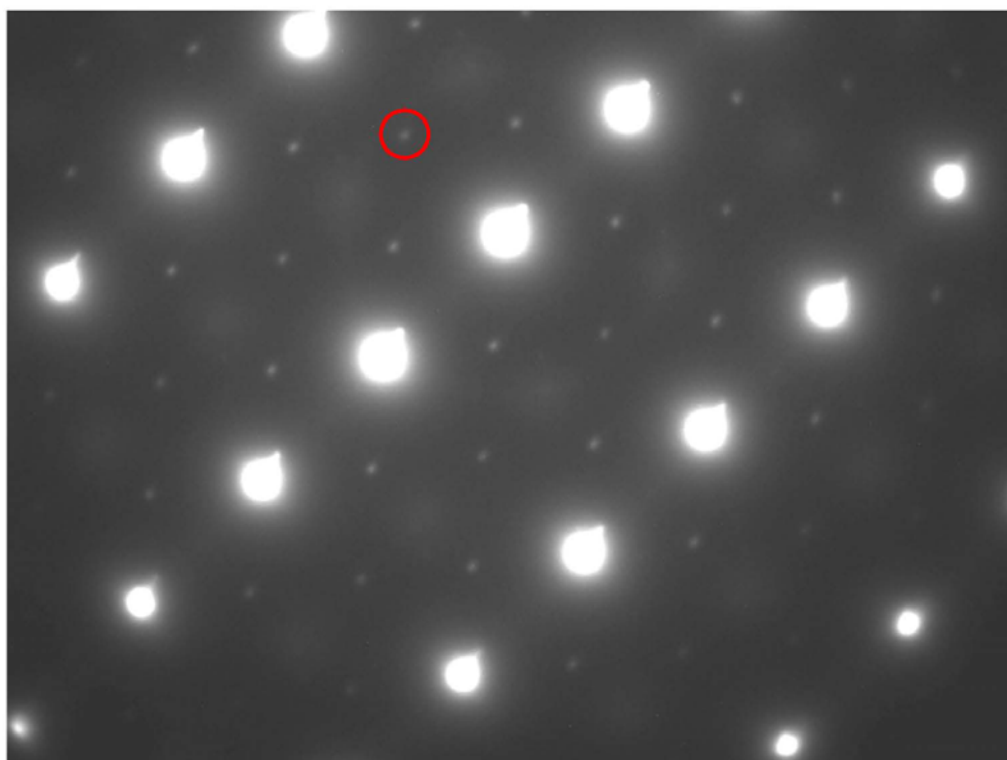
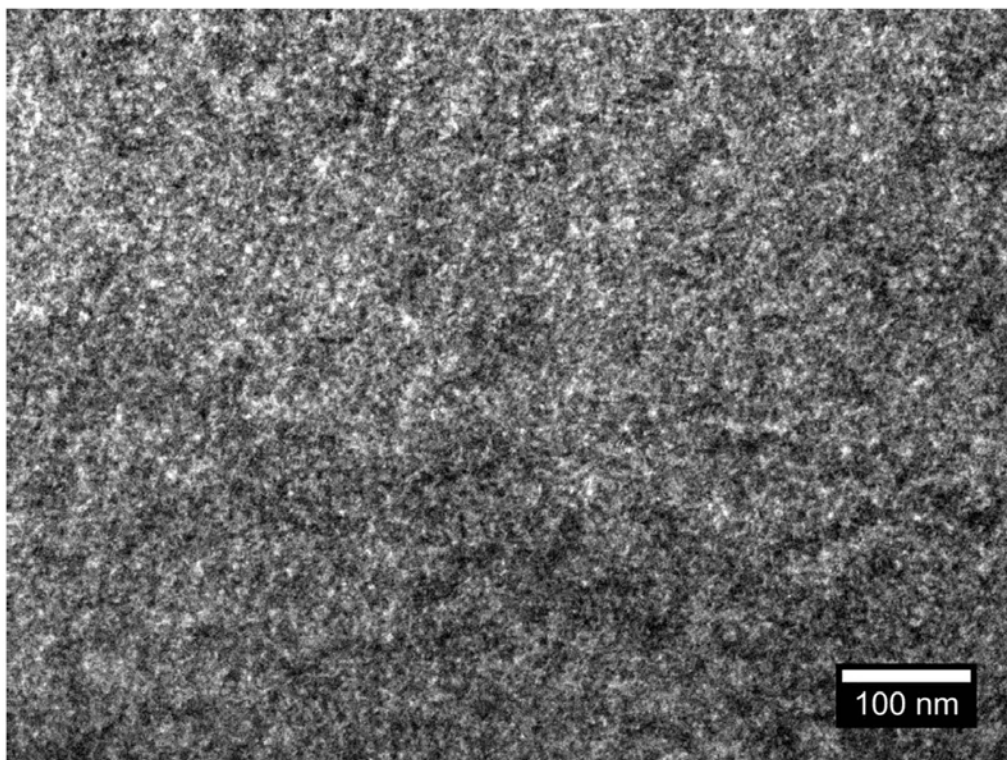
Agenda

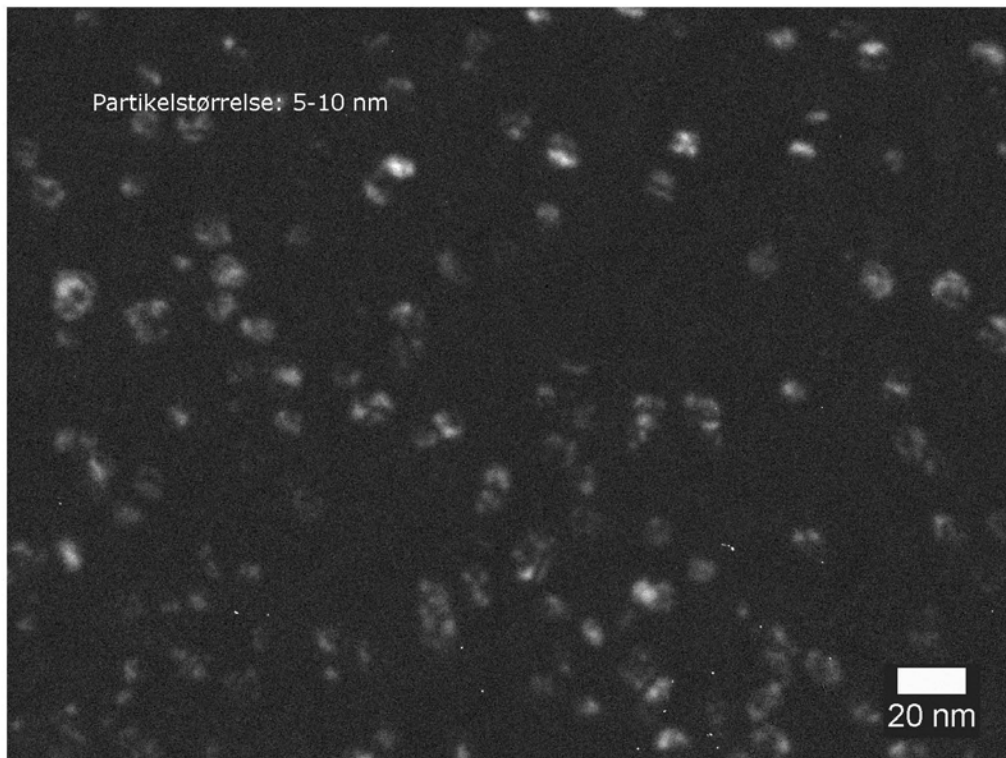
- To-takts motoren og udstødningsventilen
- Udskilningshærdning i Inconel 718
- Ny legering
- Verificering af hærdningsmekanismen i ny legering
 - Røngtendiffraktion (XRD)
 - Focused Ion Beam Imaging (FIB)
 - TEM
- Wrap-up

17

24.05.2013







Agenda

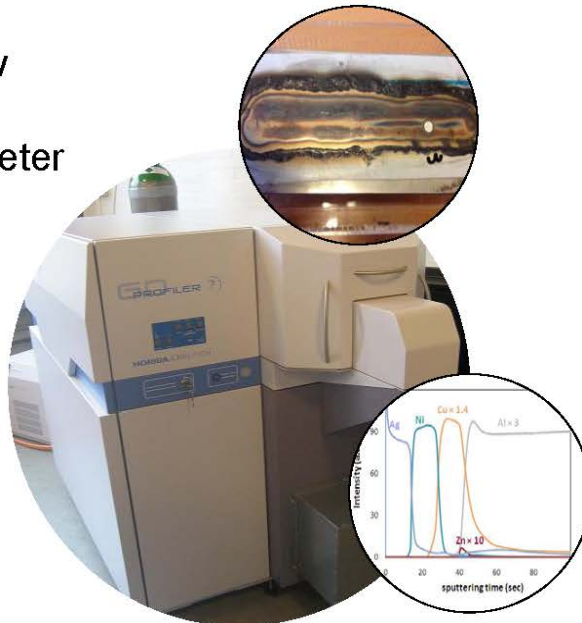
- To-takts motoren og udstødningsventilen
- Udskilningshærdning i Inconel 718
- Ny legering
- Verificering af hærdningsmekanismen i ny legering
 - Røngtendiffraktion (XRD)
 - Focused Ion Beam Imaging (FIB)
 - TEM
- Wrap-up

GD-OES applications

Io Mizushima, IPU

Anvendelse af Glow Discharge Optical Emission Spectrometer (GD-OES)

Io Mizushima
IPU



IPU

IPU: A dedicated on-campus innovation team

Side 2

- A non-profit organisation at the TU of Denmark
- Research and development projects on contract
- Commercialisation of ideas, innovations, and patents
- 50 full-time staff
- 70+ associated DTU staff
- Co-location with DTU colleagues on campus
- Turnover: ~ 6 mill EUR/yr

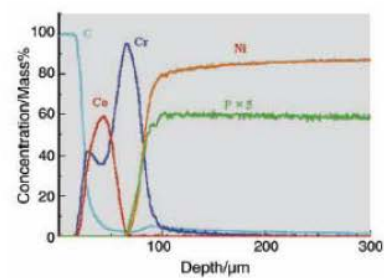
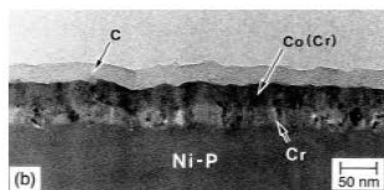


IPU

1. GD-OES - princippet
2. Fordele og ulemper ved GD-OES
3. Eksempler
 - Bulk-analyse
 - Dybdeprofiler
 - Praktiske anvendelser
4. Opsummering

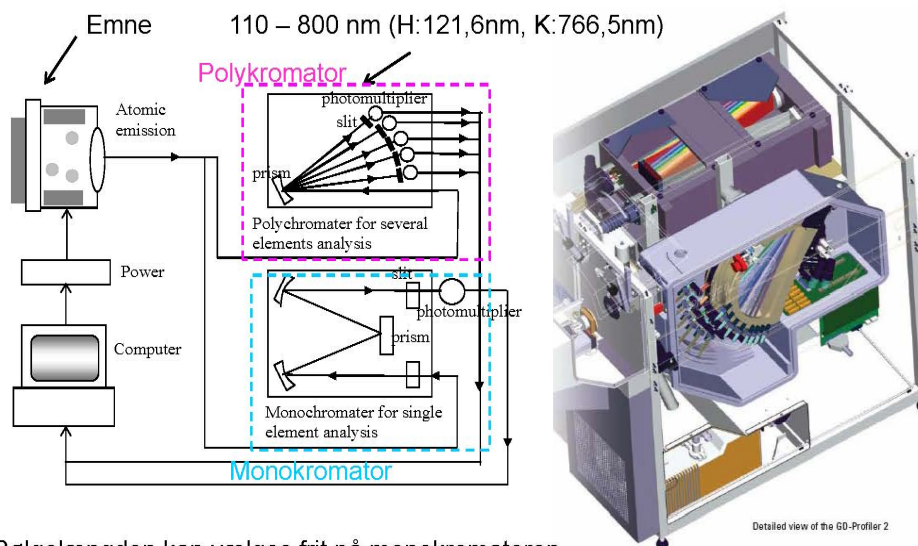
GD-OES anvendes til analyse af den kemiske sammensætning.

Både bulk-materialer og overflader kan analyseres med dybdeprofiler (0,1-100 μ m).



Machine components

Side 5



Bølgelængden kan vælges frit på monokromatoren, som i princippet kan måle alle elementer.

IPU

Optical emission lines

Side 6

H	121,567	Sb	206,833
O	130,217	Ga	417,205
Cl	134,724	Cr	425,433
N	149,263	W	429,461
Be	313,042	Pb	220,353
Nb	316,34	In	451,132
Cu	324,754	Cd	228,802
Ag	328,068	Se	241,352
C	165,701	Au	242,795
Zn	334,502	B	249,678
Ni	341,477	Hg	253,652
Co	345,351	Mn	257,61
P	178,287	Pt	265,945
S	180,734	Ge	275,459
Ti	365,35	Mg	285,213
Fe	371,994	Hf	286,637
Sn	189,989	Si	288,158
Mo	386,411	Bi	306,772
Ca	393,367	Li	670,791
Al	396,152	K	766,49

GD-OES kan måle selv lette grundstoffer som f.eks. hydrogen.

IPU

GD-OES periodic table of available elements

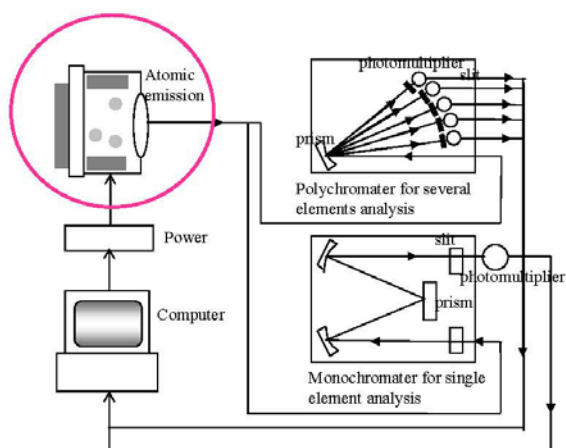
Side 7

H	Polykromator: udvalgte elementer (43) Monokromator: ekstra element kan vælges frit																He
Li	Be											B	C	N	O	F	Ne
Na	Mg											Al	Si	P	S	Cl	Ar
K	Ca	Sc	Ti	V	Cr	Mn	Fe	Co	Ni	Cu	Zn	Ga	Ge	As	Se	Br	Kr
Rb	Sr	Y	Zr	Nb	Mo	Tc	Ru	Rh	Pd	Ag	Cd	In	Sn	Sb	Te	I	Xe
Cs	Ba	La	Hf	Ta	W	Re	Os	Ir	Pt	Au	Hg	Tl	Pb	Bi	Po	At	Rn

IPU

Emission part

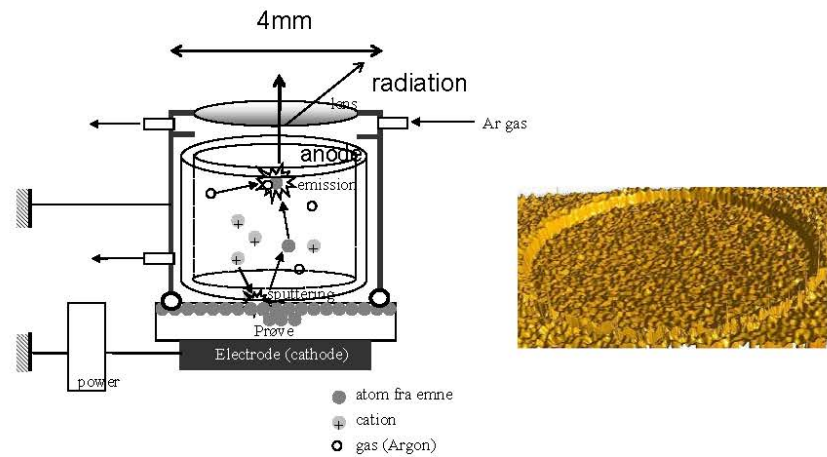
Side 8



IPU

Emission part

Side 9



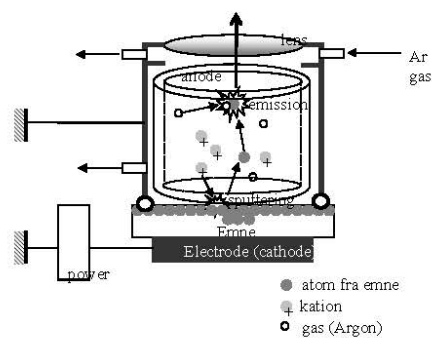
Sputtering af grundstoffer:
ioniseret argon → eksitering af grundstoffer → emission (udsender lys)

IPU

Intensitet ændring

Side 10

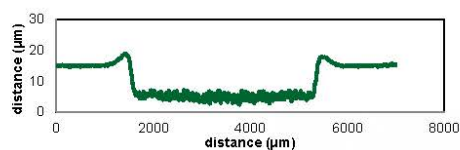
Intensitet ændres ved-
Tryk (pressure)
Spænding (voltage)
Afstand mellem anode og emne
Urenheder på linsen
Bulk materiale



IPU

Sputtering hastighed

Side 11



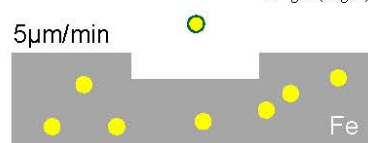
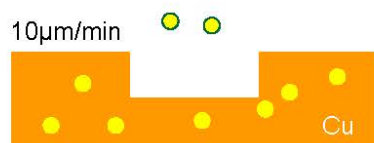
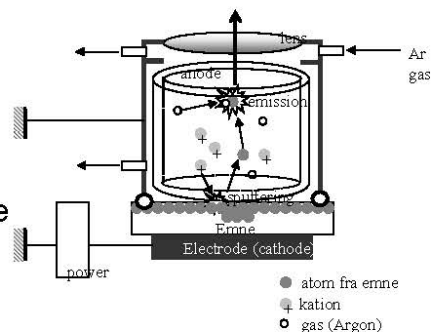
元素	濃度 (%)	スパッタリング速度 (μ/min)	密度 (g/cm ³)
Ag	99.980	22.0	10.49
Al	99.500	3.6	2.69
Au	99.950	20.0	19.26
Co	99.900	3.6	8.90
Cr	99.900	5.2	7.19
Cu	99.994	9.6	8.93
Fe	99.570	4.6	7.87
Mg	99.900	12.0	1.74
Mo	99.950	6.4	10.20
Nb	99.900	3.6	8.57
Ni	99.700	5.2	8.90
Pb	99.990	40.0	11.34
Pd	99.950	13.0	12.16
Pt	99.980	8.0	21.45
Si	100.000	2.2	2.33
Sn	99.900	18.0	7.30
Ta	99.950	4.9	16.60
Ti	99.900	2.4	4.50
W	99.950	5.6	19.30
Zn	99.990	23.0	7.13

IPU

Intensitet ændring

Side 12

Intensitet ændres ved-
Bulk materiale
Tryk (pressure)
Spænding (voltage)
Afstand mellem anode og emne
Urenheder på linsen



Udstyret skal rutinemæssigt kalibreres, og helst med standarder der er sammenlignelige med emnet der måles.

IPU

Fordele

- 43 elementer kan analyseres på én gang
- lette stoffer, bl.a. hydrogen, ilt, kul, nitrogen og klorid kan måles
- meget små koncentrationer kan måles
- hurtig måling (1-10 $\mu\text{m}/\text{min.}$)

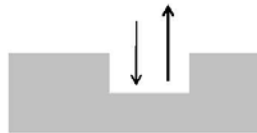
Ulemper

- emner skal være flade og skal have areal på mindst $5 \times 5 \text{ mm}^2$
- det tager lang tid at foretage kvantitative analyser grundigt
- emner skal være generelt elektrisk ledende

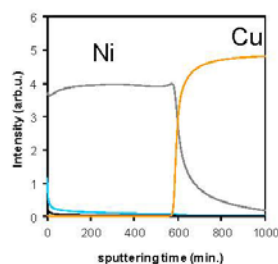
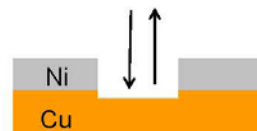
IPU

Eksempler

Bulk analyser



Dybdeprofiler



IPU

Eksempel 1 - bulk analyse

Side 15

Emne – AISi9Cu3Fe0.5 indeholdende Mn, Mg, Ti, Sr

Metode – B General Al

Referencer:

SQ-15KA Al-12%Si, 0,7%Fe, 0,5%Cu, 0,06%Mn, 1,2%Mg, 0,1%Ti, 0,03%Sr

SQ-12TL Al-1,1%Si, 0,6%Fe, 4,8%Cu, 1,1%Mn, 0,16%Mg

SQ-11PG Al-0,2%Si, 0,2%Fe, 0,5%Cu, 0,4%Mn, 3,1%Mg, 0,1%Ti

Resultat af måling på standarder:

	Si	Fe	Cu	Mn	Mg	Ti	Sr
15KA	12	0.78	0.41	0.08	1.1	0.09	0.04
12TL	0.95	0.73	3.9	1.3	0.14	-	-
11PG	0.18	0.22	0.44	0.49	2.7	0.09	

Genkalibration

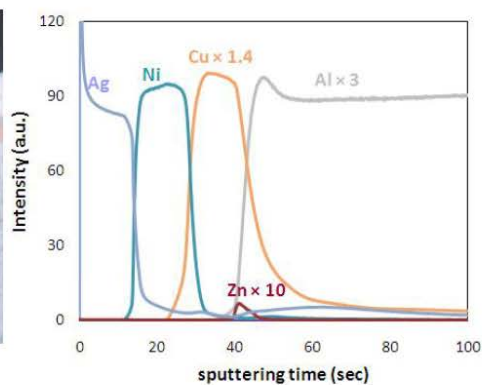
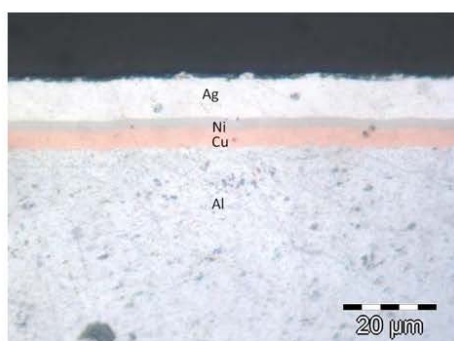
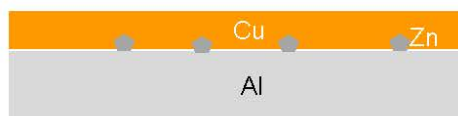
Resultat af måling på testemne:

	Si	Fe	Cu	Mn	Mg	Ti	Sr
sample	8.7	0.65	2.4	0.46	0.34	0.06	0.04

IPU

Eksempler – Zinkat behandling

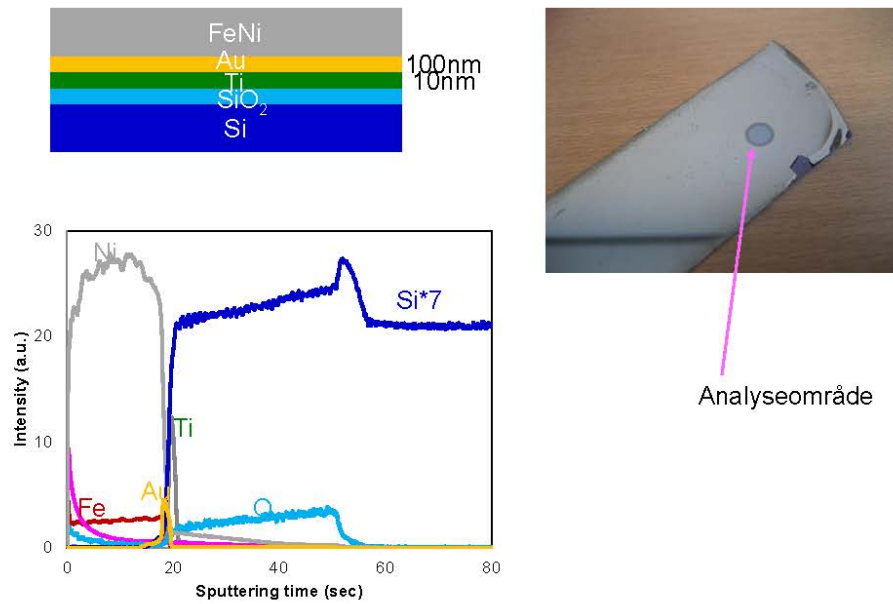
Side 16



IPU

Eksempler – Elektropletteret silicium wafer

Side 17



IPU

Eksempler – Fejl i svejsning

Side 18

Svejsning med plastiskfolie på bagside



Kan en slibning fjerne det brændte plastik fra overfladen?

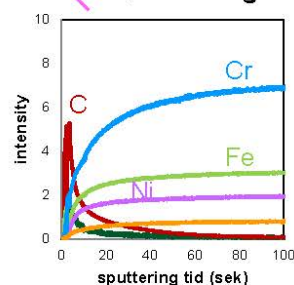
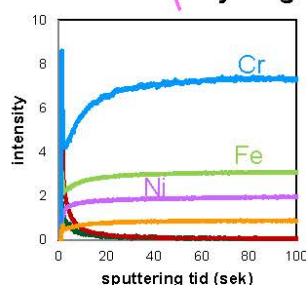
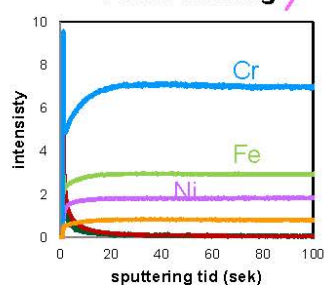
IPU



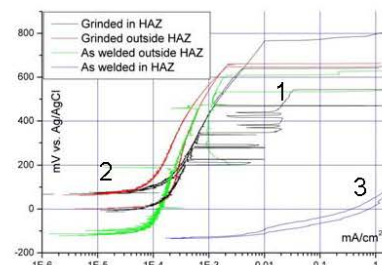
1 efter slibning

2 udenfor svejsning

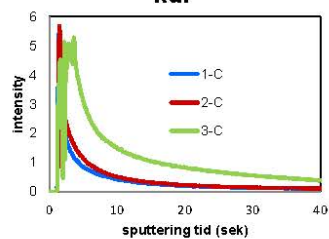
3 før slibning



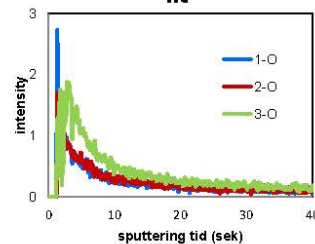
IPU



kul



ilt

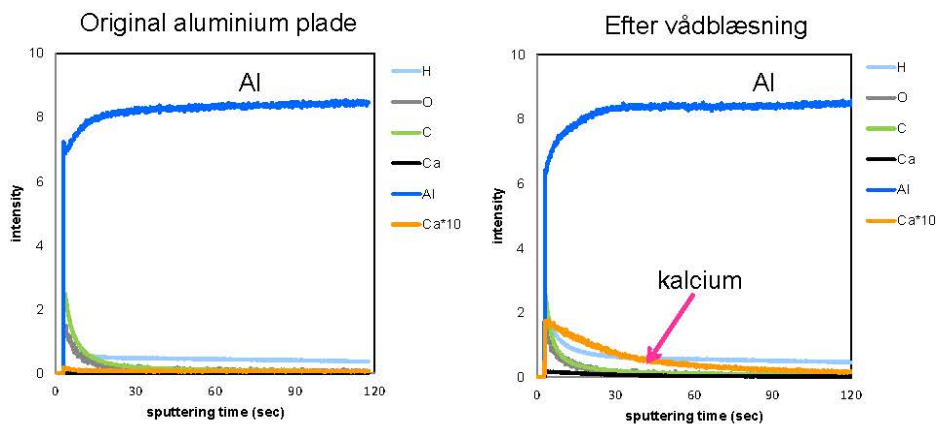


IPU

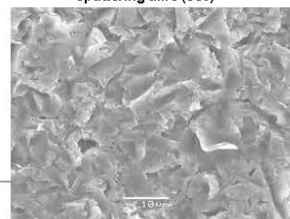
Aluminium plade forbehandlet med vådblæsning
(indeholder fint kalk pulver)



IPU



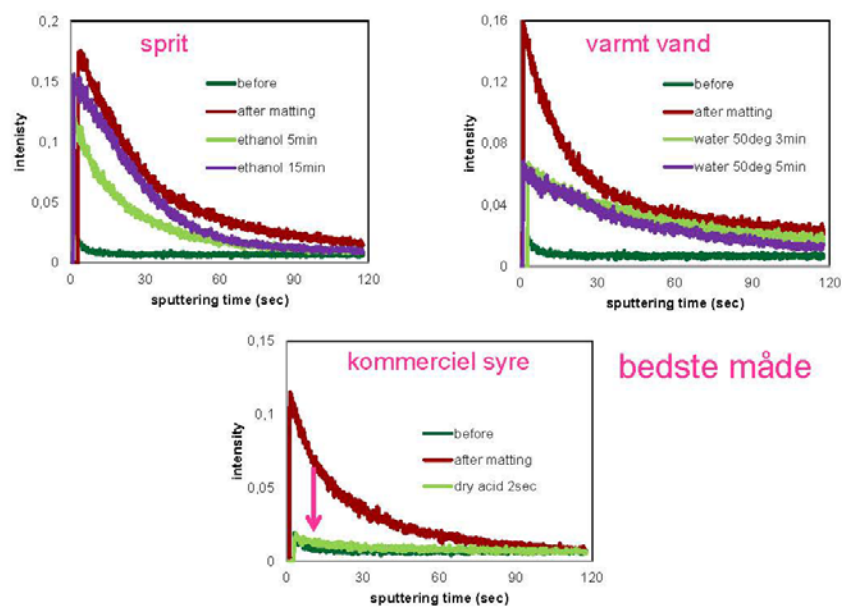
Meget calcium er stadig tilbage
→ høj pH
→ bakterier er døde



IPU

Kalcium målinger på Al forbehandlet på forskellige måder

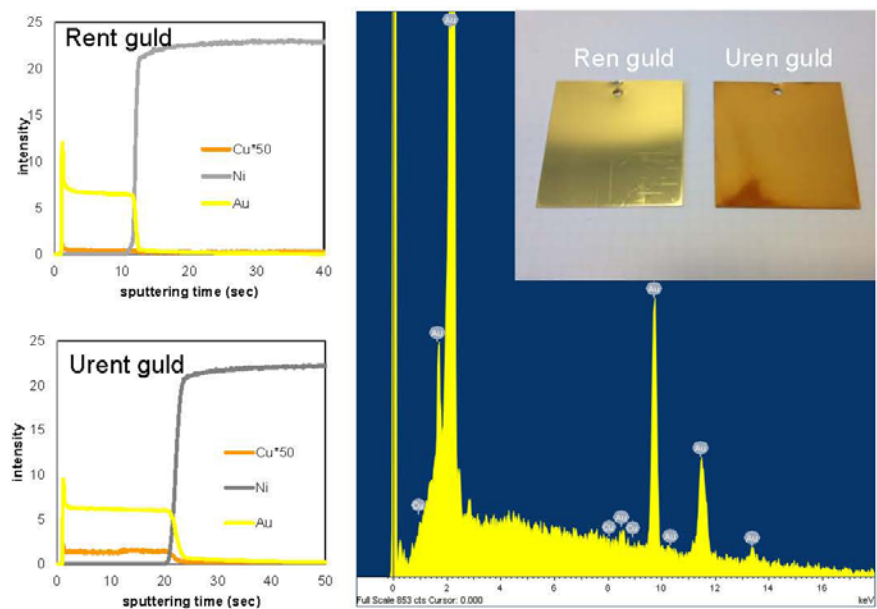
Side 23



IPU

Deponering af guld med kobberforurening

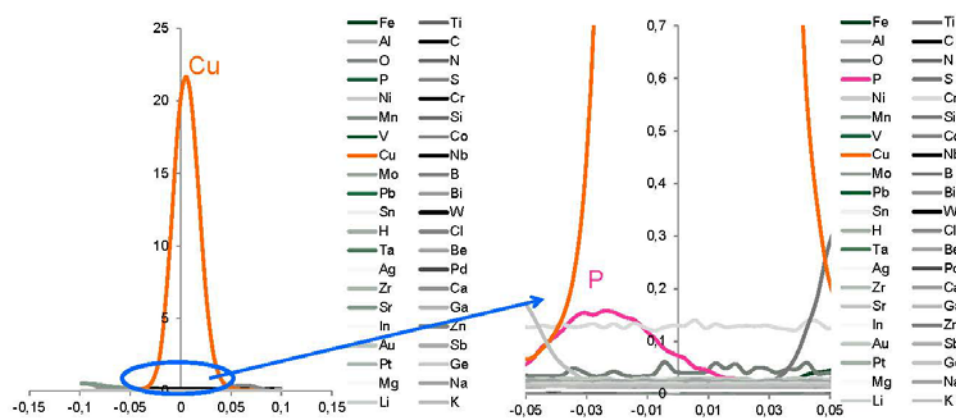
Side 24



IPU

Fosfor aktiverede kobberanoder

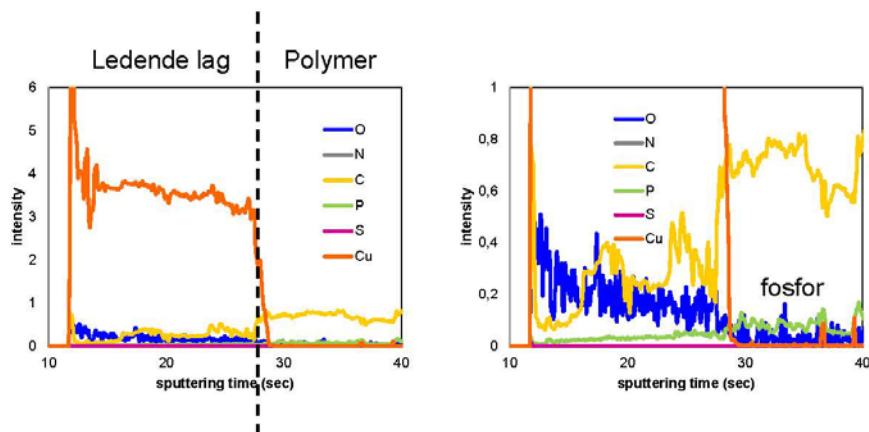
Side 25



IPU

Ikke-ledende emner

Side 26



IPU

GD-OES kan anvendes til karakterisering af sammensætning, evt. kan en dybdeprofil opnås.

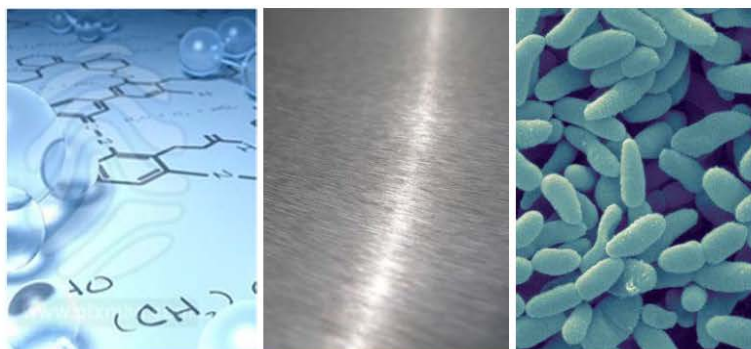
Det er vigtigt at kende fordele og ulemper ved metoden, når man foretager GD-OES måling.

Det kræver meget tid at gennemføre en ordentlig kvantitative analyse vha. GD-OES, dog er det muligt at måle selv lette grundstoffer præcist ved at bruge sammenlignelige standarder.

GD-OES kan benyttes til at måle urenheder der ikke kan detekteres med andre metoder.

Egenskaber for korrosion og rensbarhed af rustfri ståloverflader

Rasmus Lage



Præsentation – DMS Vintermøde

Korrosion og Cleanability Egenskaber for EN 1.4404 Rustfri Stål Overflader

Fredag d. 18/01 , 2013, Kolding.
Rasmus Lage – MSc Design & Innovation



Oplæg om korrosion og cleanability

Målsætning for dagens oplæg

- Gennemgå uddrag af udført studie i hvordan forskellige overfladebehandlinger kan have kraftig indvirkning på de efterfølgende egenskaber for korrosion og cleanability
- Sammenligne egenskaber for udsnit af nogle af de mest almindelige benyttede overflader i industrien
- Sammenholde ruhedsparmetre for specificering af overflader med de resulterende egenskaber

Korrosion og Cleanability Egenskaber for EN 1.4404 Rustfri Stål Overflader



Agenda

Overordnede overvejelser for korrosion og cleanability

.....●

Valgt legering og overfladebehandlinger

.....●

Resultater for overflader, cleanability og korrosionsegenskaber

.....●

Opsummering

.....●

Korrosion og Cleanability Egenskaber for EN 1.4404 Rustfri Stål Overflader



Overordnede overvejelser for korrosion og cleanability

Korrosion og Cleanability Egenskaber for EN 1.4404 Rustfri Stål Overflader



Overordnede overvejelser

Overordnede overvejelser

- Overfladetopografi har stor indvirkning på cleanability og korrosionsbestandighed af overflader, selvom de er af samme type rustfri stållegering.
- Forskellige typer af overfladebehandlinger vil introducere vidt forskellige topografier afhængigt af den enkelte behandling.
- Valg af overfladebehandling og trade-offs?
 - Cleanability
 - Korrosionsbestandighed
 - Mekaniske egenskaber
 - Visuel karakteristika
 - Eksisterende praksis
 - Fastlagte krav
 - Pris

Korrosion og Cleanability Egenskaber for EN 1.4404 Rustfri Stål Overflader



Valgt legering og overfladebehandlinger

Korrosion og Cleanability Egenskaber for EN 1.4404 Rustfri Stål Overflader



Valgt legering og overfladebehandlinger

Valgt materialetype

- EN 1.4404 stål (316L)
- Analysearbejde foretages på 2 mm pladeemner.

Hvilke overflader er tilgængelige og benyttes i praksis?

- Slebne, matteret, børstet og rystepudset
- Poleret
- Blæste
- Vibrationsslebne og vibrationspolerede
- Slyngrenset
- Kemiske og elektrokemiske

Korrosion og Cleanability Egenskaber for EN 1.4404 Rustfri Stål Overflader



Karakterisering af overflade topografi

Korrosion og Cleanability Egenskaber for EN 1.4404 Rustfri Stål Overflader



Karakterisering af overflade topografi

Karakterisering af undersøgte overflader:

For tilstrækkeligt at kunne skelne mellem konsekvenserne af de enkelte overfladebehandlinger og deres indvirkning på korrosion og cleanability egenskaber, må den introducerede topografi undersøges i dybden.

Metoder til karakterisering:

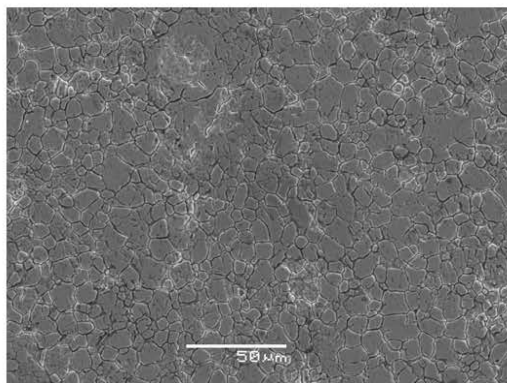
- Scanning Electron Microscopy (SEM)
- Metallographic Cross Section
- Ruhedsmålinger (R_a i særdeleshed)

Korrosion og Cleanability Egenskaber for EN 1.4404 Rustfri Stål Overflader



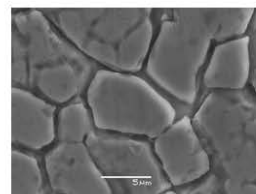
Karakterisering af overflade topografi

2B overflade



Fremstillingsproces

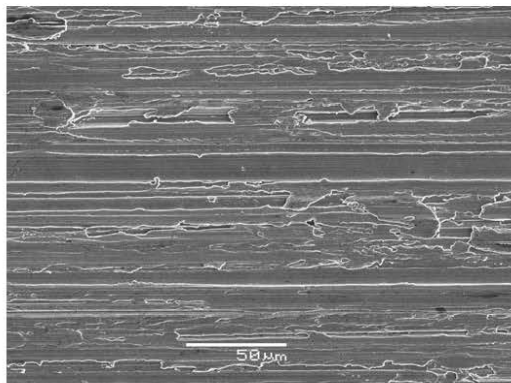
- Kold valset
- Annealed
- Bejdset
- Let valset



Korrosion og Cleanability Egenskaber for EN 1.4404 Rustfri Stål Overflader

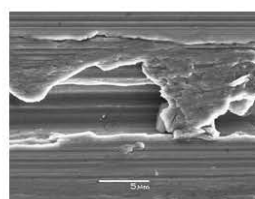
Karakterisering af overflade topografi

Slebet korn 180 overflade



Fremstillingsproces

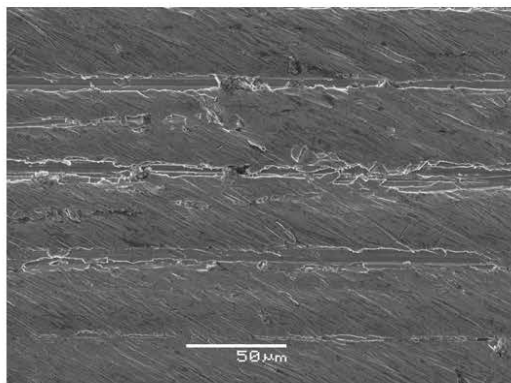
- Slebet korn 80
- Slebet korn 120
- Slebet korn 180



Korrosion og Cleanability Egenskaber for EN 1.4404 Rustfri Stål Overflader

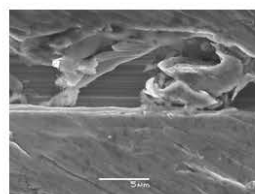
Karakterisering af overflade topografi

Matteret overflade



Fremstillingsproces

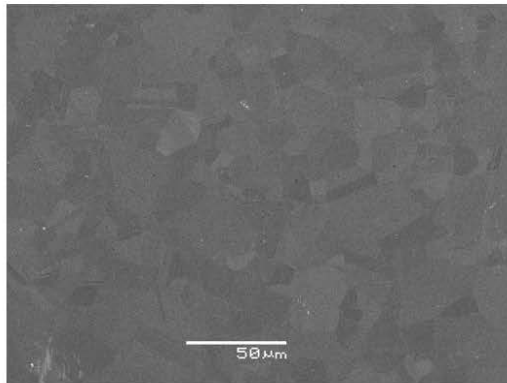
- Slebet korn 80
- Slebet korn 120
- Slebet korn 180
- Matteret m. 3M SC-BS A MED



Korrosion og Cleanability Egenskaber for EN 1.4404 Rustfri Stål Overflader

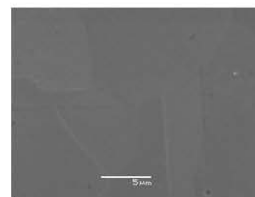
Karakterisering af overflade topografi

Electropoleret overflade



Fremstillingsproces

- Electropoleret
- 25 A/dm²
- 15 min
- 50 C°



Korrosion og Cleanability Egenskaber for EN 1.4404 Rustfri Stål Overflader

Korrosionsegenskaber og effekt af topografi

Korrosion og Cleanability Egenskaber for EN 1.4404 Rustfri Stål Overflader

Korrosionsegenskaber og effekt af topografi

Cykliske Polarisationskurver (CYP)

CYP er en accelereret test for korrosionsbestandighed, hvor en nedsænket overflade påtvinges en gradvis stigende elektrisk spænding (potentiale).

Denne spænding er et udtryk for hvor aggressivt et miljø den pågældende overflade befinder sig i.

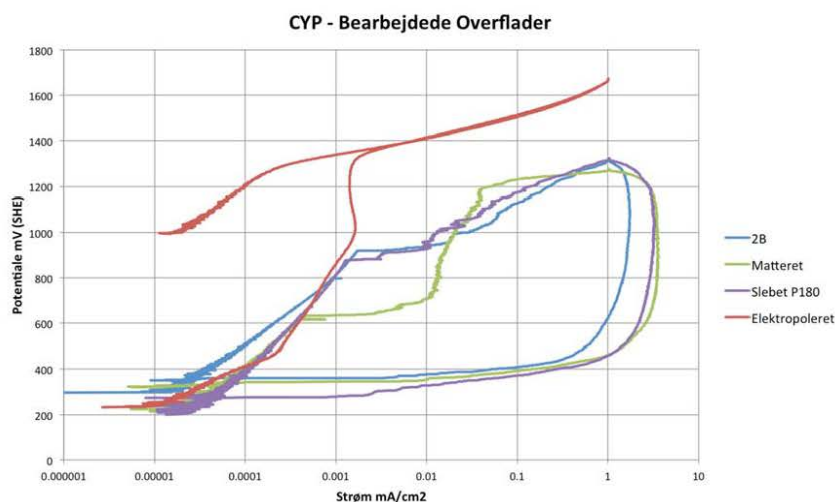
Der testes i en saltopløsning for at sikre at korrosion kan opstå.

Ved at måle den resulterende strøm mellem overflade og omkringliggende medie, kan begyndelsepunktet identificeres for korrosion (pitting potentialet)

Korrosion og Cleanability Egenskaber for EN 1.4404 Rustfri Stål Overflader

Sammenligning af korrosionsegenskaber

Cykliske Polarisationskurver



Korrosion og Cleanability Egenskaber for EN 1.4404 Rustfri Stål Overflader

Sammenligning af korrosionsegenskaber

Cykliske Polarisationskurver

Slebet korn 180 overflade



Matteret overflade



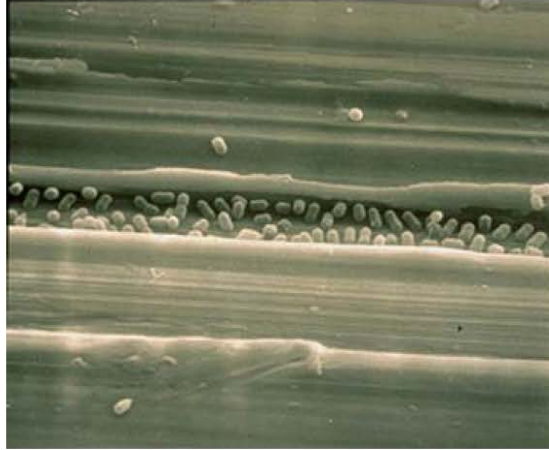
Korrosion og Cleanability Egenskaber for EN 1.4404 Rustfri Stål Overflader

Cleanability og effekt af topografi

Korrosion og Cleanability Egenskaber for EN 1.4404 Rustfri Stål Overflader

Cleanability og effekt af topografi

Cleanability som resultat af topografi?



Ref. Professor Amy Wong – Microbewiki.

Korrosion og Cleanability Egenskaber for EN 1.4404 Rustfri Stål Overflader

Cleanability og effekt af topografi

Kvantitativ metode - Impedans Analyse

Kvantitativ bedømmelse af resterende bakterier på undersøgte 10x15 mm samples efter rengøring. Antal af bakterier (Colony Forming Units - CFU) på overfladen bestemmes ved, at måle udviklingen af CO_2 der produceres af de resterende bakteries stofskifte.

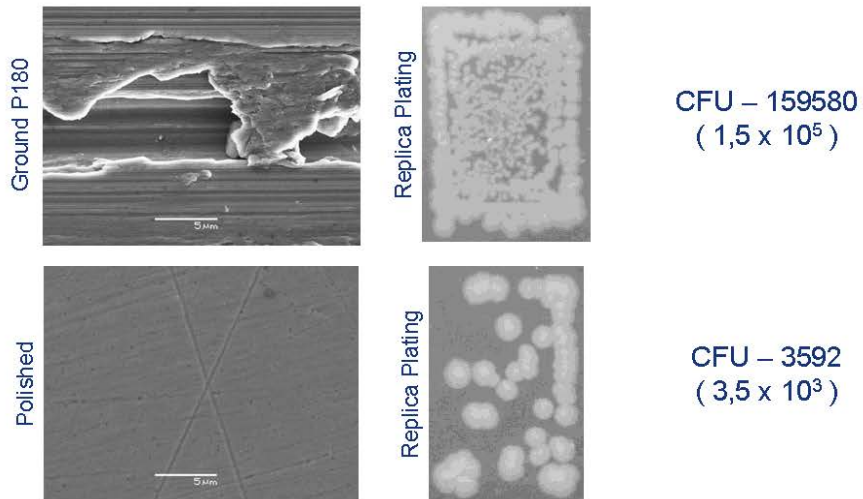
Visuel metode – Agar Replica Plating

Visuel bedømmelse af resterende bakterier på undersøgte 10x15 mm samples efter rengøring. Bakteriel overførelse fra den rengjorte overflade opnås via aftryk på Agar substrat efterfulgt af observation af den mikrobiel vækst.

Korrosion og Cleanability Egenskaber for EN 1.4404 Rustfri Stål Overflader

Cleanability og effekt af topografi

Cleanability for udvalgte overflader:



Korrosion og Cleanability Egenskaber for EN 1.4404 Rustfri Stål Overflader

Pålidelighed af ruhedsmålinger som parameter

Korrosion og Cleanability Egenskaber for EN 1.4404 Rustfri Stål Overflader



Pålidelighed af ruhedsmålinger som parameter

Nuværende brug af R_a værdier

- Mest almindelige ruhedsparemeter til specificering af overflader.
- Velkendt og let at benytte.
- Bruges i langt de fleste nuværende standarder og guidelines for design af applikationer med henblik på korrosion og cleanability.
- Anklages for at være for upræcis til tilstrækkeligt at kunne afbillede overflade topografi og overfladeregenskaber.

Korrosion og Cleanability Egenskaber for EN 1.4404 Rustfri Stål Overflader



Pålidelighed af ruhedsmålinger som parameter

Vurdering af nuværende standarder og guidelines i henhold til brugen af R_a

- R_a værdier kan ikke altid relateres til egenskaber for korrosion og cleanability.
- R_a værdier kan kun opfattes som tilnærmelser af den egentlige overflade topografi.
- R_a værdier vil for mange overflader have indlejret usikkerheder med hensyn til gengivelse af skjulte sprækker og revner.
- Nuværende standarder og guidelines tager ikke sådanne usikkerheder tilstrækkelig til efterretning.



Slebet P120

Korrosion og Cleanability Egenskaber for EN 1.4404 Rustfri Stål Overflader



Opsummering

Korrosion og Cleanability Egenskaber for EN 1.4404 Rustfri Stål Overflader

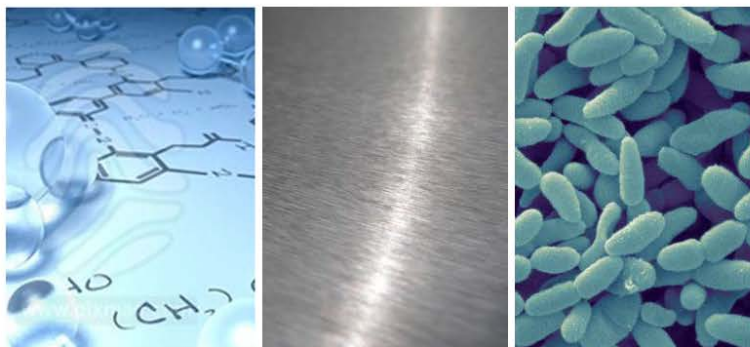


Opsummering

Opsummering

- Valg af overfladebehandling har stor indvirkning på henholdsvis cleanability og korrosionsegenskaber. Anvendt behandling og de resulterende egenskaber bør derfor overvejes i henhold til den givne applikation.
- Nuværende specificering af overfladekriterier via eksisterende standarder og guidelines indeholder flere faldgrupper. Dette skyldes især brugen af R_a værdier som overfladekriterium.
- Via overvejelser omkring effekten af topografi kan der etableres et forbedret udgangspunkt for valg af overfladebehandling. Formidlingen af disse overvejelser kan assistere med udvælgelse og forbedret forståelse af overfladespecificering.

Korrosion og Cleanability Egenskaber for EN 1.4404 Rustfri Stål Overflader



Tak

Spørgsmål?